AGHA HASAN ABEDI AUDITORIUM

CONFERENCE PROCEEDINGS

2ND PAK-TURK INTERNATIONAL CONFERENCE ON EMERGING TECHNOLOGIES IN THE FIELD OF SCIENCES AND ENGINEERING

111-13-MARCH 2019

ORGANIZED BY: GHULAM ISHAQ KHAN INSTITUTE OF ENGINEERING SCIENCES AND TECHNOLOGY

Fabrication of Nano-porous Anodic Aluminum Oxide (AAO) by varying Anodization Parameters

Asim Iltaf[1, a], Malik Hassan[2, b], Danish Tahir[1, c], Syed Irfan Raies[3,d], and Prof. Dr. Ashraf Ali[1,e]

[1] Faculty of Material Science and Engineering
Ghulam Ishaq Institute of Engineering Science and Technology
Topi, Pakistan
[2] Faculty of Mechanical Engineering
Ghulam Ishaq Institute of Engineering Science and Technology
Topi, Pakistan
[3] Department of Materials Engineering
School of Chemical and Materials Engineering
National University of Sciences and Technology
Islamabad, Pakistan

Email address: [a] asim_me06@scme.nust.edu.pk , [b] malik.hass657@gmail.com,
[c] danishtahir219@gmail.com, [d] irfan.raees17@gmail.com, and [e] drashraf@giki.edu.pk

Abstract— To produce close-packed Nano-pores using anodization process in aluminum foil by varying different process parameters of anodization process i.e. time of anodization, type of electrolyte being used, the temperature of the electrolyte, purity of aluminum foil and voltage being used. The anodized aluminum surface which is also called anodic aluminum oxide can be used to grow liquid crystal molecules in those Nano-pores and use the orientation of liquid crystal for bio-sensing and other medical applications.

Keywords—Nano-pores, anodization, electrolyte, aluminum foil, anodic aluminum oxide

I. INTRODUCTION

Aluminum anodization is a two-step electrochemical process in which an aluminum oxide layer is formed on the aluminum which was originally used [1, 2]. The aluminum oxide contains hexagonally ordered pores as a result of the anodization process. Voltage is applied to aluminum foil or sheet in the acidic electrolyte which leads to the formation of the aluminum oxide layer. The hexagonal pores structure is also called anodized aluminum oxide (AAO). The structure of AAO is a close-packed hexagonal shape array of Nano-pores which are parallel to each other and perpendicular to the surface of the underlying Aluminum substrates [3, 4]. The pore formation of AAO film was affected by several parameters, such as the anodization voltage, concentration, and nature of acid solutions, temperature of electrolyte and the first anodization time [5]. Nano-porous anodic aluminum oxide (AAO) gained exposure recently for use as a membrane in applications such as gas separation, drug delivery, and bone fixation [6]. Aluminum can be anodized in various types of acid solutions i.e. oxalic acid, phosphoric acid, and sulfuric acid [6, 7]. The required pore size and the final application in which AAO has to be used decide the type of acid solution [5]. Concentrated acid solutions give bigger size pores while small pores of AAO can be obtained using sulfuric acid. Anodization done at constant voltage with dilute acidic electrolyte is known as potentiostatic anodization. while the anodization which is performed at constant current is known as Galvano static anodization. The working voltage for oxalic acid is generally in the range

of 20-40V and for phosphoric acid it is 60-195V. Working at high voltage may result in local heat generation at the aluminum surface which can be avoided by using low temperature, but working at low temperature result in compact, thick and hard AAO layer. Anodic aluminum oxide pore size and channels depth are greatly affected by all the parameter and the final morphology of channels depends upon varying these parameters i.e. temperature, voltage, anodization time and electrolyte type [5, 8]. Pretreatments of the sample also play a significant role in anodization as improper pretreatments and handling of aluminum sample lead to the generation of local heat on sample surface which initiates the burning of the sample [9]. Besides all the parameters which affect AAO Pore size, the voltage has a linear relationship with aluminum oxide pore size. The effect of changing the voltage on pore diameter is evident by Krissada [10]. There are various electrochemical techniques which are currently being employed i.e. Electro-etching, Electro-polishing, Anodization, Corrosion protection setups and Electro-deposition. An electrochemical reaction occurs only in the presence of the following four critical components which are responsible for the initiation and continuation of reaction [11]. These critical components are described below in detail.

- Electrolyte

- Cathode

- Anode

- A connection between cathode and anode for the flow of electrons.

This electrochemical process is used for forming an oxide layer on a sample such as aluminum oxide in case of aluminum. In this case, the working electrode is anode while the counter electrode is a cathode. Electrons move from anode to cathode through the electrical

connection. The negative ions in the electrolyte are attracted to anode on which the oxide layer is formed. The schematic representation of the anodization process is shown in figure 4.

II. EXPERIMENTAL PROCEDURE

For the sample preparation, the following steps are to be followed.

1. The aluminum sample was annealed in a muffle furnace at 400º C for 5 hours of soaking time. Annealing was done to remove internal stresses and to prevent burning and cracks.

2. After annealing, the sample was electro-polished in "2 weight %" [8] NaOH and was rinsed afterward with water.

3. First anodization is done for one hour while using different voltages in the range of 0-60 for both 0.3 M oxalic acid and 5volume% phosphoric acid.

4. Pore widening is done after first anodization to increase the size of pores. It was done by dipping samples in 5volume % phosphoric acid for 30 minutes.

5. 2nd anodization is done for 2-3 hours after pore widening. It is done for the further growth of pores. It is done in the range of 0-60 V for both oxalic and phosphoric acid. The experimental setup is shown in the Figure 1.
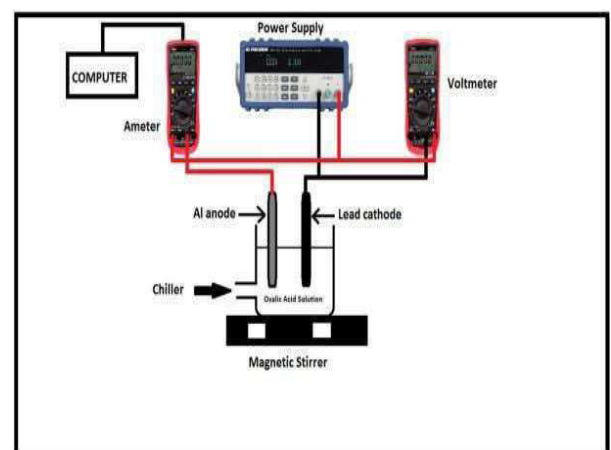

Fig. 1: Experimental setup to be used.

III. Experiments Scheme

A 1000 ml beaker was used as an anodization cell, which was placed in 2000 ml beaker, used for the recirculation of anti-freezing isopropanol solution and holding of anodization. Anodization cell consisted of a thermometer, magnetic stirrer bar, an anode, a cathode as shown in the fig.1. The thermometer was installed in the anodization cell to monitor temperature changes during the course of experimentation. A magnetic stirrer was used to minimize heat generation at the surface of aluminum. Digital ammeter was connected to the computer interface to record the current vs. time plots. Voltmeter was connected to the cell to observe voltage changes.

IV. Results and Discussions

A. Surface analysis of Aluminum obtained at 60V

For surface analysis of Aluminum obtained at 60V, the experiment conditions and pore size obtained are depicted in Table 1. The SEM image at a magnification of 5000x is shown in fig.2. As a magnification is low, it was difficult to figure out the presence of pores. It can be seen that the surface of the alumina contains some cavities, these are some intermetallic compound which forms during the process. These can be eliminated by using a foil of high purity and by performing pre-treatments. Fig.3 depicted the SEM image of same sample anodized at 60V in phosphoric acid at a higher magnification of 40000x. This shows the porous structure on the surface. As can be seen from the figure that the pores are continuous and regular.

Fig. 2: SEM image of anodized aluminum foil, anodized at 60V in 5 Vol% phosphoric acid at 5000x
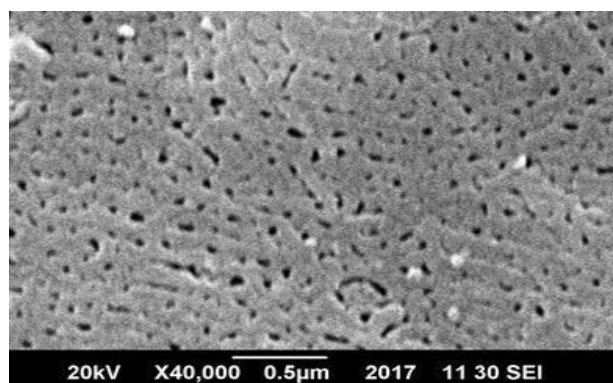
Fig. 3: SEM image of anodized aluminum foil, anodized at 60V in 5 Vol% phosphoric acid at 40000x

B. Surface analysis of Aluminum anodized at 50V

Table 2 shows the experimental conditions for surface analysis of aluminum which is anodized at a voltage of 50V. The pores size obtained after anodization is also shown in table 2.

SEM micrograph of AAO at a magnification of 30000x and 40000x is shown in fig.4 and fig.5 respectively. It is found that porous structure is obtained when anodization is performed at a voltage of 50V. The figure also shows the presence of cavities which is intermetallic compound.

Table 1: Experiment conditions for surface analysis of Aluminum obtained at 60V

Sample	Electrolyte	Time (hrs)	Temperature (ºC)	DC voltage	Pore size in nm
AO2	5 vol% phosphoric acid	2.5	-5	60	20-40

Table 2: Experiment conditions for surface analysis of Aluminum obtained at 50V

Sample	Electrolyte	Time (hrs)	Temperature (ºC)	DC voltage	Pore size in nm
AO2	5 vol% phosphoric acid	3	-2	50	20-40
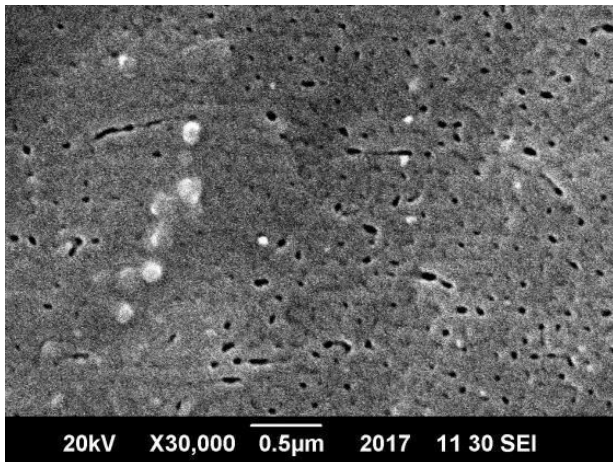
Fig. 4: SEM image of anodized aluminum foil, anodized at 50V in 5 Vol% phosphoric acid at 30000x

Fig. 6: SEM micrographs for anodization of aluminum foil performed at 25V in 0.3M oxalic acid at magnification of 50000X

D. Surface Analysis of AAO obtained at 40V

This experiment was done at relatively high voltage i.e. 40V. The voltage was increased to increase the pore size. High voltage produces heat at the surface of aluminum. To minimize the heat effect, the temperature was kept at 0°C using the recirculating chiller. Parameters used for this experiment are shown in Table 4.

As it can be seen from the fig.7 that the sample got burnt for the experiment done at 40V and 0°C. Aluminum was not anodized under these conditions due to the overheating. Overheating was probably the result of high voltage, improper pretreatments and to high temperature. Overheating also occurred due to the automatic shutdown of the recalculating chiller after achieving the desired temperature which led to the lowering of the temperature of the electrolyte. Resultantly temperature was not enough to reduce the cracks developed at the surface of aluminum. The presence of inter-metallic compounds can be seen in the fig.7. These intermetallic compounds can be reduced by doing proper pretreatments and by using high purity aluminum foil.

Fig. 5: SEM micrograph of anodized aluminum foil, anodized at 50V in 5 Vol% phosphoric acid at a magnification of 40000x

C. Surface analysis of AAO obtained at 25V

Randomly organized and relatively small pores are obtained at 25V in 0.3M oxalic acid as shown in fig.6. The parameters for the anodization done at these conditions are given in Table 3.

Table 3: Parameters for surface analysis of Aluminum obtained at 50V

Sample	Electrolyte	Time(hour)	Temperature (oC)	DC Voltage
1	0.3 M oxalic acid	1	-5	25

Table 4: Parameters for surface analysis of Aluminum obtained at 40V

Sample	Electrolyte	Time(hour)	Temperature (°C)	DC Voltage
1	0.3 M oxalic acid	1	0	40
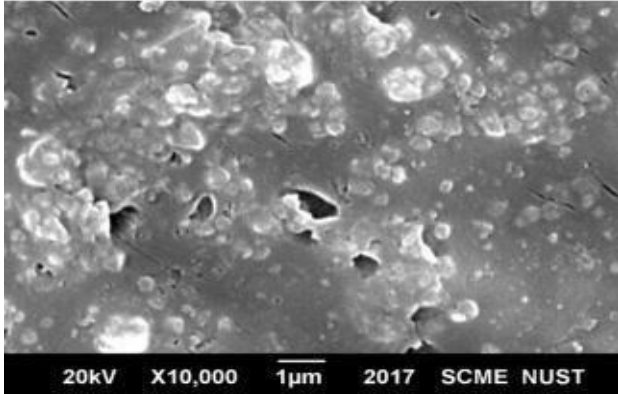
Fig. 7: SEM micrographs for anodization of aluminum foil performed at 40V

E. Surface Analysis of AAO obtained at 70V

The sample is anodized in 5 vol% phosphoric acid at a temperature of -2°C when the voltage applied was 70V. Table 5 shows the experimental conditions and pore size obtained.

Table 5: Parameters for surface analysis of Aluminum obtained at 70V

Sample	Electrolyte	Time (hrs)	Temperature (°C)	DC voltage	Pore size in nm
AO2	5 vol% phosphoric acid	3	-2	70	25-55

As the voltage is high, the sample was burnt due to the production of a large amount of heat. Fig8 shows the burnt samples.

This burning of the sample may be attributed to overheating of the sample because the temperature provided is not enough to dissipate the heat produced. After magnifyying the sample further at a magnification of 30000x, the presence of pores is shown in Fig.9.
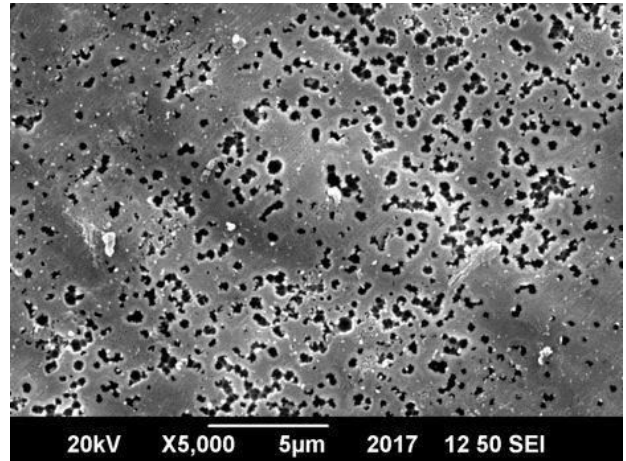
Fig. 8: SEM image for anodization of aluminum foil performed at 70V at a magnification of 5000X
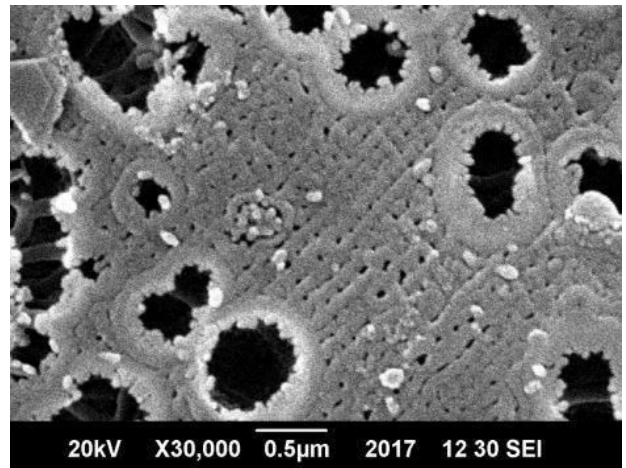
Fig. 9: SEM image of the sample at magnification of 30,000X

V. CONCLUSION

• Use of low voltage will help to achieve pores of small diameter. To get pores of large diameter, the voltage has to be increased. The applied voltage varies according to the type of electrolyte used.

5

- Magnetic stirrer will help to maintain a constant temperature in the cell and it also helps to obtain highly ordered pores.

- To compensate the local heat generated during the process, the cell temperature has to be in the range of -2°C to -7°C.

- Annealing and pre-treatment are necessary to remove any of the internal stresses present in the sample because these stresses increase the probability of burning of the foil.

- As the purity level of the sample increase, more ordered pores obtained because impurity forms intermetallic compounds on the sample.

-

REFERENCES

[1] Lv, Huiling, et al. "Anodization of dual- layer laminated aluminum foils: A facile route to through-hole porous anodic alumina templates." Journal of Alloys and Compounds 614 (2014): 182-185.

[2] Zhang, Junping, Jerrold E. Kielbasa, and David L. Carroll. "Controllable fabrication of porous alumina templates for nanostructures synthesis." Materials Chemistry and Physics 122.1 (2010): 295- 300.

[3] Jani, Abdul Mutalib Md, Dusan Losic, and Nicolas H. Voelcker. "Nanoporous anodic aluminium oxide: advances in surface engineering and emerging applications." Progress in Materials Science 58.5 (2013): 636-704.

[4] Cui, Jiewu, et al. "A facile and efficient approach for pore-opening detection of anodic aluminum oxide membranes." Applied Surface Science 258.14 (2012): 5305-5311.

[5] Chowdhury, P., et al. "Effect of process parameters on growth rate and diameter of nanoporous alumina templates." Bulletin of Materials Science 34.3 (2011): 423-427.

[6] Belwalkar, A., et al. "Effect of processing parameters on pore structure and thickness of anodic aluminum oxide (AAO) tubular membranes." Journal of membrane science 319.1-2 (2008): 192-198.

[7] Abel Santos , T.K., Dusan Losic Nanoporous Anodic Alumina: A Versatile Platform for Optical Biosensors. 2014.

[8] Yuanjing Lin, Q.L., Xue Liu, Yuan Gao, Jin He, Wenli Wang, Zhiyong Fan, A Highly Controllable Electrochemical Anodization Process to Fabricate Porous Anodic Aluminum Oxide Membrane. Nanoscale Research Letters, 2015.

[9] J. H. Yuan, F.Y.H., D. C. Sun, X. H. Xia A Simple Method for Preparation of Through- Hole Porous Anodic Alumina Membran. 2004.

[10] Krissada Surawathanawises, X.C., Nanoporous anodic aluminum oxide with a long-range order and tunable cell sizes by phosphoric acid anodization on prepatterned substrates. National Institutes of Health, 2014.

[11] Lu, Chi, and Zhi Chen. "Anodic aluminum oxide-based nanostructures and devices." Encyclopedia of nanoscience and nanotechnology 11.1 (2011): 235-259.

[12] Jin Shyong Lin, S.H.C., Ker Jer Huang, Chien Wan Hun, Chien Chon Chen, Challenges to Fabricate Large Size-Controllable Submicron-Structured Anodic- Aluminum-Oxide Film. Atlas Journal of Materials Science 2015.

Applications of nanotechnology in science and engineering; A review

Danish Tahir[1,a], Dr Ashraf Ali[2,b]

[1]Faculty of Materials and chemical Engineering, Ghulam Ishaq Khan Institute of Engineering Sciences and Technology Topi, Swabi, Khyber Pakhtunkhwa, Pakistan

[2]Faculty of Materials and chemical Engineering, Ghulam Ishaq Khan Institute of Engineering Sciences and Technology Topi, Swabi, Khyber Pakhtunkhwa, Pakistan

Email address: [a] danishtahir219@gmail.com , [b] drashraf@giki.edu.pk

Abstract—**Nanotechnology is of great importance in industry sector like medicine, security organizations, transportation and many others sectors. Today's technology at nanoscale deals with development of materials with nanoscale dimensions because manufacturing of nanoscale materials decreases the size of object. This review paper focuses the development of nanotechnology applications in recent years.**

Keywords— Science, Engineering, Environment, safety, Nanotechnology

I. INTRODUCTION

Nanotechnology is branch of science which deals with control of matter at molecular or atomic scale which is related to things that are about 100 nanometers across. For beginner level nanotechnology definition also stated as engineering branch that deals with things with a size lower as 100 nanometers. As nanotechnology use is increasing day by day in every field so here are some classified applications.

A. Sustainable energy applications

World's energy demands are increasing day by day and many researchers are looking for processes that will produce clean and renewable energy sources without burdening much on environment. If we talked about solar cells then this device is easy to install and they can be rolls if necessary. Low et al. [1] stated that nanotechnology is helping us to improve fuel efficiency by using better catalysis and furthermore this technology's use in vehicle industry makes the use of fuel consumption much low.

Fig.1: Nanotechnology applications in Science and environment [2]

Another materials scientist Najim et al. [3] researched about nano aspects in various fields especially in batteries and suggested that batteries with nano engineering have light weight, more efficient and have long life.

Chaturvedi and Dave. [4] suggested that nano-bioengineering of enzymes will convert cellulose into ethanol for fuel. Figure 1 shows the nanotechnology applications in different fields. Nanotechnology can help in obtaining clean water by using nanoscale sensors that can clean water even at low cost. For example alumina based sensors are also in used and help in detection of impurities and water purification [5,6].

B. Medicine and sensors application

Molecular signals associated with malignancy can also be detected by signals based on the nanoscale components. Along with signals nanotechnology is even used in medicine field where small nanoscale components are used to deliver drugs directly to different parts of human body. Nanotechnology makes over product cheaper, portable and safer. Biosseau and Loubaton [7]; George, [8]; Yashveer et al. [9] did very useful research on nanotechnology in areas of medicine. Diagnosing a disease is the most important part of any treatment and nanotechnology based quantum dots enhances the imaging for diagnostic. Figure 2 shows the quantum dots in medical diagnostic.
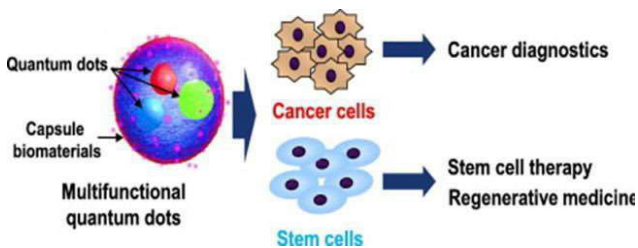
Fig. 2: Quantum dots in biological imaging for medical diagnostic [10].

These dots when exposed to ultraviolet light they emit light of bright colors which is used in identifying specific cells and other biological activities. These dots not only used in identifying but also in treatment of specific

cancerous cells in human body with minimizing risk to normal human tissue [11].

C. Future prospect in Transportation

Nanotechnology is often used in concrete, steels and other materials which not only improves these materials strengths but also increases their life and decreases their cost. Nanoscale devices have been produced which are used to monitor bridges, parking structures and rails. Nanotechnology is advancing day by day such that this technology is used to communicate between different vehicles which helps driver to maintain their lane, routes and collisions [12][13].

D. Nanomaterials with remedial technology

If we talk about the size and shape of nanoparticles then these are particles with dimensions less than 100 nanometer and upto 15000 atoms in it. They can be prepared in the form of rods, spheres, films and bulk materials. Nanotechnology is solving different problems in every field of science where these materials act as nano catalyst etc. two major properties which make nanomaterials different from bulk are small size which resulted in increase of surface area to much higher level and manipulations of molecular level produces desired characteristics in these materials.

Bowman et al. [14] researched about removal of contaminations and he divided his work into two processes where contaminants sorption occurs on a certain medium. Another step involves the transformation of contaminants into a compound which is non-toxic in nature. Lie et al. [15] did an outstanding research where multi-walled nanotubes are used for removal of contaminants which are chlorinated aromatic compounds. Figure 3 illustrate the acidic generation on MWNT.
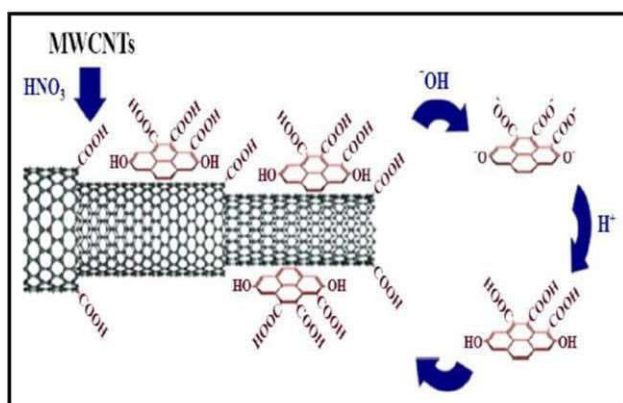
Fig. 3: Generation of acidic groups with covalent nature on MWNT [15]

He suggested that many processes have been developed to remove contaminants from different liquids but sorption method is most common method, cost effective and efficient.

E. Nanoparticles with In Situ applications

Application method at nanoscale is mostly dependent on site and geology of treatment zone. Along with these two factors way of injection of nanoparticles is also important and is mostly injected through wells and piezometers. Injection well involves injection of particles in wells with up gradient slope and down gradient usually extract water at ground. Nanoparticles are mixed with this ground water and injected.

Scientists are doing research on methods of injection where nanomaterials can maintain their high reactivity and distribute their self easily on the surface. nZVI has been created successfully from plant phenols and this material is better for contaminants and less dangerous in preparation method [16].

F. Nanoparticles with In Situ applications

Food and agriculture are very important field for people residing in any country. According to reports about 50% of total population is living in an Asia. Many countries face daily food shortage because of environmental impacts. To improve yield every developing country is focusing to develop pest resistant crops to secure their food. Nanoparticles are also being used in food industry as a medium for food packaging. Bionanocomposites are used to protect the food and this package based on nanotechnology is more environments friendly because it reduces the use of plastic.
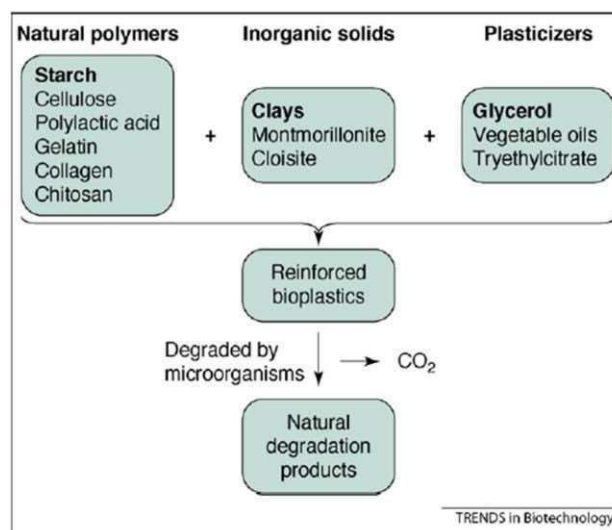
Fig. 4: Formation of bionanocomposite [17].

Figure 4 show the schematic for the preparation of bionanocomposite and these are more useful than traditional packaging because traditional packaging includes materials which are nondegradable and these return results in environmental pollution.

Fryxell et al. [18] examined that nanotechnology has a potential to reduce the waste and pollution concept. In other words due to small scale science this technology reduces resource consumption. Along with these advantages some hazards also associated with these very fine particles. Salata et al. [19] talked about hazards of these nanomaterials and how can we control them.

II. CONCLUSION

Using this review it has been revealed that nanotechnology played a vital role in every field of science and engineering. This technology is taking the fields of medicine, agriculture, construction materials and food to new level of advancement. Some research on replication of natural systems generates complexities in this field. Nanomaterials are also a wide growing area where alteration in properties make a useful product for the benefit of particular industry and following same route we will see a new world of Nanoscience in future.

REFERENCES

[1] Low J, Yu J, Ho, W. (2015). Graphene- Based Photocatalysts for CO2 Reduction to Solar Fuel. The journal of physical chemistry letters, 6(21): 4244-4251.

[2] Jalaja K, Naskar D, Kundu S.C, James NR. (2016). Potential of electrospun core–shell structured gelatin–chitosan nanofibers for biomedical applications. Carbohydrate polymers, vol. 136, 1098-1107.

[3] Najim M, Modi G, Mishra YK, Adelung R, Singh D, Agarwala V. (2015). Ultra-wide bandwidth with enhanced microwave absorption of electroless Ni–P coated tetrapod-shaped ZnO nano-and microstructures. Physical Chemistry Chemical Physics, 17(35): 2923-2933

[4] Chaturvedi S, and Dave PN (2014). Emerging applications of nanoscience. Paper presented at the Materials Science Forum, 152-159

[5] Rabbani MM, Ahmed I, Park SJ. (2016). Application of Nanotechnology to Remediate Contaminated Soils Environmental Remediation Technologies for Metal-Contaminated Soils. Springer, 219-229.

[6] Mishra Y, Chakravadhanula V, Hrkac V, Jebril S, Agarwal D, Mohapatra S, Adelung. R (2012). Crystal growth behaviour in Au- ZnO nanocomposite under different annealing environments and photo switch ability. Journal of Applied Physics. 112(6): 301-309.

[7] Boisseau P, Loubaton B. (2011). Nanomedicine, nanotechnology in medicine. Comptes Rendus Physique, 12(7): 620-636.

[8] George S. (2015). Nanomaterial Properties: Implications for Safe Medical Applications of Nanotechnology Nanotechnology in Endodontics, Springer, 45-69.

[9] Yashveer S, Singh V, Kaswan V, Kaushik A, & Tokas J. (2014). Green biotechnology, nanotechnology and bio-fortification: perspectives on novel environment-friendly crop improvement strategies. Biotechnology and Genetic Engineering Reviews, 30(2): 113-126.

[10] Daisuke Onoshima. (2015). Multifunctional quantum dots-based cancer diagnostics and stem cell therapeutics for regenerative medicine. Advancec drug delivery review. Pages 2-14

[11] Adam M, Wang Z, Dubavik A, Stachowski G.M, Meerbach C, Soran-Erdem Z, Eychmüller A. (2015). Semiconductor Nanocrystals: Liquid–Liquid Diffusion-Assisted Crystallization: A Fast and Versatile Approach Toward High Quality Mixed Quantum Dot-Salt Crystals (Adv. Funct. Mater. 18/2015). Advanced Functional Materials, 25(18): 2783-2783.

[12] Golestani B, Nam B.H, Nejad F.M, Fallah R. (2015). Nanoclay application to asphalt concrete: Characterization of polymer and linear nanocomposite-modified asphalt binder and mixture. Construction and Building Materials, 91: 32-38.

[13] Sobolev K. (2015). Nanotechnology and Nano engineering of Construction Materials Nanotechnology in Construction, Springer, 3-13.

[14] Bowman RS. (2003). Applications of surfactant-modifiedzeolites to environmental remediation. Microporous and Mesoporous Materials, 61(1): 43-56.

[15] Liu X, Pi B, Wang H, Wang XM (2015). Self-assembling peptide nanofiber hydrogels for central nervous system regeneration. Frontiers of Materials Science, 9(1): 1-13.

[16] Hart S.L, Milstein M.B. (2003). Creating sustainable value. Academy of Management Executive. 17: 172-180.

[17] Nasli Sozer. (2009). Nanotechnology and its applications in the food sector. Trends in Biotechnology, Pages 82-89

[18] Fryxell G.E, Lin Y, Fiskum S, Birnbaum J.C, Wu H. (2005). Actinide sequestration using self-assembled monolayers on mesoporous supports. Environ Sci Technol, 39: 1324-1331

[19] Salata OV. (2004). Applications of nanoparticles in biology and medicine. Journal of Nano biotechnology; 2(3):16-22.

Effect of Stack Geometry, Material, and Position on the Performance of Thermoacoustic Refrigeration System

Malik Hassan[1, a], Samar Abbas[1, b], Zeeshan Ahmad[1, c], Naeem Ullah[1, d], Asadullah Khan[1, e], and Ghani Khan[1,f]

[1] Faculty of Mechanical Engineering
Ghulam Ishaq Institute of Engineering Sciences and Technology
Topi, Pakistan

Email address: [a] malik.hass657@gmail.com , [b] samarabbas@giki.edu.pk , [c] zeeahmad253@gmail.com ,
[d] naeem6960@yahoo.com , [e] giki2015081@gmail.com , and [f] ghanikhan2015113@gmail.com

Abstract— Development of the refrigeration system based on Thermoacoustic technology is a new solution for the present day need of cooling without causing ecological risks. With added advantages of less moving parts and no recirculating refrigerant, the thermoacoustic refrigeration Systems can produce very low temperatures with compact size. There are many parameters (such as stack shape, length, position, material, resonance frequency and working fluid etc.) involved in thermoacoustic refrigeration cycle which affects the efficiency of this cycle. In this study, the effect of stack shapes, material, and position on the temperature difference has been determined.

Keywords— Refrigeration system, Thermoacoustic refrigeration System, Stack, Refrigerant

I. INTRODUCTION

Refrigeration is one of the most required and important needs of humans beings. Almost everywhere in the world, conventional refrigerators are used for obtaining low temperature. The traditional refrigerator uses the following processes

1) Compression

2) Condensation

3) Expansion

4) Evaporation

The main issue with these conventional refrigerators is that they use refrigerants which is harmful to the environment and causes global warming. The major issue caused by these refrigerants is the depletion of the ozone layer. Ozone layer blocks the harmful ultraviolet radiations of the sun coming to earth. These ultraviolet radiations are very harmful to human beings and may cause skin cancer. As the population is increasing day by day and definitely the needs of refrigeration also increase. As a result, the emissions of these gases can increase dramatically. Fig.1 shows the concentration of different refrigerants used in different years.

One of the possible solutions to this problem is the use of a thermos-acoustic refrigeration system which does not use these harmful gases as a refrigerant. Thermo-acoustic is a combination of thermodynamics and acoustics. Thermo-acoustic refrigeration System utilizes the thermodynamic characteristics of pressure sound waves. As the sound wave propagates, the gas medium undergoes pressure oscillations accompanied by corresponding temperature oscillations. Sound waves travel in the form of compressions and rarefactions. In compression, the density and pressure of air increases and as a

result the temperature also increases while in rarefaction the density and pressure of air decreases which results in the decrease in temperature at the rarefaction. This system uses the concept that when air compresses its temperature increases and can transfer heat to the surroundings while in rarefaction the temperature of the air decreases and can accept heat from the surroundings and, hence producing cooling. This is actually done with standing waves caused by resonance in the air column inside the tube. In resonance, the amplitude of vibrations and also the pressure differences becomes maximum due to which greater temperature differences can be achieved. The particles behavior, amplitude of vibrations of the particles, and pressure variation during the process are depicted in fig.2. In fig.2 (a) the behavior of air particles in the tube during the resonance is shown. The dense areas represent the compressions while the rare areas show the rarefaction. Fig.2 (b) shows the amplitude of the particles along the length of the tube. The parts of the wave where the amplitude is zero are called displacement nodes while those having maximum amplitude are called displacement antinodes. Whereas the fig.2 (c) shows the pressure variation along the tube. Pressure nodes are the points where the pressure is equal to atmospheric pressure whereas, the pressure variation is maximum at pressure antinodes. The displacement nodes and antinodes are pressure antinodes and nodes respectively.

For thermoacoustic refrigeration, the most suitable position for the stack is the pressure antinode where the pressure variation is the maximum i.e. pressure increases to a high value above the atmospheric pressure and then decreases below the atmospheric pressure to a low value.
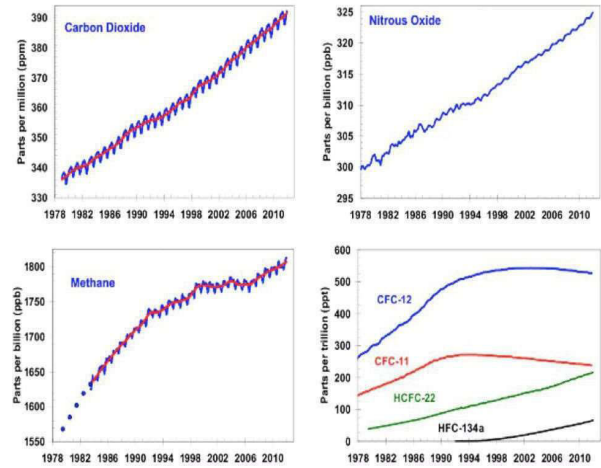
Fig. 1: Concentration of different refrigerants at a different period of time [1].
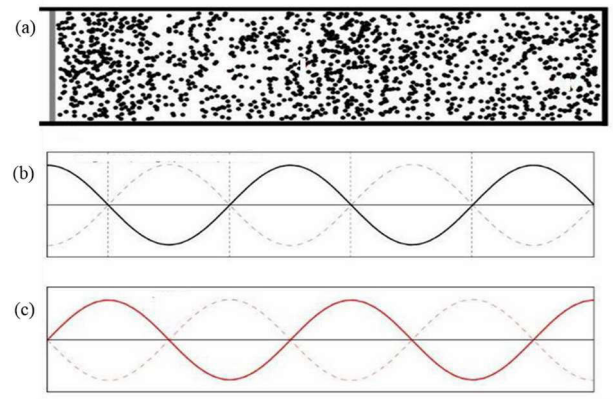
Fig. 2: (a) particles behavior in resonator (b) amplitude of vibrations of the particles along the length of resonator (c) pressure variation along the length of the resonator [2]

II.   LITERATURE REVIEW

Thermoacoustic induced oscillation has been observed for the centuries. This phenomenon was first observed during the glassblowing process (glass manufacturing process). It was observed by Taconis & Beenakker in 1949 [3] that blowing the hot bulb at the end of the cold narrow tube causes sound waves to generate. Byron Higgins was the first who made a scientific observation of this phenomenon and explained this phenomenon as the conversion of heat energy into acoustical oscillation [4]. Different scientists gave different explanations of the thermoacoustic oscillations phenomena observed at a different time. It was Kramer in

1949 who first gave a formal theoretical study of thermoacoustic when he generalized the Kirchhoff's theory of attenuation of the sound wave at a constant temperature to the case of attenuation of the sound wave in the presence of temperature gradient [5]. After that, the acoustic part of thermoacoustic was linked to the thermodynamics theories by the Swift in 1988 [6]. Different research exertions have been done to improve the efficiency of the thermoacoustic refrigeration cycle.

[7] Showed the effect of stack geometry and stack material on the cooling load of the thermoacoustic refrigeration. [8] worked on the optimization of performance and cooling load of the thermoacoustic refrigeration. They showed the effect of working gas, stack length and stack position in term of non-dimensional parameters on the performance and cooling load of thermoacoustic refrigeration. [9] showed the effect of stack length, stack spacing, thickness and stack cross section on the cooling load using non-dimensional parameters and graphical approach. They used Helium as working gas in a resonance tube of 58.8 cm with a pressure of 10 bar and achieved a cooling load of 4W. [10] showed the optimization of stack geometry in thermoacoustic refrigeration. They showed the effect of optimized normalized stack length and center position stack position on the COP of thermoacoustic refrigeration. A cooling load of 4.71W was achieved for optimized stack length and stack position. [11] described the complete design of thermoacoustic refrigeration using linear theory and showed the effect of different process parameters on the COP of the system in term of non-dimensional parameters.

III. EXPERIMENTS SCHEME

Thermoacoustic refrigerator consists of the following components.

- FUNCTION GENERATOR
- SOUND AMPLIFIER
- LOUDSPEAKER
- RESONANCE TUBE
- WORKING FLUID
- STACK

The function generator is a device which generates a sound tone of required frequency and shape. It can produce sine, triangular, square and sawtooth sound waves. In this work, NCH tone generator software was used to generate a sound wave. The sound waves produced by the function generator has a low amplitude. For increasing the amplitude a sound amplifier is used. It is connected with the function generator to receive a sound signal and amplify it. In order to have an audible sound of the given frequency, a loudspeaker is used. The amplified sound wave from the amplifier is fed into the loudspeaker which produces sound waves in the tube. The loudspeaker is connected to one end of a resonance tube. The other end of the resonator is closed. Length of the resonator determines the frequency required to produce a standing wave or vise versa. The standing waves of quarter wavelength were produced in resonance tube as portrayed in fig.3. The temperature difference between the two ends of the stack depends upon the fundamental resonance frequency in such a way that with the increase in frequency, the compressions and rarefactions will also increase resulting in a higher temperature difference between the ends of the stack. The most important part of the thermoacoustic refrigerator is a stack. It is placed inside the resonance tube and the best place for it is the pressure antinode. It is a perforated component. It consists of channels in the axial direction so that air molecules can freely vibrate inside it.

There are many stack geometries as shown in fig.4. The stacks used in this work are the parallel plate and spiral stack as shown in fig.5. The experimental setup used in this work is shown in fig.6.
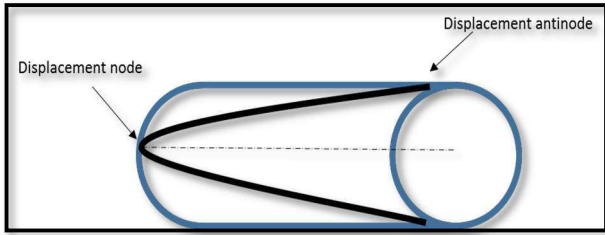
Fig. 3: Quarter wavelength resonator
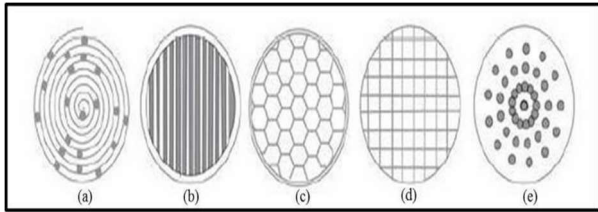
Fig. 4: Stack geometries: (a) Spiral (b) Parallel plate (c) Honey comb (d) Corning celcor (e) Pin array
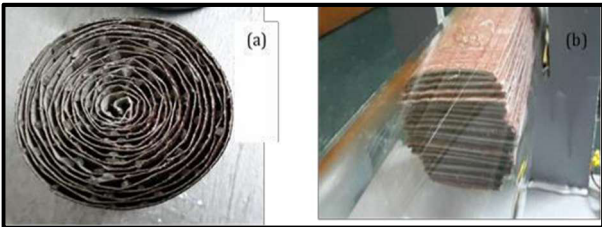
Fig. 5: Stack geometries (a) Spiral (b) Parallel plate
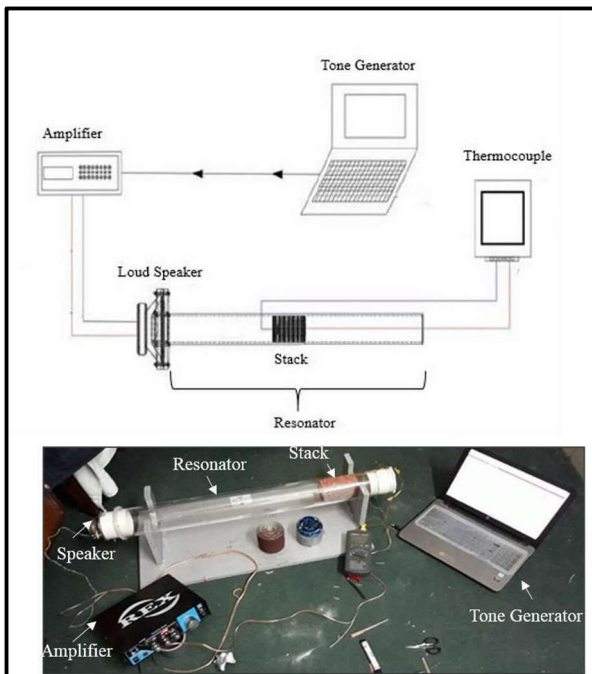
Fig. 6: Experimental Setup of Thermoacoustic refrigeration system

IV. CALCULATIONS

The resonance tube is closed at one end. The relation for the wavelength and tube length, during resonance, is given as

$$\lambda_n = \frac{4L}{n} \tag{1}$$

n=1,3,5,7…

λ_n are the nth harmonic wavelength and n shows the harmonic number, for fundamental wavelength, n=1. For periodic waves, the relation between velocity frequency and wavelength is given as

$$V = f\lambda \tag{2}$$

By putting equation (1) in (2) gives

$$f = \frac{V\,n}{4L} \tag{3}$$

In this case v=344m/s , L=90cm, n=1 for fundamental harmonic. The fundamental frequency comes to be f=96 Hz.
Thermal penetration depth is given as

$$\delta_t = \sqrt{\frac{K_a}{\pi f \rho C_p}} \tag{4}$$

Where K_a is the thermal conductivity of air, ρ is the density of air and C_p is the specific heat of air. Putting the values in the equation gives the thermal penetration depth to be δ_t=0.27mm. The thermal penetration depth is the distance that heat can diffuse in one time period. It's the thermal penetration depth which decides the optimum spacing s between the stack layers. It is four times the thermal penetration depth and is given as

$$s=4\,\delta_t \tag{5}$$

14

The optimal spacing comes to be s=1.08mm. It is evident that higher frequency is required in order to achieve higher efficiency and smaller unit size. However, for increase in frequency, stack of small size is required, which become expensive, and difficult to manufacture. In this work, stack length was chosen to be 8cm. Also, the position of the stack is very important. The best position for the stack is to place it near pressure antinode.

V.   RESULTS AND DISCUSSION

Table 1 shows the effect of changing the stack position upon the temperature difference between the two sides of the stack. However, in this case, the resonance frequency was kept constant to the fundamental frequency and the stack material used was polypropylene sheets and the stack geometry was spiral.

Table 1: Stack position and corresponding temperature difference for polypropylene stack having spiral shape

Stack position (cm)	Temperature difference ΔT (∘C)
8	2 . 8
16	1 . 7
24	2 . 2

When the stack was made of Gasket material, the change in temperature obtained is shown in Table 2.

Table 2: Stack position and corresponding temperature difference for stack made of gasket material having parallel plate shape

Stack position x_s (cm)	Temperature difference ΔT(∘C)
10	2
8	3
6	2

When the stack shape was a parallel plate, made of sandpaper, the change in temperature obtained is shown in Table 3.

Table 3: Stack position and corresponding temperature difference for stack made of sandpaper having spiral shape x_s

Stack position (cm)	Temperature difference ΔT (∘C)
10	3
8	4
6	3

The experimental study was performed to investigate the effect of stack material and geometry on the cooling load of system. Highest temperature difference is achieved for the spiral stack geometry made of polypropylene. This increase in temperature difference obtain for polypropylene stack is due to low thermal conductivity of polypropylene. Thus the stack material having lower thermal conductivity yield greater change in temperature.

REFERENCES

[1] https://www.esrl.noaa.gov/gmd/aggi/
[2]   http://www.acs.psu.edu/drussell/Demos/StandingWaves/StandingWaves.html
[3] Jin Shyong Lin, S.H.C., Ker Jer Huang, Chien Wan Hun, Chien Chon Chen, Challenges to Fabricate Large Size-

Controllable Submicron-Structured Anodic- Aluminum-Oxide Film. Atlas Journal of Materials Science 2015.

[4] Jinshah, B.S., Ajith Krishnan, R. and Eep, V.S., 2013. Study on A Standing Wave Thermoacoustic Refrigerator Made of Readily Available Materials.

[5] Rott, N., 1969. Damped and thermally driven acoustic oscillations in wide and narrow tubes. *Zeitschrift für angewandte Mathematik und Physik ZAMP*, *20*(2), pp.230-243.

[6] Swift, G.W., 1988. Thermoacoustic engines. *The Journal of the Acoustical Society of America*, *84*(4), pp.1145-1180.

[7] Nayak, B.R., Pundarika, G. and Arya, B., 2017. Influence of stack geometry on the performance of thermoacoustic refrigerator. *Sādhanā*, *42*(2), pp.223-230.

[8] Herman, C., Lavin, C. and Trávníček, Z., 2008, January. Performance of Thermoacoustic Refrigerators: Cooling

Load and Coefficient of Performance. In *ASME 2008 Heat Transfer Summer Conference collocated with the Fluids Engineering, Energy Sustainability, and 3rd Energy Nanotechnology Conferences* (pp. 755-760). American Society of Mechanical Engineers.

[9] Dhuley, R.C. and Atrey, M.D., 2016. Design Guidelines For a Thermoacoustic Refrigerator. *ArXiv preprint arXiv:1601.05149*.

[10] Atiqah Zolpakar, N., Mohd-Ghazali, N. and Ahmad, R., 2017. Optimization of the Stack Unit in Thermoacoustic Refrigerator. *Heat Transfer Engineering*, *38*(4), pp.431-437.

[11] Tijani, M.E.H., Zeegers, J.C.H. and De Waele, A.T.A.M., 2002. The optimal stack spacing for thermoacoustic refrigeration. *The Journal of the Acoustical Society of America*, *112*(1), pp.128-133.

Techno-Economic Feasibility Analysis of Optimal Hybrid Renewable Energy System for South Punjab Rural Area of Thal Canal

Muhammad Ali Aqdas Rehman Qazi[1, a], Saeed khan[2, b], Saba Zia[3, c], Muhammad Zunair Zamir[4, d]

[1]University College of Engineering Science and Technology (UCEST), Lahore Leads University
[2] Faculty of Electrical Engineering University College of Engineering Science and Technology (UCEST),
Lahore Leads University
[3] Ph.d * Scholar National University of Science and Technology
[4] Faculty of Electrical Engineering Riphah International University Faisalabad Campus

Email address: [a)] engr.aliaqdas@gmail.com, [b)] drmsaeedkhan@ucest.edu.pk [c)] saba.zia@ucest.com.pk
[d)] engineer.mzunairzamir@gmail.com

Abstract— Since more than a decade shortage of electricity in rural areas of Pakistan is a main issue of concern. This kind of problem can be eliminated by prompting optimal hybrid combination of renewable energy systems along-with existing infrastructure for utilization of power supply also present generation has proved to be expensive and unreliable. This combinational (solar, micro-hydro, grid connected, Diesel Generator and storage batteries) hybrid renewable energy systems are superior because they are less injurious to environment and least time consuming. This method is scalable and can be used in any test system. Different renewable hybrid Combinational Systems (DCS) will be implemented and comparison will be made in terms of COE and total production of electricity. The research tool HOMER (hybrid optimization models for electric renewable) software by NREL (national renewable energy laboratory) is used to perform techno- economic analyses for the hybrid renewable system. Moreover, sensitivity analysis will perform to get best suitable combination in terms of cost and resources, also evaluate the effect of uncertainty and improbability in the variables.

Keywords— Thal Canal, Feasibility Study, Renewable Energy, HOMER.

I. INTRODUCTION

Energy plays significant role for the economic and industrial growth of developing countries like Pakistan. Although there are a lot of natural renewable energy resources as like wind, solar and biogas which are present in Pakistan but still the country is facing worst energy crisis from past few decades. There is a huge gap of almost 5000 MW between generation and demand [1]. which becomes wider in summer season due to increment in load and we can expect that this gap will go on increasing in absence of proper energy utilization and generation policies. This situation has created an alarming condition. Country is facing worst load shedding of 10 to 18 hours per day [2].Overview of electricity generation from 2001 to 2011 in Pakistan is given in Table-1:

TABLE I. Electricity generation during 2001 to 2011

Generation Sources	Use in total Generation
Coal	0.09%
Oil	35.06%
Gas	27.34%
Hydro-Electric	33.61%
Nuclear	3.61%
Imported	0.28%

In 2014, Pakistan has energy usage of about 70.1 billion KWh, 38.6% were used by industry,43% for domestic, 16% for commercial, 1.6% for agriculture and 0.8% other miscellanies use [3].

The present energy scenario clearly indicates that there must be a reliable solution to fulfill the energy demands of this country is to maximize the use of renewable energy resources in our generation [4]. These resources are clean and always available and renewable energy resources must be developed to overcome the present energy shortfall [5].

Hybrids systems are gaining worldwide attention these days. Many researchers from different countries are working on these types of systems. S. Shezan., et.al proposed hybrid system including the components pv-wind-diesel-battery. The results confirmed that the cost of energy of the optimized system is about $0.209/kWh, the NPC of the optimized system is about $33,310.00 and the operating cost is $2,037/year [6]. A. N. Khan., et.al discussed techno-economic analysis and suggested three cases, standalone solar PV system, wind system and a hybrid combination of both centralized standalone solar and wind. COE of PV is 0.771/KWh, 0.4/KWh and lowest is 0.381/KWh [7]. M. Nurunnabi., et.al, Presented off-grid and on-grid models, results showed that grid connected PV/Wind system is more efficient and economical as compared to PV/Wind/Battery for the same load of off-grid model [8]. J. B. Fulzele., et.al carried out sensitivity analysis in terms resources. By varying the resources, the COE is $0.503/KWh and Without considering of sensitive variables the cost of energy is slightly inclined $0.550/KWh [9].

R. H. Kumar et.al Suggested feasibility study of PV-Biomass Generator, 69% of electricity was supplied through PV modules and remaining through biomass generator and optimum cost of energy is USD 0.186/KWh. Emission of gases percentage is slightly higher and need to be minimized for future sustainability [10]. M. M. Rahman et.al Techno-economic assessment of a stand- alone off-grid solar Photovoltaic system COE $0.72. Sensitive analysis was conducted and suggested that interest rate, life time and cost of the battery has direction relation with cost of the energy [11]. Ali, A et.al described the renewable energy hybrid system of pv/wind/biomass and battery. Three scenarios, when only grid is supplying to load, when maximum share of hybrid system delivering to load, when storage capacity is added. COE of energy is $0.099/KWh, $0.060/KWh and $0.067/KWh [12]. M. R. B. Khan et. al made techno-economic analysis along-with seasonal assessment of load and availability of renewable energy. The outcome specifies that hydro-diesel-battery system is the most optimal hybrid system followed by Pv-diesel-battery system based on the current energy situation [13].

II. TOPOGRAPHY OF THE LOCATION

The proposed location Layyah has been selected, which is one of the rural areas of Thal Canal. It is one the district in the Punjab and positioned in the southern part of the province. The weather is hot and most of the area is desert. Geographically it lies between 30°58'N latitude, 71° 06'E. The elevation is 148 meters height [14].

A. Estimation of Available Energy Resources

The zone under investigation, Solar radiations are present in the official NASA surface meteorology website. It is important to mention here that values of the available resources of the NASA are accepted all over the world. The valuable data for hydro resources is taken from Punjab Irrigation Department (PID). The selected period of the data is taken from October 2016 to September 2017.

B. Solar Energy

Solar radiation profile of selected area over last one-year started from October 2016-September

2017. The maximum radiation is in the month of June and least in December i-e 6.74 KWh/m²/day and 2.1 KWh/m²/day. Middle months of the year have moderate radiations. The annual average radiation 4.42 KWh/m²/day, clearness index value remains between 0.5 to 0.6. The solar radiation is quite pleasant in chosen area. The average annual temperature is 24.07°C which quite moderate. [15].
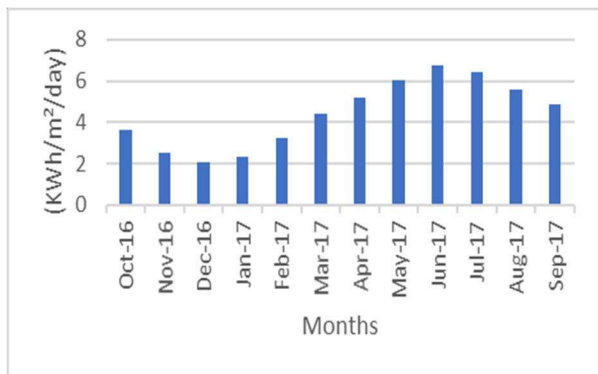
Fig. 1. Annual average solar radiation

C. Hydro Resources

Thal Canal one the most water carrying canal is lower Punjab, Pakistan. It feeds water to many branches and distributaries. Indus branch, solitary branch of Thal Canal and Layyah Distributary is taken out from it. The detailed information of Layyah distributary is given in Table-II.

TABLE II: DETAILED INFORMATION OF

LAYYAH DISTRIBUTARY

Parent channel	Indus Branch
Sub Division	Bhagal
Channel Type	Distributary
Circle	Thal
Section	Bhagal
Flow type	Perennial
Division	Layyah
Authorized Head discharge	233.00 Cc
Remarks	Layyah distributary is first preference

Fig. 2. shows the discharge rate of Layyah Distributary. The data under consideration is from October 2016-September 2017. The maximum discharge rate in the months of May to September, moderate February to April and minimum in January [16].
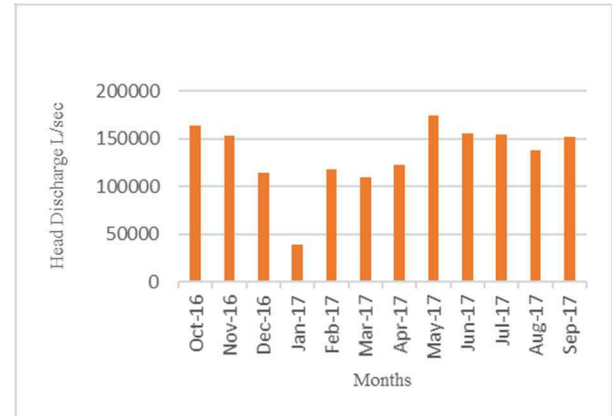
Fig. 2. Annual Average Head Discharge Liter per second

III. ELECTRIC LOAD DEMAND PROFILE

The electrical energy supplied from combinational hybrid renewable energy system is broadly characterized in two subdivisions, domestic and commercial users. Domestically, it is characterized in such a manner that the village consists of 57 rich families, 82 medium income families, 107 low and very poor income families, sum up with total 246 houses. It has 25 stores, 5 banks, 7 primary and secondary schools. The load demand in Summer Season is 1457.395 KWh/day which reduces in Winters and become 972.85 KWh/day but to address stochastic variations of the load, a random variability of 4% (hourly) and 3% (daily) is added [17].

$$\alpha = 1 + \varsigma_d + \varsigma_t$$

A. *Summary Load*
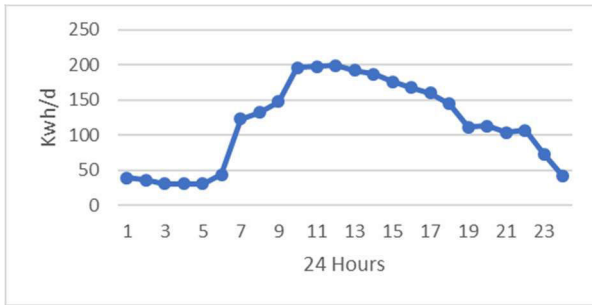
Fig. 3. Summer Season total load of 24-Hours

The above curve shows the load of both domestic and commercial users of summer season. The minimum load at 01:00-02:00am is 36.2 KWh which increases at 05:00-06:00am 44 KWh. At 06:00-07:00am the load incline dramatically to 122.9 KWh, on word it keeps inclination. The highest peak is achieved at 11:00 am besides load is 198.51 KWh. The load goes down to 111.8 KWh at 17:00-18:00 onward it steeply drops to 41.5 KWh at 23:00.

B. *Winter Load*

The load of both domestic and commercial users of Winter Season. The minimum load is at 02:00-04:00 am which is 14.37 KWh. The vividly raise in load starts at 06:00-09:00am and acquire a rising peak of 97.5 KWh and continue till 124.155 KWh at 12:00-13:00. Onward it gradually dejected.
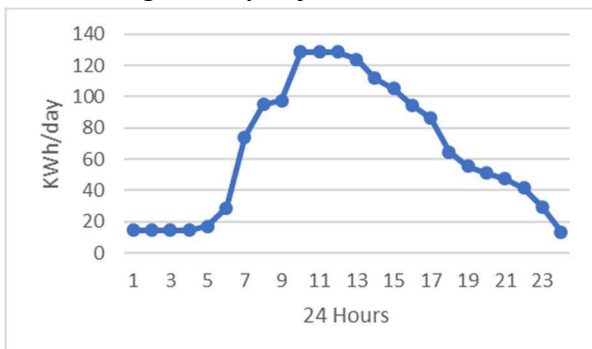
Fig. 4. Winter Season total load of 24-Hours

C. *Comparison of Summer and Winter Load*

The below Fig. 5. shows the comparison graph of Summer and Winter season. It reflects significant variation of load demand in both seasons. The pattern of rising and dropping of line graph is similar but the wattage utilized in described seasons are momentously different. It is because appliances used in summer season having high wattage and their time of uses are large.
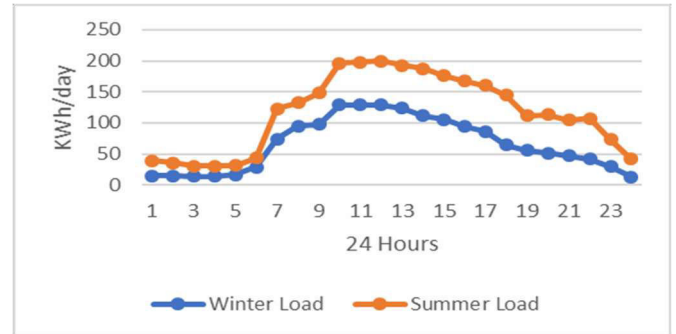
Fig. 5. Load comparison of Summer and Winter Season

IV. COMBINATIONAL HYBRID SYSTEM AND COMPONENT COST

A. *Combinational Hybrid Scenario*

The simulation work consists of five different scenarios that are taken into consideration. The below Table. 3 shows the combinations of considered scenarios.

Table iii. Different combinational scenarios

Scenario	Considered Combinational Scenario
Scenario I	Diesel Generator, Grid, Batteries
Scenario II	Grid, PV System, Micro-Hydro
Scenario III	Micro-Hydro, Diesel Generator, Grid
Scenario IV	Micro-Hydro, PV System, Batteries
Scenario V	PV System, Diesel Generator, Batteries, Grid

These different scenarios are simulated to get minimum Cost of Energy and least Net Present Cost. Sensitive Analysis also be taken in to consideration for most suitable scenario.

B. Cost of Component

The cost of components is main area of concern. The key parameters taken into consideration are capital cost, Replacement cost and O & M cost. They are depending upon unit size and international market values of brands.

TABLE IV. Input data on option cost

Option	Capital cost	Replacement cost	O & M cost
Micro-Hydro ($)	83,520	18,600	800
Solar	1,600	1,600	100
Diesel Generator	31,480	28350	0.30/hr
Battery	1,200	1,200	0
Converter	300	300	0
Grid Extension	300	300	10/yr

C. PV Module

The *PV* output majorly depends on the available solar radiation, the lesser the solar radiation the lesser the *PV* output. Generic Flat Plate PV, manufactured by Generic is used [18].

TABLE V. PV module cost and information

Description	Cost/Information
Capital cost ($)	1600 per KW
Replacement cost ($)	1600 per KW
O & M cost ($)	100/year
Life time(year)	25
De-rating Factor	80%
Panel azimuth angle	232.8
Slope	39.4degree
PV Tracking system	No Tracking

D. Diesel Generator

Perkins Diesel Generator is chosen. Diesel price affects by continuous varying of Dollar rate in local market. The fuel price fluctuates between $0.75 to $0.90. The selected price for simulation is taken $ 0.85/liter [19].

Table VI. Diesel generator cost and information

Description	Cost/Information
Capital cost ($)	31,480
Replacement cost ($)	28,000
O & M cost ($)	0.5/hour
Lifetime (Operating hour)	20,000

E. Battery Storage

The Surrette 6CS25P batteries by Rolls Battery Engineering was simulated as part of hybrid system. The batteries are connected in series forming a string and he strings are connected in parallel forming a battery bank [20].

TABLE VII. Storage battery cost and information

Description	Cost/Information
Capital cost ($)	1,200
Replacement cost ($)	1,200
O & M cost ($)	15/year
Life time(year)	15

F. Micro-Hydro

The below TABLE VIII shows the properties of Micro-hydro [21].

Table VIII. Properties of micro- hydro

Properties of Micro-Hydro	
Capital cost ($)	83,520
Replacement cost ($)	18,600
O & M cost($/year)	800
Size (Kw)	98
Lifetime(year)	25
Available Head (m)	8
Design Flow rate (L/s)	1050
Minimum flow ratio (%)	90
Maximum flow ratio (%)	120

Efficiency (%)	75
Pipe head loss (%)	7

G. Convertor and Inverter

As the hybrid energy system has AC as well as DC sources of energy so Converter is required to convert AC power to DC and inverter will invert DC power to AC. The is due to the fact PV plant and batteries output is DC while load requires AC power [22].

TABLE IX. Convertor cost and information

Description	Cost/Information
Capital cost ($)	260
Replacement cost ($)	260
O & M cost ($)	0
Life time(year)	15
Efficiency (%)	95

H. Current Tariff Plan

MEPCO (Multan Electric Supply Company) provides electricity to the selected location. They have tariff of $ 0.131/KWh on peak hours rates. Grid is used as power supplier and excess power absorber [23].

I. System Economics

The average values of nominal interest rate, inflation rate is 12.51% and 8.03% which means that annual real interest rate is 4.18%. The project life time is 25 years [12].

V. ECONOMICS ANALYSIS

It would be relatable that economic analysis should be made while trying and attempting to optimize the size of combination hybrid renewable energy generation systems which is favorable and an affordable unit price of power produced. The economical approach is developed to be the best indicator of economic profitability of system cost analysis in this study.

A. Total System Annualized Cost

Total system annual cost includes annual replacement cost A_{RPC}), annual operation & maintenance cost (A_{OMC}), annual fuel cost (A_{FUC})and annual miscellaneous cost A_{MLC}). The miscellaneous cost includes salaries of higher officials, junior stuffs and taxes [24].

$$C_{Tsac} = A_{RPC} + A_{OMC} + A_{FUC} + A_{MLC} \qquad (2)$$

B. Annualized Capital Cost

Annualized Capital Cost A_{cpc}) of each system component consists of component price, the cost of civil work and installation cost.

$$A_{cpc} = [\sum Solar_{pv} * \sum Unit_{pv}] + [\sum \mu.hydro * \sum unit_{,uh}] + [\sum Battery * \sum unit_{,b}] + [\sum Inverter * \sum unit_{,Inv}] + [\sum D.Gen * \sum unit_{,DG}] + C_o \qquad (3)$$

Where C_o is a cost of civil work and installation [25].

C. Annual Operation and Maintenance Cost

It can be represented as a function of capital cost and reliability of components. It is oblivious that more reliable component needs less attention. But as the reliability of a component escalate, its cost will also increase. So, there is a mutual consideration between the capital cost and reliability.

$$A_{OMC} = \frac{1-\lambda}{y} \qquad (4)$$

Where λ reliability factor of the system component.

The components involve in that system includes repairing, maintenance and other charges to operate the system and can be expressed as

$$Compoments_{MRPC} = R_{RC} M_{MC} \qquad (5)$$

Where R_{RC} and M_{MC} is the hourly, weekly or monthly repairing and maintenance cost of the components.

D. Annual Replacement Cost

Annual Replacement Cost A_{RPC}) is the annual value of replacing expenditure of components during the project lifetime. Since the lifetime of the other components are equal to the lifetime of the project (chosen as 25 years), Batteries are needed to be replaced in this case and for generator, lifetime is the number of running hours.

$$A_{RPC} = C_{rep}S_{FF}(i, x_n) \qquad (6)$$

Where C_{rep} is the replacement cost. So, it can easily be understood that the replacement cost of the component is nothing but its capital cost. S_{FF} is the Sinking Fund Factor
The lifetime (number of years) of a generator can be calculated as

$$N_{gen,1} = \frac{N_{gen,Lt}}{N_{gen,h}} \qquad (7)$$

$N_{gen,Lt}$ is generator lifetime.
$N_{gen,Lt}$ is the number of hours operating during one year [26].

E. Fuel Cost of Diesel Generator

Hourly fuel consumption based on the load characteristics of the diesel generators. It can be calculated by equation:

$$F(fhr) = (0.246 * P_{DG}(t) + 0.08415 * P_r) \qquad (8)$$

$F(fhr)$ Fuel cost per litter ($)
(P_r) Rated capacity of the diesel generator (kW)
$P_{DG}(t)$ Power generated by the DG (kW) [27].

F. Grid Purchase and Sale Amount

The total amount of electricity purchased from the grid.

$$E_{gp} = \sum_0^{8760} P_{gp} \qquad (9)$$

The total price of electricity purchased from the grid.

$$C_{gp} = E_{gp} C_g^p \qquad (10)$$

C_g^p Unit cost of electricity ($/kwh) or (Rs/kwh) purchased from the grid.
P_{gp} Maximum grid purchase capacity.
The total amount of electricity supply to grid.

$$E_{gp} = \sum_0^{8760} P_{gs} \qquad (11)$$

The total price of electricity sells to grid.

$$C_{gs} = E_{gs} C_g^s \qquad (12)$$

C_g^s Unit cost of electricity ($/kwh) or (Rs/kwh) sold to grid.
P_{gs} Maximum grid sold capacity [25].

G. Capital Recovery Factor (CRF)

CRF is the capital recovery factor defined as the ratio to calculate the present value of a series of equal annual cash flow.

$$CRF(i, n) = \frac{i(1+i)^n}{(1+i)^n - 1} \qquad (13)$$

n The project life time and i annual interest rate.

H. Annual Real Interest Rate

Annual Interest real rate consists of nominal interest rate i_{LOAN} (the rate at which a loan can be obtained) and annual inflation rate, F, by the equation [28]

$$i = \frac{i_{LOAN} - F}{1 + F} \qquad (14)$$

VI. SIMULATION TOOL

Hybrid Optimization Model for Electric Renewable (HOMER) is software developed by the National Renewable

Energy Laboratory (NREL). Already used in many renewable energy studies in order to simulate supply systems configurations and also allowing technical and economical scenarios to be tested. The basic representation of this software is shown in given Fig. 6. [29], [30].
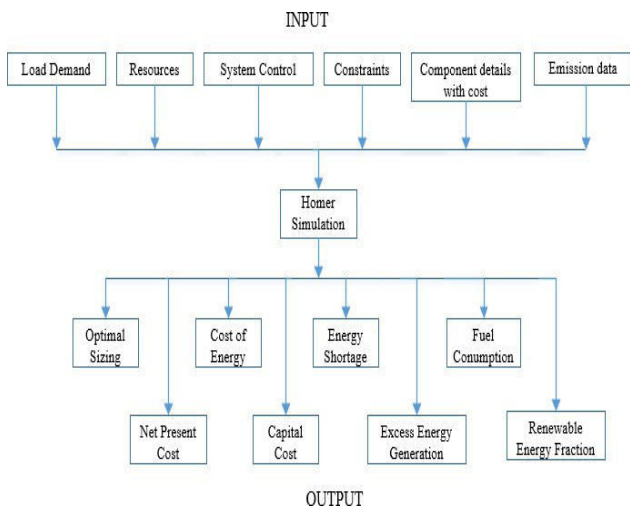
Fig. 6. Homer basic working principle

VII. RESULT AND DISCUSSION

In this section, five different combinational scenarios are constructed in order to determine the most favorable option in terms of cost and recovery of net present cost. In Scenario I, Grid is connected and electric power is being supplied with Diesel Generator and for backup, Batteries are connected. In Scenario II, Micro-Hydro which has incredible resources in selected area is combination with PV System and Grid. In Scenario III, previous combination of Micro-hydro and grid is taken in to consideration and Diesel Generator is used in order to magnify the variation in cost of energy. In Scenario IV, the cost is increased

because large number of batteries are used. Scenario V, PV Panels and Diesel Generator made the net present cost high.

In comparison, the scenarios are compared through cost of energy, production of electricity from different components and Payback duration of Net Present Cost (NPC).

A. Production of Electricity from Diesel Generator
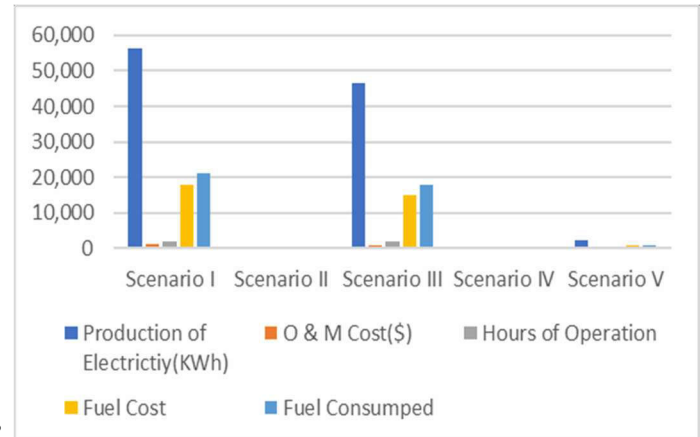
B.

Fig. 7. Electricity production and cost comparison

In first and third scenario, production of electricity mainly depends upon Diesel Generator. They produce 56,453KWh in scenario I and 46,411KWh in scenario II. There direct impact prolongs the working operational hours and fuel consumption.

C. Electricity Purchased and Sold to Grid

Fig. 8. Describes that in scenario I, energy 4,75,796 KWh is purchased from grid and not a single unit is sold to grid. Scenario II and Scenario III, 6,92,081 KWh and 4,49,991KWh is sold to grid which reduces the cost of energy. In Scenario V, 1,86,850 KWh purchased and 3,36,054 KWh is sold.

D. Production of Electricity from Solar PV

The unit size of PV in Scenario V is 504 KW, which incline the Capital cost. Scenario II

uses 218KW, the capital cost reduce significantly also reduces production of electricity kilowatt hour per year. The hours of operation in all the scenario is taken as 4381 hours/year.

Fig. 8. Energy Purchase and Sale by Grid
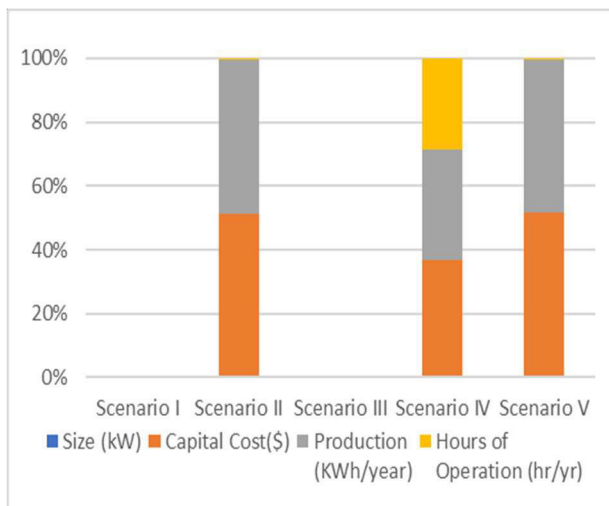
Fig. 9. Unit sizing, Cost and Production of Electricity

E. Production of Electricity from Micro-Hydro
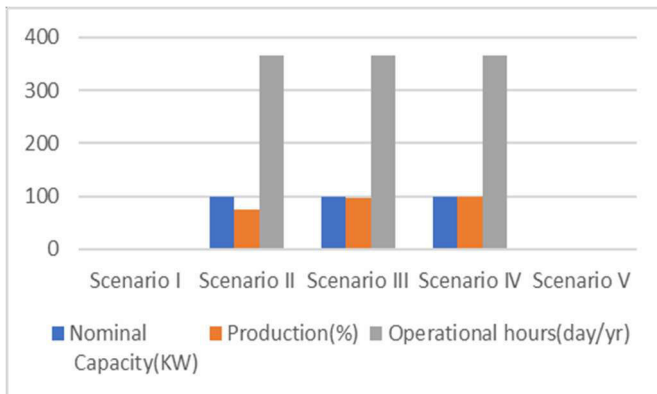
Fig. 10. Production of Electricity from Micro-hydro

In the Fig. 10. the Nominal Capacity of Micro-Hydro is taken as 98.9 KW and Optional hours are 8760 hours/yr. The production of electricity in Scenario II, Scenario III and Scenario IV is 74.2%,95.3% and 99.4%.

F. Production of Electricity

Electricity Production in Scenario II is maximum 1260MWh, slightly less in Scenario III, Scenario IV and minimum in Scenario I which is 532MWh. Excess electricity is produced Scenario IV which needs extra storage or can sale to grid.
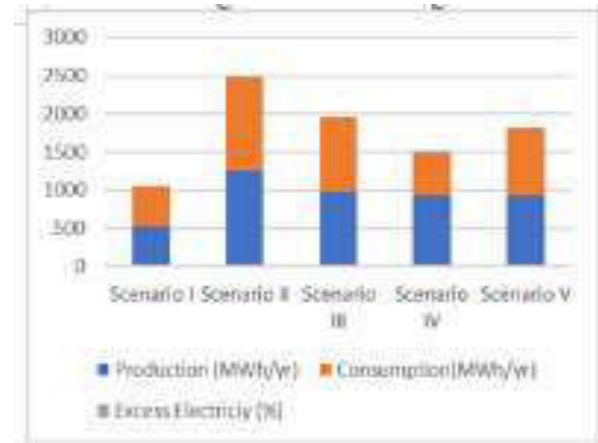
Fig. 11. Production and Consumption of electricity of all Scenario

G. Emissions Analysis

Different types of pollutants (CO_2, CO, SO_2, NO_x) are emitted during the combustion of fossil fuel to produce electricity. The combustion of diesel is the only source of operational emissions. The below figure shows that Scenario-I and Sensitive Scenario-III emits extreme emissions to environment. Emission factors are based on the diesel properties that are shown in Table IX. [27]:
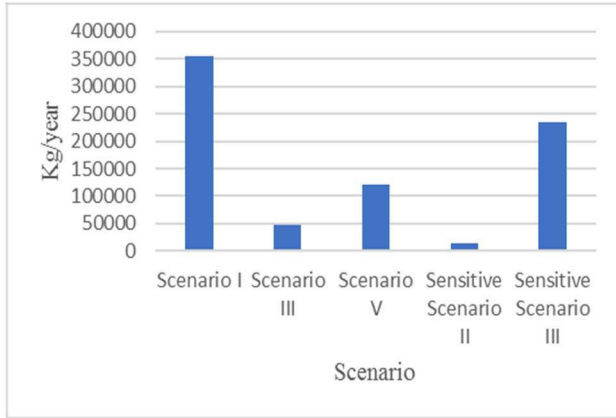
Fig. 12. Emissions analysis

Table X. Diesel properties

Property	Value
Low heating value	43.3 MJ/Kg
Density	820 kg/m3
Carbon content	88%
Sulfur content	0.33%

VIII. SENSITIVITY ANALYSIS

This analysis is taken into consideration for the selection of best optimal combination in worst case scenario. In this analysis the cost of equipment will increase to 30% and resources will decrease to 30% and determine the cost of energy.

table XI. Sensitive component cost analysis

Cost of Compo n ent	Micro - Hydro	Solar	Conver t or	Diesel Gener a tor
Capital cost ($)	$1085 76	$2080	$338	$40924
Replace ment cost ($)	$8450 0	$2080	$338	$36830
O & M cost	1950 $/yr	130 $/yr	20 $/yr	0.65 $/hr

The Diesel price is increased and considered as $1.11. Other constraints such as annual interest rate and inflation rate has increased to 8.45% and 5.44%. Stochastic variations of

load in daily and hourly also increased to 5.2% and 3.9% respectfully.

Average annual solar radiation cuts to 3.09 KWh/m²/day from 4.42 KWh/m²/day. Average annual temperature goes down to 16.85 °C and annual average Head discharge rate become 93004.4 L/s.

A. Sensitive Analysis of Scenario II and Scenario III

The below TABLE XII. defines unit sizing of components of scenario II and scenario III.

Table XII. System architecture and unit sizing

System Architectu re	Scenario II	Scenario III
Diesel Generato r (kw)	NA	105
Grid (kw)	100	100
Batteries	NA	NA
Converter (kw)	317	NA
Micro-Hydro (kw)	70	70
PV (MW)	1.62	NA

Table XIII. Cost analysis of scenario ii and scenario iii

Items	Scenario II	Scenario III
COE($)	0.121	0.0618
NPC($)	7.02 M	2.36M
Operating cost($/year)	85,513	54,684
Initial Capital Cost($)	3.61 M	172,900
Fuel Cost($/year)	NA	52,191

The above TABLE XIII. shows the variation of cost in both scenarios. Initial and Net Present Cost have considerable difference, which affects Cost of energy.
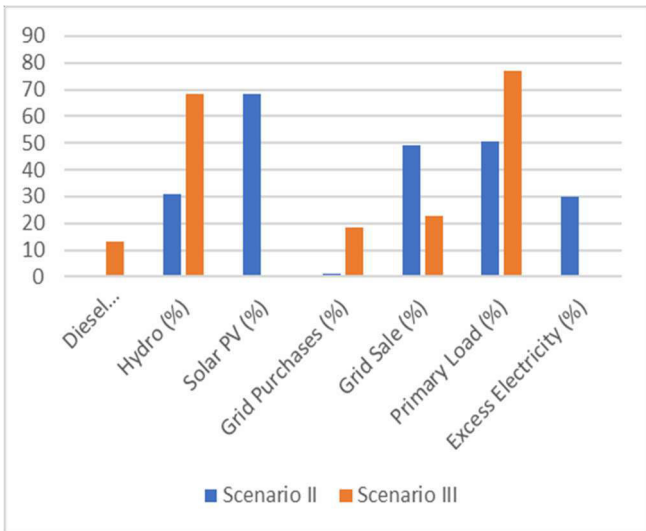
Fig. 13. Comparison of Scenario II and Scenario III

The Fig. 13 shows the involvement of components used in Scenario II and Scenario III. The Diesel Generator, Micro-hydro involvement for the production of electricity in Scenario III is greater than scenario II. Electricity purchased and sale to the Grid has not much alteration.

In Scenario II, Production of electricity from Micro-hydro is quite less than Scenario III but utilization from Solar PV is maximum. Electricity sale to Grid is hefty than the purchasing.

IX. PAY BACK PERIOD OF NET PRESENT COST
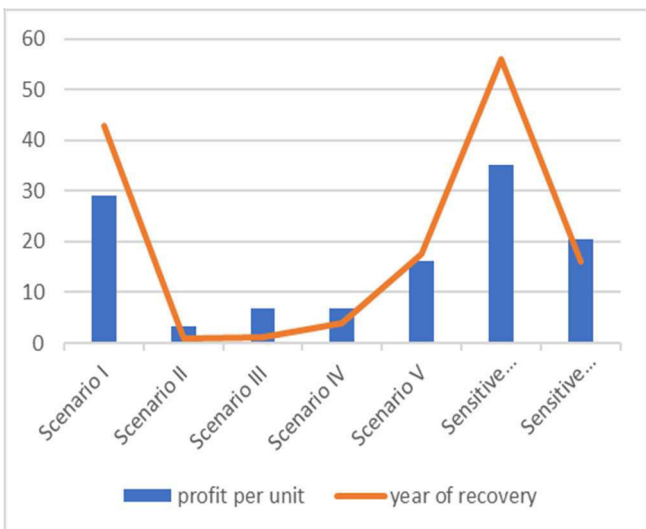
Fig. 14. Recovery Period of Net Present cost

The Fig. 14. defines that line drawn above the peak show years of recovery of Net Present Cost. Which directly relates the profit on Cost of Energy. Higher the profit rate sooner will be recovery period. Scenario II, III and IV has least cost of energy, lesser Net present cost and profit per unit is moderate. So, their payback period will not exceed from one year to four years. Scenario I and Sensitive Scenario IV would take maximum years.

X. CONCLUSION

In Scenario I, Net present cost is very high, which seriously effects cost of energy. Capital Recovery duration is being prolonged and Not a single unit being sold to grid. Scenario II, Maximum energy is produced from micro-hydro because of supreme resources are available. Their participation is about 74.2%. Total electric power of 56.5% to be sold to grid. Which reduces the cost of energy per kilo-watt. Net present is very less as compare to first scenario. Capital Recovery duration is reduced to almost one and half year. Scenario III, not a single unit is being purchased from gird. Micro-Hydro participation is 95.3%. and total electric power of 45.8% is to be sold to grid. The fuel consumption is 1.18% less than the first scenario. Net present cost is less than first scenario but slightly higher than the second. Capital Recovery duration is one year and two months.

In Scenario IV, Production from solar is reduced drastically 61.3% as compare to second scenario. Net present cost is slightly higher than the third combination. Capital Recovery duration touches the four year. Scenario V, Maximum energy is produced from PV system their participation is about 79.9 %. 19.9 % is purchased from grid. Net present cost is high which seriously affect the capital recovery duration.

27

For sensitive Analysis Scenario II, Results reflects that reducing the resources, increasing in unit price per kilowatt. The capital cost increased to 2.76% from the second scenario. These changes affected seriously on system overall cost and increase the payback period.

For sensitive Analysis Scenario III, it reflects that DG consumption increased to 13.1 % and Micro-hydro decreased 68.5%. The system Net present cast increased to 6.8% which directly enhances the per unit cost and capital recovery factor.

REFERENCE

[1] W. Aslam, M. Soban, F. Akhtar, and N. A. Zaffar, "Smart meters for industrial energy conservation and efficiency optimization in Pakistan: Scope, technology and applications," *Renewable and Sustainable Energy Reviews,* vol. 44, pp. 933-943, 2015.

[2] M. Farooq and A. Shakoor, "Severe energy crises and solar thermal energy as a viable option for Pakistan," *Journal of Renewable and Sustainable Energy,* vol. 5, p. 013104, 2013.

[3] "Pakistan:Energy Sector Appraisal Report", Paper prepared by Sustainable and developmentpolicyInstitute(SDPI),2013:pp.1- 24.

[4] Nayyar, Z.A., N.A. Zaigham, and A. Qadeer, *Assessment of present conventional and non-conventional energy scenario of Pakistan.* Renewable and Sustainable Energy Reviews, 2014. 31: p. 543-553.

[5] Khalil, H.B. and S.J.H. Zaidi, *Energy crisis and potential of solar energy in Pakistan.* Renewable and Sustainable Energy Reviews, 2014. 31: p. 194-201.

[6] S . Shezan, N. Das, and H. Mahmudul, "Techno-economic analysis of a smart-grid hybrid renewable energy system for Brisbane of Australia," *Energy Procedia,* vol. 110, pp. 340-345, 2017.

[7] A. N. Khan, P. Akhter, and G. Mufti, "Techno-Economic Evaluation of the Centralized Hybrid Renewable Energy Systems for Off-Grid Rural Electrification," 2016.

[8] M. Nurunnabi and N. Roy, "Grid connected hybrid power system design using HOMER," in *Advances in Electrical Engineering (ICAEE), 2015 International Conference on*, 2015, pp. 18-21.

[9] J. B. Fulzele and M. Daigavane, "Optimization of PV-wind hybrid renewable energy system for rural electrification," in *Emerging Trends in Engineering and Technology (ICETET), 2015 7th International Conference on*, 2015, pp. 101-105.

[10] R. H. Kumar, "Feasibility study of photovoltaic (PV) modules, and biomass generator to supply electricity to Auckland City, North Island Context-New Zealand," *J Clean Energy Technol,* vol. 2, pp. 374-378, 2014.

[11] M. M. Rahman, A. S. Islam, S. Salehin, and M. A. Al-Matin, "Development of a Model for Techno-economic Assessment of a Stand-alone Off-grid Solar Photovoltaic System in Bangladesh," *International Journal of Renewable Energy Research (IJRER),* vol. 6, pp. 140-149, 2016.

[12] A. Ali, M. Amjad, A. Mehmood, U. Asim, and A. Abid, "Cost effective power generation using renewable energy based hybrid system for Chakwal, Pakistan," *Science International,* vol. 27, pp. 6017-6022, 2015.

[13] M. R. B. Khan, R. Jidin, J. Pasupuleti, and S. A. Shaaya, "Optimal combinations of PV, wind, micro-hydro and diesel systems for a seasonal load demand," in *Power and Energy (PECon), 2014 IEEE International Conference on*, 2014, pp. 171-176.

[14] http://layyahonline.net/Union-Council-wise-Information-Layyah/Union-Council-Wise-Information-about-Layyah.html

[15] Online data Access from "NASA Surface meteorology and Solar Energy: HOMER Data

[16] irrigation.punjab.gov.pk/

[17] Abbas, Muhammad Khurum. "Economic power generation for an off-grid site in Pakistan." *Power Generation System and Renewable Energy Technologies (PGSRET), 2015.* IEEE, 2015.

[18] Solar Panel Prices have checked from solar panel store (SPS) & Q-cell Company from its Official websites.

[19] Perkins Diesel Generator price list are avaibale online & its conparsion with other Generator prices are also given; Generator are Chine Made;2016

[20] Battery Storage prices can be checked from Trojan Company site, Manufactured in USA.

[21] Turbine price checked from smart Hydro Power (GmbH) company, Manufactured in Germany.

[22] Inverter & Charge Controller Prices can be Checked from Voltronics Company Official Site.

[23] www.mepco.com.pk

[24] R. Khare and Y. Kumar, "Techno economic analysis for PV-wind-DG-battery IHRES with SGA," in *Power India International Conference (PIICON), 2014 6th IEEE*, 2014, pp. 1-6.

[25] S. Singh and S. C. Kaushik, "Optimal sizing of grid integrated hybrid PV-biomass energy system using artificial bee colony algorithm," *IET Renewable Power Generation,* vol. 10, pp. 642-650, 2016.

[26] R. Khare and Y. Kumar, "Techno economic analysis for PV-wind-DG-battery IHRES with SGA," in *Power India International Conference (PIICON), 2014 6th IEEE*, 2014, pp. 1-6.

[27] S. Arun, S. Kumaravel, and M. Selvan, "Unit size optimization of hybrid energy system," in *Innovative Smart Grid Technologies-Asia (ISGT Asia), 2014 IEEE*, 2014, pp. 79-83.

[28] M. Nurunnabi and N. Roy, "Grid connected hybrid power system design using HOMER," in *Advances in Electrical Engineering (ICAEE), 2015 International Conference on*, 2015, pp. 18-21.

[29] M. D. Al-Falahi, S. Jayasinghe, and H. Enshaei, "A review on recent size optimization methodologies for standalone solar and wind hybrid renewable energy system," *Energy conversion and management,* vol. 143, pp. 252-274, 2017.

[30] J. L. Bernal-Agustín and R. Dufo-Lopez, "Simulation and optimization of stand-alone hybrid renewable energy systems," Renewable and Sustainable Energy Reviews, vol. 13, pp. 2111-2118, 2009.

Review of Net Metering Techniques for Low Income Communities

Muhammad Shoaib Khan[1, a], Mohammad Adil[2, b]
[1]Researcher, Department of Civil Engineering UET Peshawar
[2]Assistant Professor, Department of Civil Engineering UET Peshawar

Email address: [a] 15pwciv4320@uetpeshawar.edu.pk , [b] adil@uetpeshawar.edu.pk

Abstract: Many countries are using net metering techniques as an energy resource and their public are taking benefits from it but in Pakistan financial, social and unawareness with technology are barriers for implementation. Although Pakistan is one of the most power crisis struck country but average income per capita is 148 USD per month which is very less and they cannot afford such techniques, only a small percentage and relatively rich group of population is using this facility. The importance of Distributed Generation is increasing continuously because electricity generation from other centralized facility like fossil fuel plants have negative impact on environment. In this paper a review on net metering techniques has been studied. It can be seen that Pakistan has high solar irradiance with an average of 4.5 to 5 kWh/m² per day and solar energy can be used as a source through net metering technique which can reduce demands on centralized facility and resolve electricity shortage problem of the country to a large extent.

I. INTRODUCTION

Researchers have identified that solar energy technologies are the feasible source of sustainable electricity production [13] and for this renewable energy techniques are getting popularity [14, 15]. Using fossil fuels plant for energy production has many negative impacts on environment and this has forced community to use an alternative that must be environmental friendly and to sustain increased energy loads. Energy production from solar is one of the renewable techniques having less negative impact on environment [10]. Renewable energy techniques has many advantageous while decreasing greenhouse gas emission, CSIRO are suggesting solar energy most efficient and effective [11] and their cost is also going toward declination [16]. New techniques are increasing for developing low cost PV cells [17].

Distributed Generation is one of the benefit of renewable technology which is decentralize generation and produce power from small sources. Most of the countries are producing power from centralized facilities such as fossil fuels, nuclear plants and hydropower plants but these plants are transmitting power over long distances and have negative impact on environment both locally and globally while on the other side distributed generation have less negative on environment. Benefits of DG for utilities, customers and also to the environment is highly loaded but studies shows that it has a lot of benefits to utility companies [17]. By using such techniques customer will become prosumers and will consume and produce power which will be connected to grid but excess power will feed into grid. To get benefit of this system utility will connect DG to available grids and interconnection, associated rights and responsibilities are managed through net metering agreements.

Net metering techniques can be used as a choice to get benefits of renewable energy techniques and distributed generation. Net metering has bring revolution in renewable energy techniques by running a meter backwards in which excess power is feed into electrical grids that can balance energy demand, manage loads and going toward clean, green and sustainable electricity production. Net metering is developed to encourage owners to install and link their renewable energy generators with grids and hence to develop distributed generation. It is a low cost program that will use customer investment for renewable energy techniques. If customer produce electricity from solar and connect it to the grid then its demand on centralized generation by utilities will be decreased and hence customer and utility companies will get benefits from net metering. Also it will reduce negative impact on environment [18] by converting source production to the renewable techniques which will also decrease carbon emissions [19]. Utility and solar power plant are connected in a two way power flow that will help to feed the excess energy to grid during abundant of sunlight or during least demand and will get power back from grid mostly at night when there is no excess power. So net metering will also reduce wastage of energy. Figure 1 shows net metering functional conventional system.

Figure 1, 2 shows working of net metering in which solar power which produce direct power must be integrated with inverter to convert into AC power to make it usable in houses etc. and during abundant sunlight, excess power generation will be feed into grids which can be measured through two way meter.
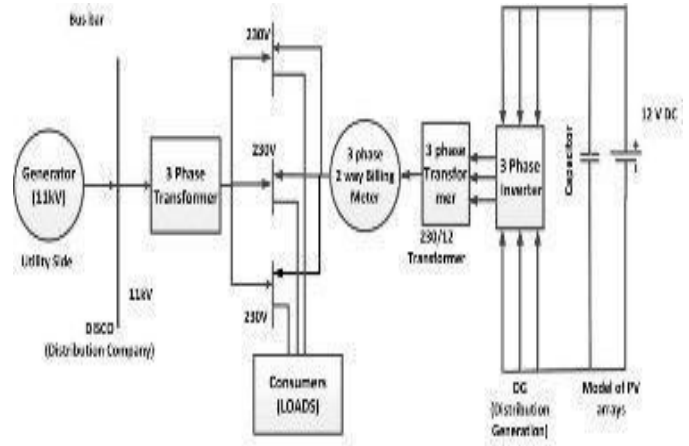
Figure 1. Two Way Net Metering [20]
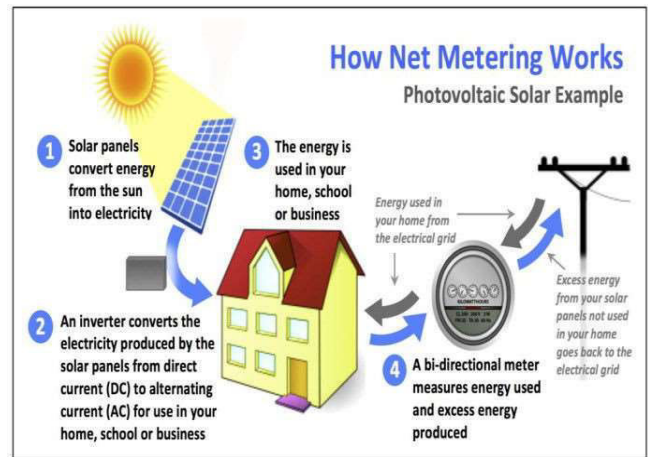
Figure 2. Working of Net Metering [20]

II. BACKGROUND

In 1983, the concept of net metering is developed in United State of America in which small scale solar panels and wind turbines are installed and connected with grids [1]. It has been adopted in different countries in the world like Canada, Italy, Japan, Denmark, Germany etc. In renewable energy technology production from solar energy has got second highest annual growth rate of 28% [7]. In 2008 over 6GW of solar thermal power are announced by different countries [8] and solar technology is increased from 2009 to double in

Table 1. 10 COUNTRIES USING SOLAR ENERGY

S.No	Country Name	Installation in 2017 (GW)	Total Installed Capacity (GW)
1	China	53	131
2	USA	10.6	51
3	Japan	9.1	49
4	Germany	7	42
5	Italy	2.6	19.7
6	India	1.8	18.3
7	UK	1.25	12.7
8	France	1.2	8
9	Australia	.9	7.2
10	Spain	.9	5.6

2010 which is 16 MW by European Photovoltaic Industry Association [9].

There are a lot of countries in the world using solar panels for electricity production. The PV market is increased in 2017 like 2016 after it has limited growth in 2014 and slow in 2015. In 2017 it has broken records while reached to threshold of 100GW and that's all because of China which accounts for almost 54% of total installed capacity in 2017 more than 2016 [12]. According to A SNAPSHOT OF GLOBAL PV: 2017, A YEAR OF CONTRASTS by International Energy Agency IEA among 10 top countries in the world having installed capacity are shown in table 1 and 8 out of 10 countries have more than 1GW installed capacity in 2017. China household income per capita is 4805.935 USD [28] which is very large as compare to Pakistan 649.972 USD [27].

Denmark introduced the concept of net metering and due to increase in electricity bills has attracted household to adopt such techniques and also in Denmark more than 50% of total price is tax so households having net metering facility are exempt from tax which also encourages peoples. At the end of 2011, Denmark PV power installation reached to 17 MW [2]. Federal energy regulatory agency (ANEEL) of Brazil has established new policies to develop distributed generation in April 2012. For this customer small scale generator of 1MW or less is developed to offset their utility bills ad customer will get benefits from ANEEL and for this customer generator are classified into micro (100kw and less) and mini distributed generators (100kw and 1MW). In this regulation customer will install system but for routine maintenance and checking utility distributer will be responsible. First renewable technology in developing country was implemented in Thailand in May 2002. In Thailand net metering idea was approved and implemented in May 2002 for very small renewable energy power producers (VSREPP) and has a generator with renewable source which sells 1MW or less power to the distributed utility. VSREPP has introduced and forced utility to purchase power from customer and also its tariff are differentiated, if customer produce electricity more than they use than consumer will be paid with average bulk supply tariff but if produce less than they produce customer will pay normal retail tariff. 95 projects are developed under VSREPP till July 2006 and 67 include solar projects [3]. California has also been using net metering techniques. In October 2009 a law was signed to support net energy metering production by

customers by utilities and in 2010 California had 48% of production from solar mostly on rooftop and has set to achieve 12,000 MW through net metering till 2020 [4].

The development of net metering techniques are increasing in the world. This idea of using renewable energy techniques is also developed in African countries. The Deutsche Gesellschaftfurinternationali Zusammenarbeit (GIZ) had studied benefits of solar PV to low voltage and had concluded to promote net metering techniques and program of 1 million roofs is being developed. The idea of using solar PV for electricity generation in Kenya has been grown. Kenya and Germany are included in World top countries that produce more power percentage from solar energy but only difference is Kenya is using off grid while Germany has on grid system [5, 6]. South Africa has also developed idea for net metering. NERSA (National Energy Regulator of South Africa) has approved to developed micro technology for power production which include Net Metering techniques and now in the process.

III. NET METERING FOR PAKISTAN

Pakistan has ultimate solar irradiance through full year and this energy must be used efficiently and in effective manner to overcome the energy demand. Conventional system in Pakistan is already developed which is off grid system in which customer produce power and stored it in batteries which is uneconomical, with least reliability and need extensive maintenance. These batteries make the system ineffective and decrease efficiency of system while other techniques are available in which customer will produce power and

through interconnection this power will go to grid making on grid system from off grid which has more benefits to the customers as well as to the utility companies. Location of Pakistan is very favorable and solar radiation occur with peak and almost most of area has 7 to 8 hours sunlight [21]. Pakistan has average solar irradiance of 2400 kWh/m2 [22]. US National Renewable Energy Laboratory (NREL) generated solar maps for Pakistan and it concludes that some areas of Pakistan have high solar irradiance averaging 5-7 kWh/m2 per day [23]. Average solar irradiance for Pakistan is shown in figure 3 [24] and show that average are 4.5 to 5 kWh/m2 per day represented by yellow color and also areas of 7 to 7.5 kWh/m2 per day are also exists near Quetta while Baluchistan and northern area goes to high irradiance of 6.5 to 7kWh/m2 per day. But the problem is with income level of Pakistan and most of community have very low income which is financial barrier to get benefit from solar energy through net metering techniques. Monthly income per capita of Pakistan is 148 USD in June 2015 [25] while household income per capita is 649.972 USD [26] which is less and they cannot meet with this income to implement net metering in their houses and get benefits from solar energy.
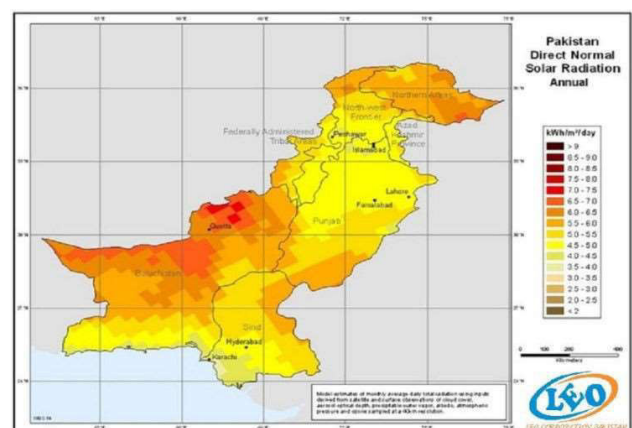

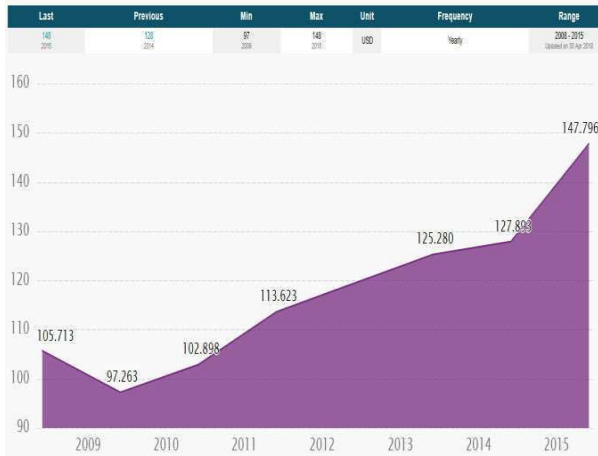Figure 3. Solar irradiance map of Pakistan
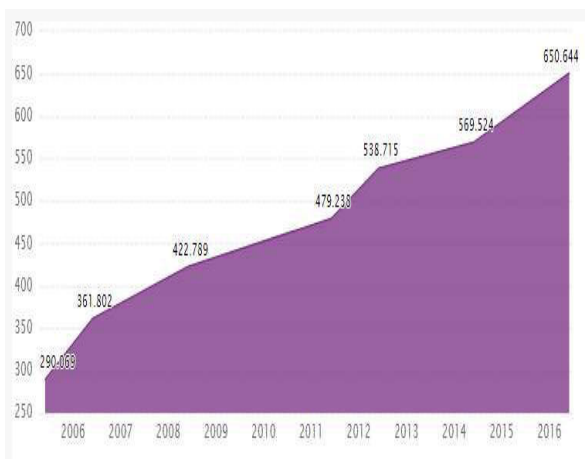
Figure 4. Per Capita monthly Earning [27]

Figure 5. Annual house hold income per Capita [27]

IV. CONCLUSION

Pakistan has serious electricity shortage in present days although its solar irradiance is high throughout the year. If this high solar energy is used in effective manner then total demand on centralized system can be reduced to large extent and excess will be feed to the grids through net metering system that will resolve electricity shortage Pakistan to a large extent. Solar irradiance for Peshawar is from

4.5 to 5 kWh/m^2 per day shown in figure 3. So Peshawar has high value and this can be used to produce power in Peshawar from solar

energy and to develop net metering technique in Peshawar. Power production from solar is clean, green and sustainable and using with net metering idea will reduce electricity bills and using of batteries for power storage.

ACKNOWLEDGMENT

REFERENCES

[1]. http://www.ren21.net/status-of-renewables/global- status-report/

[2]. Lindahl, J. (2014). National survey report of pv power applications in Sweden. *Uppsala University and International Energy Agency: Uppsala, Sweden.*

[3]. International review of regulatory schemes for PV.
Henrik Jensen, July 2006

[4]. Net Energy Metering. California Public utilities commission, 2012.

[5]. Grid Connection of Solar PV- Technical and Economical Assessment of Net Metering in Kenya,
George hilly et al. Michael Franz, December 2011

[6]. https://www.reeep.org/index.php?id=9353&special =viewitem&cid=54

[7]. M. Amer and T. U. Daim, "Selection of renewable energy technologies for a
developing county: a case of Pakistan," Energy for Sustainable Development,
15(4): 420-435(2011)

[8]. Bahadori, A., & Nwaoha, C. (2013). A review on solar energy utilisation in Australia. *Renewable and Sustainable Energy Reviews*, *18*, 1-5.

[9]. Despotou, E., Gammal, A. E., & Fontaine, B. (2010). Global market outlook for photovoltaics until 2014. *Brussels, Belgium: European Photovoltaic Industry Association*.

[10]. Solangi, K. H., Islam, M. R., Saidur, R., Rahim, N. A., & Fayaz, H. (2011). A review on global solar energy policy. *Renewable and sustainable energy reviews*, *15*(4), 2149-2163.

[11]. https://www.csiro.au/en/Research/Energy/About-Solar-power

[12]. http://www.iea-pvps.org/index.php?id=266

[13]. Heywood, V. E. (1956). *U.S. Patent No. 2,772,611*. Washington, DC: U.S. Patent and Trademark Office.

[14]. Linehan, M. M., Korslund, K. E., Harned, M. S., Gallop, R. J., Lungu, A., Neacsiu, A. D., ... &

Murray-Gregory, A. M. (2015). Dialectical behavior therapy for high suicide risk in individuals with borderline personality disorder: a randomized clinical trial and component
analysis. *JAMA psychiatry*, *72*(5), 475-482.

[15]. greenberg, m. (2009). moral concepts and motivation 1. *philosophical perspectives*, *23*(1), 137-164.

[16]. Feldman, D., Barbose, G., Margolis, R., James, T., Weaver, S., Darghouth, N., ... & Wiser, R. (2014). Photovoltaic system pricing trends. *US Department of Energy*.

[17]. Schelly, C., Louie, E. P., & Pearce, J. M. (2017). Examining interconnection and net metering policy for distributed generation in the United States. *Renewable Energy Focus*, *22*, 10-19.

[18]. Hsieh, D., Qian, D., Wray, L., Xia, Y., Hor, Y. S., Cava, R. J., & Hasan, M. Z. (2008). A topological Dirac insulator in a quantum spin Hall phase. *Nature*, *452*(7190), 970.

[19]. Tsikalakis, A. G., & Hatziargyriou, N. D. (2007). Environmental benefits of distributed generation with and without emissions trading. *Energy Policy*, *35*(6), 3395-3409.

[20]. http://floraoflangkawi.org/solar-net-metering-wiring-diagram/solar-net-metering-wiring- diagram-copy-solar-irradiance-on-grid-solar- power-systems-with-net-metering-of-solar-net- metering-wiring-diagram-at-solar-net-metering- wiring-diagram/

[21]. Chaudhry, M. A., Raza, R., & Hayat, S. A. (2009). Renewable energy technologies in Pakistan: prospects and challenges. *Renewable and Sustainable Energy Reviews*, *13*(6-7), 1657-1662.

[22]. Ilahi, T., Abid, M., & Ilahi, T. (2015, June). Design and analysis of thermoelectric material based roof top energy harvesting system for Pakistan. In *Power Generation System and Renewable Energy Technologies (PGSRET), 2015* (pp. 1-3). IEEE.

[23]. Amer, M., & Daim, T. U. (2011). Selection of renewable energy technologies for a developing county: a case of Pakistan. *Energy for Sustainable Development*, *15*(4), 420-435.

[24]. https://energydata.info/dataset/pakistan-solar-measurement-wbg-esmap

[25]. https://www.ceicdata.com/en/indicator/pakistan/monthly-earnings/amp?fbclid=IwAR1ij1ILcbvVl30m9mg7ZhWSy2EMGHLU3yBktsGzL6Qvam6bpiMIKzi5 XbI

[26]. https://www.ceicdata.com/en/indicator/pakistan/an nual-household-income-per-capita

[27]. https://www.ceicdata.com/en/our-insights

[28]. https://www.ceicdata.com/en/indicator/chin a/annual-household-income-per-capita

Numerical Modeling of Reinforced Concrete Beam Column Joint Damageability

Muhammad Shoaib Khan[1,a], Abdul Basit[2,b] and Ubaidullah[3,c]

[1]Graduate Student Researcher Structural/Earthquake Engineering, University of Engineering & Technology, Peshawar, Pakistan

[2]Graduate Student Researcher Structural Engineering, University of Engineering & Technology, Peshawar, Pakistan

[3]Graduate Student Researcher Structural Engineering, CECOS University of IT & Emerging Sciences, Peshawar, Pakistan

Email address: [a] shoaibuet10@gmail.com, [b] abdulbasit111g@gmail.com and [c] ubaidullah714@yahoo.com

Abstract— The behavior of reinforced concrete moment resisting frame structure is reflected by beam-column joint during an earthquake. The reversal of stresses on joint makes it one of the most crucial zone when subjected to lateral loads. This may cause distress and often failure when not design and detailed properly. The analysis of reinforced concrete frame is significantly affected by beam column joint flexibility. In this research study top external beam column joint of a five storey reinforced concrete structure is modeled through software SAP2000 and analyzed for time history of two famous earthquakes
a) Kobe and b) Kocaeli, using different modeling techniques; a) Normal design b) rotational springs and c) rigid links. The nodal displacement of joint recorded during numerical simulation show significant difference for different techniques. Rotational springs show more displacement, as it counts the shear deformations occurring at joint core as compared to normal design and rigid link elements.

Keywords—Time history analysis, beam column joint, joint flexibility, finite element modeling, SAP2000

I. INTRODUCTION

Reinforced concrete moment resisting frame structures, steel structures, and composite structures are used throughout the world because of it enrich gravity load carrying capacity. In the recent decades numerous experimental and numerical studies have been done focusing on the seismic behavior of these structures. The portion of structure that is of prime importance during a seismic event is the beam column joint. According to the definition of ACI-352 [1], joint is the portion of column within the depth of the beam framing into the column. Joint is an extremely important portion affecting the overall performance and capacity of the structure under gravity and earthquake loadings. Upon the action of loads the joint is under the combination of shear, axial, and bending stresses. During an earthquake the reversal of stresses occurs at joint, making it one of the most crucial zone and the failure of joint often leads to the failure of whole structure as shown in the "Fig. 1", Such a behavior was also observed in Kashmir/Balakot earthquake of 2005 as shown in the "Fig. 2".

Fig. 1. *Structural collapse during 1999 Kocaeli earthquake, [2]*

Fig. 2. *Failure of beam column joint in Kashmir earthquake 2005*

The behavior of joint is dependent on various factors including load pattern, concrete strength, amount and detailing of reinforcement. Many researchers pointed out that the use of different materials and various reinforcement patterns at joint can increase the load carrying capacity to a certain level. Reference [3] replaced normal concrete and transverse reinforcement with ECC (Engineered Cementitious Composites) in joint zone, and found that the shear capacity & ductility of the joint is increased by using ECC.

Various rehabilitation and retrofit techniques are used by many researchers to strengthen beam column joint including jacketing [4] and FRP composites [5], [6], [7].

Several analytical models are developed by many researchers throughout the years to model the inelastic response of beam column joint. Reference [8] introduced zero length rotational spring elements at joints, while Reference [9] modeled joint by providing a rigid zone at the end of beam and column. Reference [10] provided two rotational springs at the beam column intersection to capture shear deformations and anchorage failure. The research of [11], summarized a four node, 12 degrees of freedom element for joint investigation.

The objective of this research study is to model reinforced concrete beam column joint through a finite element software SAP2000 (Structural Analysis Program) using various elements and to observe the variations among

the joint response analyzed for time history of past earthquakes.

II. MODELLING DESCRIPTION

The reinforced concrete joint is modeled with dimensions (355.6mm * 508mm) and (355.6mm * 355.6mm) for beam and column respectively. Four techniques are followed to model the joint flexibility. The first one is the centerline model which falls in the category of normal design. The beam section is continued to the center of column as shown in the "Fig. 3". "Fig. 4" represents rotational spring at the intersection of beam and column. A rigid link is provided to connect the end of a beam to the centerline of column presented in "Fig. 5". "Fig. 6" represents a link which runs at half-length from joint to column and beam.
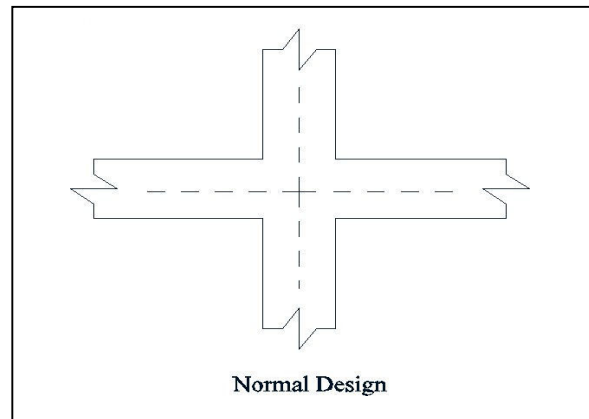
Fig. 3. *Centerline connection of beam and column*
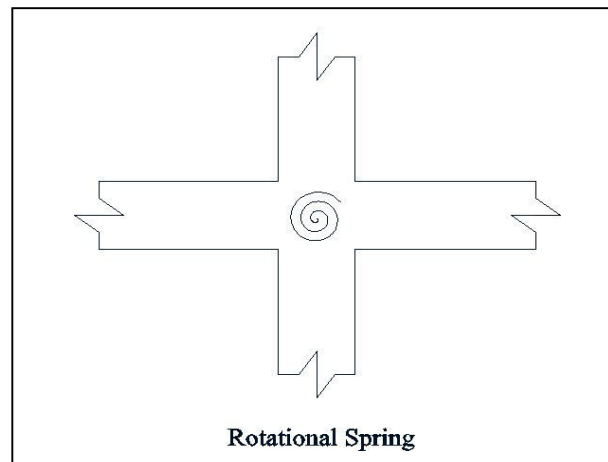
Fig. 4. *Rotational spring at the center of beam column intersection*
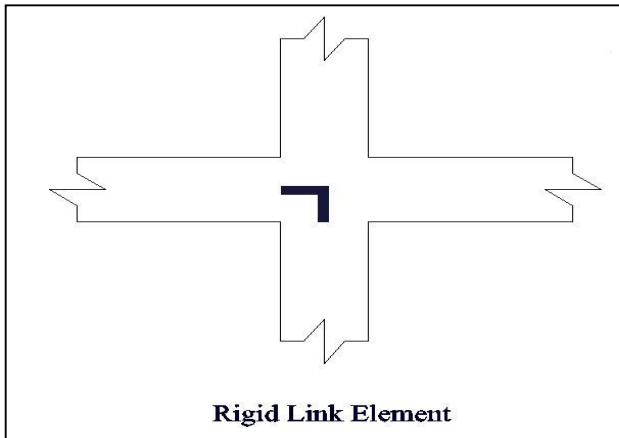
Fig. 5. *A Rigid link element runs from the center of beam to column*
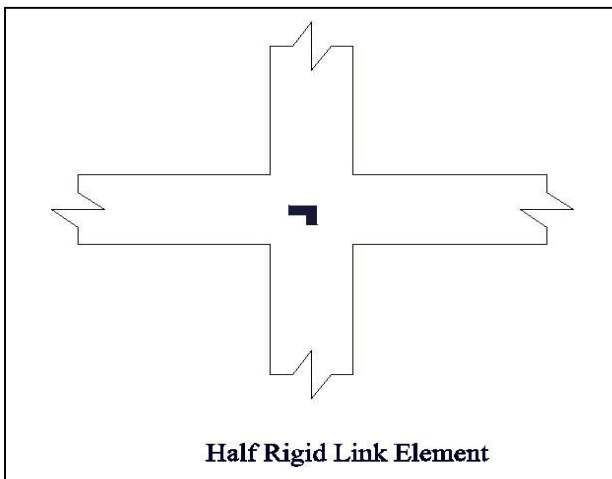
Fig. 6. *Half rigid link element provided at the beam column intersection*

III. ANALYSIS, RESULTS AND DISCUSSION

A five storey reinforced concrete structure having bay width of 15 feet in both X and Y direction, and storey height of 12 feet is analyzed in SAP2000 for the time history of past earthquakes; a) Kobe also known as the Great Hanshin earthquake and b) Kocaeli obtained from PEER (Pacific Earthquake Engineering Research).

The top exterior joint as shown in the "Fig. 7" is modeled for four cases; a) Normal design **b)** Rotational spring c) Rigid link and d) half rigid link element.
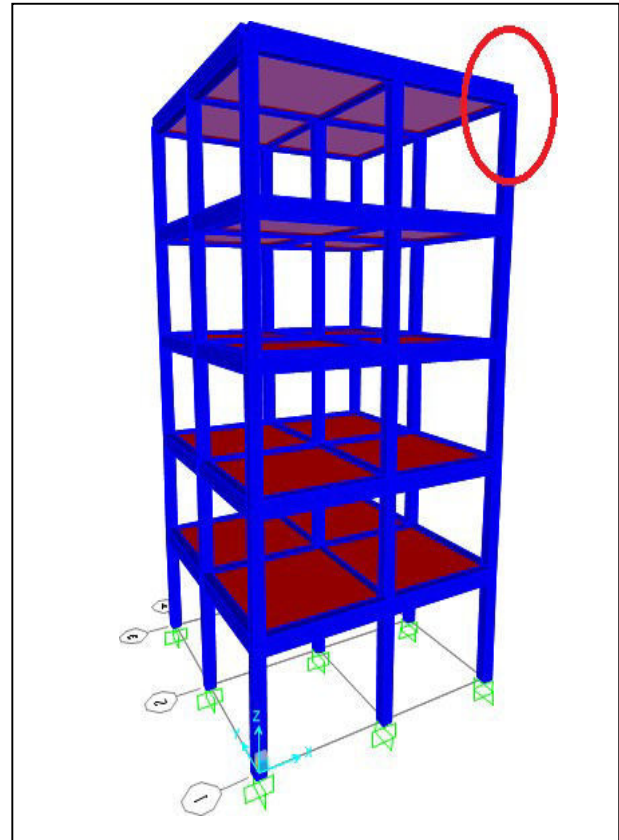
Fig. 7. *Isometric view of the model*

The nodal displacement of joint in millimeters recorded versus time in seconds for the above-mentioned cases against the time history of Kobe earthquake is shown in the "Fig. 8.", Fig. 9", "Fig. 10" and "Fig.11", which concluded that the rotational spring provided at joint show more deformations overall. The deformations are less in the case of normal design followed by half rigid and full rigid link elements respectively.
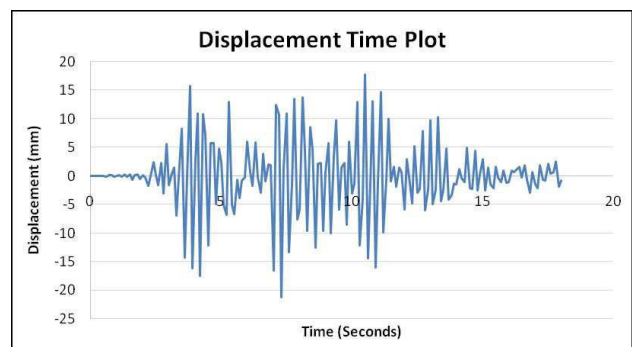
Fig. 8. *Displacement time plot for normal design*
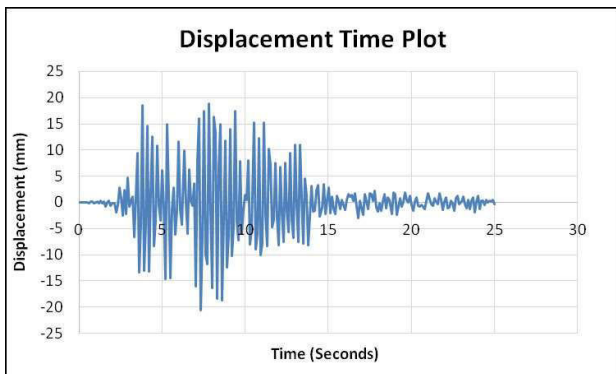
Fig. 9. *Displacement time plot for rotational spring*
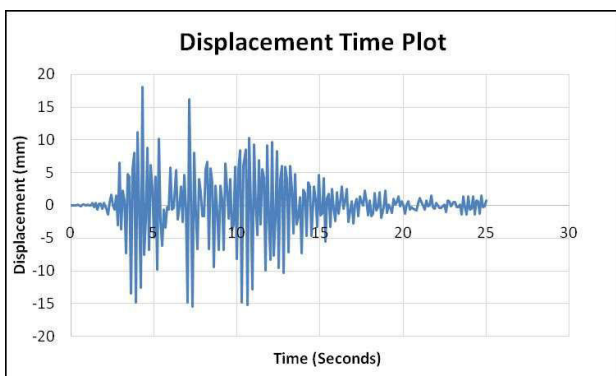
Fig. 10. *Displacement time plot for half rigid link*

Fig. 11. *Displacement time plot for full rigid link*

Results obtained for Kocaeli earthquake followed the same pattern, where the joint deformations are noted increased in case of rotational spring element as shown in the "Fig. 12", "Fig.13", "Fig.14" and "Fig.15".

Fig. 12. *Displacement time plot for normal design*

Fig. 13. *Displacement time plot for rotational spring*

Fig. 14. *Displacement time plot for half rigid link*
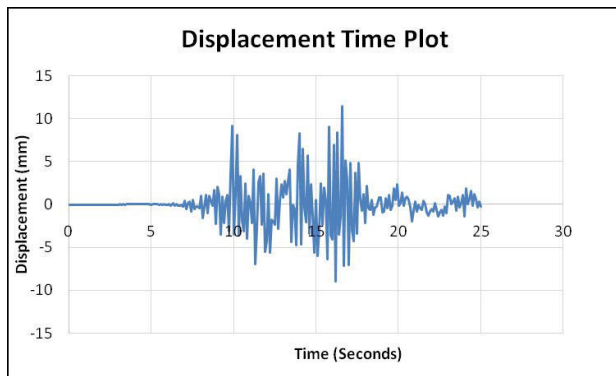
Fig. 15. *Displacement time plot for full rigid link*

IV. CONCLUSIONS

This study has investigated various approaches to model the response of beam column joint under lateral loads using SAP2000. The response of beam column joint under lateral loads is defined by the nonlinear shear response of the joint panel and the bond slip response of longitudinal beam reinforcement. The normal design (centerline model) is a common practice for the modeling of beam column joint under gravity loadings. Results showed that the normal design and half rigid link element ignores up to certain extent the joint flexibility and deformations occurring at joints during a seismic event. While the displacements in the case of full rigid link element are very low concluding the complete ignorance of joint flexibility. The deformations recorded for rotational spring element are significantly high as compared to other models. This summarizes rotational spring as element considering the shear deformations occurring at the core of the joint which is ignored in the rest of the models. An experimental study is necessary to compare the experimental data against the numerical data captured by SAP2000.

V. ACKNOWLEDGMENT

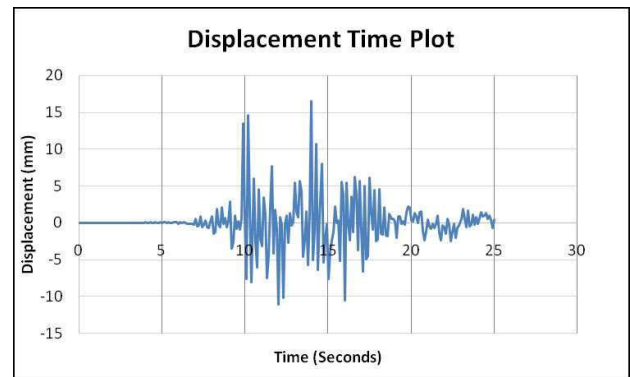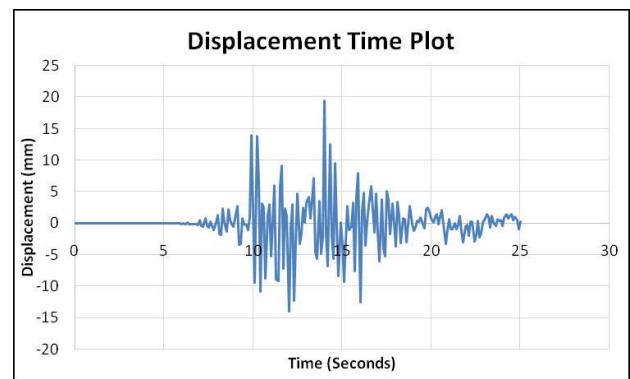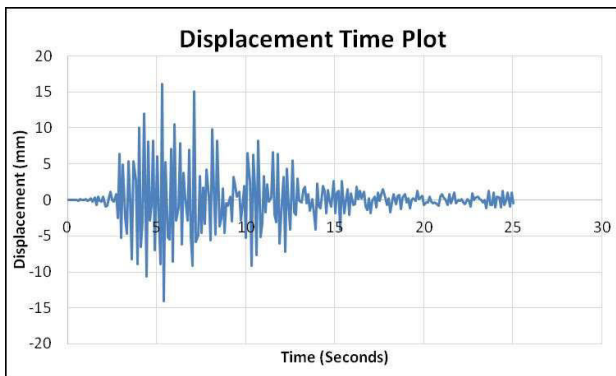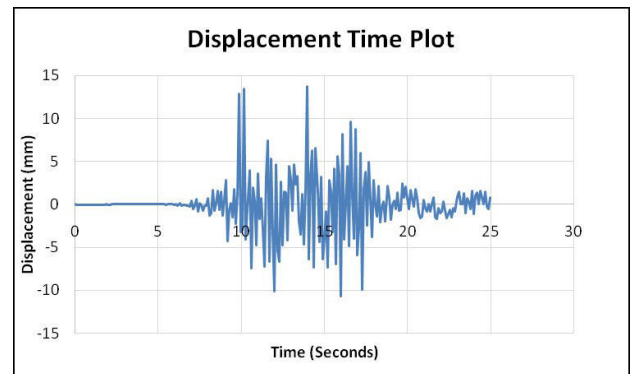The authors are extremely grateful for the help and guidance provided by the Faculty of Civil Engineering, University of Engineering & Technology, Peshawar, Pakistan.

VI. REFERENCES

[1] ACI 352, "Recommendations for design of beam column joints in monolithic reinforced concrete structures," American Concrete Institute, Committee 352, ACI 352R-02, 2002.

[2] M. Saatcioglu, D. Mitcheel, R. Tinawi, N. N. Gardner, A. G. Gillies, A. Ghobarah, D. L. Anderson and D. Lau, "The August 17, 1999, Kocaeli (Turkey) Earthquake- Damage to Structures," Canadian Journal of Civil Engineering, vol.28, No.4, pp.715- 737, 2001.

[3] S. H. Said, "Effect of replacing the transverse reinforcement with Engineered Cementitious Composites in RC exterior beam column joints subjected to cyclic loading," Proceedings of the Eleventh International Conference on Composite Science and Technology, Sharjah, United Arab Emirates, pp.15-10, 2017.

[4] S. M. Alcocer and J. O. Jirsa, "Strength of reinforced concrete frame conncetions rehabilitated by jacketing," ACI Structural Journal, vol.90, No.3, pp.249-261, 1993.

[5] A. Prota, G. Manfredi, A. Nanni and E. Cosenza, "Capacity assessment of GLD RC frames strengthened FRP," Proceedings of the Twelfth European Conference on Earthquake Engineering, London, UK, Paper No. 241, 2002.

[6] C. P. Antonopoulos, T. C. Triantafillou and G. Papanicolaou, "Experimental Investigation of FRP Strengthened Beam Column Joint," Non Metallic Reinforcement for Concrete Structurres – FRPRCS5, Cambridge, pp.309-318, 2001.

[7] C. P. Pantelides, C. Cylde and L. D. Reaveley, "Rehabilitation of RC Building Joints with FRP Composites," Twelfth World Conference on Earthquake Engineering, New Zealand Society for Earthquake Engineering, New Zealand, Paper No.2306, 2000.

[8] S. E. El-Metwally and W. F. Chen, "Moment rotation modeling of reinforced concrete beam column connections," ACI Structural Journal, vol.85, No.4, pp.384- 394, 1988.

[9] S. Alath and S. K. Kunnath, "Modelling inelastic shear deformation in RC beam column joints," Engineering Mechanics: Proceedings of Tenth Conference, Univeristy of Colorado at Boulder, Boulder, Colorado, 1995, American Society of Civil Engineers, vol.2, pp.822-825, 1995.

[10] A. Biddah and A. Ghobarah, "Modelling of shear deformation and bomd slip in reinforced concrete joint," Structural Engineering and Mechanics, vol.7, No.4, pp.413-432, 1999.

[11] L. N. Lowes and A. Altoontash, "Modelling reinforced concrete beam column joints subjected to cyclic loading," Journal of Structural Engineering ASCE, vol.129, No.12, pp.1686-1697, 2003.

A model for Big Data Adaption in Cloud Computing

Waheed Ullah Khan[1,a] and Abdul Wahid Khan[2,b]

[1]Department of Computer Science, Gomal University D.I. Khan

[2]Department of Computer Science, University of Science & Technology, Bannu

Email address: [a)] waheedmwtbcs@gmail.com

Abstract— Big Data and cloud computing are two important area of today research. We have planned to develop a model from vendor's perspective to overcome the challenges faced by vendor organisation in adapting Big Data in Cloud Computing. There are two basic components of this model: first to identify the challenges and second to identify practices for the identified challenges. These challenges and practices will be identified through Systematic literature review (SLR). The finding of SLR will be validated through empirical study. The proposed model will assist vendor organizations to measure their level to overcome on the challenges as they faced in adaption of Big Data in cloud computing. The proposed model will be evaluated in real world through case studies in software industry.

I. INTRODUCTION

Today is an information technology (IT) era. Each one (organizations, companies, education departments ,science and etc) in the world desire to have a lot of information for their further uses, In order to get whenever they will be needed in any stage of lifespan. But the problem is that how these huge of information can be stored, because of this information is created from different sources i.e. Multimedia, social media, internet of things, sensors and etc) having its own individual characteristics i.e. format, velocity, volume, variety, complexity etc which is difficult for traditional database management system and recent

software technology to support it. These information was named later by john Mashey [1]in 1998 as "big data and the next wave of infers stress"[1]. The starting point of the term "big data" is due to the fact that every day we are creating a large amount of data, so big data can be define as "the description of data [2, 3] having massive volume either in structure or in unstructured or in both form having the following properties i.e. high-volume, high-velocity, high-variety, high complexity as well as high variability in order so that it is difficult to store, manage and process for a traditional DB (database) and recent software technologies. In order to collect, store, process and manage such a huge and complex data as discussed above a technology we used is Cloud Computing. The cloud computing was originated in 1960 by John McCarthy [3]an American scientist. This service was later lunched in 2006 [3] when a lot of companies started an interest to create cloud base-infrastructure. The cloud computing term was used for the purpose to show a new class of network based computing, that works over the internet or a model that work on a large, centralized data bank to store and process a large volume of information.

In order to analyze [4] a huge and complex data and to recognize the main theme of that data it must be store, manage, process and share large amount of complex data securely. On the other hand cloud has its own challenges face during the storage of data on cloud because the data owner itself does not have any command on that data where that data is placed. The reason towards that is, when one wants to gain the advantages of cloud, they must also utilize the allocation of that resources as well as the scheduling handed by the controls. Furthermore, we will require data privacy because cloud consists of many complexities.

In this paper [4] the authors described some special approaches in order to provides security to clouds. They have suggested to create such a scalable system that's have the ability to handle a large numbers of site as well as process large and huge amount of data. We know that state of the art system using HDFS(Hadoop distributed file system) and MaReduce are some scalable improvement in big data as well as cloud computing, but are not completely enough because they do not facilitate required security feathers to protect important and sensitive data. While on the other hand Hadoop framework facilitates some basic feathers in order to solve problems as well as manage data easily with the help of verity techniques i.e. merging the k-means with data mining techniques [5]. To develop our proposed model we will try to know in detail about cloud computing and big data concept.

A. Cloud computing

Cloud computing [4] is nothing but a technology used for to share a computing resource with those having local server or personal devices. The local servers or personal devices are used to handle an application or services to the users provided by cloud. In cloud computing the words cloud used, which means

an "internet", so we can also define the cloud computing as" that type of computing through which services are shared via internet", the main purpose of the cloud computing is to create such a system that have the ability to increase the computing power in order to execute million of instructions in unit time. Example of cloud computing applications are Gmail, Drop box, Google Calendar and Google Docs etc. There is a lot of benefits of cloud computing but the most benefits among theme is cost, means reducing the cost of computing resources[6]. Cloud consists of various computer networks. A cloud resolves cost related problems because it reduces the cost of both software as well as hardware on the user side. Cloud actually consists of two parts, the front end and back end. The front end consists on the user interface software and the cloud network, while the back end consists of varies computers, servers, database system that actually creates cloud.

B. Big Data

From its name[4] it is cleared that big data is the data which is so massive either in structure format or in unstructured format having properties of high volume, velocity, variety that is difficult for the recent database system as well as software technologies to process it. Such a massive volume of data produced mostly from social media, multimedia, internet of things, sensors and etc.

C. Hadoop

A Hadoop[4] is a free framework written in java-programming language that have the capability to support processing of big data datasets in distributed cloud computing environment. An Apache project how produced the hadoop sponsored by a foundation known as Apache Software Foundation. Hadoop cluster that uses a structure known as Master/Slave structure [7]. However by using hadoop a huge amount of data can be processed that is divided

among a servers in cluster form as well as an applications run on a system having thousand numbers of nodes associated thousands numbers of terabytes. The characteristics of hadoop distributed file system are the quick data transformation rates as well as fault-tolerant capability. This approac minimize the failure risk of the entire system, even a node failures occur in significant numbers. Hadoop framework used in many companies like Amazon, Google, IBM and Yahoo etc due to the characteristics of fault tolerant, flexibility, cost effectiveness and scalability in order to support an application that is used for big data. A framework Hadoop is further divided into two sub-projects known as Map Reduce vs. Hadoop Distributed File System (HDFS).

D. MapRedus

A framework Hadoop MapRedus [4, 8] used for the purpose to write applications. This writing application retained the capability to process massive amounts of data that is in parallel mode by using groups of commodity resources i.e. hardware resources in a fault-tolerant as well as in reliable manner. The mapping work first divides the data into separate chunks that are processed by map jobs in parallel. Then the output of the map sorted by the framework is the input for reduced operations. Generally input and job output are both stored in a file system. Failure of scheduling, monitoring as well as re-executing tasks is taken care of by the framework.

E. HDFS

The Hadoop Distributed File System(HDFS) [4, 9] is a file system that is the capability to spreads all of the nodes in a cluster known as Hadoop cluster for purpose of data storage. This file system connects to the local node simultaneously so that it can be made up of a hug file system. To correct the node failure, HDFS improves the reliability by creating a replication of data in many sources.

II. LITERATURE REVIEW/BACKGROUND

The etymology of the word 'Big Data' started for the first time in 1998 during a Silicon Graphics (SGI) slide building by John Mashey with the name 0f "Big Data and the Next Wave of Infra Stress". It was the word that he used for the data sets which is so large and complex that is up to imposable for current database management system tools and methods to process and manages them. The main purpose of the word 'Big Data' was creating a massive amount of data produced every next day [1].While the idea of cloud computing started in 1990s [10].

In 2015 a Paper was published by Dr.Jangala.Sasi Kiran., et al. [1]to discuss the "present Issues as well as Challenges associate with Big Data adaption in Cloud computing ". According to the paper, a big data is one of the most important things in today business environment as well as in education departments, science field and etc. Therefore it must be secure in the view of privacy as well as security rules and authority. They mentioned in the paper those five levels of security that's increasing the security level introduce by International Data Corporation are: privacy, compliant-driven, custodial, and confidential as well as lockdown. Cloud computing precipitate the role of backbone in protecting important data, infrastructure and application etc with some polices recent technologies, big data tools as well as controls. In the paper they discussed Security challenges faced by cloud environment are categorized into 4-level as: network level, authentication level, data access and generic issues. They have also addressed some advancement in the existing challenges. In the

view of future perspectives they mentioned that we have to developed more understandable solution of the existing challenges faced by big data in cloud computing, especially big data analysis and design methodology.

Big data in cloud computing faced a very critical challenges. For this purpose a number of publications were made in order to struggle for eliminating those challenges faced by big data in cloud computing environment. In 2014 [11] a paper was published on the rise of big data and cloud computing along with their review as well as open research problems. In this publication they mentioned varies aspects of big data i.e. big data definition, classification and characteristics. They also motioned cloud computing, relation between big data and cloud computing, storage system of big data, case study as well as Hadoop technology. Furthermore they highlight those points that are the key point of this publication is: research challenges. These challenges are: scalability, availability, data integrity, data transformation, privacy, legal and regulatory challenges as well as governance .At the last they present all those challenges faced by big data and cloud computing, that required some specific research efforts called open research challenges. In the future all the existing issues and challenges faced either big data or cloud computing required significant effort to solve then in order so that to explore new territories in the field.

Cloud computing are widely used in industry and research aspects, therefore it is needed to secure it in all point of view, because they want to place all the important data of the organization on cloud. In security issues point of view in 2016 [12] a paper was shared in which they discussed the big data and cloud computing issues. According to the paper security issues is one of the most critical challenge to big data and cloud computing, therefore they focus all the attention

on the security issues and challenges faced by big data and cloud computing. So those challenges that is discussed in this paper associate with big data and cloud computing are: plumbing, security, cost modeling, charging modeling and service level agreement. But on the other hand also present some suggested solution of the existing problems. Furthermore they also mentioned some other security issues associate with cloud computing. In future point of view they discussed trends of big data because big data are doubling each year and for that we have to improve more and more security issues and challenges in better way, so that to adequate service delivery.

In 2015 [13] a publication was made on the challenges faced by big data in cloud computing and their future research review. According to the publication now a day data management is one of the critical challenges in term of big data, because now a day data are produced in drastically manner not in term of increasing size but also in variety. Therefore it is difficult to solve the entire problems associate with those hug and flexible data. Some of the issues are up to solve by using Google Distributed System as well as MapReduce functionality, but lot of the challenges up to now faced by the cloud computing in term of big data analysis . In future we can overcome on these existing challenges faced by big data in cloud computing and for that we have to developed an efficient tools as well as technologies.

Big data adaption in cloud computing play an important role in today business environment, science, education etc, but they faced a lot of security challenges during or after the adaption of that data in cloud computing because the in environment is changed for the big data. Therefore in 2014 [14] a paper was shared on the security issues faced during the adaption of big data in cloud computing along with the security

issues produced in MapReduce as well as Hadoop environment. Those security issues associated with big data adaption in cloud computing are categorized in network level, authentication level, data level and generic type, They also motioned some approaches to solve the existing challenging issue up to some level. Furthermore they also discussed big data and cloud computing in broad manner i.e. what is cloud computing and big data, Hadoop, Map Reduce, HDFS, big data applications, big data advantages, need of security for big data as well as motivation vs. related work,

Big data is a data analysis technique that started a new era in the field of IT. For the big data accommodation a large amount of storage space required. Cloud computing facilitate large storage space for the big data. Data warehouse facilitate a large amount of storage space for the data, but failed in to provide reasonable response time .the 4v's of big data creates for data management as well as analytics'. In 2018, Samir A. EI-Seoud et al. [15] shown big data and cloud computing trends as well as their challenges. They discussed varies aspects of big data as well cloud computing in the paper i.e. big data vs. cloud computing literature review, genial concept and definition of big data, moving data management to cloud, managing of big data in cloud computing, solution vs. methodologies for the big data storage, data processing vs. resource management, advantages of big data applications advantages vs. risk of big data vs. cloud computing integration. The main focus of the study on the security challenges. By integrating big data and cloud computing, in resulting to create a new form of platform, due to which they create new challenges of security. In the paper they mentioned some challenges create due to the new form of platform. These challenges are: Heterogeneity, nature of data and its lactation, optimization of big data .That also mentioned

that it is possible to overcome on these challenges in indirect manner, because they required straggle to invest money for creating a suitable environment for operation of massive data.

K. Shanmugapriya et al. [4] focused on the big data security in cloud computing. According to them how we can solve the security problem of big data in cloud computing. They discussed different security issue faced by cloud computing, big data Hadoop, MapReduse as well as Hadoop distributed file system, but the main focus on the security issues associate with big data and cloud computing. It is clear that cloud computing consists of varies technologies, therefore cloud faced varies security challenges. So for varies technologies varies security solution will be needed. Therefore they discussed varies approaches so that to improve the security issues. Furthermore they also mentioned big data applications as well as advantages.

We know that security challenges is one of the most critical problem in the world of big data and cloud computing. Therefore publication was made on Big Data Services Security and Security Challenges in Cloud Environment. In this publication [16] they discussed those security challenges faced by big data whenever it is uploaded on cloud computing to store it in order so that later it is shared with customer and those methodologies that improve the storage issues of big data in cloud computing. In this publication they also mentioned, that some of the challenges faced by big data in cloud computing was acknowledge and some of the challenging issues are under the discussion associate with cloud computing. Furthermore they also highlighted big data analysis in term of classification.

Big data and cloud computing plays impartment roles in today business as well as

academia environment along with some challenging issues. Pedro Calderia Neves et al. [17] analyzed the features as well challenging issues of them. According to them big data are increasing in such a manner that is difficult for the recent technology as well methods to store and process them. So we have a technology to store as well as process such a complex and varied volume of data. Cloud facilitates a suitable environment having the characteristics of reliability, availability, fault-tolerant and scalability. They discussed varies challenges i.e. security, privacy, scalability, data governance, heterogeneity, disaster recovery and some other problems associated with big data and cloud computing. But they also mentioned that some of the exiting problems are up to solve in the next few years.

J. Raja et al.[18] focused on the storage of big data in cloud computing and its security challenges .The main focus of this paper on those security challenges faced by the cloud storage. In this paper they present some techniques that's solve cloud storage problems and challenges up to some level They also present some methods in the paper having the capability to solve big data management problem in cloud computing securely. Furthermore they discussed some of the data optimization tools and big data management in cloud computing. They also explore their idea about cloud storage security in future point of view that is still under the development and required some more enhancement are needed in future.

Data security as well as data access control in cloud computing environment faced a lot of challenges. Today is an IT era. Each user wants to upload their data over cloud. Therefore it is necessary to prove a security for such type of data, so that user can access their data security. In 2012 [19] a publication was made on the data

security in cloud computing .In this publication they mentioned that during the exchange of data in cloud computing faced a lot of challenges. According to the publication, that during sharing of data by using cloud computing services faced different types of security issues and problems, such as key generation, data security and authentication. Therefore the use some control technique so that to minimize an existing security issues and problems, in order so that only authorize users can access their data. Those control technique are: RSK algorithm and TORDES algorithm along with them they also mentioned the propose system model and their performance as well as verified the test cases of the model. They also discussed they satisfied output of their struggle in term of data access and data sharing application.

In 2018,[20] a publication was made on the bid data, cloud computing and their increasing challenges in future. According to the publication today data a creating in such a large scale that it is difficult for an organization to handle and process such a large scale data because current technologies, methods as well as infrastructure management are hanging to handle such a large scale data. Therefore it is needed for an organization to thinks and chose such a way to handle as well as process such a large scale data .Cloud computing plays a key role to handle such a large scale data, but also faced some security challenges .Those challenges faced by the cloud computing are categorized in network level, user level, authentication level, data level as well as generic issues. Some big data needs a special security with respect to privacy and security laws and regulation. Therefore they discussed those five levels of increasing security define by the International Data Corporation. Those are: privacy, compliance-driven, custodial, confidential, and lockdown hey also stated that it is necessary to clearly define these security

levels for perform their matching with the current law and current analysis. They mention about the challenges faced by the web scale storage in now handle by Google file system(GFS).In future point of view they spread their views that we have to create such an algorithm having the capability to handle the randomize personal data amount big data in order to ensure privacy problem.

From the start data is passing with big security issue in the field of information technology. But from the corner of cloud computing security issue increase up to some level due to the distributed properties in all the globe. Therefore it is necessary to concentrate their focus on the data security as well as privacy protection. In 2014 [21] a paper was published about the data security and privacy protection. In order to improve or eliminate the challenges of data security and privacy protection they perform a comparative research analysis of the all ready perform work done on the data security as well as privacy protection techniques that is mostly used in cloud computing environment .The main benefit of this study is to explore varies security and privacy techniques as well as challenges either related to software or hardware in cloud environment for the purpose of to improve the data security as well as privacy protection for the trustworthy cloud computing platform. They also say that data security along with privacy issue in future point of view is very necessary for cloud computing technology that participate in academia and industries.

Data security as well data access vs. data transformation become a challenging issue in cloud computing. To solve these above problems a publication was made in 2012 [22] in order to improve these challenging issues. According to the publication current technologies are failed in the computational problem of keys generation as well as their

secure exchange. In this publication they address three challenging issues i.e. key generation as well as their transformation, data security and authentication problem. To overcome on these problems the use some access control technique so that to ensure that only registered user can access their outsource data. In order to ensure the data security not only on the cloud but also during the transmition from the third part hacker they used the Deffi-Hellman key exchange algorithm while for key generation they used the Symmetric key algorithm who's remove the disadvantages of cryptography access control model. While for authentication problem they used a two-way authentication for accessing their account. Furthermore they also mentioned function specification, analysis, simulation advantages and benefits as well as future scope of her proposed model.

III.   RESEARCH QUESTION

RQ1. What are the major challenges faced by vendor organization in adaption of Big data in Cloud Computing?

RQ2. What are the practices as discussed in the literature to overcome on the challenges in adaption of Big Data in Cloud computing?

IV.   RESEARCH NETHODOLOGY

A. *Systematic literature review*

Systematic literature review (SLR) plays a vital roles as a methodology in the field of software engineering research [23].A Systematic literature review facilitate researchers as well as practitioner a well-trained methodology that point as well analyze a supporting resources belongs to a specific area, interest or phenomena[24]. Systematic literature review (SLR) work in a procedural manner .First of all they create a comprehensive protocol

means arrange plane, after that they started reviewing process consists of several steps and at the last as they collect and document results.

B. Empirical Research

Empirical research plays a vital role in our proposed research. Empirical research consists of different methodologies such as questionnaire survey and case studies. A questionnaire survey used for the validation of findings. After the questionnaire survey case study has conducted for the purpose to test an outsourcing software organizations for the purpose evaluation our proposed model. Niazi et al. [25] has defined that "Empirical research is the type of research which is based on observed and measured phenomena that derives knowledge from experience rather than from theory".

V. RESEARCH GAP/PROBLEM STATMENT

- We know that cloud computing provides a well-defined environment i.e. scalable, fault-tolerant and available for the big data storage as well as transformation. The concept of big data is so large and complex that is out of the scope of traditional data base system to store as well as technology to process them. Therefore it is very importance for the today industries and academies to store such a massive volume of data on the cloud.

- However associate with the above facilities provided by cloud computing to the industries and academes they also faced some special challenges about privacy and security. Therefore most of the industries and academes hesitate to store their important data on using the above concept.

- To solve these above problems, our search work will investigate several

options to make the cloud more secure. We have found through literature review that numbers of challenges have been discussed by the different researchers in their research articles but not found any specific model to overcome on these issues. We have plane to develop a model using SLR concept from vendors' perspective that will assist them to overcome on these challenges during the adaption as well exchange of big data in cloud environment.

VI. SIGNIFICANCE OF WORK

If a vendor organization follows this model in cloud environment then it provides the following significance as given below:

- Reduce the complexity faced by vendor organization in adaption of big data in the cloud.

- The vendor organization will overcome on the issues in adaption of big data in the cloud.

- Vendor organization can know in advance about their status using this model.

- Vendor organization will enhance their weaknesses to improve their status for such kind of activities.

- The client organization can also know about the status of vendor organization before signing contract with them.

VII. STRUCTURE MODEL

A. A Modal of Big Data Adaption in Cloud Computing Development

The model shown in Figure 1 defines the underline planed structure that is of A Modal of Big Data Adaption in Cloud Computing (MBDACC). The structure of model shows the relationship between the different type of phases

used that is the factor (CBs) as well as different practices put into practice so that to identified factors. The MBDACC level shows how management potential as well as empirical results will be incorporated into a management levels from the factor (CBs) and different measuring practices.

Following dimensions show MBDACC structure:

- Factor (CBs) Level Dimensions
- Implementation Dimensions

The main classification of MBDACC dimensions comes that from the model known as maturity mode. A maturity model used in order to implement the software Process improvement [48]. The first dimension will determine the factor (CBs) level that will leads us to avoiding from varies key barriers. Different practices that will lead us for the correct implementation of identified factors.

B. A Modal of Big Data Adaption in Cloud Computing Evaluation

In order to evaluate MBDACC, case study methods will be used and important information can be provided in the real world [26]. The goal is to find five outsourcing organizations (suppliers) to evaluate MBDACC. The effectiveness of MBDACC will be assessed through a study of five cases. A focus group meeting [27] will be arranged with the participants to obtain feedback on "A Modal of Big Data Adaption in Cloud Computing". The main theme of the group meeting was to get feedback from researchers as well as experts in the outsourcing organization and to get more information about the various issues that could not be achieved through interviews with individuals [27].

REFRENCES

[1] E. A. Jangala. Sasi Kiran.Dr, "Recent Issues and Challenges on Big Data in Cloud Computing," *InternatIonal Journal of Computer SCIenCe and teChnology,* vol. 6, p. 5, AprIl - June 2015.

[2] A. S. a. R. R. S. Narasimha Inukollu.Venkata, "Security Issues Associated With Big Data in Cloud Computing," *International Journal of Network Security & Its Applications,* vol. 6, p. 12, May 2014

[3] W. M. a. H. G. R. Katal.Avita, "Big Data: Issues, Challenges, Tools and GoodPractices," *Institute of Electrical and Electronics Engineers,* p. 6, August 2013.

[4] M. M. a. S. K. Shanmugapriya.k, "Security Issues Associated With Big Data in Cloud Computing.," *International Journal of Computer Science and Information Technologies.,* vol. 6, p. 5, 2015.

[5] H. C. a. Y. Qiao., ""Research of Cloud Computing based on the Hadoop platform.",," presented at the 2011 International Conference on Computational and Information Sciences, 2011.

[6] L. L. Amanatullah.Yanuarizki, Purnomo Ipung.Heru, and Juliandri.Arkav., ""Toward Cloud Computing Reference Architecture: Cloud Service Management Perspective"." presented at the International Conference on ICT for Smart Society., Jakarta, Indonesia., 2013.

[7] H.-s. C. a. T.-t. H. Lu.Huang, ""Research on Hadoop Cloud Computing Model and its Applications"," presented at the 2012 Third International Conference on Networking and Distributed Computing., Hangzhou, China., 2012.

[8] T. R. V. a. A. G. Jiang.Wei, ""A Map-Reduce System with an Alternate API for Multi-core Environments". ," presented at the 10th IEEE/ACM International Conference on Cluster, Cloud and Grid Computing., Melbourne, VIC, Australia., 2010 .

[9] K. K. A. a. Chitharanjan.K., ""A review on hadoop — HDFS infrastructure extensions"," presented at the 2013 IEEE Conference on Information &

Communication Technologies., Thuckalay, Tamil Nadu, India, India., 2013.

[10] S. R. .M., ""Big Data and Current Cloud Computing Issues and Challenges "." *International Journal Of Engineering And Computer Science.,* vol. 5, p. 12, April 2016. 2016.

[11] e. a. Abaker Targio Hashem.Ibrahim, ""The rise of "Big Data" on cloud computing: Review and open research issues "," *Information Systems .* vol. 47, p. 18, July 2014 2014

[12] e. a. O.Awodel, ""Big Data and Cloud Computing Issues "," *International Journal of Computer Applications .* vol. 133, p. 6, January 2016 . 2016.

[13]   E. A. Kumar Majhi.Santosh ""Challenges in Big Data Cloud Computing And Future Research Prospects: A Review "," *Smart Computing Review.,* vol. 5, p. 6, August 2015. 2015.

[14]   e. a. Narasimha Inukollu.Venkata, ""SECURITY ISSUES ASSOCIATED WITH BIG DATA IN CLOUD COMPUTING "," *International Journal of Network Security & Its Applications* . vol. 6, p. 12, May 2014 2014.

[15]   e. a. A. El-Seoud.Samir, ""Big Data and Cloud Computing: Trends and Challenges "." *International Journal of Intractive Mobile Technologies.,* vol. 11, p. 19, 2017.

[16]   e. a. Alsufyani.Raed, ""Big Data Services Security and Security Challenges in Cloud Environment "." presented at the In Proceedings of the International Conference on Internet of Things and Big Data., 2016.

[17]   C. Neves.Pedro., ""Big Data in Cloud Computing: features and issues "." presented at the International Conference On Internet of Things and Big Data., 2016.

[18]   e. a. Raja.J, ""A Comprehensive Study on Big Data Security and Integrity Over Cloud Storage"." *Indian Journal of Science and Technology.,* vol. 9, October 2016 2016.

[19]   M. A. K. rao.Leena., ""Centralized Database Security in Cloud"." *International Journal of Advanced Research in Computer and Communication Engineering.,* vol. 1, p. 6, October 2012 2012.

[20]   M. K. . ""Challenges of Cloud on Big Data "." *International Journal of Management, Technology And Engineering.,* vol. 8, p. 8, OCTOBER/2018 2018.

[21]   e. a. Sun.Yunchuan, ""Data Security and Privacy in Cloud Computing"." *International Journal of Distributed Sensor Networks.,* vol. 10, p. 9, 16 July 2014 2014.

[22]   e. a. H.Patil.D, ""Data Security over Cloud "," presented at the International Conference on Emerging Frontiers in Technology for Rural Area., 2012.

[23]   e. a. Kitchenham.Barbara, ""Systematic literature reviews in software engineering– a systematic literature review"." *Information and Software Technology.,* vol. 51, p. 9, 12 November 2008. 2008.

[24]   Kitchenham.Barbara., ""Procedures for Performing Systematic Reviews".", Software Engineering Group Department of Computer Science Keele University Keele, Staffs ST5 5BG, UK . 2004

[25]   e. a. Niazi.Mahmood, " " A Maturity Model for the Implementation of software process improvement: ,"." *The Journal of Systems and Software.,* vol. 74, 2005.

[26]   Yin.R, " "Application of Case Study Research"," 1993.

[27]   D. L. Morgan, ""Focus Groups as qualitative research"," presented at the Qualitative Research Methods Series, 1997.

Numerical Investigation of VR-7 Airfoil Dynamic Stall Under Steady and Transient Conditions

Tariq Ullah[1,a], Adeel Javed[2,b]
1Center for Advanced Studies in Energy
National University of Sciences and Technology
H-12 Islamabad, Pakistan

Email address: [a] 17teetariq@uspcase.nust.edu.pk , [b] adeeljaved@uspcase.nust.edu.pk

Abstract—This paper carry out a comprehensive study on transient pitch oscillating boing VR-7 airfoil, in order to correctly encapsulate the dynamic stall and airfoil responses. A two dimensional computational fluid dynamics analysis has been performed for steady and transient conditions at fixed Reynolds number and varying angle of attack. Different models were studied to analyze the aerodynamic behavior of airfoil with pitching motion being about quarter of the chord axis. The Reynolds Averaged Navier-Stokes K-omega shear stress transport model is used to predict turbulence. Y plus has been kept below one. A dynamic mesh technique with smoothing and re-meshing was used along with user defined function for unsteady pitch oscillating airfoil. Consequently, the proposed approach is appropriate and it can be used to capture dynamic stall phenomenon in various lifting objects e.g. helicopter rotors, wind turbine rotors and aircraft wings.

Keywords—VR-7 airfoil, dynamic Stall, computational fluid dynamics (CFD), performance modeling

I. INTRODUCTION

Studying transient pitching and oscillating airfoils are important due to aerodynamic instabilities, particularly dynamic stall. Dynamic stall (DS) is the phenomena of delayed flow separation, when the angle of attack (AOA) surpasses static stall angle due to variations in incoming flow and gusts. The delay in flow separation not just leads to vortex formation near the leading edge (LE) of the airfoil but also significant increase occurs the lift and drag forces until the vortex starts shedding. Once the LEV sheds, the airfoil goes into a state of deep stall [1]. The unsteady features associated with the dynamic stall phenomena are important in different aerodynamic applications including wings of aircraft, propellers, helicopter rotors and wind turbines. D Favier and his colleagues made incredible efforts to simulate the effects of fluctuating incidence and velocity simultaneously on the 2D aerodynamic performance of a NACA0012 airfoil [2]. A pitch oscillating airfoil for low Reynolds number (Re~10^5) was investigated numerically to understand dynamic stall of lifting bodies under varying free stream velocities. The results show that the high phase difference reduced the aerodynamic loads almost three to four times but increased the vortex growth times [3]. Numerical CFD analysis was performed on a large scale vertical axis wind turbine (VAWT) airfoil to investigate the influence of increasing Reynolds number, the results indicated that dynamic stall effects are delayed to higher angle of attack and consequently a higher maximum tangential coefficient is attained. In addition, increase in the freestream turbulence provided

better resistance to flow separation and also displays evidence of earlier flow reattachment following stall [4]. Reduced frequency also effect DS phenomena specially the LEV formation, delay in flow separation occurred at high incidence as the reduce frequency increased but the life time of LEV on the suction side decreased [5].

II. SPECIFICATIONS OF SIMULATED CASE

A VR-7 airfoil during steady state was pitching at fixed angle of attack (AOA) from 00 to 300. For transient analysis, the airfoil performs sinusoidal pitching motion about quarter (1/4) of chord length. The sinusoidal motion is described by instantaneous AOA equation

$$\alpha = \alpha_m + \alpha_a \sin(\omega t) \qquad (1)$$

Where α_m is mean AOA, α_a is oscillation amplitude and ω represents angular frequency. The oscillation amplitude 10^0 was kept constant throughout the CFD analysis [6]. Reduced frequency (k) is also a useful parameter which describe the unsteady aerodynamic behavior of an airfoil. It is used to illustrate the steadiness and unsteadiness of the flow. When k = 0, the flow is in steady state. For $k \geq 0$ and $k \leq 0.05$ the flow is called in quasi-state where the steadiness effects are small. Reduced frequency is described in terms of the airfoil chord, angular frequency and free stream velocity. Mathematically,

$$k = \frac{\omega * c}{2v_{\alpha}} \qquad (2)$$

Where v_{α} the free stream velocity and c is the chord length of airfoil.

III. NUMERICAL SETUP

A. Turbulence model

For CFD simulation ANSYS Fluent 15 [7] was used to model the flow field for constant and oscillating airfoil under constant incoming velocity. K-ω SST turbulence model was used for the simulations. It capture flow structures of dynamic airfoils near the surface as well as in the far field. Also, for a wide range of Reynolds numbers, K-ω SST model give better flow visualization. It is strongly recommended where highly accurate resolution of boundary layer is critical. According to k-w SST criteria, the value of Y plus (Y+) is kept below one [3][8].

B. Grid generation

An O-grid layout has been created with ICEM CFD 15 [9] as shown in Fig. 1. Different grid sizes were used to analyze the independency of the results. The final mesh grid has 20704 cells and 208004 nodes around the airfoil while the distance of the first row of cells from airfoil surface is kept 0.002. For accurate and stable numerical computations, quality of mesh plays an important role. Quality of the given mesh is around ninety percent (90%). The main domain of the fluid is fifteen times the chord length (15c) of the airfoil (Fig. 2). Freestream velocity is defined at inlet boundary condition from all sides.
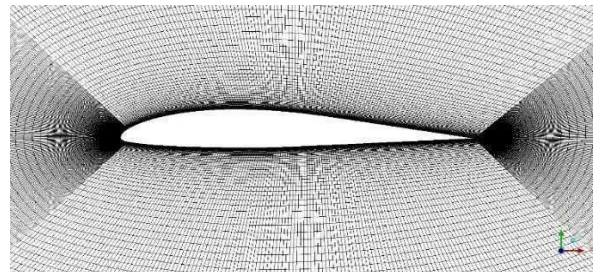

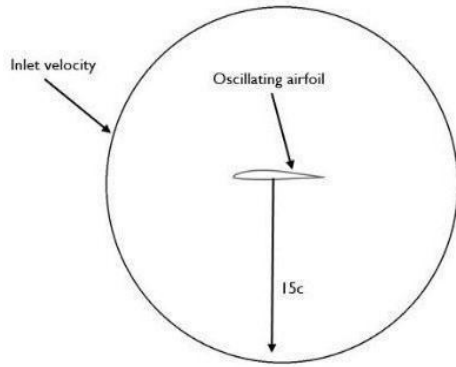Fig. 1. Structured mesh of VR-7 airfoil

Fig. 2. 2D airfoil, circular CFD domain

C. Solver setup

A dynamic mesh technique with smoothing and re-meshing is used along with UDF code for CFD analysis of 2-D VR-7 oscillating airfoil. The DM function is used for moving the airfoil mesh which is deforming with each time step. UDF is programmed in C language and compiled in FLUENT solver [9]. It is used to calculate the aerodynamic characteristics of an airfoil. The lift and drag coefficients are calculated against AOA for the VR-7 airfoil during steady and unsteady conditions. The pressure based Navier Stokes solution algorithm was chosen due to incompressible flow and SIMPLEC algorithm was preferred for the pressure/velocity coupling scheme. The residuals were (10^{-6}) in magnitude for the convergence criteria. The numerical results are compared with experimental data to check the validity of suggested numerical approach. The time step size 0.0001 is used for calculation over 50000 number of time steps (5 sec) for transient pitch oscillation of the airfoil.

IV. RESULTS AND DISCUSSION

The numerical simulation based on K-ω SST turbulence model are plotted for 200000 Reynolds number and reduced frequency value 0.10. To check the accuracy of the numerical simulation, the NASA results for VR-7 airfoil [6] are compared for steady and unsteady sinusoidal airfoil with oscillating amplitude of 100. The experimental and numerical results for lift and drag coefficients are plotted, under steady conditions in Fig. 3 and Fig. 4 respectively. Although the obtained numerical results are for transient flow. Fig. 5 and Fig. 6 represent comparison between K-ω SST turbulence model and the experimental results for lift and coefficient at mean angle of 10^0.

The acquired numerical results for Cl and Cd are approximated well with the experimental report of NASA. It is shown in Fig. 3 that the dynamic stall occurred early than experimental results, approximately at 13^0 degree as the roughness on airfoil surface is not accounted. Roughness have significant effects on the flow over airfoil. For stall region, the lift coefficient increase for rough surface over corresponding value for smooth surface, with higher increase for higher roughness size. Also, for pre stall region, it causes reduction in Cl. The minimum value for the Cd increasing with increasing roughness. Since smoothness is responsible for early dynamic stall, therefore separation mechanism is significantly affected by roughness size. Roughness leads to delay in flow separation on the airfoil surface, although airfoil efficiency decreasing with roughness [10]. Fig. 9 illustrates velocity contours at different angle of attack, dynamic stall phenomena occurred at 15^0.
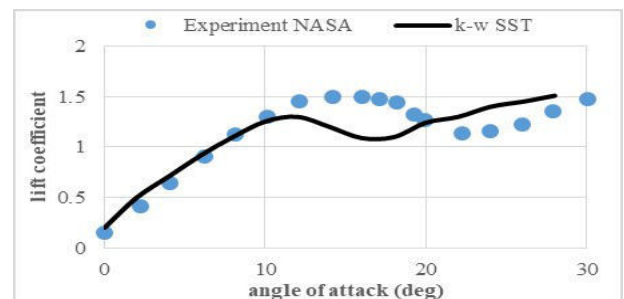
Fig. 3. Steady state coefficient of lift
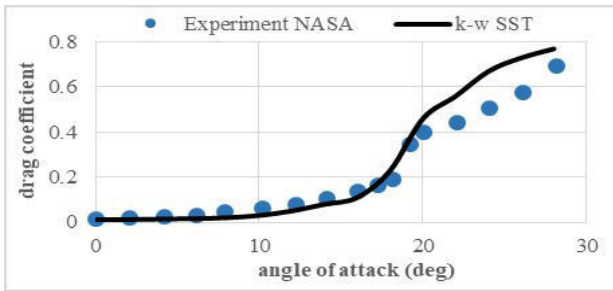
Fig. 4. Steady state coefficient of drag
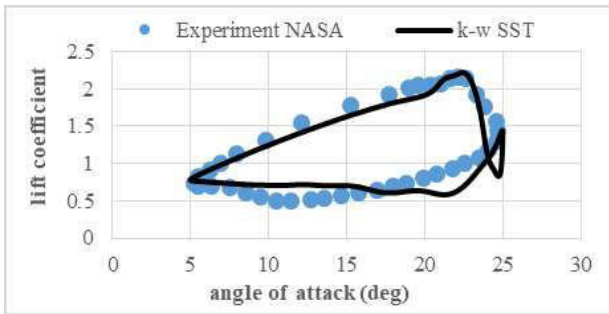
Fig. 5. Lift hysteresis for $\alpha_m = 15^0, Re = 20000 \ and \ k = 0.10$
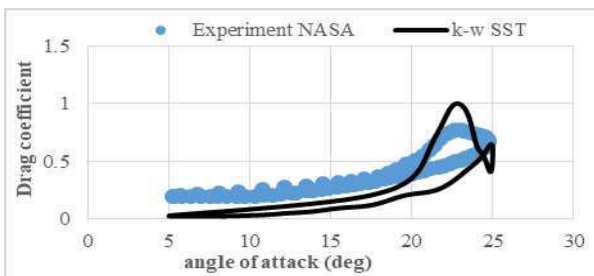
Fig. 6. Drag hysteresis comparison between experimental data and SST model
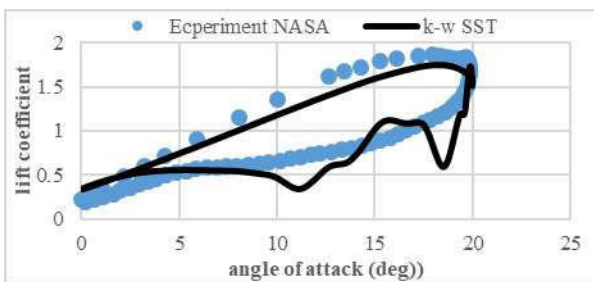
Fig. 7. Lift hysteresis for $\alpha_m = 10^0, Re = 20000 \ and \ k = 0.10$
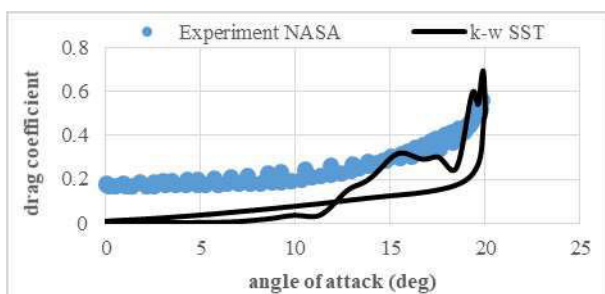
Fig. 8. Drag hysteresis loop
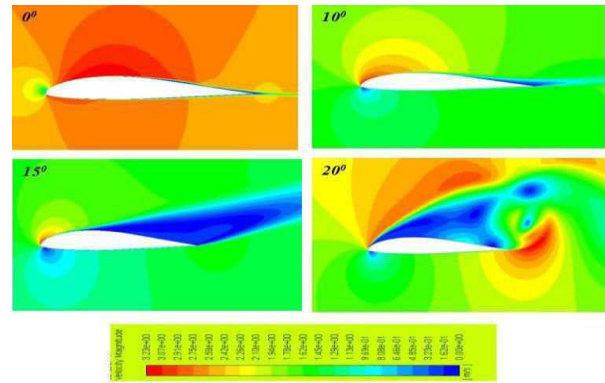
Fig. 9. Velocity contours at various AOA

V.   CONCLUSION

A pitch oscillating VR-7 airfoil was simulated numerically to understand dynamic stall phenomena in lifting objects at average Reynolds number. In the present study, although k-ω SST turbulence model is usually used for 3-D computations flow, here this model is used to capture the two-dimensionality of flow behavior well. Because of the comparatively good correspondence between experimental data and obtained airfoil numerical characteristics, it supposes the suitable choice of approaches including differencing scheme and grid resolution. Therefore, it can be concluded that the use of k-ω SST model capture reasonably well the dynamic stall region for 2-D VR-7 computations of pitch oscillating airfoil.

REFERENCES

[1]   A. Choudhry, M. Arjomandi, and R. Kelso, "Methods to control dynamic stall for wind turbine applications," *Renew. Energy*, vol. 86, pp. 26–37, 2016.

[2]   D. Favier, A. Agnes, C. Barbi, and C. Maresca, "Combined Translation / Pitch Motion: A New Airfoil Dynamic Stall Simulation," vol. 25, no. 9, pp. 805–814, 1988.

[3]   K. Gharali and D. A. Johnson, "Dynamic stall simulation of a pitching airfoil under unsteady freestream velocity," *J. Fluids Struct.*, vol. 42, pp. 228–244, 2013.

[4]   B. Hand, G. Kelly, and A. Cashman, "Numerical simulation of a vertical axis wind turbine airfoil experiencing dynamic stall at high Reynolds numbers," *Comput. Fluids*, vol. 149, pp. 12–30, 2017.

[5]   N. Guillaud, G. Balarac, and E. Goncalvès, "Large Eddy Simulations on a pitching airfoil: Analysis of the reduced frequency influence," *Comput. Fluids*, vol. 161, pp. 1–13, 2018.

[6]   K. W. Mcalister, C. Tung, and N. Aeronautics, "Suppression of Dynamic Stall with a Leading-Edge Slat," *Aviation*, 1993.

[7]   L. Wizard, "Release Notes," *Notes*, no. March, pp. 2–4, 2011.

[8]   A. Confidential, "Lecture Theme," 2014.

[9]   C. ANSYS, "Ansys Inc," *Canonsburg, PA, USA*, vol. 15317, no. November, p. http://www.ansys.com/es_es, 1998.

[10]   A. A. Abdel-Rahman and W. M. Chakroun, "Surface roughness effects on flow over aerofoils," *Wind Eng.*, vol. 21, no. 3, pp. 125–137, 1997.

Finite Element Analysis of Brick Masonry

[1,a] Faisal Rahman, [2,b] Shahid Ali Khan, [3,c] Saddiq Ur Rehman, [4,d] Muhammad Shoaib Khan, [5,e]Umer saleem.
[6,f]Shehroze Mughal, [7,g]Shahid Ahmad, [8,h]Muhammad Asim Aman

[1] Assistant professor, Civil Engineering Department UET Peshawar

[2,3,4] Researcher, Civil Engineering Department UET Peshawar

Email address: [a] faisal@uetpeshawar.edu.pk ,[b] 15pwciv4302@uetpeshawar.edu.pk,

[c] 15pwciv4335@uetpeshawar.edu.pk ,[d] 15pwciv4320@uetpeshawar.edu.pk , [h] Muhdasimaman@gmail.com.

Abstract--In this study numerical modeling of unconfined masonry is carried out using finite element analysis software Abaqus. The model selected for this study is concrete damaged plasticity which has the ability to describe the behavior of compression and tension in plastic range. Modeling is done in three diverse ways i.e. Micro-mechanical, Simplified-micro mechanical and Macro-mechanical, out of which macro- mechanical modeling was chosen, where the constituents of masonry is homogenized as an isotropic or anisotropic continuum. Testing of model for different pre-compression ratios is carried out and its load displacement curve and total energy versus time curve are plotted. At different limit state the numerical and experimental results are compared in term of drift ratio. The results of numerical modeling and experimental modeling are in good agreement.

Keyword—Abaqus, Masonry, continuum, load displacement curve, isotropic, pre-compression.

I. INTRODUCTION

Most of the structure in Pakistan are made up of brick masonry. In early stages of masonry structures, designs were normally based on a great exact insight without scientific or prescient techniques. It is still broadly utilized because of its ease of construction and simplicity with low material expense and aesthetics. It's a composite of two different materials in which blocks (a building unit made of any specific material e.g. brick) are laid upon each other with binder or cohesive material i.e. mortar in between them. Materials are distinguished from each other by their mechanical properties and have different response towards loading. Brick masonry are used in structure due to its loads transfer mechanism but it has poor performance and needs confinement when subjected to in plane lateral loadings. This behavior causes the masonry to damage and its response towards such loadings has to be measured experimentally and numerically to get benefits from masonry. For this masonry model is tested for different material and mechanical properties in physical to find its response for different conditions and then mathematical technique is used for numerical modeling using software. Predicting the complex behavior in any computational framework is a significant challenge for researchers. The modern development in technology has enabled the researchers somehow to model the masonry with its complexities using Finite Element Analysis. For the consideration of every brick and joint separately complex model can be created but in practice the use of simple models are of more importance where less analysis time is desired. For accurate, precise and complex analysis developed, such as ANSYS, LS-DYNA, ABAQUS, etc. In this study ABAQUS has

been chosen as a tool for the numerical modeling of masonry.

Abaqus is a finite element analysis application which helps in solving the analysis problems ranges from simple linear analysis to complex nonlinear analysis (1). Abaqus can solve problems that contain modeling of different elements by associating the material and geometry of each element and then selecting their interactions. This software chooses convergence tolerances and load increments in nonlinear analyses. In this way Abaqus adjust the different conditions for insuring that an accurate result is obtained for complex and simple problems.

II.   METHODOLOGY

This part represents modeling procedure of masonry walls.the model isotropic homogeneous one as simple .The model is considered as "concrete damaged plasticity model" defined in ABAQUS meterials .

A. MODEL GEOMETRY

The model is defined as only one part and then their properties and section is defined and then material assigned.At the end the part module is meshed for which global seed of(0.05) is assigned.similarly interaction properties is also defined for this part. Element type is explicit 3D stress element.
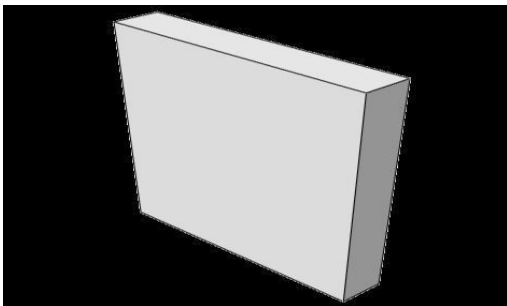
Figure 1: Masonry Wall
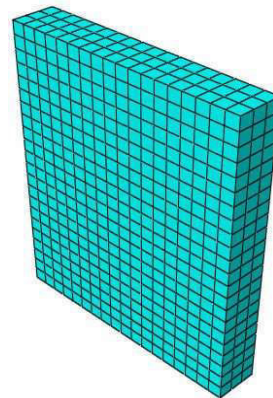
Figure 2: Meshed Masonry Wall

B. MATERIALS:

In this module we have defined the material properties to define for model. Generally three types of properties are required for the model i-e, density, plasticity and concrete damaged plasticity for the wall masonry .

The process is prescribed as under.

i.   Plasticity

The plastic parameters used in brick masonry model is tabulated here in Table.1

Table 1: Plasticity Parameters				
Dilation Angle	Eccentricity	f_{b0}/f_{c0}	K	Viscosity Parameter
45	0.1	1.3	0.51	0

ii.   Compressive Behavior

The   compressive   strength(4.79MPA) calculated from an empirical equation is very   close   to   an   experimental value(4.54MPA).So   the   compressive strength versus strain can be determined using empirical equation(2).the value of strain is assumed to be around 0.004 because their exact value is not known(2).Instead of 0 .27 various values are used and finally 0.4 for the model is taken. For the stress strain graph, the remaining values are calculated using equation 1 to 3.

$$f^l_m = f_i + (f'_m - f_i)\left(\frac{2\varepsilon_m}{\varepsilon'_m} - \frac{\varepsilon^2_m}{\varepsilon'^2_m}\right)^{0.8} \tag{1}$$

$$f^2_m = f'_m + (f_{mid} - f'_m)\left(\frac{\varepsilon_m - \varepsilon'_m}{\varepsilon_{mid} - \varepsilon'_m}\right)^2 \tag{2}$$

$$f^3_m = f_r + (f_{mid} - f_r)^{2\left(\frac{f_{mid}-f'_m}{\varepsilon_{mid}-\varepsilon'_m}\right)\left(\frac{\varepsilon_m-\varepsilon_{mid}}{f_{mid}-f_r}\right)^{1.5}} \tag{3}$$

Where,

f'_m Is the crushing strength

ε'_m Is the peak strain at the crushing strength

$f_i = \frac{1}{3}f'_m$ (Initial stress)

$f_{mid} = \frac{1}{2}f'_m$ (Mid stress)

$f_r = \frac{1}{4}f'_m$ (Rupture Stress)

ε_{mid} Is 2.25 times greater than ε'_m
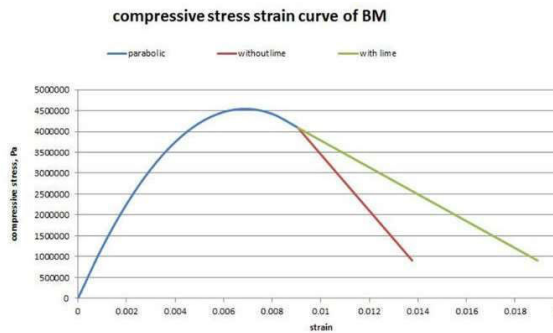
Figure 3: Compressive Stress-Strain Curve

In case of compressive stresses outside elastic range, a stress σ_c versus inelastic deformation is defined as a tabular function shown in fig.4

Plastic strains are determined automatically by ABAQUS program from inelastic strains.

Compressive Elastic strains are determined by an equation(4)

$$\varepsilon^{el}_{c0} = \frac{\sigma_c}{E_0} \tag{4}$$

Using equation (5) we can determine inelastic deformation

$$\varepsilon^{in}_c = \varepsilon_c - \varepsilon^{el}_{c0} \tag{5}$$

Equation(6) are used to calculate plastic deformation

$$\varepsilon^{pl}_c = \varepsilon^{in}_c - \frac{d_c \sigma_c}{(1-d_c)\,E_0} \tag{6}$$

Figure (4) shows graphical representation of equation(4) to equation(6)
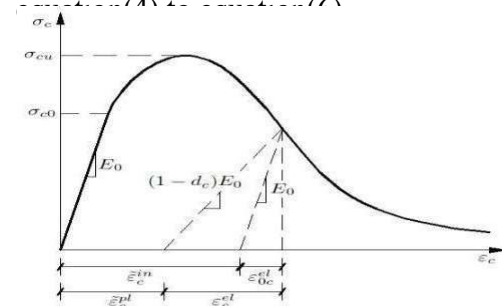
Figure II: Definition of Compressive Inelastic Strains

Equation(7) is used to calculate the damaged parameter(dc)

$$d_c = 1 - \frac{\sigma_c}{\sigma'_c} \tag{7}$$

The compressive strength of masonry is represented by σ'_c in equation(7)

Table (2) represents inelastic strains and damaged parameters corresponding to yield stresses.

i. Tensile Behavior

Here the wall is under the shear compressive load and their behavior under such condition is shown in Fig(5)

Table 2: Compressive Behavior		
Yield Stress (10^6 Pa)	Inelastic Strain	Damage Parameter
1.224175	0.00051	0
2.256534	0.001097	0
3.097077	0.00176	0
3.745805	0.002501	0
4.202718	0.003318	0
4.541097	0.005182	0
4.422563	0.00623	0.026102
4.112214	0.007354	0.094445
4.088188	0.007422	0.099736
0.908486	0.0134	0.799941
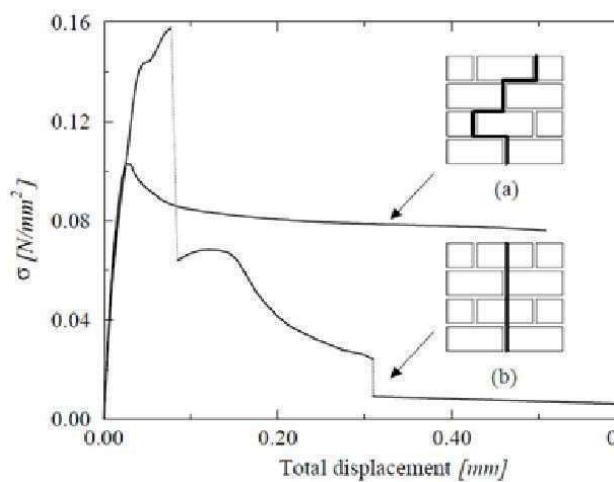
Figure 5: Results of the Tensile Test Parallel to the Bed Joint (Backes (1985)) (4)

Here it has be noted that when the crrack propagates and opens then the friction forces between the bricks develops and increases, so the masonry has also considerable strength even after cracking starts and opens.Therefore a masonry wall has some stresses at ultimate strain shown in Fig(6).At value of 0.2 the" C" the experimental results.Stress strain curve are shown in fig(6)
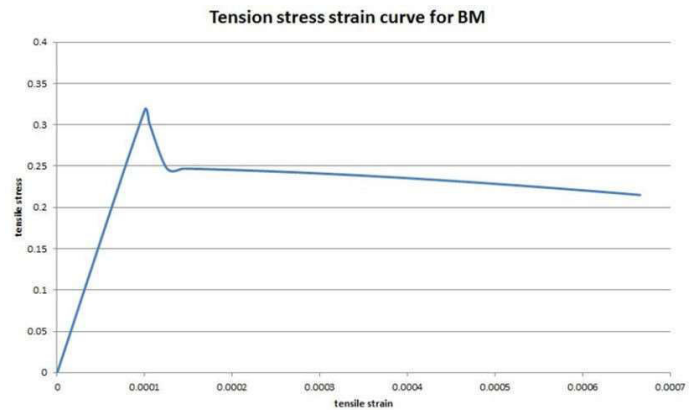
Figure 6: Tensile Stress-Strain Curve

Similar to the compression strain, tensile inelastic strains are calculated.Tensile inelastic strains can be determined by using equation(8)

$$\varepsilon_{t0}^{el} = \frac{\sigma_t}{E_0} \qquad (8)$$

Inelastic strains can be determined by using equation(9)

$$\varepsilon_t^{in} = \varepsilon_t - \varepsilon_{t0}^{el} \qquad (1)$$

Plastic strains are calculated using equation(10)

$$\varepsilon_t^{pl} = \varepsilon_t^{in} - \frac{d_t}{(1-d_t)} \frac{\sigma_t}{E_0} \qquad (2)$$

Figure(7) represents graphical representation of equation(8) to equation(10)
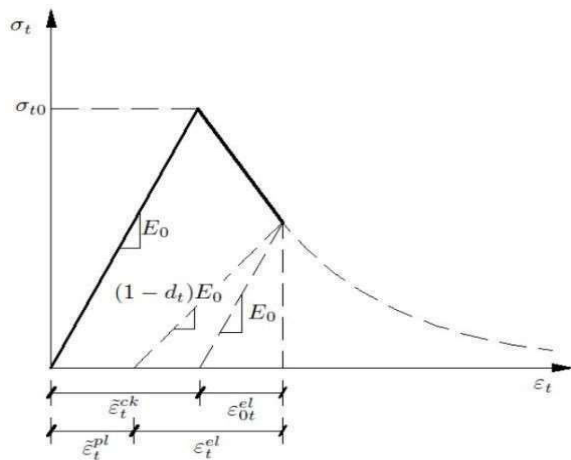
Figure 7: Definition of Tensile Inelastic Strains

Damaged parameter (dt) can be determined using equation(11)

$$d_t = 1 - \frac{\sigma_t}{\sigma'_t} \qquad (3)$$

Masonry tensile strength is represented by , σ'_t

Table(3) represents damaged parameters and inelastic strain correspondence to yield stresses.

Table 3: Tensile Behavior		
Yield Stress $(10^6 \, Pa)$	Cracking Strain	Damage Parameter
0.263	0	0
0.247	0.000029	0.06325
0.235	0.000057	0.10819
0.226	0.000084	0.14267
0.218	0.000111	0.17044
0.212	0.000138	0.19356
0.207	0.000164	0.21328
0.203	0.000190	0.23042
0.199	0.000216	0.24554
0.195	0.000242	0.25904

0.192	0.000268	0.27120
0.189	0.000293	0.28226
0.186	0.000319	0.29238
0.184	0.000345	0.30170

Table(2) and Table(3) are used to assigned values to "concrete damage plasticity model"

Two parts are created.one is concrete and the other one is masonry. Both are assigned solid homogeneous sections in a property module

C. STEP DEFINITION

Dynamic explicit step is more suitable for this model because masonry wall in this case has Quasi-static in plane lateral loads.(3)

In ABAQUS program only one step is defined by default(initial step. Here we defined two additional steps.one is displacement controlled step in case of lateral loads and one is precompression step for pre-compressive loads. For displacement controlled step time increment defined is 1200sec and for precompression step 30 sec is defined. Computationally the analysis is very time consuming and costly so we defined the time scaling for the speeding of analysis process having a scale factor of 1000 defined in semi-automatic mass scaling option which helps in increasing the density of meterials(3).

D. ASSEMBLY

As we defined two parts in part module(Masonry wall and beam). To assemble both of these parts Assembly module is used where the beam is placed at the top of masonry wall. Tie constraint is used to tie the beam to the top of masonry wall using interaction module where discretization method has been used.by using coupling type constraint a Refrence

point is constrained to the bottom of the wall.
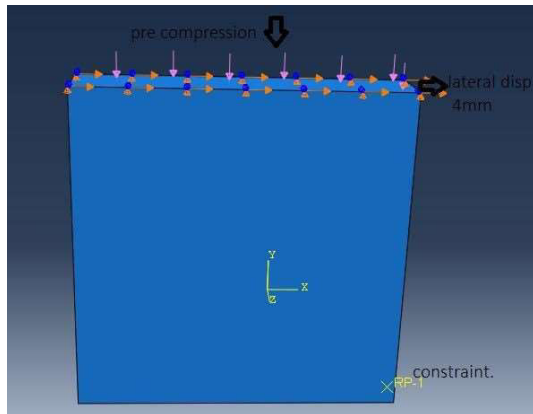
Figure 8: The Assembled Model

E. BOUNDARY CONDITIONS & LOADS

The boundry condition is applied to the refrence node(RP-1) and boundry condition is ENCASTER type.Displacement type boundry condition is applied to beam. The vertical displacement is restrained so putting (U3=o) and lateral displacement is allowed(U1=0.004m).The procedure of operation is such that it is placed undercompression in precompression step and then subjected to displacement continuous step upto end.

F. OUTPUT REQUESTS

In output request define those variable which are of interest.we added compression and tension damage variables for all analysis procedure and time of 5 second are set for the frequency of output values.Reaction force(RF) in X-direction is also defined in output history request for which refrence point is considered as domain and added to a set.also displacement in x-direction (U1) is also defined for which domain at the top of wall is considered and added as a set.

III. RESULTS AND DISCUSSION

Finally job module is used to run the analysis and X-Y plots are extracted as the analysis completes.Also stress strain curves is extracted from output history request.

A. LOAD-DISPLACEMENT CURVE

Fig(9) Represents lateral load-lateral displacement curve
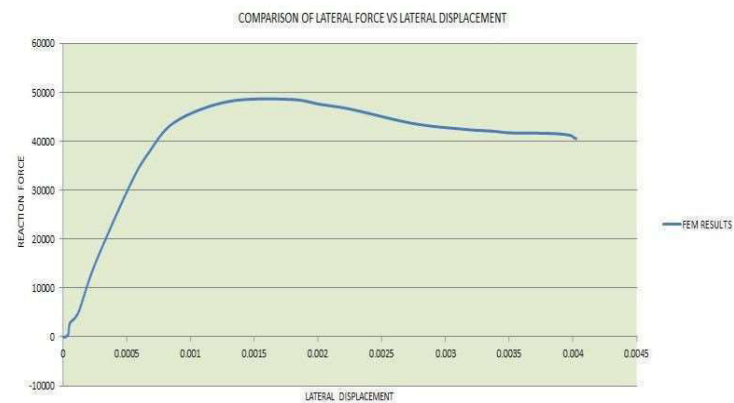
Figure 9: Load-Displacement Curve of FEM model

At lateral force of 48KN and lateral displacement of 0.51mm flexural tension damage starts and for that performance level of operational(O) is considered.At the center of the model significant damage starts due to tensile stresses at 0.90 displacement.The crack propagates diagonally towards the corners of the wall and correspondence horizontol load is 25KN.At 55kNload and corresponding displacement of 1mm, diagonal crack appears and regarded as intermediate occupancy level(IO) performance.

B. COMPARISON WITH LAURENCO

LEURENCO Positive direction hystereses results for model was compared with Getdata graph digitizer(5) and plotted as shown in Fig(10).Metric units are converted to imperial for comparisoin
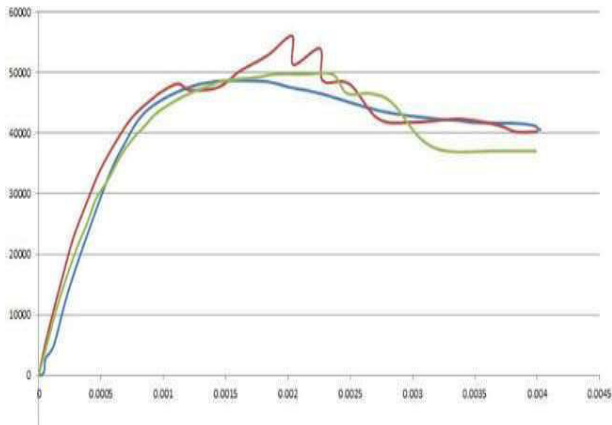
Figure 10: Comparison of the Results

C. STRESS-STRAIN VISUALIZATION

Contours of stress strain results are illustrared here where plastic strains and stresses are shown.
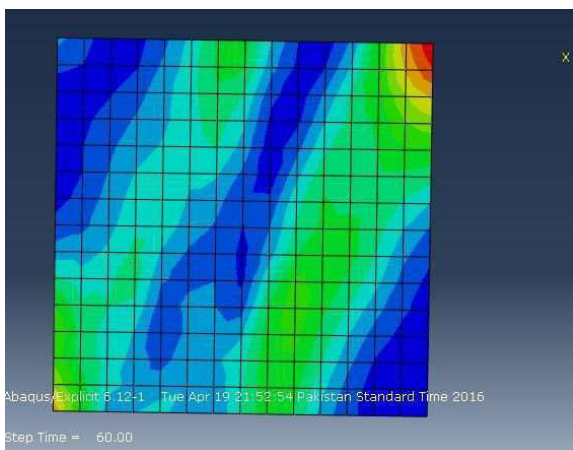
Figure 11: plastic strains
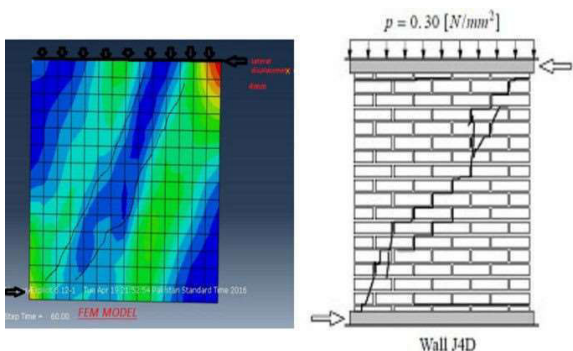
Figure 12: comparison of results

IV. CONCLUSION AND RECOMMENDATION.

This numerical study was carried out on already experimental study of masonry structure by Lourenco P.B. (1996) and its load displacement curve was compared for different limit state.

In this study, the numerical model is elastically calibrated with the experimental result with the help of empirical equation and elastic modulus found out to be 4070 MPa.

Concrete Damaged plasticity is used as an inelastic model which can easily show the damage in the both tension and compression. The default values of tension and compression are determined from mathematical expressions and using these default values as a starter the plasticity parameters are determined by trail test.

Masonry is constituent of brick and mortar therefore it has to be modeled anisotropic to show more realistic behavior in numerical modeling. For anisotropic modeling three methods can be adopted.

First method is anisotropic homogenous method in which the input is two different material properties in vertical and horizontal. Abaqus show anisotropy only for elastic behavior while for inelastic behavior user defined material compiled in FORTRAN is recommended.

Second method is building the model brick by brick and join the by a binder or cohesive material whose thickness is negligible or act as interface. Half of the binder (mortar) thickness is added to brick all dimensions. This method very helpful and simple and is recommended by most of the researchers.

Third method is building the model brick by brick by taking into the account the mortar thickness between the bricks. This method

takes too much time so it is not recommended for large modeling e.g. walls. It is only helpful for micro level modeling of masonry for homogenization.

It was found out that the procedure is not helpful in case of cyclic loading so it is recommended for future study that FORTRAN compiler should be used for cyclic loading.

V. REFERENCES:

1. Abaqus Analysis User's Guide – "Fully coupled thermal-stress analysis,"

2. Hemant B, Kaushik, Rai D.C., and Jain S.K. (2007), "Uniaxial Compressive Stress-Strain Model for Clay Brick Masonry", Current Science, 92(4), Indian Academy of Sciences, Bangalore, India, 25 February 2007, pp.497-501.

3. "Abaqus/Aqua analysis," Section 6.11.1 of the Abaqus Analysis User's Manual

4. Backes, H. P. (1985), Behavior of Masonry Under Tension in the Direction of the Bed Joints, PhD thesis, Aachen University of Technology, Aachen, Germany.

5. Lourenco, P.B. (1996), Computational Strategies for Masonry Structures, PhD thesis, Delft University of Technology, Delft, The Netherlands.

Dual-Mode Triboelectric Nano-generator for harvesting Energy

Syed Abbas Raza[1,a], M. Imran Khan[1,b], Mairaj Ahmed[1,c], Danish Tahir[1,d], Asim Iltaf[1,e], Nayab Jamal[1,f]

[1]Ghulam Ishaq Khan Institute of Engineering Sciences and Technology, Topi, 23640, KPK.

[a]gmm1846@giki.edu.pk; [b]imrankhan@giki.edu.pk; [c]gmm1845@giki.edu.pk; [d]gmm1844@giki.edu.pk; [e]gmm1843@giki.edu.pk; [f]nayab.jamal@giki.edu.pk

Abstract- *Tribo-electricity, also referred to as Static Charge which is explained as the phenomena of production of a charge on material by bringing it into contact with an object of opposite nature. The Dual Tribo-Electric Nano-Generator is a construction used for harvesting energy from water by two principles, the first focus being the charge carried by water and the second being the kinetic energy of water from moving source. A robust setup is used consisting of an integrated separator. The negatively charged material employed is Poly-Vinyl Chloride (PVC) and the positively charged material is Silicon Dioxide. The PVC sheet was procured locally and the SiO₂ thin layer was deposited via E-beam evaporation. In addition to these main components, additional parts also played a crucial role. SiO₂ mono-spheres were deposited over the SiO₂ layer to increase the overall contact area). The SiO2 spheres were produced by Stober Method.) Then, since the primary purpose of this Tribo-electric Nano-Generator was to serve under the impact of water, a hydrophobic layer was necessary to negate any absorbance of water by the exterior PVC film, so as to prevent failure of the TENG. The method employed for this task was Chemical Bath deposition (CBD) of Titanium Dioxide Nano-Materials Layer on the PVC film. The resultant layer was adherent and prone to flaking off due to the flexibility of the film substrate. It was dipped into a stearic acid solution after which it showed hydrophobicity. The substitute to Silicon Dioxide was Glass Fiber which according to the authors was comparatively more positive Tribo-electrically against Silicon Dioxide. Both Nano-Generators were compared in terms of output.*

Keywords--- *Tribo-electric, Energy harvesting, Titanium Dioxide, Thin film, SEM, AFM, Potential.*

I. INTRODUCTION

The demand for energy has continued to grow amid increasing digitization of the infrastructure and continued increase in human population with an expected overall increase by up to 50% until 2030. On top of that legitimate dangers concerning ozone depletion and the resultant greenhouse effect have given rise to more concentrated efforts to shift towards green energy. The lead has shifted towards nano-technology as the new frontiers for energy harvesting and powering modern devices. From these pioneering concepts came forth the idea of Nano-Generators in 2006 at Georgia Institute of Technology by [1]. The initial development of this device was based on ZnO based nano-material in conjunction with piezo-electric devices. However, with progressive research overtime, additional branches/sources of energy have been developed successfully; namely the pyro-electric and Tribo-electric effect[2].

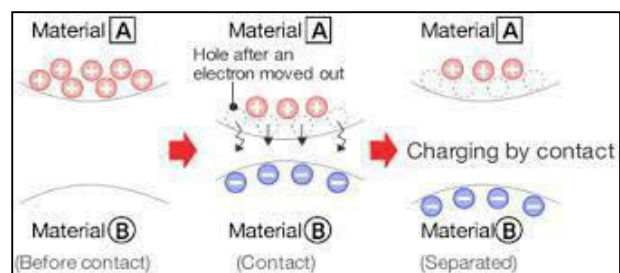Tribo-electrification (fig.1) is a concept of physics which has existed for extensive time

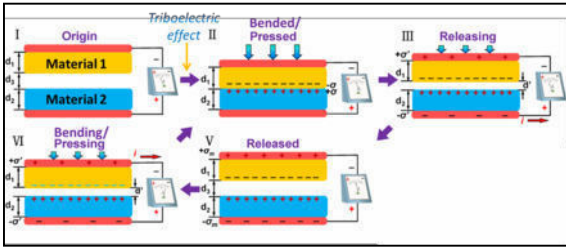Fig. 1 Shows the triboelectrification

Fig. 2 Shows the contact separation mode.

Figure 4 Single electrode mode

prior to utilization, usually being associated with negative consequences, until its potential was recognized as a favorable energy source[3], [4]. Utilization of energy with devices associated with the tribo-electric effect involves contact between oppositely charged materials to generate a potential difference which would drive a current around a closed loop circuit. This however, has not been the first attempt at the utilization of this phenomena with the Van De Graff and Wilmshurst machine representing the more traditional approach to the tribo-electric phenomena.

What currently makes up as a hinderance for researchers is a lack of clarity with regards to the tribo-electric effect. Previous research has involved efforts to collect charge from rolling particles and measure them via interaction with AFM. However, they have their shortcomings as they fail to understand the *in situ* mechanism of electrostatic charge formation. Currently, due to exceptional pace and innovation, the tribo-electric nanogenerator has been designed and categorized into four different working principles which are as follows:

A. Vertical-Contact based Separation Mode

This is the first working principle in the field of Triboelectric nanogenerator. Two films are brought into physical contact possessing both different electron affinity and upon separation develops a potential difference between the two films. Being connected by a load would result in

Figure 3 The in plane sliding mode

the flow of electrons between the two films hence current formation occurs. The continuous closing and opening of the contact between the two layers results flow of current back and forth hence an AC current generation occurs. This particular principle has two mods of operation. They are[2]:

1.) Dielectric-to-Dielectric Mode: This form of TENG involves Interaction between two different types of polymer sheet by mechanical forces oriented or applied vertically and upon release charge generation and potential difference forms and provides additional benefit given the fact that the polymers have ability to retain charge extended long times of up to hours make it an interesting prospect to work with [2]. The potential of the top electrode can be calculated by the following formula if the potaential of the bottom electrode is taken as zero:

$$Ute = -\frac{\sigma d'}{\epsilon 0}$$

Where the symbol σ represents triboelectric charge density, ϵ_0 represents vacuum permittivity, and d_0 is the gap between the layers at a given distance.

2.) Metal-to-Dielectric Mode: This form of TENG operation involves contact between highly negatively charges tribo- electric material and positive materials such as that of Teflon and copper. Which subsequently results in generation of the negative charge on Teflon for example and positive on copper and gold. Electrons flow to the copper on account of its electro positive nature from ground
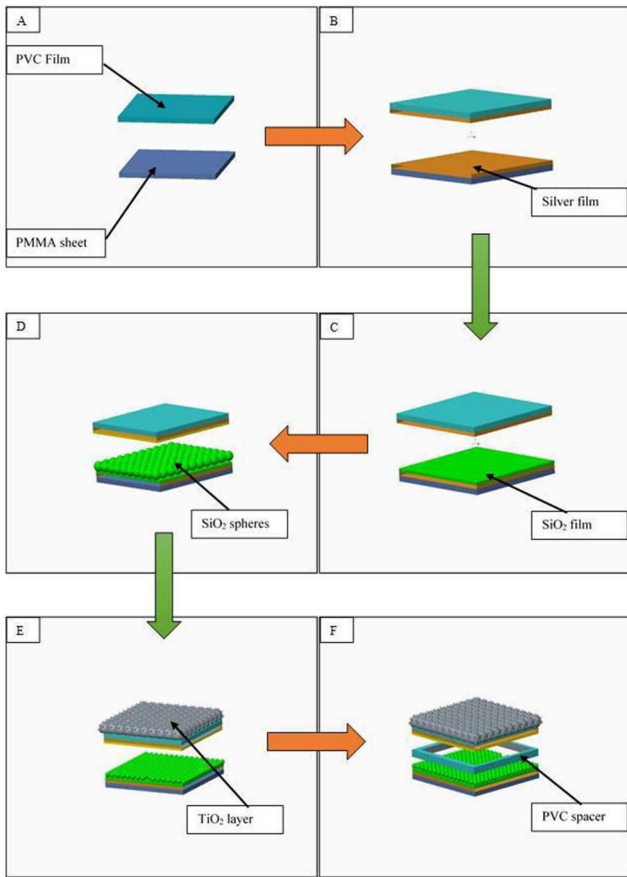
Fig. 5 Shows substrate (a) the substrates, (b) Silver deposition, (c) SiO$_2$ film deposition, (d) SiO$_2$ Spheres, (e) TiO$_2$ film and (f) integration with PVC spacer.

connection. This results in accumulated charge density on the surface of the electrode which can be calculated as follows:

$$\sigma 1 = - \cfrac{\sigma}{1 + \cfrac{d1}{d2\epsilon rp}}$$

Here, the term ϵ_{rp} and d_1 represent permittivity and thickness of the negative charged layer whereas d_2 represents the interlayer distance between the positive and negatively charged material surfaces. Therefore, when two material move closer it causes a positive current to flow between them where by drifting them apart results i the generation of the negative current.

B. In-Plane Sliding Mode

The underlying principle of this mode of TENG operation is the same as any other [1], resultant contact and separation between materials of opposite triboelectric polarities being brought in conjunction with each other the resultant contact generates charge on the surface of both materials, which leads to the current flow in the closed circuit in conjunction with the position of the charge generated (fig. 3). This can be more practically elaborated between two trbo-electrically polar materials such as Teflon and Aluminum which come into contact via sliding action driving them towards each other. The resultant alignement between the electrodes determins the current direction and its generation such that when the electrodes are in complete contact there is zero net charge no current flows however as sliding occurs so net charge results which causes a flow of electron from the aluminum to teflon and current flows. As such constant sliding between the surfaces of the material results in alternating charge flow or alternating current generation.

C. Single Electrode Mode

In the previously two elaborated methods of Nanogenerator fabircation and operation principle, the electrodes in question had to be physically in connection so that charge transfer and current generation can take place (fig. 4). However such design conception lead to considerable number of limitations given the fact that nanogenerator concept invoked the matter of flexibility in power generation from nature assisted stimulii so such hinderances are not to be expected [5], [6]. The single electrode mode of the nanogenerator was developed with the focus in mind to resolve this particular issue.

A more conformed example of this mode of operation can be seen in Figure. 4 where the single installed elctrode acts as charge collector with the question being dry human skin and PDMS polymer. AS previously mentioned in our discussions, when both the skin and the
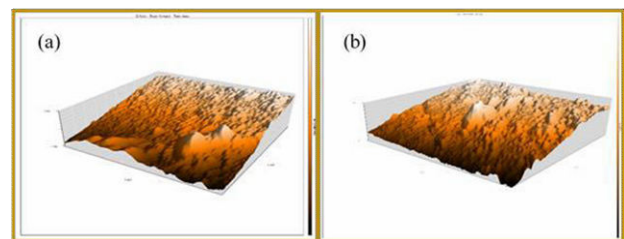
Figure 6. the silver film at (a) 5 µm, (b) 10 µm
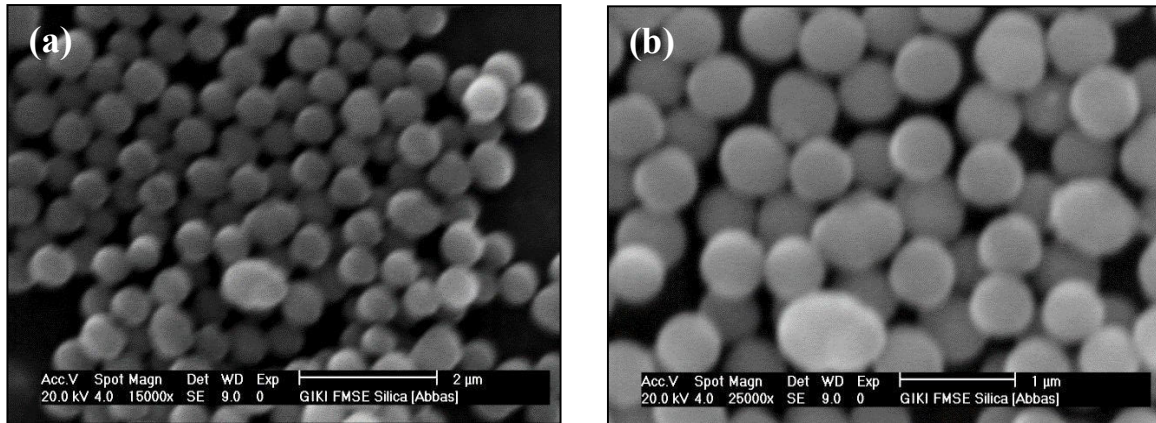
Figure 7 (a) the silica spheres at 15000x and (b) 25000x.

PDMS are in complete contact the net charge flow across them is zero. Upon releaase excesss negative charge prompts the formation of positive charge on the ITO substrate which causes flow of electrons from the ground to the substrate hence current is generated.

TENG has stemmed from the extensive focus of electronics to minimze and space and maximize potential towards electronics possessing flexibility and multiple functionality which alloes for greater value on the device. The TENGs have been modelled based on their smart potential as sensors over the decade.

Furthermore, they have been utilized successfully for harvesting potentially extensive mechancial energy of water from ocean and other moving sources of water whereas their chemical and design characteristics have allowed for them to be utilized as ethanol sensors and pressure sensors.

The in plane sliding and single ontact sliding devices have excelled In harvesting energy from wind for energy generation whereas the single electrode design has been used in harvesting energy from tires, wind and more

II. EXPERIMENTAL WORK

Engineering has progressed remarkebly to incorporate unique devices which allow for a smarter lifestyle and workspace and as th TENG is concerned they tuilize certain from of mechanical stimulii to work or operate (fig. 5). The research focus that was implemented was made to harvest tribloelectric energy from the charge on tap water and the mechanical force of the water falling from the tap.

The Lower TENG began with the substrate (PMMA) and ended with the Top most layer SiO_2 spheres. The step by step is as follows:
1) Clean the PMMA Substrate (2 mm thick).
2) Depositing the Silver thin film by thermal evaporator route.
3) Deposit of Silica Thin Film by E-beam evaporation
4) Deposition of silica mono-dispersed spheres by drop casting.

A. The Separator

The spacer was fabricated with a nominal thickness of 0.6 mm with the outer width of the edges being approx. 2 mm. The spacers were, to maintain form and uniform dimension, were fabricated via CNC machine.

B. The Upper region of TENG

The upper TENG began with a PVC of thickness 50 μm and was later used as the base or deposition of Nano-materials. T:
1.) Deposition of Superhydrophobic layer of TiO_2 on the upper layer[7],
2.) Uniform layer of Silver deposited on the lower part of the film.
3.) The lower part was attached to the spacer.

C. Deposition of Silver and Silicon Dioxide

The electrode materials deposited on the PVC and the PMMA substrate was silver as uniform thin films approx. 100 nm thick which were
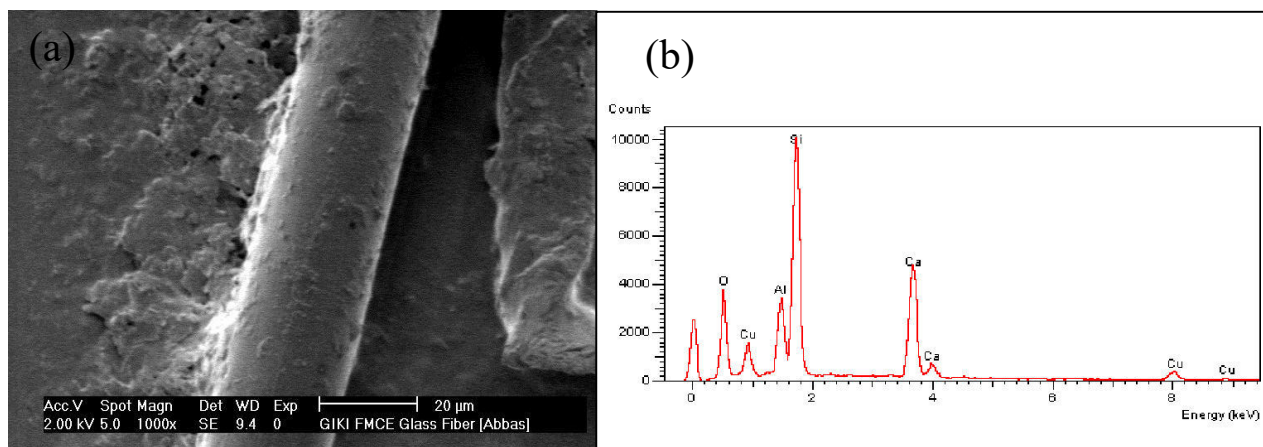
Figure 8 (a) SEM at 1000x magnification, (b) EDS Analysis.

deposited on the substrate via Edwards Auto 306 thermal evaporatar via resistive heating inside a graphite crucible. On the other hand, the Silicon Dioxide thin film was deposited on the substrate via e-beam based evaporation deposition. The resultant thin layer of both electrode and oxide was evaluated using Nanosurf Atomic Force Microscopy.

D. Preparation of Silica Particles

Two solutions were prepared simultaneously for the synthesis of this product. Solution A consisted of mixing 135 ml Ethanol and 9 ml of Tetraethyl Orthosilicate (TEOS) in a separate beaker which was stirred at room temeprature for a duration of 15 minutes. The second solution was prepared in this duration and consisted of adding of 8 ml of 32% Ammonia solution to 10 ml of DI water which was slowly added to the stirring solution A and the mixture was left to stir at 600 rpm for 6 hrs. and then stored overnight. The sol was then stirred in centrifuge machine at 3000 rpm and washed alternately with ethanol and DI water with last washing by DI water. The speheres were dried in air at 120˚C followed by calcination at 500˚C. substitute for them were Glas fibres which were characterized via SEM, EDS analysis.

E. Titanium Dioxide film

The nanostructured layer of Titania was deposited on the PVC substrate. A transparent glass bottle of 1 Litre capacity and glass stopper was used and rnsed with De-Ionized (DI) water.

A mixture of 100 ml DI water and 12 ml Titanium Tri-Chloride was added to it. The PVC substrate was placed in the bottle (floating) and the solution was kept at 120˚C for 12 hours. The substrate was removed from the bottle and the excess layer (unbonded) was removed by rinsing via ethanol and then dipped in stearic acid solution followed by being left to dry.

III. RESULTS AND DISCUSSIONS

A. The Silver electrode
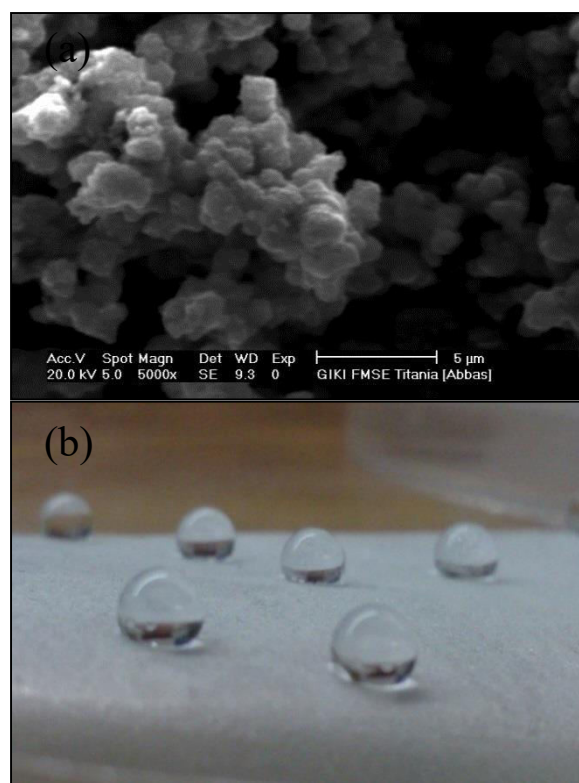
Figure 9 show (a) microstructure of film (b) surface treated film
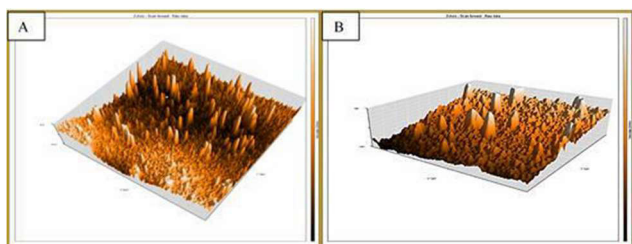
Figure 10 show (a) higher deposition rate film, (b) lower deposition rate

The AFM imaging on the silver substrate shows the formation of depressions underlying the fact that certain degree of discontinuous regions exist in the film with the obtained mean roughness, R_m, of -1036.3 nm. The surface morphology of the the silver shows lesser degree of non uniformity in the roughness of the film deposited. The high degree of roughness is a measure of the distance between the electrode and the source which produces the resu;ts when coupled with the slow depostition rate used in the process in roder tom minimize distortion of the substrate due to heat effect coupled that with

Additionally, given the relatively lower degree of silver adherence compared to copper , silver being a oble metal, the film could have
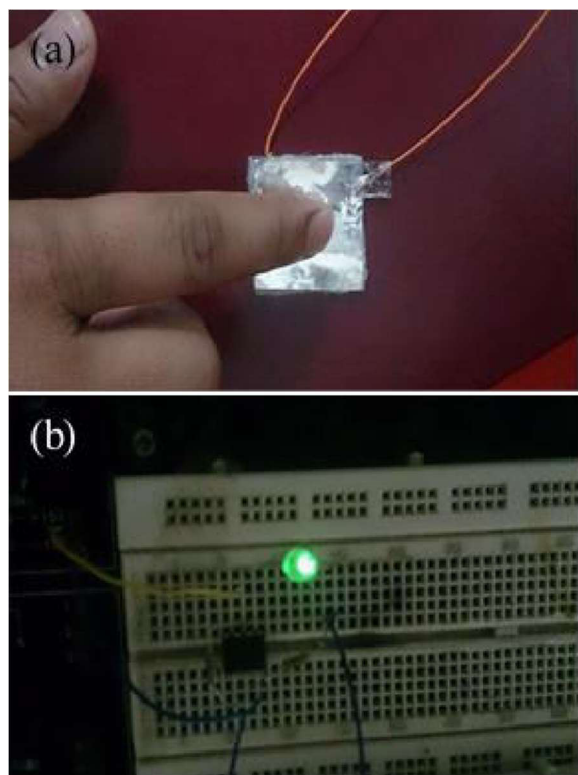
Figure 11 (a) compression of TENG, (b) LED lighting.

undergone tarnishing due to handling or movement..

B. The Silicon Dioxide Spheres and Glass Fiber

The BSEM images taken of the calcined silica nano-spheres shows them to have an approximate (fig. 7). The ratio of the ammonia added, which acts as a catalyst, was lower end which contributed to the smaller size of the particles. This is due to the fact that the rate of hydrolysis and condensation are both directly proportional to the concentration of ammonia in the solution[8], [9]. Decrease in the concentration of ammonia in the solution leads to a decrease in the formation of the intermediate $[Si (OC_2H_5)_{4-x} (OH)_x]$ as result of slower hydrolysis rate.[10], [11] and when it reaches the supersaturated state the nucleation period increases which leading to greater quantity of nuclei formation and resulting in a decrease in Colloid formed of the SiO_2. The glass fiber characterized via SEM showed to have a diameter of 20 micrometer and EDS (fig. 8) analysis showed it to have a major composition of Aluminum Oxide and Calcium Oxide which indicated that this is a E-type fiber[12].

C. Titanium Dioxide Film

The deposited layer of TiO_2 showed a unique nanostructured morphology of pin like growth on the surface of the island like growth of TiO_2 on the PVC surface. The resultant behavior after being treated in stearic acid solution showed that the static angle behavior with superhydrophobic behavior and the sliding angle of relatively high of the nano-structured layer.[13], [14].

D. Silicon Dioxide Thin Film

The morphology of the deposited layer of the Silica showed discontinuous structure which is attributed to vapor forming nature of the silica due to its high boiling point which cause short vapor burst to form and travel towards the substrate in the evaporation chamber leading to a more island like film formation[15], [16]. Furthermore, the deposition rate which is
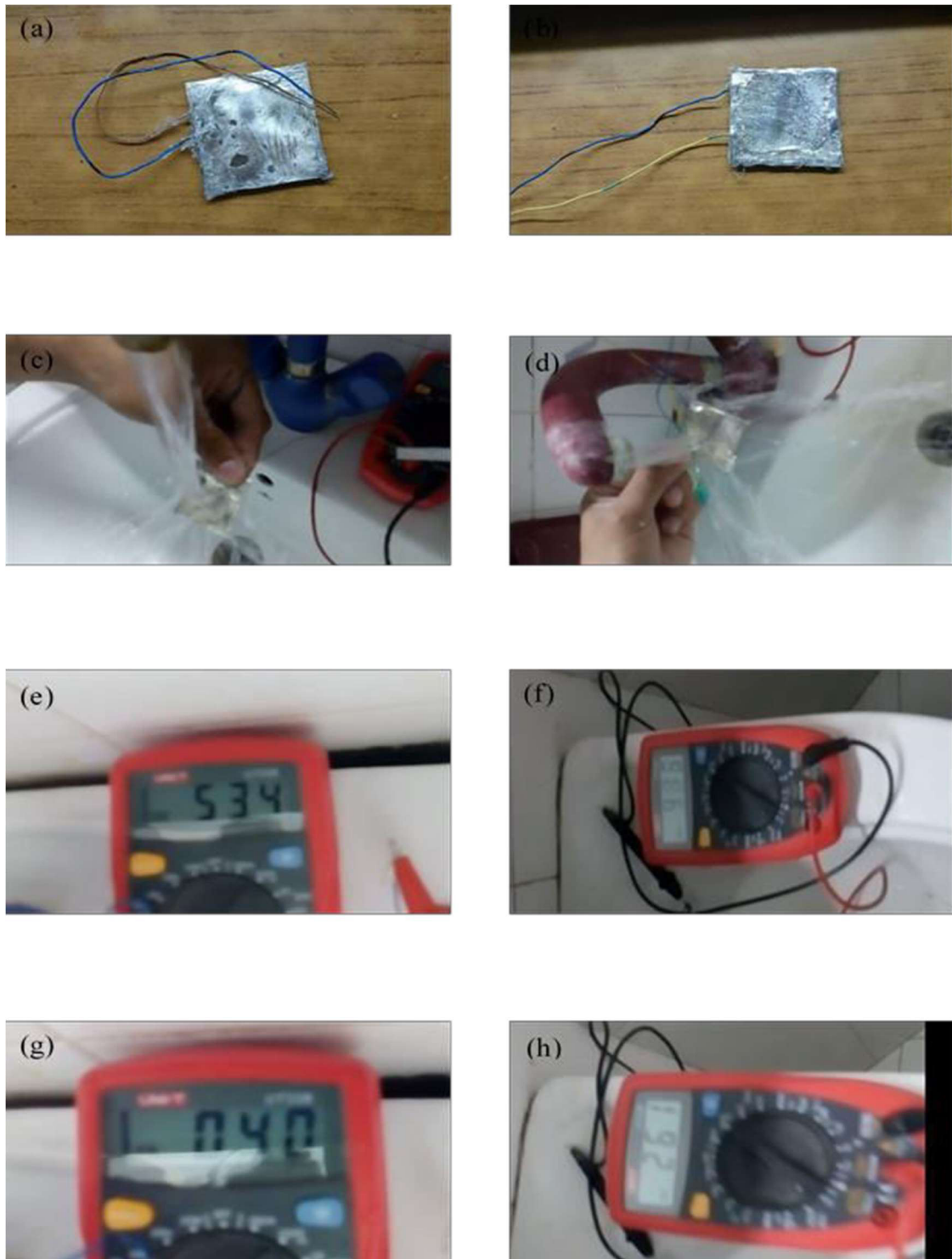
Figure 12 Shows the Assembled generators of (a) Silica , (b) Glass Fibers, Their function under tap water (c) and (d) and their resultant open circuit voltages at (e), (f), (g) and (h).

affected by the current magnitude also increases the morphology to a more columnar structure which inhibits the hinderance of the silica to the substrate (fig. 10) (PMMA).

E. Assembling the Generator

The first attempt at fabricating our device involved the device fabrication without the deposition of the Titania nano-material layer. The Upper TENG was highlighted as the positive electrode whereas the lower portion of the TENG is considered as negative one. The

alternating potential reached a peak value of 14 mV then the output potential was amplified via Integrated Circuit (IC), LM 741C. The result can be seen as shown in the figure 11. which the application of the mechanical force causing the upper and lower TENG to come into contact and the potential is generated across the device (fig. 12). The second phase of experimentation and assembling involved the deposition of the superhydrophobic Titania layer as well as substitution of the Silica spheres with glass fibers as well. The output measures showed the peak voltage of Silica based TENG to have an Open-Circuit Potential of 534 mV and as opposing as low as -80 mV. Comparatively speaking, the Glass Fiber glass fiber substituted TENG measured a peak Open Circuit Potential of 324 mV. The flow and impact of tap water causes a fluctuating level of mechanical stresses on the device that exhibit short delay times (In range of milliseconds or/and less) which is lower than the minimal range of recordable response time for the commercially available (DMM), therefore it is likely that most values (peaks) could not be observed by the DMM (fig. 12). For that we require more sensitive measurement devices such as nanovoltmeter and pico-ammeter. Both nano-generators showed the aspects discussed above. The glass fibers could were not separated into individual strands remaining slightly agglomerated which also reduced their total contact surface area. Also the other fact that the diameter of the glass fiber (20um) was larger than the diameter of the spheres (500 nm) and the thickness of the silica Film, hence the contact area is inherently lower. Glass fibers can be employed to overcome this issue with finer diameter to increase their contact surface area, however the fact of replacing them with finer fiber diameters only complicates the matter of arranging them, adding to that the use PVC film as the triboelectric negative materials instead of the PTFE film with double thickness (50 um instead of 25 um) only added to degradation of the output of the Nanogenerators since both the PVC and SiO$_2$ function as dielectric materials and greater thickness leads to reduced output.

IV.   CONCLUSION

From the results we can conclude the following:

- Measurements revealed that the open circuit voltage of the Silicon Dioxide based Nanogenerator was higher than the Glass Fiber based Nano-Generator as the which has been attributed to the larger surface area of the Silicon Dioxide Assembly and the conglomerate formation in the glass fibers.
- Finer glass fibers are recommended albeit the issue to handle them must be taken into consideration.

V.   ACKNOWLEDGEMENT

VI.   REFERENCES

[1]   Z. L. Wang, "Triboelectric Nanogenerators as New Energy Technology for Self-Powered Chemical Sensors," no. Xx, 2013.

[2]   Z. L. Wang, G. Zhu, Y. Yang, S. Wang, and C. Pan, "Progress in nanogenerators Besides targeting at the worldwide energy needs at a large scope , we have," *Mater. Today*, vol. 15, no. 12, pp. 532–543, 2012.

[3]   S. Nanosystems, Z. L. Wang, and W. Wu, "Nanotechnology-Enabled Energy Harvesting for Self- Powered Micro- / Nanosystems Angewandte," pp. 2–24, 2012.

[4]   S. Wang, Y. Xie, S. Niu, L. Lin, and Z. L. Wang, "Freestanding Triboelectric- Layer-Based Nanogenerators for Harvesting Energy from a Moving Object or Human Motion in Contact and Non- contact Modes," pp. 2818–2824, 2014.

[5]   Z. Lin, "Triboelectric nanogenerators as new energy technology and self-powered sensors – Principles , problems and perspectives 2 . Fundamental principle modes of triboelectric," *Faraday Discuss., vol. 00, pp. 1–12,2014.*

[6]   M. S. El-Eskandrany and A. Al-Azmi, "Potential applications of cold sprayed Cu50Ti20Ni30metallic glassy alloy powders for antibacterial protective coating in medical and food sectors," *J. Mech. Behav. Biomed. Mater.*, vol. 56, pp. 183–194, 2016.

[7]   H. E. Press, "Preparation and formation mechanism of CdS nano-films via chemical bath deposition," vol. 3, no. 1, pp. 18–22, 2008.

[8]   E. Cristina, D. O. Nassor, L. R. Ávila, and P. Fabiana, "Influence of the Hydrolysis and Condensation Time on the Preparation of Hybrid Materials," vol. 14, no. 1, pp. 1–6, 2011.

[9]   S. Method and C. Growth, "Simple Method for the Controlled Growth of SiO 2 Spheres," vol. 3, no. 4, pp. 237–242, 2013.

[10]   H. Giesche, "Synthesis of Monodispersed Silica Powders I . Particle Properties and Reaction Kinetics," vol. 14, pp. 189–204, 1994.

[11]   J. Eur, C. Soc, and H. Giesche, "Giesche , H . Synthesis of monodispersed silica powders II . Controlled growth reaction and continuous production," no. January, 2016.

[12]   G. F. Types, "Glass Fibers," vol. 21, no. Ref 19, 2001.

[13]   P. Roach, N. Shirtcliffe, P. Roach, N. J. Shirtcliffe, M. I. Newton, and P. Roach, "Progess in Superhydrophobic Surface Development Progess in superhydrophobic surface development," no. January, 2008.

[14]   Y. Pu *et al.*, "Surface Passivation of TiO 2 Nanowires Using a Facile Precursor- Treatment Approach for Photoelectrochemical Water Oxidation," 2014.

[15]   A. Mubarak, E. Hamzah, and M. R. M. Toff, "review of physical vapour deposition (pvd) techniques for hard coating," no. 20, pp. 42–51, 2005.

[16]   P. Vapor and D. Pvd, "II . Thin Film Deposition General Characteristics of Thin Film Deposition."

Fabrication of Aluminium Based Lab-Scale Cross Flow Printed Circuit Heat Exchanger

Aubaid Ullah[1], Khalid Waheed[2], Rab Nawaz[3], Waseem Siddique[4], Mazhar Iqbal[5]

[1-5] Department of Nuclear Engineering, Pakistan Institute of Engineering and Applied Sciences, Nilore
Islamabad, Pakistan

Email address: [1] aubaidullah@pieas.edu.pk, [2] khalidwaheed@pieas.edu.pk

Abstract— **Heat exchanger is an essential component of all chemical and mechanical industries. Industry needs compact heat exchanger to reduce the capital and maintenance costs. Compactness in a heat exchanger can be achieved by reducing the area of flow channel. In current work aluminium based Printed Circuit Heat Exchanger (PCHE) with cross flow pattern was fabricated indigenously. Heat exchanger was consisted of total 7 layers of plates and 32 flow channels per plate. Flow channels were 1.5mm in square shape and fabricated on 2.5mm thick plate using Computer Numerical Control (CNC) machine. Plates were arranged in cross wise pattern and bonded using diffusion bonding method under high pressure of 30MPa and high temperature equals to the 80% of melting point of aluminium i.e. about 550 ºC. Flow headers were fabricated separately and welded through TIG welding with PCHE. For experimentations, water at normal pressure i.e. 1MPa was used as working fluid. Experiments were performed using different hot inlet temperatures and all four outlet temperatures were measured using thermocouples and data acquisition device and mean heat transfer rate was calculated.**

Keywords— Printed circuit heat exchanger, Square channel, Diffusion bonding

I. Introduction

With many advances in heat transfer field, researchers are trying to boost the efficiency of heat transfer devices. In this context heat transfer area to volume of a particular heat exchanger (m^2/m^3) is one of the most important parameter. Performance of heat exchanger increases by increasing this quantity[1]. This quantity depicts the compactness of heat exchanger. To make one heat exchanger compact, flow area of its channels should be smaller and smaller. Usually micro sized channels fabricated on thin plates are used in compact heat exchangers.

Printed Circuit Heat Exchanger (PCHE) is one of best-known compact heat exchangers. Fluid channels of size comparable to a millimeter are fabricated on thin plates. These micro channels can be fabricated using chemical etching techniques[2], or by any other mechanical mean such as Computer Numerical Control (CNC) machine etc. Due to the difficulty in binding techniques such as welding, these thin plates are bonded together using diffusion bonding technique[3]. A schematic of fabrication procedure is shown in Figure 1. Construction material for this heat exchanger are selected depending upon their thermal, diffusion bonding and other mechanical properties. In the current work, a lab scale Printed Circuit Heat Exchanger is fabricated indigenously to be used in further research in this field. Coming chapters will provide details of geometric parameters of the model and fabrication techniques adopted.

The Heat Exchanger (HX) will find its application in next generation nuclear power plants such as HTGR, VHTR and SMRs[4]. In small modular reactor this heat exchanger is very suitable due to its small size and weight[5].
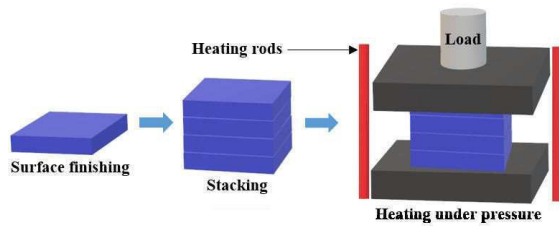
Figure 1: Schematic diagram of diffusion bonding process

II. METHODOLOGY

Aluminium metal was selected to fabricate the heat exchanger because it has comparatively low melting point i.e. about 660℃ and ease of machining process. Flow channels of size 1.5x1.5mm were made on 10x10cm plates with 32 channels on each. Flow channels were prepared on 7 plates, out of which 4 were given to cold fluid and 3 plates to hot fluid. Individual plates was 2.5mm thick which gave identical wall thickness all around each flow channel i.e. 1mm. A 5mm thick plate was placed at both top and bottom to minimize the heat losses and to strengthen the exchanger core. Cross flow pattern was selected because flow headers can easily be made on all four sides i.e. two hot sides and two cold sides. Geometric parameters of model are presented in Figure 2.

Table 1: Geometrical parameters of model

Metal-plate material		Aluminum
Dimensions of PCHE (W × L × H), mm		$100 \times 100 \times 23.5$
Dimensions of plates (W × L × H), mm		$100 \times 100 \times 2.5$
Dimensions of end plates (W × L × H),		$100 \times 100 \times 3$
Number of plates	Hot side	3
	Cold side	4
Number of channels per plate		32
Channel width,		1.5
Channel height,		1.5
Land (solid) width,		1

Operating temperature during diffusion bonding process was kept at ℃ i.e. 80 to 85% of the melting point [6]. Heating was done in electrical muffle furnace for continuous 4 hours. Pressure is defined as normal force applied per unit area of the body surface, hence it was calculated using geometric parameter of the heat exchanger and came out about 30MPa. High pressure is applied using hydraulic press by placing the heat exchanger core between 1in thick MS plates and then maintained the applied pressure using bolts as shown in Figure 3.
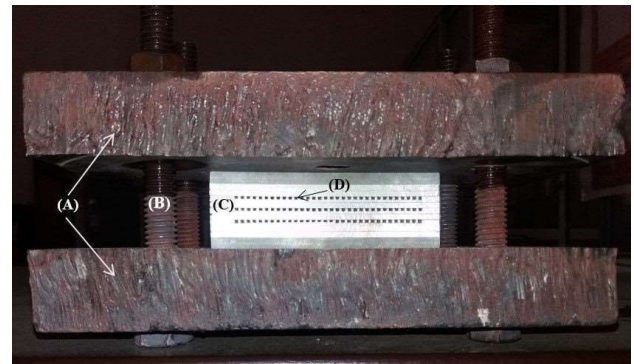
Figure 2: (A) Pressure holding plates, (B) Screw and bolts, (C) Heat exchanger core and (D) Flow channels
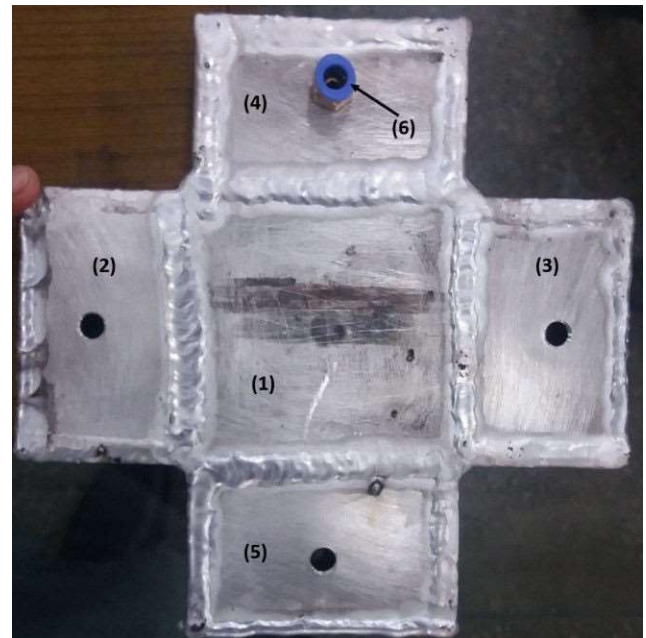
Figure 3: Complete PCHE module as (1) PCHE core, (2) hot fluid in, (3) hot out, (4) cold in, (5) cold out, (6) push connector

After diffusion bonding, flow headers were welded across the core as shown in figure 3. Dimensions of flow headers were comparable to the heat exchanger i.e. 100mm x 50mm x 23.5 mm. Flow header were also made of aluminium so that welding could be made easy due to similar metals. Tig welding technique was used to weld the headers. Fluid inlet and outlet push connectors of 1cm diameter were connected to flow headers.

III. EXPERIMENTATION

For experimentation, hot water was supplied by a constant temperature heated water source and cold water was normal tab water. Temperatures were measured by using K-type thermocouples and data was recorded on computer using data acquisition device as shown in Figure 4. Four experiments were performed using different flow rates.
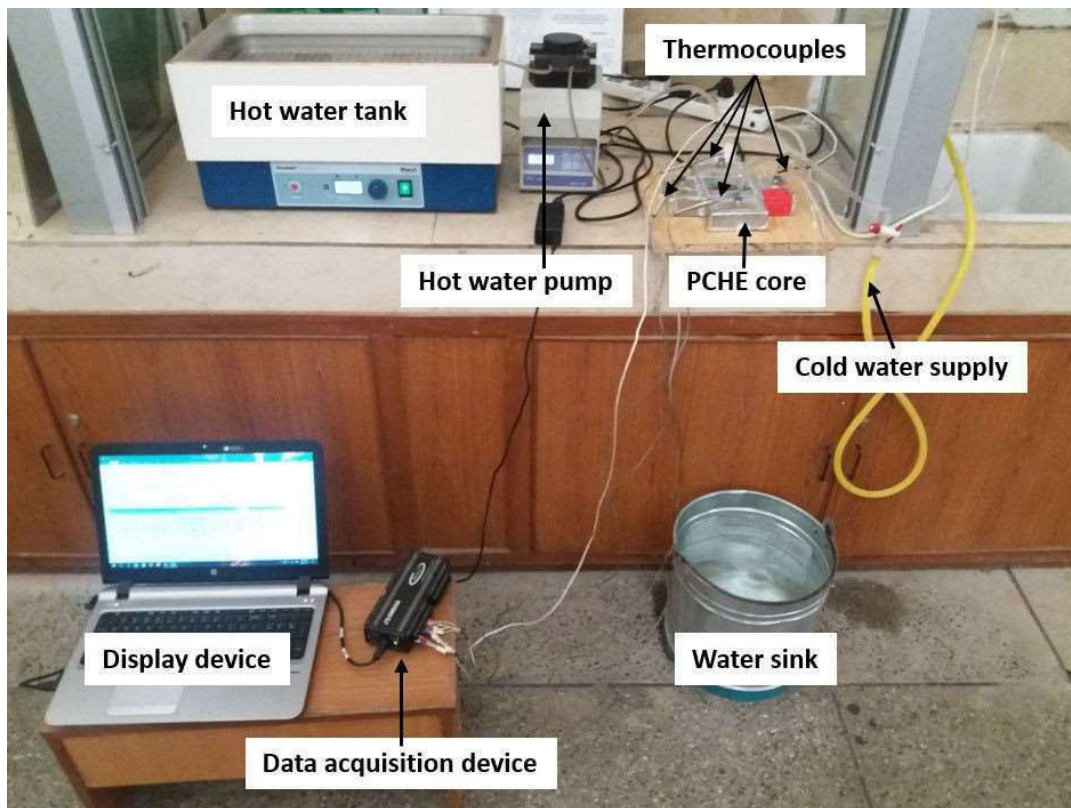
Figure 4: PCHE experimental facility

Mean heat transfer rate (Q_m) of experiment was calculated using following equations.

$$Q_c = m_c C_{p_c} \Delta T_c \tag{1}$$

$$Q_h = m_h C_{p_h} \Delta T_h \tag{2}$$

$$Q_m = \frac{Q_c - Q_h}{2} \tag{3}$$

Table 2: Experimental data and calculated results

Exp. No.	Cold flow rate	Hot flow rate	T_c inlet	T_c outlet	T_h inlet	T_h outlet	Q_m
	ml/min	ml/min	K	K	K	K	W
1	42.6	46.2	300.16	309.16	315.66	307.66	24.5
2	41.4	52.8	300.66	310.66	316.66	308.96	24.2
3	36.6	54.0	300.86	310.96	315.16	309.86	28.9
4	36.0	54.0	300.76	311.16	315.36	309.66	26.7

IV. Conclusion

In this work a lab scale facility of Printed Circuit Heat Exchanger was fabricated indigenously at the institute using aluminium metal. Experimentations were also performed to test any leakage in exchanger core. Furthermore, experimentations will be performed to evaluate the heat transfer coefficient of this exchanger using different working fluids along with the pressure drop. The experimental setup itself will also be improved to get more reliable results.

Acknowledgment

This work was not possible to perform without the valuable collaboration and expertise of the faculty of Pakistan Institute of Engineering and Applied Sciences (PIEAS).

References

[1]   P. B. Thakre and P. R. Pachghare, "Performance Analysis on Compact Heat Exchanger," *Mater. Today Proc.*, vol. 4, no. 8, pp. 8447–8453, 2017.

[2]   F. Xin, T. Ma, Y. Chen, and Q. Wang, "Study on chemical spray etching of stainless steel for printed circuit heat exchanger channels," *Nucl. Eng. Des.*, vol. 341, pp. 91–99, 2019.

[3]   M. V. V Mortean, L. H. R. Cisterna, K. V Paiva, and M. B. H. Mantelli, "Development of diffusion welded compact heat exchanger technology," *Appl. Therm. Eng.*, vol. 93, pp. 995– 1005, 2016.

[4]   I. H. Kim and H. C. No, "Physical model development and optimal design of PCHE for intermediate heat exchangers in HTGRs," *Nucl. Eng. Des.*, vol. 243, pp. 243–250, 2012.

[5]   C. W. Shin and H. C. NO, "Experimental study for pressure drop and flow instability of two-phase flow in the PCHE-type steam generator for SMRs," *Nucl. Eng. Des.*, vol. 318, pp. 109–118, 2017.

[6]   J. Varmazyar and M. Khodaei, "Diffusion bonding of aluminum- magnesium using cold rolled copper interlayer," *J. Alloys Compd.*, vol. 773, pp. 838–843, 2019.

Proposition of New Rheological Model for Supplementary Cementitious Materials Incorporated Mortars

Dr. Maria Idrees

Department of Civil Engineering, Middle East Technical University, Ankara, Turkey

Abstract- Rheology is a very sophisticated tool to measure the flow properties of mortars and concretes. Till now workability is a general term used in civil engineering to show the flow-ability of concrete because of its inexpensiveness and ease to use. But this term is insufficient to depict the flow behavior completely. Determining flow properties is very important because they control all other properties of mortars and concretes in the hardened state, including strengths and durability. Rheological parameters such as yield stress (for starting flow) and plastic viscosity (for continuing flow) for plain and mineral admixtures incorporated mortars are investigated in this research. Fly ash (FA), silica fume (SF) and ground granulated blast furnace slag (BFS) are used in different amounts to partially replace portland cement (PC) on mass basis with different water-binder ratios and constant polycarboxylate based high range water reducing admixture and are tested by using a two-probe eBT2 rheometer. A new model is proposed and checked for suitability to the experimental data obtained both for plain portland cement and mineral admixture- incorporated cement mortars. The proposed model is found to be a better fit than commonly used Bingham model to represent the flow data.

Keywords_ Rheology; mortar, mineral admixtures; flow models; relative yield stress; relative plastic viscosity; proposed model

1. Introduction

Workability is a key property to control all other characteristics of cement based materials. It is defined as the ease/effort with which the mortar or concrete can flow. The required hardened properties of cement-based materials are achieved after an initial period of plasticity within which the pastes, mortars, or concretes are to be easily mixed and transported, uniform within batch and between batches, compacted without excessive effort, and finished properly without significant segregation during placing and compaction (Mindess and Young, 1981). In other words, the properties of fresh concrete are important since they affect almost all of the properties in the hardened state. Workability of concrete is the property of freshly mixed concrete which determines the ease and homogeneity with which it can be mixed, placed, consolidated and finished' as defined by ACI Standard 116R-90 (ACI 1990b).

Generally the workability represents the flow-ability of mortars and concretes. Additives, both mineral and chemical have reasonable effect on the workability of concrete. The term workability that covers all these properties of cementitious systems is being used to describe their behavior within the plastic stage. Workability of

fresh concrete can be measured by numerous different test methods which are generally categorized as slump test, compaction tests, flow tests, remolding tests, penetration tests, mixer tests (Mindess and Young, 1981) and (g) rheometer tests (Banfill, et al, 2001). Although almost all of these tests are empirical, it is significant to measure the workability and the available methods provide at least some information on its variations. The development of new and special concretes, such as self-compacting concrete and high performance concrete, requires more sophisticated tools rather than simple slump tests. The devices which are called concrete rheometers use rheology methods to measure the flow properties of fresh concretes. Basically, they measure the shear stress at varying shear rates (Banfill et al, 2001).

The term "workability" is not enough to explain these flowing behaviors. Hence the term rheology (flow property) is preferable and is comprised generally of flow parameters i.e. yielding stress and plastic viscosity, both of which control the flow characteristics.

The yield stress is the stress required to initiate the flow. In mortars and concretes, we prefer the less effort to start the flow, i.e. less yield stress is required. The ease and effort to keep its flow once the flow has started is called "plastic viscosity". The stability properties i.e. bleeding and segregation of mortars and concretes are controlled by their plastic viscosity. Lower plastic viscosity of mix causes higher bleeding and segregation of mortars and concretes and vice versa.

Bingham model nowadays, which has been derived from Maxwell equation, is the most commonly used and well accepted model for non Newtonian

considered as heavily concentrated suspensions of cement and aggregate particles in water, represented by Bingham Model which is described by Equation 1:

$$\tau - \tau_y = \eta \frac{d\gamma}{dt} \qquad (1)$$

fluids like mortars and concrete. It is a common practice to approximate the flow behavior of fresh mortar or concrete which may be

Where τ_y is the yield stress, η is the coefficient of viscosity, and is the time rate of shear strain. Such behavior is shown in Figure 1. Flow takes place only at stresses above the yield value. It also follows that upto the yield stress the material behaves as elastic solid which is able to carry loads without permanent deformation. Materials that show this behavior are named as Bingham bodies (Jastrzebski, 1959).
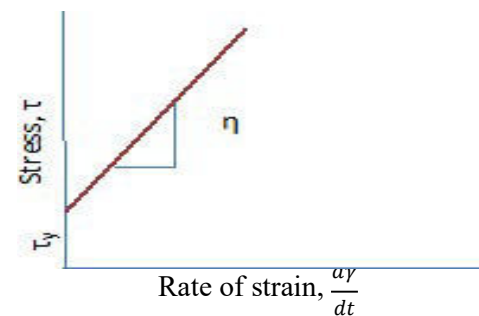
Figure 1 Flow behaviour of the Bingham body.

The actual rheology of cementitious systems, however, is more complex than that can be described by Bingham Model. Bingham model represents a linear data but actual data obtained, for mortars and concretes, from rheometer is nonlinear. The best fit model is one which represents the data correctly. The rheological properties are time dependent because of the continuing hydration reactions in the very early stages even right after mixing cement with water. Furthermore, shear thinning or shear thickening phenomena may usually be observed. Fresh mortars and concretes may also show thixotropy which is decrease of coefficient of viscosity under stress or sometimes anti- thixotropy (Mindess and Young, 1981).

Besides these, there are several other parameters of cementitious materials such as (1) interparticle forces like Brownian, van der Waals, viscous, and liquid bridging forces, (2) particle shape, (3) particle size distribution and fineness, and (4) surface charge which may result in the flocculation or dispersion of particles that may affect the rheological behavior of cementitious systems (Nehdi et al, 1998; Moosberg-Bustnes, 2003). Consequently, numerous other models have been proposed by different researchers to predict the rheological properties of fresh cementitious systems (Hu, 2005).

The use of mineral admixtures in cementitious systems had long been a common practice due to economical, ecological, and technical advantages that they may provide. Whether they are used to partially replace the portland cement or as an addition in concrete they affect the workability and rheological properties as well as the rest of the fresh and hardened properties. Effects of mineral admixtures on concrete workability are usually related to the changes they cause in the water requirement of the mixture.

The goal of this study is to determine the effect of mineral admixture type and amount on the rheological properties of mortars to propose a new model based on the experimental data obtained.

Three control mortar mixes were prepared by using portland cement (PC) as the only cementitious material. Fly ash (FA), silica fume (SF) and ground granulated blast furnace slag (BFS) were used in different amounts to partially replace PC on mass basis. All mixtures had a constant amount of polycarboxylate based high range water reducing admixture. Rheology measurements were taken as rotational speed and corresponding torque by a two-probe eBT2 rheometer. The data obtained were statistically analyzed and yield stresses and

Plastic coefficients of viscosity were determined and a new model is proposed.

1.1. Research Significance

The Bingham model is used commonly to depict data obtained by rheometer for cement based materials. Data obtained is nonlinear while Bingham model shows linear behaviour. To depict the data more accurately, a new model is proposed. The solver in Microsoft Excel accurately guesses all the unknown parameters. New model is bit complex but a best tool for modern researchers. It may be used for guessing rheological parameters for many materials other than mortars and concretes. Hence researchers/users may apply the proposed model to other materials to find its applicability for them.

2. Experimental investigation
2.1. Properties of the Materials Used

In preparing the fresh mortars Portland cement (PC), fly ash (FA), ground granulated blast furnace slag (BFS) and silica fume (SF) were used as the cementitious materials. The sand used was natural sand, the particle size distribution of which was brought to that of a standard sand described in EN 196.1 (2005). All mortar mixtures contained a polycarboxylate based high range water reducing agent (HRWRA).

PC which was obtained from Votorantim Ankara Cement Factory was CEM I 42.5 R. Its properties were in accordance with EN 197.1 (2012). Its chemical composition and physical properties are given in Table1. FA was a low lime fly ash obtained from Tunçbilek Thermal Power Plant. BFS and SF were obtained from Ereğli Steel plant and Antalya Ferrochromium Plant, respectively. The properties of the mineral admixtures are

also given in Table 1. Particle size distributions of the cementitious materials used were determined by laser particle size (Malvern Mastersizer 2000) and given in Figure 2. The sand used in the mortars was natural river sand with a bulk specific gravity of 2.65. Its granulometry is shown in Figure 3.

Table 1 . Properties of the Cementitious Materials Used.

Chemical Composition				
Oxide (%)	PC	FA	BFS	SF
SiO_2	20.27	53.2	42.96	84.14
Al_2O_3	5.09	22.89	11.28	0.17
Fe_2O_3	3.16	6.15	0.87	0.31
CaO	60.98	6.28	33.01	0.58
MgO	1.59	2.22	6.16	5.24
SO_3	2.7	1.15	1.45	1.33
Na_2O	0.39	0.92	0.33	0.4
K_2O	0.53	1.41	0.66	2.88
TiO_2	nd	1.09	0.6	0.01
Loss on Ignition	4.65	2.98	0.33	3.62
Physical Properties				
Blaine Sp. Sur. Area (m^2/kg)	362	421	468	---
Median size (μm)	18.48	17.56	13.00	7.70
Density (g/cm^3)	3.07	2.38	2.85	2.27
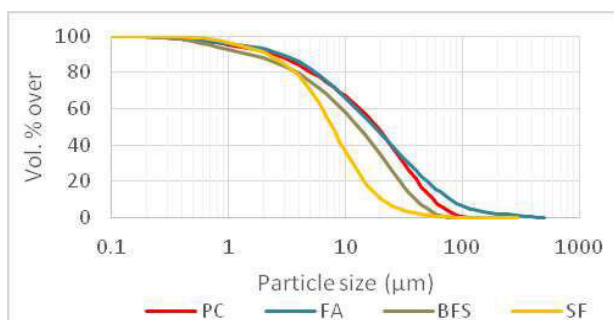
Figure 2. Particle size distributions of the cementitious materials used .
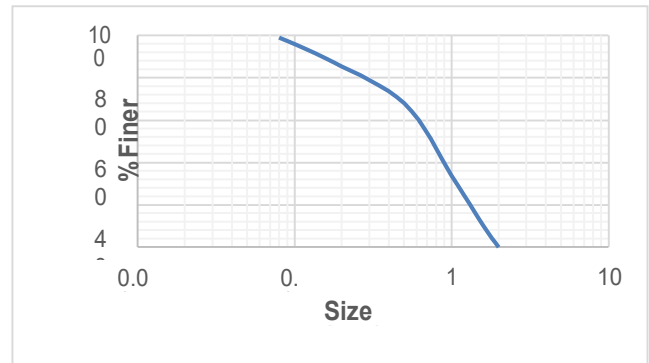
Figure 3. Granulometry of the sand used.

2.2. Mortar Mix Proportions

All mortar mixtures used had 1:3 (by mass) cementitious material to sand ratio and a constant HRWRA content of 2% (by mass of cementitious material). Mineral admixture incorporated mortars contained different amounts of FA, BFS, or SF that were used to replace equal amounts of portland cement. Mortar mix designations and relative proportions of the ingredients for each mix are given in Table 2. Some other mix were tested but discarded due to being too dry or too wet.

Table 2 Mortar Mixes Used.

Mineral Admixture Used	Mix Designation	Relative proportions of the ingredients (by mass)						
		PC	FA	BFS	SF	Sand	Water (net)	HRWRA
None	PC 0.3	1	-	-	-	3	0.30	0.02
	PC 0.6	1	-	-	-	3	0.60	0.02
	20FA 0.45	0.8	0.2	-	-	3	0.45	0.02
	40FA 0.55	0.6	0.4	-	-	3	0.55	0.02
Blast Furnace Slag	10BFS 0.4	0.9	-	0.1	-	3	0.40	0.02
	10BFS 0.5	0.9	-	0.1	-	3	0.50	0.02
Silica Fume	5SF 0.4	0.95	-	-	0.05	3	0.40	0.02
	5SF 0.5	0.95	-	-	0.05	3	0.50	0.02

2.3. Apparatus and Test Methods

The mortar mixtures were prepared in batches of 80 to 90 kg, mixed in a pan-type mixer (Figure 4). The mixing procedure consisted of adding first the sand into the mixer, and then about half of the mixing water is added and mixed for one minute. Then cement and mineral admixtures are added and mixed for another 2 minutes. HRWRA was introduced into the mix together with the remaining mixing water and mixing continued for two more minutes. Finally, after one minute of rest, the mortar was mixed for two more minutes. Right after mixing is finished, the fresh mortar is transferred into the container of the rheometer to take the initial flow data. Besides these flow table test (ASTM C 230, 2003) was carried out and bleed water amount was measured up to 40 minutes after mixing by a similar method (no vibration was applied) described in ASTM C 232 (2004) for mortars with water-cementitious material ratio of 0.45.

3. TEST RESULTS AND DISCUSSIONS

Cement paste, mortar, or concrete are concentrated suspensions of solid particles. Therefore, particle migration may become an important phenomenon in the rheology of these materials. The solid particles will have the tendency to move to the regions of lower shear rates and due to the differences in the densities of the suspended particles and the liquid medium, vertical segregation is also possible. Furthermore, the time dependent behaviour of these materials may result in changes in the rheological properties due to thixotropy, structural breakdown, or loss of workability (Feys, 2009; Hafid et al, 2010). These would result in measurement artifacts the magnitudes of which depend on the

characteristics of the suspension, the working principle of the rheometer, and the shear flow geometry used. Thus, flow curves obtained by means of rheometers may sometimes have various anomalies. The data deviating more than two times the standard deviation of the linear relationship obtained with the original data were eliminated.

Actually data obtained from rheometer is very random and one can not guess the parameters unless data is averaged with the help of models (equations). The best fit model is able to depict most accurate rheological parameters.

3. Results and Discussions
3.1. Flow Data Obtained
The torque induced versus the speed of the rheometer probes were obtained as initial data after mixing as soon as the mortar is placed into the container of the rheometer.

Since the rheometer used was stated to be designed on the basis that the fresh mortar (or concrete) behaves as a Bingham body, the linear relationship between the torque and speed were determined, also. Figure 4 shows the flow curves obtained by software attached to eBT2 rheometer

Figure 4. Pan type mixer and eBT2 rheometer

3.2. Relative Yield Stress and Relative Viscosity Values

As it was previously mentioned, the rheometer used assumes Bingham body behavior for fresh cementitious systems. Therefore, using the data obtained, relative yield stresses and relative plastic viscosities of the mortars were obtained by using the following equation 2.

$$\Gamma = g + Vh \qquad (2)$$

Where g (Nm) and h [Nm/(m/sec)] are constants corresponding to relative yield stress and relative plastic viscosity, respectively. Figure 5 shows a typical plot of torque (Γ in Nm) versus speed (V in m/sec). Linear regression analysis was performed on the data. The slope of the line defines relative plastic viscosity (h) and the intersection point with the y-axis defines relative yield stress (g). The results are shown in table 3. However, analysis of these parameters is out of scope of this paper.

Table 3 Rheological Parameters for mortars

PC 0.3	**Bingham**	T_o	μ		RMSE
		0.664	46.649		0.0243
	Proposed	To	a	b	RMSE
		0.664	28.294	1.649	0.0239
PC 0.6	**Bingham**	To	μ		RMSE
		0.21070	26.81343		0.00310
	Proposed	To	a	b	RMSE
		0.19621	1.21590	23.60771	0.00308
20 FA 0.45	**Bingham**	To	μ		RMSE
		0.356433	61.58067		0.05684
	Proposed	To	a	b	RMSE
		1.333382	0.53418	214.7681	0.053351
40 FA 0.55	**Bingham**	To	μ		RMSE
		0.027793	1.463216		1.47E.05
	Proposed	To	a	b	RMSE
		0.018452	0.046054	55.77056	1.09E.05
10 BFS 0.40	**Bingham**	To	μ		RMSE
		0.8523	72.6616		0.0383
	Proposed	To	a	b	RMSE
		0.8521	19.7373	3.6845	0.0382
10 BFS 0.50	**Bingham**	To	μ		RMSE
		0.0824	13.7681		0.0008
	Proposed	To	a	b	RMSE
		0.0824	17.6550	0.7799	0.0007
5 SF 0.4	**Bingham**	To	μ		RMSE
		0.4820	25.6293		0.0059
	Proposed	To	a	b	RMSE
		0.3559	0.6576	66.7839	0.0044
5 SF 0.5	**Bingham**	To	μ		RMSE
		0.228139	74.82824		0.05257
	Proposed	To	A	b	RMSE
		0	1.927316	56.93589	0.041545

3.3 Flow Model

A flow model is considered to be a mathematical equation that describes rheological data such as shear rate and shear stress in a convenient manner (Rao, 1999).

3.3.1. Bingham Model

Bingham model is the simplest and the most widely used model till now. It is a 2 parameter model. In this model, graph is drawn between shear stress and shear rate, the intercept gives the yield stress and slope of straight line reveals plastic viscosity. So the graph is drawn between torque applied and velocity to obtain relative yield stress and relative plastic viscosity by eBT2 rheometer.

$$\tau = \tau_0 + \mu\dot{\gamma} \qquad (3)$$

One of the main discrepancies of Bingham model is its linearity. It does not give any idea about shear thinning and shear thickening behavior.

4 Model Proposed in This Study

The new model "Proposed model" has been proposed and is described by equation 3.

$$T = T_, + a\sin bv \qquad (4)$$

Where, T represents shear stress, a and b are parameters representing relative viscosity and flow coefficients, and T_o is yield stress. V represents shear strain rate. Sine is used because the graph obtained by rheometer resembles sine wave.

4.1 Methodology Adopted

Experimental values of velocity (V) and Torque (T) are plotted on graph. By applying model equation, T model is plotted against experimental V on the same graph. Parameters are selected by minimizing root mean square error for T model and V experimental.

Some models cannot describe the experimental values, so they are rejected for mortars. The models well describing and most suitable for the data are the successful models for mortar.

A new model is proposed for the mortar. Table 3 describes experimental data from many SCM incorporated mix and the applied proposed model. Hence it is visible that the model is a best fit for all of the cases. RMSE represents root mean square error. Higher RMSE means higher error and lower accuracy. The other way to verify the suitability of model is that "The model representing average of experimental data is the better fit model, it shows less deviations from obtained experimental data from rheometer. Figure 4 to figure8 represents the actual data obtained by rheometer along models to find out rheological parameters.

The comparison between Bingham model and Proposed model is visible. It can be seen that proposed model is representing most of the experimental data coorectly.
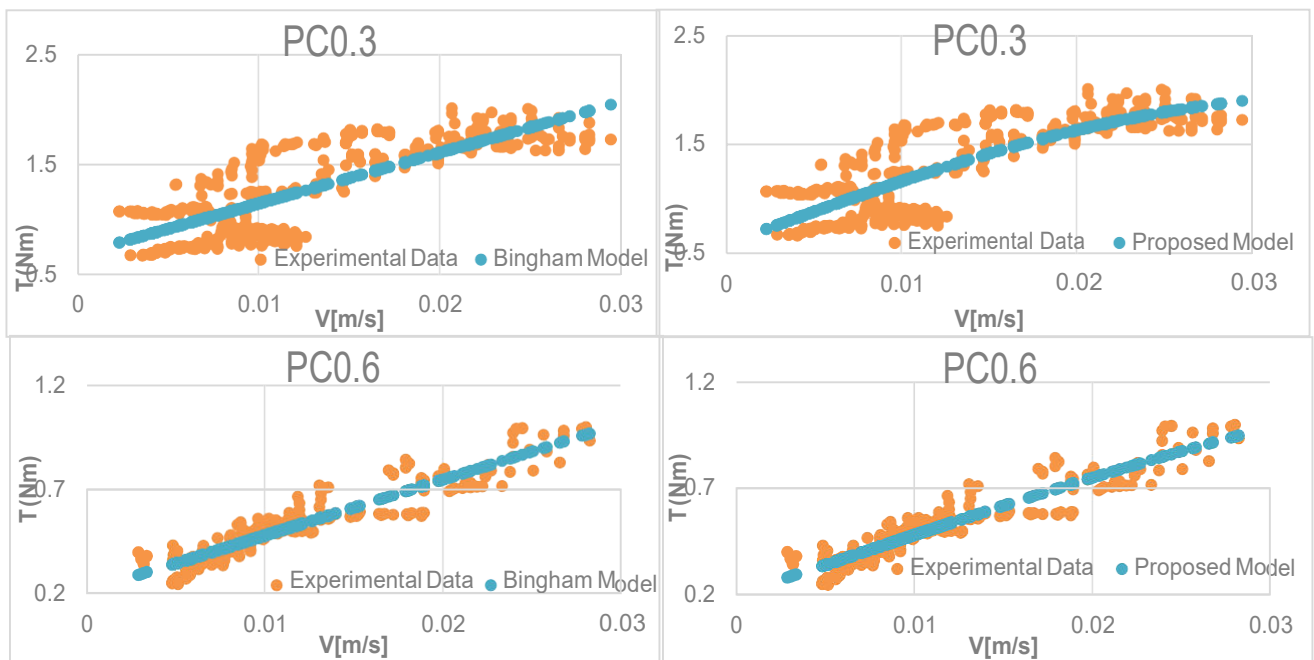
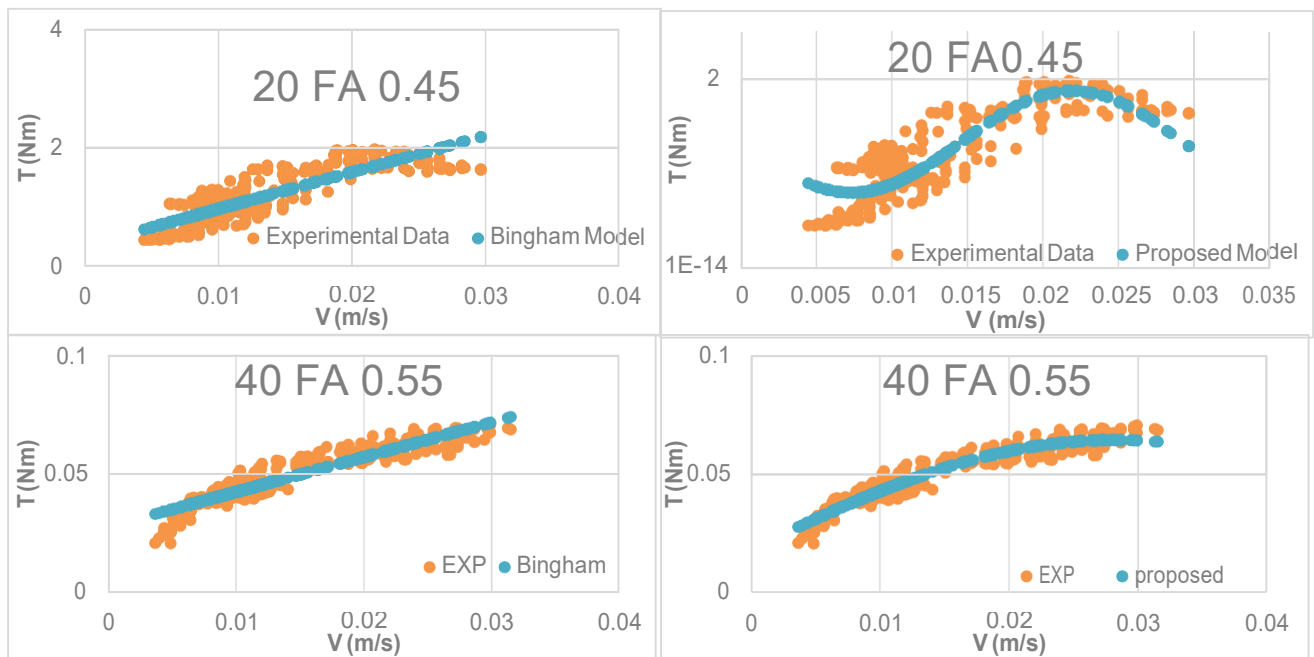Fig 5: Bingham and Proposed Models of PC 0.3, PC 0.6

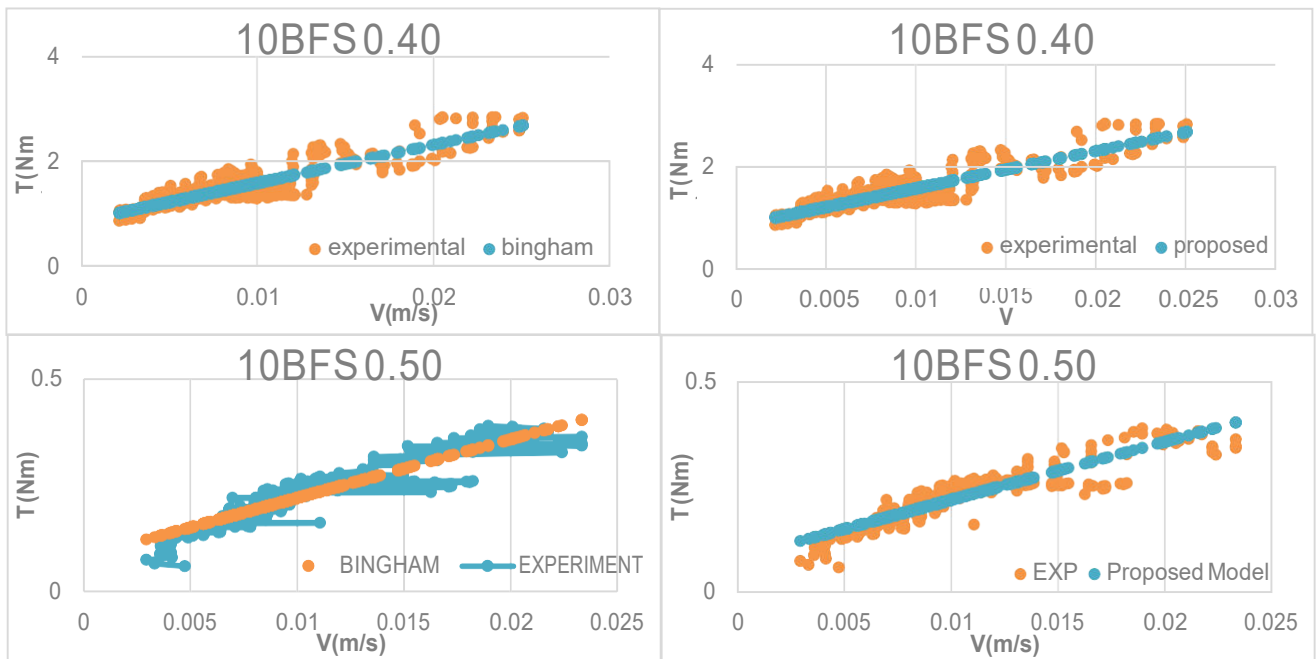Fig 6: Bingham and Proposed Models of 20 FA 0.45, 40 FA 0.55

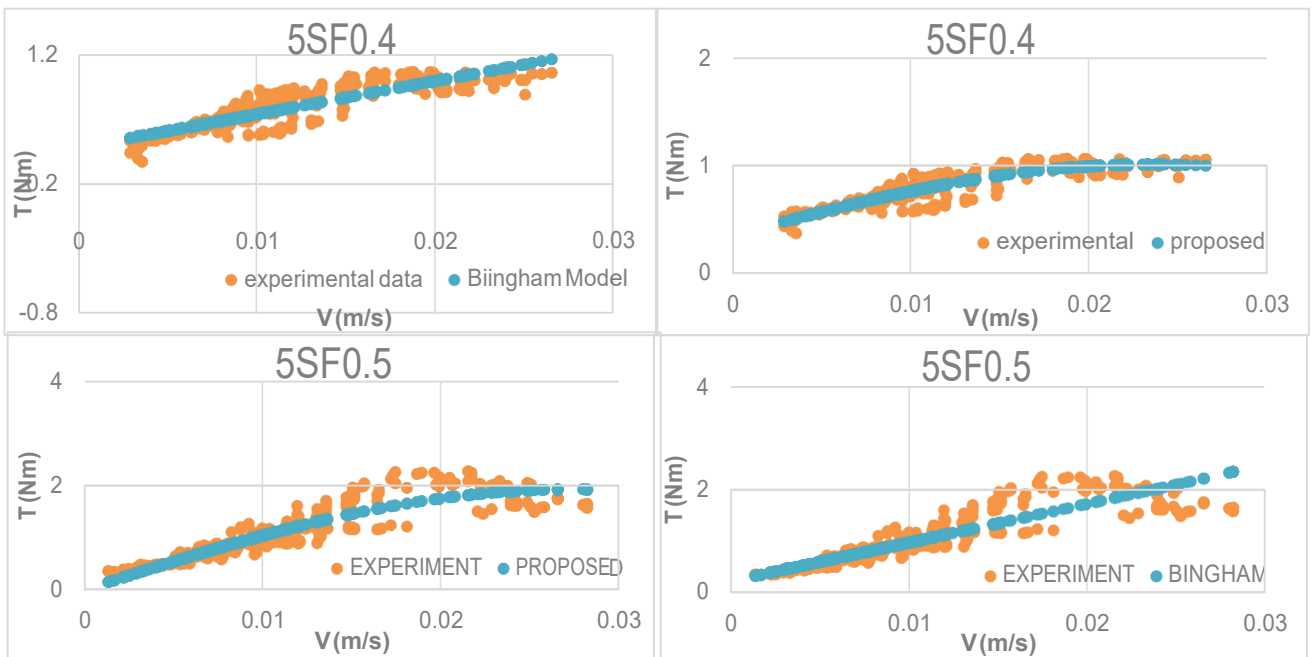Fig 7: Bingham and Proposed Models of 10 BFS 0.40, 10 BFS 0.50

Fig 8: Bingham and Proposed Models of 5 SF 0.4, 5 SF 0.5

4. Conclusions

"Proposed" model is the best fit models, even when admixtures are added in mortar. In many cases, it was the best fit and in other cases, it was very well suited model. It never failed and never showed negative values. It can be easily and efficiently used for cement based materials. The use of Microsoft excel solver optimize all unknown parameters of equations and provides the best possible solutions. The tool is more helpful for young researchers and learners.

NOTE

Further information on data and analysis can be found on following website:

http://etd.lib.metu.edu.tr/upload/12620623/index.pdf

ACKNOWLEDGMENT

REFERENCES

Ferraris, C, de Larrard, F., and Martys, 2001. Fresh Concrete Rheology: Recent Developments, in Materials Science of Concrete VI (Eds. S. Mindess and J. Skalny), pp. 215-241, The American Ceramic Society. Banfill, P.F.G. 2003. The Rheology of Fresh Cement and Concrete – A Review, in Proc. 11th Int Cement Chemistry Congress (Ed. H. Justnes), Durban, South Africa.

Wallevik, O.H. and Wallevik, J.E. 2011. Rheology as a Tool in Concrete Science: The Use of Rheographs and Workability Boxes, Cement and Concrete Research, 41, 1279-1288.

De Larrard, F. Ferraris, C.F. and Sedran, T. 1998. Fresh Concrete: A Herschel-Bulkley Material, Materials and Structures, 31, 494-498.

Lu, G. 2008. Rheological Studies on the Flow Behavior of Two-phase Solid-Liquid Materials. Retrospective Theses and Dissertations. Paper 15884. Iowa State University.

Banfill, P.F.G. 2006. Rheology of Fresh Cement and Concrete, Rheology Reviews, The British Society of Rheology, 61-130.

Tokyay, M., Delibaş, T., Aslan, Ö. 2010. "Effects of Mineral Admixture Type, Grinding Process, and Cement Fineness on the Physical and Mechanical Properties of BFS-, Natural Pozzolan-, and Limestone- incorporated Cements, Working Paper AR-GE 2010/01-B, Turkish Cement Manufacturers' Association (TÇMB), 45p. (in Turkish)"

Idrees,M., Tokyay, M., 2016. Thesis "Effects of Mineral Admixture on rheology of concrete." http://etd.lib.metu.edu.tr/upload/12620623/index.pdf

Analysis of Hybrid Solar Desiccant Air Conditioning for building application

Rehan Khursheed[1,a] , Abdul Hameed Memon[1,b] , Mahesh Kumar[1,c] and Yuehong Su[2]

[1] Mechanical Department, Hamdard University, Main Campus Karachi-Pakistan

[2] Institute of Sustainable Energy Technology, University Park Campus,
The University of Nottingham, Nottingham-UK

Email: [1,a)] rehan.khursheed@hamdard.edu.pk ,[1,b)] hameed.memon@hamdard.edu.pk,
[1,c)] mahesh.kumar@hamdard.edu.pk and [2)] yuehong.su@nottingham.ac.uk

Abstract - Solar desiccant air conditioning system for an office building in Karachi was analyzed to determine its applicability. Energy plus 7.2 was used to analyze the building for calculation of cooling load. The analysis was carried out by considering ASHRAE 189.1-200 (Climate 4-8) HVAC standard. For the selection of desiccant wheel, the NovelAire desiccant wheel software was used. The regeneration process was accomplished by solar energy using evacuated tubes with collector area $20m^2$ at tilt angle of 15°. The COP for peak summer conditions was found to be 0.9. It was observed that desiccant wheel rpm has effect on the humidity and exit air temperature, both parameters found to be decrease slightly with increase of wheel rpm. The effect of variation of cooling load on COP was assessed and it was found that COP decreased at when load reduces from 30% to 40% and at further at increasing load, the COP started increasing. Simulations results indicated that solar desiccant system can be applied effectively for building air conditioning using solar energy. However, for continuous application hybrid system may be developed utilizing solar energy in daytime and in the absence of solar energy, auxiliary heating system may be used to provide the required heat energy.

Key Words —*Desiccant, Regeneration, Humidity, Coefficient of Performance*

I. INTRODUCTION

About 40% of total energy consumed in building is used for HVAC systems.[1,2]. Mostly Vapour compression systems are commonly used air conditioning systems around the world. This system uses working fluid known as 'refrigerant'. [3]. Vapour compression systems are mechanical powered driven by electric power. Globally, the energy consumed by vapour compression is 15% [4,5]

The refrigerant contains many conventional fluorocarbon refrigerants which have significant environmental effects e,g. HFC–134a and HFC–410A both having global warming potentials (GWPs) around 1,370 and 2,100 times of carbon dioxide (CO_2) respectively [6].

Pakistan is blessed with excellent renewable energy resources which include as hydropower, solar, biomass and wind. it is observed that Pakistan has daily solar insolation of 5-7 KWh/m^2/day suitable for efficient operation of evacuated tubes [7].By taking into consideration above factors, the present study looks for application of solar desiccant air conditioning system which is substitute to the usual air conditioning technology.

A. Desiccant Mechanism

Desiccant system is a combination of two processes together: evaporative cooling and dehumidification. The general system layout of desiccant air conditioning is shown in Fig 1 and parameters of this system are shown on psychrometic chart in Fig 2. Working principle of desiccant wheel is based on the difference in vapour pressure between the water side (which is hold by desiccant) and the air side. Air side vapour pressure is higher and so in this way, air dehumidifies. For the reuse of desiccant, it must be heated so the vapour pressure gets reversed i.e. it holds more vapour pressure in

1

desiccant wheel as compared to air so desiccant gets dehumidified. This vapour pressure changing process is called 'Regeneration'[8]. The regeneration temperature can be achieved by using renewable technology such as solar energy or burning biomass. This will also reduce fuel costs and in particular emissions levels in the environment [9].
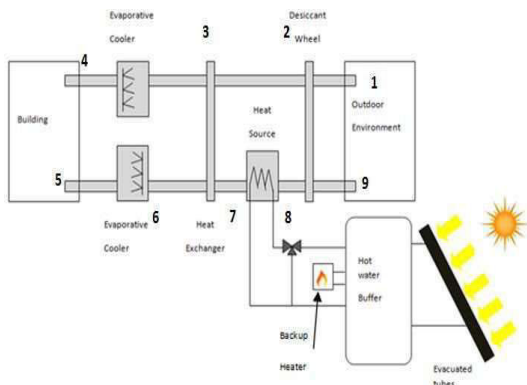
Fig 1. Solid desiccant air conditioning system using solar energy for regeneration.
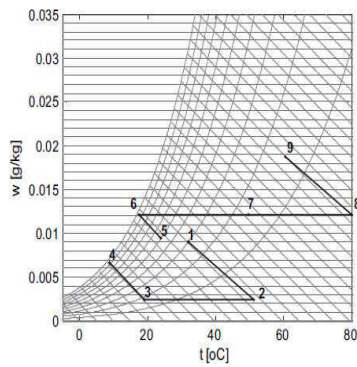
Fig.2. Desiccant air conditioning process on psychometric chart.

II. METHODLOGY

For the present work, Dalda office building comprising of five floors, was taken as case study for the city of Karachi. The Google Sketchup software was used to model the building and extract the plan area of the

building as Fig 3. The building cooling load was evaluated by EnergyPlus software. Following dimensions were evaluated: Width (East facing): 15.07 m, Width (South facing): 11.51 m, Height of building: 20 m.
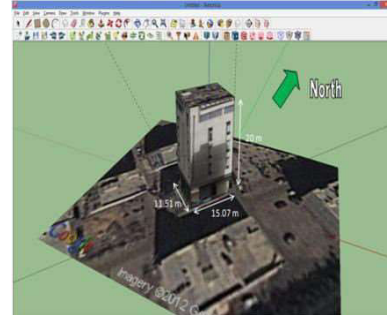
Fig 3 3D model of Dalda Office building in Google sketch up.

For analysis purpose, the floor plan of the building for each floor is assumed to be divided into six spaces as shown in Fig 4 and the final model is illustrated in Fig 5.
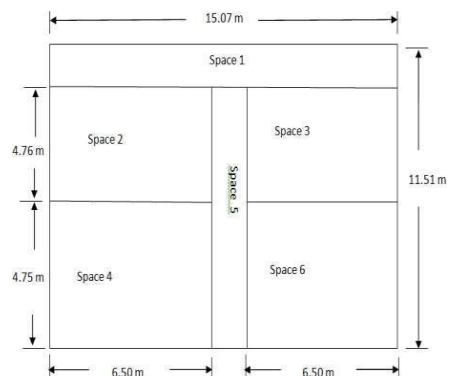
Fig 4. A proposed layout for a floor of the building.
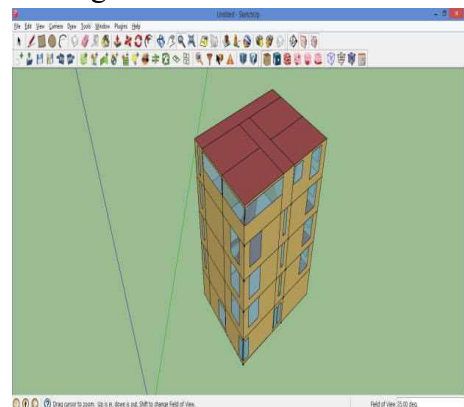
Fig 5: Building modeled in Google sketch up.

2

The building cooling load alongwith parameters were calculated using Open Legacy studio software using the ASHRAE 189.1-200 (Climate 4-8) as standard. The following fixed conditions were fixed for the simulation: Outdoor temperature = 40°C (Dry bulb) and 28.3°C (Wet bulb), humidity (w_1= 19.6g/kg) and Indoor temperature 26°C, relative humidity 50% and density of air ρ = 1.127 kg/m^3. [10]

Table 1. Standard values obtained after simulation from Open Legacy studio software

S.No.	Parameter	Evaluated Value
1	Sensible Load ($Q_{sensible}$)	24.8 kW
2	Air Volume flowrate	4624 cm^3/hr
3	Air mass flow rate	1.47 kg/s
4	Humidity (building)	10.57 g/kg

A. Selection of Desiccant Wheel & Evacuated Tubes

For the required conditions, the selected desiccant wheel Model No: WSG 1220x 220 having following characteristics as shown in table 2. [11]

Table 2. Specification of desiccant wheel

Specification	Value
Wheel diameter	1220 mm
Depth of wheel	200 mm
Cassette Width	1371.6
Cassette depth	330.20 mm
Drive motor	1/40 hp

For regeneration process, evacuated tubes (flat absorber) of Thermomax company were selected with following specifications: solar collector efficiency 69.9%, Area of single

module 1.975 m^2 (for T = 50 K, 800 W/m^2) [1]. The number of modules of evacuated tubes required = 9

III. CALCULATIONS

To evaluate the parameters describing HVAC conditions were evaluated by the equation proposed in references [10-11] & [12-16] alongwith the Novel Aire desiccant wheel selection software and psychometric charts. The evaluated results are presented in table 3.

Table 3: Different values of parameters at various points of desiccant system.

S. No	Temperature (°C) Dry Bulb	Humidity Ratio (g/kg)	Enthalpy (kJ/kg)
1	40.0	19.6	91.0
2	70.0	10.6	100.0
3	28.7	10.6	57.5
4	20.8	10.0	46.0
5	26.0	10.6	53.0
6	21.5	13.1	55.0
7	62.7	13.1	96.0
8	88.0	13.1	128.0
9	58.0	22.1	117.0

3

IV. SYSTEM ANALYSIS

The analysis of the system is carried out on two scenarios as shown below:

A. Effect on exhaust temperature to outdoor on changing wheel RPM

Table 4. Effect of wheel speed on outdoor

Conditions

RPM	Exhaust Temperature (ºC)	Humidity Ratio (*w*)
24	58.0	22.10
30	57.2	22.00
35	56.6	22.06
40	56.4	22.03
45	56.0	22.03
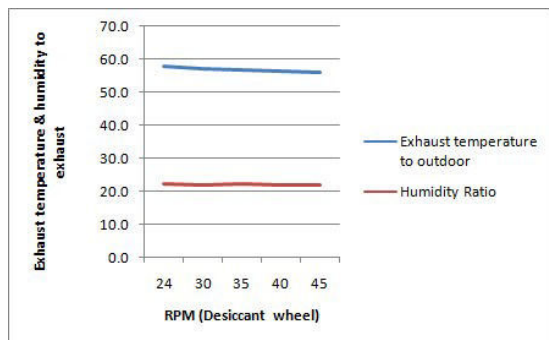
Fig. 6. Changes in exhaust temperature with desiccant wheel speed variation.

When the desiccant wheel RPM increased from 24 to 45 RPM, the exhaust temperature of the air at point 9 of the system reduces from 58ºC to 56ºC which makes a good positive impact on the environment

B. Changing COP with varying cooling load

The regeneration temperature is fixed at 88ºC and also the indoor/outdoor conditions.
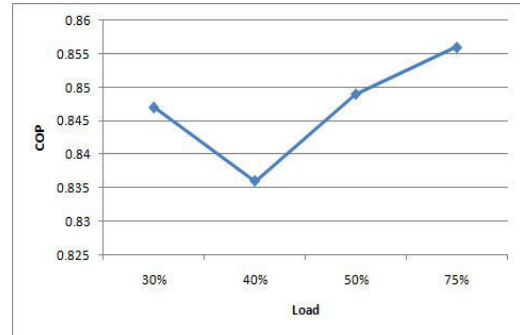
Fig. 7. Graph showing changing COP with respect to varying load conditions.

The COP of the system is calculated at different cooling loads and COP increased very slowly with the increasing cooling load.

V. CONCLUSIONS

The COP for this desiccant system found as 0.9. The WSG 1220 x 200 desiccant wheel is selected having regeneration temperature range 80ºC to 170ºC. The regeneration temperature is achieved using proper selection of evacuated tubes.

The system's performance analysis was carried out on changing parameters.. From the analysis, it was found that the wheel RPM to be increased so as to reduce the exhaust air temperature. The changing regeneration temperature will reduce the COP. So for achieving maximum COP, the regeneration temperature should be maintained at 88ºC.

Future work could be carried using hybrid system like using gas heaters for reheating since gas is cheaply available in Pakistan and further the rotation of wheel could be made using photovoltaics.

4

V. REFERENCES

[1] Henning, H.-M. , "Solar-assisted air conditioning in buildings", A handbook for planners by hans-martin henning, springer, 2007.

[2] Xin Zheng, Hing-Qi Li, Ming Yyu, Gang Li and Qi-Ming Shang, "Benefit Analysis of Air Conditioning Systems using Multiple Energy Sources in Public Buildings", Applied Thermal Engineering, vol. 107, 2016, pp. 709-718.

[3] Chambers, B. "Vapour Compression Refrigeration cycle, An Introduction for GE Appliance Salesmen", 2009, accessed 7th January'2019

[4] Ascani Maurizioa, Cerri Giovannib,
De Francesco Eduardoc, "Power Reduction in Vapour Compression Cooling Cycles by Power Regeneration", Energy Procedia, 2015, pp 1184-1197.

[5] V.M. Nguyen, S.B. Riffat, P.S. Doherty, "Development of a Solar Powered Passive Ejector Cooling System", Applied thermal engineering, 2000, pp 157-168.

[6] William Goetzler, Robert Zogg, Ji, Young, Caitlin Johnson, "Alternatives to Vapor- Compression HVAC Technology",Ashrae Journal, 2014.

[7] Sheikh, M.A., "Renewable Energy Resource Potential in Pakistan", Renewable and Sustainable energy reviews, 13, 2009, pp 2696-2702

[8] Sayigh, A.A. M. & Mcveigh, J.C., "Solar Air Conditioning and Refrigeration", Pergamon Press, 1992.

[9] Mehta, J. & Rane, M. Liquid, "Desiccant Based Solar Air Conditioning System with Novel Evacuated tube collector as regenerator", Procedia engineering, \51 , 20113 pp 688-693.

[10] The national energy conservation center Pakistan, Building energy code of Pakistan, 1990 [pdf], accessed 5th Aigust 2016.

[11] Novelaire technologies (heat and mass transfer products), desiccant dehumidification wheel, accessed 6thAugust 2016

[12] Panaras, G., Mathioulakis, e., belessiotis, & Kyriakis, N., "Theoretical and experimental investigation of the performance of a desiccant air conditioning system", Renewable energy 35, 2000,pp 368-1375.

[13] Sensible heat ratio (general design values, accessed November, 2017

[14] Air changes for typical room and buildings. Accessed August 2016.

[15] Panaras, G., Mathioulakis, E. & Belessiotis, V, "Solid Desiccant Air- Conditioning Systems-Design Parameters. Energy, Vol. 36, 2011, pp 2399-2406.

[16] Li, H., Dai., Li, Y., La, D. & Wang, R., "Case study of a two-stage Rotary Desiccant Coolin/Heating System driven by Evacuated Glass tube Solar Air Collectors", Energy and Buildings, Vol. 47, 2012, pp 107-112

A Novel Approach of Parametric Modeling of Real Space (NAPMRS)

Syed Atif Ali Shah [1,a], Zubia [2,b]

[1]Northern University, Nowshera, Pakistan

[2]Qurtuba University, Peshawar, Pakistan

[a] atif@northern.edu.pk , [b] dboss009@yahoo.com

Abstract—The recent complicated appliances however, really valuable are distinct by the need of platform; competent enough with strong computing power and with the grand efficiencies. Conventionally a uni-dimensional structure were able to managing the hassled up issues up to some level, now with steadily higher clock speeds surrounded the other features; thus produced a demand for a new ground called multiple-dimensional. The initiative was to use several individual dimensions and split the pack in the way that the unity of dimensions is made more effectiveness. The rapid progression in computation enforced scientists to grasp the Allan Turing's Computational model for extremely multifaceted problems. 3D Euclidean space covers the three- dimensional space of Euclidean geometry. In this paper, 3DTM is used for modeling the 3 Dimensional Digital Spaces (3DDS), this representation is smarter while presenting and resolving three-dimensional space of Euclidean geometry, having pretty professional appearance on 3DDS tribulations. This procedure passes the techniques of algebra and calculus to bear on matters of plain and analytical geometry and includes the benefit that it simplifies easily to Euclidean spaces on Turing Machine.

Keywords— Euclidean Space, 3D Space, Geometry, 3D Graph, Turing Machine.

I. INTRODUCTION

The swift advancements in semiconductor processing technology enabled designers to realize the Allan Turing's predictions even today. The increased logic density on has made it possible to fabricate very complex problems. While a decade back, efficiency of the system was increased by increasing the clock's speed, which resulted in higher power demands; and/ or with complex CPU organizations by reducing the size of chip. Now architects believe in simpler logical solutions for that for achieving higher performance. A multi dimensional Turing machine system deploys multiple tapes with different directions. At this juncture the problem with most of these techniques is limited by the computational convolution. 3DTM is proficient of solving 3D problems competently. Instead of using single infinite tape or multi infinite tapes; it uses 3Dimensional Euclidean geometry / Graph to resolve numerous issues.

A. Euclidean space

In geometry, 3D Euclidean space is also known as the three-dimensional space of Euclidean Geometry. Conventionally the geometry describes them by means of some laws and belongings of these 3Ds were figured out as theorems. Calculus modeling is a common tool to delineate normal figures. whilst algebraic and arithmetic study grow to be developed enough, this comparison upturned and currently it is further general to describe ES using CC and the view of analytical geometry. It reveals that elements of the space are depicted with gathering of real values (numbers), and equations and inequalities to represent geometric figures. This technique passes the systems of algebra and calculus to set on issue of calculus and has the benefit that it simplifies straightforwardly to Euclidean spaces system

for further dimensions. Euclidean space is usually represented by means of Cartesian coordinates. It is then mold by the real coordinate space (Rn) of the same dimension. For One Dimension, it's a real line; for Two Dimensions it's a Cartesian plane; and in Three Dimensions it is a coordinate space with three real number coordinates. Mathematicians symbolize the MD (Multi Dimensional) Euclidean space by En to highlight its Euclidean character, but Rn is used as well since the second is understood to have the customary Euclidean structure.
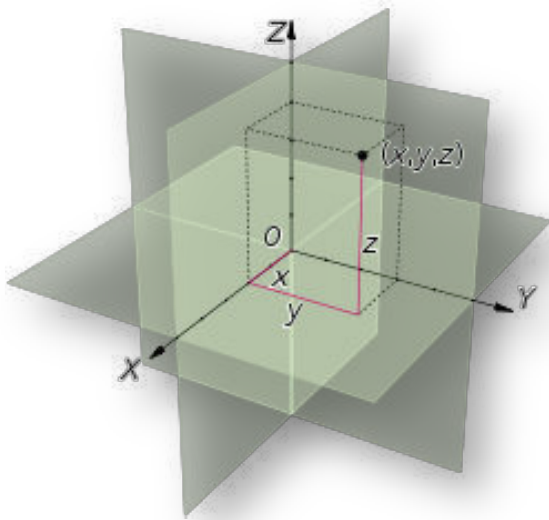
Fig 1. Euclidean Space

B. 3D Space

Tri-dimensional space or 3D space or 3-space or 3 dimensional spaces is a geometric domain in which 3 parameters are needed for deciding the location desired component; which is point. In physical sciences, a series of numbers is visualized as a position in 3D space is called three-dimensional Euclidean space; represented as Ř3. This provides a three-parameter form of the physical universe (i.e the spatial part. Nonetheless, this space is only one example of a large variety of spaces in three dimensions called 3-manifolds. In this conventional example, when the three parameters refer to

capacity in diverse directions (coordinates), any 3 directions can be selected, provided that vectors in these directions don't all lie in the same two space. Moreover, in this case, these 3 parameters can be tagged by any arrangement of 3 selected from the elements height, depth, and breadth.
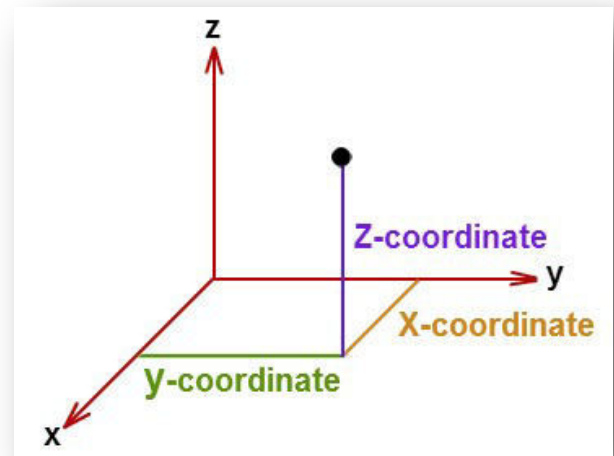
Fig 2. 3D Coordinates

C. 3DTM

Three Dimensional Turing's Machine (3DTM) is another variant of single tape Turing's Machine. Though the power of all variants is same but there is disparity of time trade. A three dimensional Turing's machine computes same way as other TM; it is alike 3Tape TM, with the difference of work space. A 3T TM uses 3 tapes while 3DTM is using 3 dimensional spaces system.

Formally a 3Dimensional Turing machine is a 7-tuple, (Q, $\sum$, Γ, δ, q0, qa, qr), where Q, $\sum$, Γ are all finite sets.

1. Q is the set of states.

2. $\sum$ is the input alphabet not containing the special blank symbol ␣.

3. Γ is the tape or work alphabet.

4. q0 is the start state.

5. qa is the accept state.

6. qr is the reject state.

7. δ: Q × Γ → Q × Γ × {L,R} × {U,D} × {I,O} is the transition function.

Just like an ordinary TM it performs computation, with the distinction of only head movement; for each step it has to work the following way (X□Y, L/R, U/D, I/O), where the

- X is a ∑ (input alphabet)

- Y is a Γ (output alphabet)

- → is transition from input to output

- L/R Left or Right, travels with X axis of the coordinates

- U/D Up or Down, travels with Y axis of the coordinates

- I/O In or Out, travels with Z axis of the coordinates

D. 3DDS/3DES

3D Euclidean Space or 3D Cartesian Coordinate System or 3 Dimensional Digital Space System is a virtualization of the real world, a 3 Dimensional Space, generally speaking a 3Dimensional Graph.
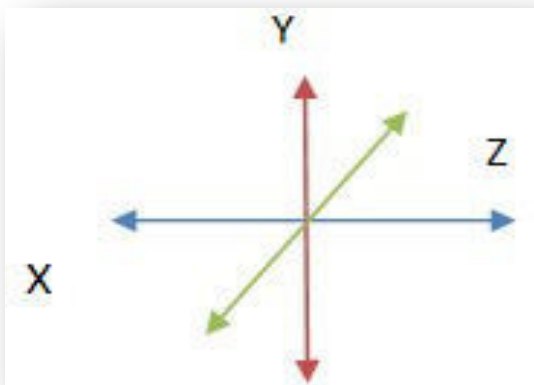
Fig 3. 3D Axis

The three dimensional Cartesian coordinate system is shown in the following diagram X and Y coordinate are axes which are together at right angles, just like two-dimensional structure

and an additional third axis, called Z axis that is also perpendicular to both X and Y axes. Find below a more clear 3D figure of 3D coordinate system.
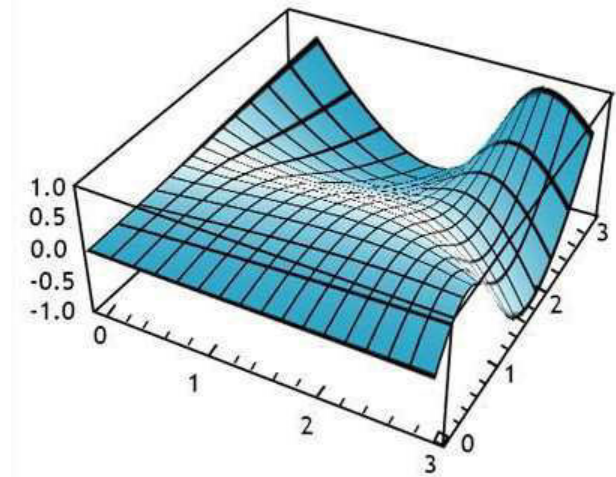
Fig 4. 3D Graph

E. Connecting a Point to Base

Now we'll connect a point (present anywhere in 3 Dimensional Space / 3D Euclidean space) to the base i.e (0,0,0) using 3DTM. In other words we are discovering the shortest distance to the said point from origin.

Below is the description of the Turing Machine to execute the problem.

- $\Sigma = \{Pi, Pf, .\}$

- $\Gamma = \{Pi, Pf, ., \_\}$

- Start state.

- Accept state.

- $Q \times \Gamma \rightarrow Q \times \Gamma \times \{L,R\} \times \{U,D\} \times \{I,O\}$ is the transition function.

Fig 5. 3DTM
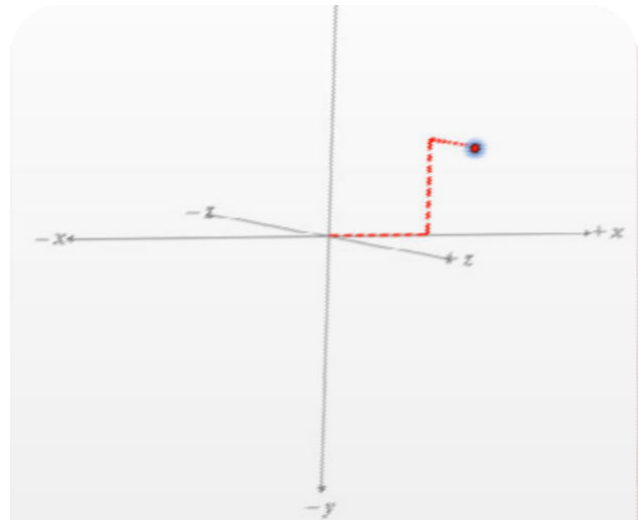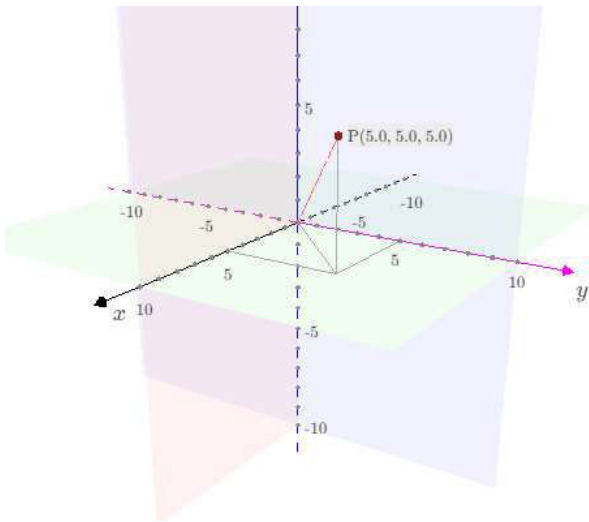
F. Simulation of 3DTM

This machine starts its working from base location, here we taking base location or initial point $(0,0,0)$ and call it Pi and Pf or simply 'P' as final point . It's not necessary to take 0 as base location, we can start from anywhere. But here we taking $(0,0,0)$ as our base location or initial point. This machine takes (_) as input and converts it to (.) as output, in our diagram we represented (_) as X and (.) as Y; for convenience.

$$\rightarrow q\, P_i \_\_\_\_ P_f \_$$
$$\rightarrow \_P_i\, q_0 \_\_\_\_ P_f \_$$
$$\rightarrow \_P_i . \, q_0 \_\_\_ P_f \_$$
$$\rightarrow \_P_i . . \, q_0 \_\_ P_f \_$$
$$\rightarrow \_P_i . . . \, q_0 \_ P_f \_$$
$$\rightarrow \_P_i . . . . \, q_0 P_f \_$$
$$\rightarrow \_P_i . . . . P_f q_a \_$$
$$\rightarrow q\, P_i\, xxxx\, P_f \_$$
$$\rightarrow \_P_i\, q_0\, xxxx\, P_f \_$$
$$\rightarrow \_P_i\, y\, q_0\, xxx\, P_f \_$$
$$\rightarrow \_P_i\, yy\, q_0\, xx\, P_f \_$$
$$\rightarrow \_P_i\, yyy\, q_0\, x\, P_f \_$$
$$\rightarrow \_P_i\, yyyy\, q_0\, P_f \_$$
$$\rightarrow \_P_i\, yyyy\, P_f\, q_a \_$$

Fig 6. 3DTM Modeling

II. FUNDAMENTAL APPLICATIONS

- Computer vision

- Computer Graphics

- GIS

- 3D animations

- Auto CAD/CAM

- 3D Geometry /Calculus

- Gaming industry

- Medical Imagining

- Bioinformatics

- Structural Engineering

III. CONCLUSION

The recent complicated appliances although very valuable, are noticeable by the necessity of dais competent of sky-scraping resolution supremacy beside immense competences. Conventionally a uni-dimensional structure were able to managing the hassled up issues up to some level, now with steadily higher clock speeds surrounded the other features; thus produced a demand for a new ground called multiple-dimensional. The initiative was to use several individual dimensions and split the pack in the way that the unity of dimensions is made more effectiveness.

In geometry, 3D Euclidean space is also known as the three-dimensional space of Euclidean geometry. Conventionally the geometry describes them by means of some laws and belongings of these 3Ds were figured out as theorems. Calculus modeling is a common tool to delineate normal figures. whilst algebraic and arithmetic study grow to be developed enough, this comparison upturned and currently it is further general to describe ES using CC and the view of analytic geometry. It
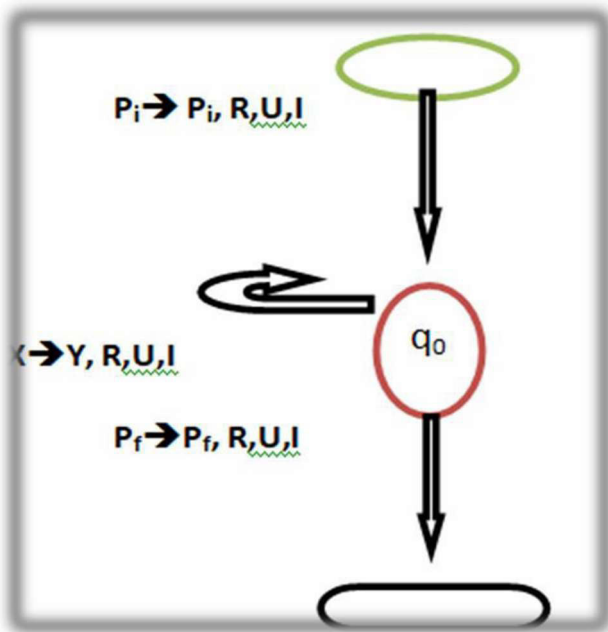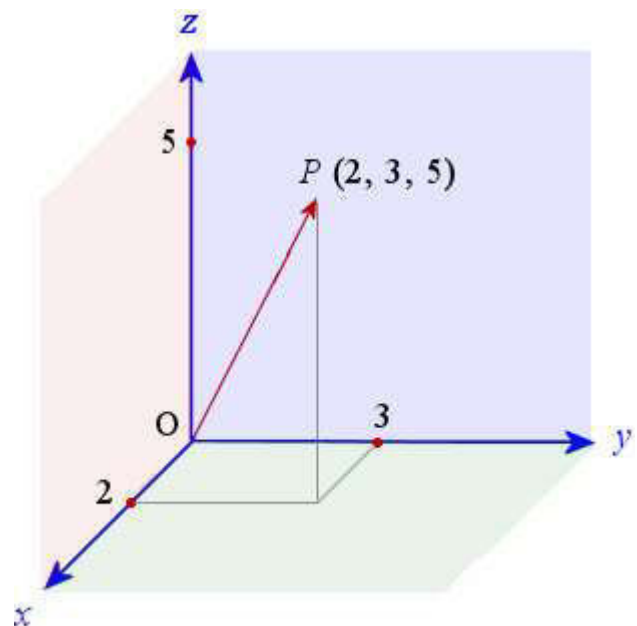
reveals that elements of the space are depicted with gathering of real values (numbers), and equations and inequalities to represent geometric figures. This technique passes the systems of algebra and calculus to set on issue of calculus and has the benefit that it simplifies straightforwardly to Euclidean spaces system for further dimensions. Euclidean space is usually represented by means of Cartesian coordinates. It is then mold by the real coordinate space (Rn) of the same dimension. For One Dimension, it's a real line; for Two-Dimensions it's a Cartesian plane; and in Three Dimensions it is a coordinate space with three or more real number coordinates.

A multi dimensional Turing machine system deploys multiple tapes with different directions. At this juncture the problem with most of these techniques is limited by the computational convolution. 3DTM is proficient of solving 3D problems competently. Instead of using single infinite tape or multi infinite tapes; it uses 3Dimensional Euclidean geometry / Graph to resolve numerous issues. It is mainly concerned with the 3 Dimensional Digital Spaces (3DDS), this is a smarter version for presenting and resolving three-dimensional space of Euclidean geometry, having pretty professional appearance on 3DDS tribulations. This technique passes the tools of algebra and calculus to bear on questions of geometry and has the benefit that it generalizes easily to Euclidean spaces on Turing Machine.

REFERENCES

[1]. Ya.D. Sergeyev. Numerical computations and mathematical modeling with infinite and infinitesimal numbers. Journal of Applied Mathematics and Computing, 29:177–195, 2009.

[2]. A. Church. An unsolvable problem of elementary number theory. American Journal of Mathematics, 58:345–363, 1936.

[3]. S. Barry Cooper. Computability Theory. Chapman Hall/CRC, 2003.

[4]. M. Davis. Computability & Unsolvability. Dover Publications, New York, 1985.

[5]. A.N. Kolmogorov and V.A. Uspensky. On the definition of algorithm. Uspekhi Mat. Nauk, 13(4):3–28, 1958

[6]. J.P. Mayberry. The Foundations of Mathematics in the Theory of Sets. Cambridge University Press, Cambridge, 2001.

[7]. Reengineering the Industrial CMMI, S Atif A S. Volume 4, Issue 3, Summer 2018, Page 135-208. Journal of Advances in Computer Engineering and Technology (JACET). http://jacet.srbiau.ac.ir

[8]. K. (Vela) Velupillai, "Computability and Complexity in Games," Working Papers _010, University of California at Los Angeles, Center for Computable Economics.

[9]. Francesco Luna & K. (Vela) Velupillai, . "Notes on Learning Rational Expectations under Computability Constraints," Working Papers_009, University of California at Los Angeles, Center for Computable Economics

[10]. Formulating DNA Chains Using Effective Calculability, S atif a s. 1 (2018) > shah. international journal of computer (ijc). http://ijcjournal.org

[11]. UC 2011 - 10th International Conference on Unconventional Computation, Turku, Finland, June 6 - 10, 2011.

[12]. TAMC 2011 - 8th Annual Conference on Theory and Applications of Models of Computation, Chofu, Tokyo, Japan, May 23 - 25, 2011.

[13]. Decoding 3-Dimensional Euclidean Space using 3DTM. S Atif Ali Shah. 3rd Abasyn International Conference on Technology and Business Management

[14]. Francesco Luna, . "Learning in a Computable Setting: Applications of Gold's Inductive Inference Model," Working Papers _008, University of California at Los Angeles, Center for Computable Economics.

[15]. Transforming a company with OOP Andrea Rinaldi Director, Business Software Development Group Microarea S.p.A. Via Renata Bianchi,

[16]. on squaring a number and t-semi prime numbermohammed khalid shahoodh

[17]. Applications of Multidimensional Time Model for Probability Cumulative Function to Brownian motion on fractals to Kinetics of Chemical Reactions and other areas of chemical research, Michael Fundator

Identification of Critical Factors Influencing Cost Escalation In Public Sector Construction Projects

Zohaib Qadeer[1,a], Nafees Ahmed Memon[2,b], Muhammad Aslam Leghari[3,c], Aftab Hameed Memon[4,d] and Fida Hussain Siddiqui[5,e]

[1]Mehran U.E.T., Jamshoro, Sindh, Pakistan
[2]Mehran U.E.T., Jamshoro, Sindh, Pakistan
[3]NESPAK Consultancy, Hyderabad, Sindh, Pakistan
[4]QUEST, Nawabshah, Sindh, Pakistan
[5]Mehran U.E.T.,Jamshoro Sindh, Pakistan

Email address: [a]zohaibqadeer66@gmail.com, [b]nafees.memon@faculty.muet.edu.pk, [c]leghariaslam@gmail.com, [d]aftabm78@hotmail.com and [e]fida.siddiqui@faculty.muet.edu.pk

Abstract—*The Pakistan Construction Industry plays vital role in both economic growth and poverty reduction. Cost related issues are also faced by Pakistan like many other developing countries. Cost escalation is defined as change in the cost of particular services or goods in a certain economy over a period of time. The continuous increase in labor and material cost has raised serious problems on the efficiency of work contracts. It has been observed that cost escalation in many public sector projects of Sindh is very critical issue. Pakistan's economy largely depends on agriculture. Therefore, water sector projects are important from the development point of view. The present situation also indicates that some of the projects in this sector have been affected by cost escalation. This research therefore considers the study of cost escalation in construction projects related to water sector. Thus, the identification and evaluation of factors influencing cost escalation in public sectors projects becomes necessary. This was achieved by conducting a questionnaire survey. Based on the analysis of survey, this study identifies critical factors influencing cost escalation with main focus on water sector construction projects in Sindh.*

Keywords—*Cost Escalation, Project Cost, Water Sector Projects, Critical Factors, Sindh*

I. INTRODUCTION

Construction industry in all over the world is to be considered one of the vital industry having activities such as installation, construction, alteration, extension as well as demolition [1]. It plays a significant role in the economic as well as physical development of any country [2, 3]. Construction sector has a share of 20% in total GDP (gross domestic product) of the country and it consumes up to 50% of the countrywide 5 years plan expenditures. Many construction projects such as medium to large construction takes many years for their completion in such condition labor prices and material prices increases regularly which causes many problems in the management of any project. Since last several years construction sector has been suffering from many problems due to rapid increase in interest charges, equipment cost, labor cost and material cost. Cost escalation defined as change in the cost of particular services or goods in a certain economy over a period of time. Escalation comprises general inflation related to the supply of money, it is also determined by variation in applications, technologies and specifically supply and imbalance demand that are specific to a particular service or good in a given economy. For example, Due to the imbalance supply-demand in the year 2003-2007 the general inflation in the US was less than 5% and steel prices was increased by over 50%. Generally, Cost overrun of project may occur due to Cost escalation. In particular, the construction industry faces a major problem due to this increase [4]. In the past many construction projects have been suffered due to schedule and cost overruns. There are many examples where the final cost of project was greater than the estimated cost prepared and released at the start

of construction [5, 6]. By estimator's point of view, escalation is an important risk that must be estimated [7]. Cost escalation has usually been observed in many of the construction projects. The completion of highway projects usually takes long period of time as in the case of Holland tunnel which experienced increase in cost. Nearly 50% of large highway projects in America have exceeded their original cost. Research and study work have revealed individual factors resulting in escalated project cost [8]. A study has been carried out by Minsochol, to improve the cost escalation system calculate the fluctuation rate and calculate the price fluctuation of whole material [9]. Expenses of projects also include escalation therefore for tendering process and budget it is necessary to calculate cost escalation [10].

It has been observed that cost escalation in many public sector projects of Sindh is very critical issue. It is difficult to calculate cost escalation accurately therefore cost of the public sector project becomes high due to escalation. Consequently, the cost of public sector projects increases and additional funds are required for completion of projects.

II. FACTORS INFLUENCING COST ESCALATION IN PUBLIC SECTOR PROJECTS

Construction and engineering services sector within Pakistan is the most neglected one despite its great contribution towards the GDP and employment about 9% of the total labor force. In Pakistan Construction projects generally run over cost and time schedules and do not necessarily meet user requirements [11]. Cost escalation is the adjustment or settlement of unit price of contract component which includes labor, construction materials and equipment to contract the value during bid and is almost inevitable in large construction projects [24]. Cost related issues are also facing by Pakistan like many other developing countries among which cost escalation is considerably prominent [12]. Cost control is very critical issue in construction project management [13, 14]. It is a phenomenon which is widely practiced by all construction

stakeholders. Cost escalation has negative implications for both construction stakeholders and the industry in general [14, 15]. When actual cost exceeds the previously estimated values then cost escalation occurs [16, 17]. Today's construction industry is expected to face the trend of cost escalation even in future because of the race of experts and funds. This trend has caused a great deal of uncertainty and uneasiness among the project owners who will have to face exceeded expenses towards the projects than the budgets which was fixed prior to the current market place escalation. This escalation pushes them to redesign the process to coincide the previously fixed funds or manage for the surplus funds to handle the new demands [18]. The suggestions provided by current procedures that there is lack of methods of planning and logical strategy of cost escalation to achieve a proper examination of cost at the initial stage of schemes and throughout the construction processes [19]. Construction performance in terms of cost leading to risk due to several governing factors [25]. The structure delivery through its construction industry describes the capital of any nation. Due to its volatility and enormous size, the construction industry requires huge capital outlays. ChabotaKaliba (2009) highlighted some causes and impacts of increased cost and schedule delays in infrastructure projects. The main factors influencing cost escalation highlighted in his study were: inflation, scope changes, bad weather, technical challenges, strikes, environmental protection, schedule delay and local government pressures [17]. K.Vamsidhar and D.A.Eshwarswaroop (2014), suggested the following main factors which influence cost escalation: increase in transportation fare, fluctuation in price of material, increase in labor cost charges, increase in equipment charges, increase in lending rate for various small-scale industries sector, power cuts, increase in electricity charges, increase in demand for residential building, increase in VAT and Service taxes [4].Some factors influencing cost escalation in construction projects were also given by Anderson (2007), which include: Schedule changes, failure to account for risks,

complexity, scope changes, errors of omission and scope creep [20]. Jennifer S. Shane (2009), in his study mentioned some internal and external factors influencing cost escalation which include: engineering and construction complexities, poor estimating, inconsistent application of contingencies, delivery/procurement approach, faulty execution, ambiguous contract provisions, contract document conflicts and project schedule changes, effects of inflation, local concerns and requirements, scope changes, scope creep, unforeseen events, unforeseen conditions and market condition [6]. Some factors influencing the cost escalation in civil engineering projects were also given by Nasiru Zakari Muhammada (2015). Those factors include: fluctuation of price of materials, variation, government policies, change of government and political instability, wrong method of estimation, poor financial control on site, long period between design and tendering time, design errors, lack of coordination between contractors and consultant, poor supervision and liquidation damages, previous experience of contract, inadequate production of raw materials, effect of weather and absence of construction cost data [14].The major factors causing cost escalation in construction industry as identified from literature are: labor cost, cement, bricks, steel, composite materials, aggregate and equipment cost [4]. Common factors influencing cost escalation reported in literature were summarized and taken for further study.

III. RESEARCH METHODOLOGY

Factors identification was done through literature review and from unstructured interviews by the experts of professionals having experience in water sector related projects. On the basis of factors identified, the questionnaire was designed. The questionnaires were distributed to the professionals of the public sector to assess the rank of cost escalation factors. There were mainly two parts of the questionnaire, part one and part two. Part one asked about the respondent's demographics i.e. personal information. Part two asked about

the information related to significant level of identified cost escalation factors. It was arranged in the order of priority scale from not significant (1) to extremely significant (5).

IV. DATA COLLECTION AND ANALYSIS

One hundred twenty questionnaire proforma were distributed to the professionals of clients, consultants and contractors. Ninety-eight fully filled questioners were received from professionals of the public sector. Data analysis was carried out from 5-point Likert scale, the scale read as follows, 1 = Not Significant, 2 = Slightly Significant, 3 = Moderately Significant, 4 = Very Significant, and 5 = Extremely Significant. Considering the five-point Likert scale of measurement adopted for this study, 1 was subtracted from 5 which equal to 4. After that, the 4 was divided by 5 which is equal to 0.8. Thus, the difference between values is 0.8. See Table IV.I for the ranges and interpretations [23]. The results obtained from the feedback of the questionnaires were analyzed using SPSS version 20.0 (statistical package for the social sciences) software. SPSS provides a broad range of capabilities for the entire analytical process. All data and information from the questionnaires were entered into SPSS program for statistical analysis in order to obtain mean value and rank of identified cost escalation factors.

TABLE IV.I INTERPRETATION OF THE LIKERT SCALE MEASUREMENT

Interpretation	Value Range Allocation
Extremely Significant	4.2-5.0
Very Significant	3.40-4.20
Moderately Significant	2.60-3.40
Slightly Significant	1.80-2.60
Not Significant	1.00-1.08

V. RESULTS AND DISCUSSIONS

Tables V.I below show the results of the identified cost escalation factors in public sector

projects respectively mean value and ranked in order to identify critical factors which causes cost escalation.

TABLE V.I COST ESCALATION FACTORS IN PUBLIC SECTOR OF PAKISTAN

Factors	Mean Value	Rank
Fluctuation in price of material	4.3352	1
Frequent changes in design	3.8681	2
Frequent change orders during construction by client	3.7802	3
Financial difficulties faced by client	3.7418	4
Changes in scope of work	3.6978	5
Long duration between design and tendering	3.5769	6
Inadequate planning and scheduling	3.5000	7
Increase in labor charges	3.4890	8
Increase in transportation charges	3.4725	9
Delays in decisions making by client	3.4132	10
Increase in value added tax (VAT) and Service taxes	3.2967	11
Inadequate quality assurance and quality control plans by Client	3.2582	12
Wrong estimation	3.2527	13
Suspension of work by client	3.1813	14
Poor site supervision by client	3.1758	15
Unforeseen ground condition	3.1648	16
Long duration between award of work and execution	3.1638	17
Increase in equipment charges	3.1593	18
Inadequate modern equipment	3.1484	19
Delay in delivering the site to the contractor due to site	3.1209	20

Factors	Mean Value	Rank
issues		
Changes in law and regulatory framework	3.0989	21
Lack of coordination between client and contractor	3.0987	22
Delay in getting necessary permissions from relevant departments	3.0659	23
Delay in delivery of equipment	3.0604	24
Increase in electricity charges	3.0275	25
Unavailability of required equipment	2.9725	26
Inadequate technical specification of material	2.7747	27
Shortage of material	2.6099	28
Delay in delivery of material	2.4890	29
Effect of weather	2.2747	30

The factors having the mean value of 3.4 or greater than 3.4 are considered as critical factors which causes cost escalation. It is observed from above Table 5.1 that out of these factors which causes cost escalation in public sector projects are, fluctuation in price of material ranked 1st with mean value of 4.3352, followed by frequent changes in design ranked 2nd with mean value of 3.8681, frequent change orders during construction by client ranked 3rd with mean value of 3.7802, financial difficulties faced by client ranked 4thwith mean value of 3.7418, changes in scope of work ranked 5th with mean value of 3.6978, long duration between design and tendering ranked 6th with mean value of 3.5769,inadequate planning and scheduling ranked 7th with mean value of 3.5000, Increase in labor charges ranked 8th with mean value of 3.4890, increase in transportation charges ranked 9th with mean value of 3.4725, delays in decisions making by client ranked 10th with mean value of3.4132are critical factors which causes cost escalation. It is also observed that from above table that the factors having mean value less than 3.4 are

increase in value added tax (VAT) and Service taxes, inadequate quality assurance and quality control plans by client, wrong estimation, suspension of work by client, poor site supervision by client, unforeseen ground condition, long duration between award of work and execution, increase in equipment charges, inadequate modern equipment, delay in delivering the site to the contractor due to site issues, changes in law and regulatory framework, lack of coordination between client and contractor, delay in getting necessary permissions from relevant departments, delay in delivery of equipment, increase in electricity charges, unavailability of required equipment, inadequate technical specification of material, shortage of material, delay in delivery of material and effect of weather.

VI. CONCLUSION

Construction industry is seriously affected every year by cost escalation causing many difficulties and a large number of constructors to rearrange the projects. Construction projects are delayed due to cost escalation and scope of projects is being reduced due to cost escalation. The clauses of cost escalation could also seriously affect the public sector projects because of the fact that submitted prices are not being guaranteed for long period of time. The findings of this study provided the knowledge related to critical factors influencing cost escalation in construction projects. Factor identification was done through literature review and from unstructured interviews by the experts of the concerned field. The questionnaire of identified cost escalation factors was distributed to the professionals of the public sector to assess the rank of cost escalation factors. The results obtained from the feedback of the questionnaires were analyzed using SPSS version 20.0 (statistical package for the social sciences) software. This study found thirty factors influencing cost escalation in water sector projects. Top ten identified significant factors are: fluctuation in price of material, frequent changes in design, frequent change orders during construction by client, financial

difficulties faced by client, changes in scope of work, long duration between design and tendering, inadequate planning and scheduling, increase in labor charges, increase in transportation charges, delays in decisions making by client. Addressing the above identified factors at appropriate stage of project life cycle will help the project stakeholders in mitigating the occurrences of cost escalation in water sector projects of Sindh.

REFERENCES

[1] Gupta, B.L.G.a.A., Constrution Management, Machinery and Accounts. Third Edition 2005, ed. Bikaner. 1995, India: Prabhat Offset Press, Dehli.J. Clerk Maxwell, A Treatise on Electricity and Magnetism, 3rd ed., vol. 2. Oxford: Clarendon, 1892, pp.68–73.

[2] Enshassi, A., S. Mohamed, and S. Abushaban, "Factors affecting the performance of construction projects in the Gaza strip". Journal of Civil Engineering and Management, 15(3): p. 269-280. (2009).K. Elissa, "Title of paper if known," unpublished.

[3] Pinto, A., I.L. Nunes, and R.A. Ribeiro," Occupational risk assessment in construction industry–Overview and reflection". Safety Science, 49(5): p. 616- 624. (2011).

[4] K. Vamsidhar, D. A. Eshwarswaroop, K. Ayyappapreamkrishna, R. Gopinath. "Study and Rate Analysis of Escalation in Construction industry". Journal of Mechanical and Civil Engineering (IOSR- JMCE) e- ISSN: 2278-1684. (2014).

[5] Flyvbjerg, B., Holm, M. K. S., Buhl, S. L. "Underestimating costs in public works projects: Error or lie?" J. Am. Plan. Assn., 68(3),279–295. (2002).

[6] Jennifer S. Shane, A.M.ASCE1; Keith R. Molenaar, M.ASCE2; Stuart Anderson, M.ASCE3; and Cliff Schexnayder, Dist.M.ASCE. " Construction Project Cost Escalation Factors", JOURNAL OF MANAGEMENT IN ENGINEERING © ASCE / OCTOBER 2009.

[7] John K. Hollmann; Larry R. Dysert, "Escalation Estimation: Working With Economics Consultants", AACE International Transactions, AACE International, Morgantown, (2007).

[8] Jennifer S. Shane, Keith R. Molenaar, Stuart Anderson, and Cliff Schexnayder "Construction Project Cost Escalation Factors" J. of Management. Eng, Vol 25,Issue 4. (2009).

[9] Minsoo Choi, Jinu Kim and Moohan Kim, "A study on the price escalation system in a construction contract" J. of Civil Engineering, Vol 10, Number 4. (2006).

[10] Andrew N. Blair, Leonard M. Lye, W. J. Campbell, "Forecasting construction cost escalation" J. of Canadian Journal of Civil Engineering, Vol 20,Issue 4. (1993).

[11] Engr. Rizwan U. Farooqui CBM-CI International Workshop, Karachi, Pakistan.

[12] Rizwan U. Farooqui "First International Conference on Construction In Developing Countries (ICCIDC–I)"Advancing and Integrating Construction Education, Research & Practice" August 4-5, Karachi,, Pakistan. (2008).

[13] Amusan, Lekan Murtala. "Neural Network- based Cost Predictive Model for Building Works". Unpublished Thesis for the Ward of PhD Degree Covenant University Nigeria. (2011).

[14] Nasiru Zakari Muhammada, Ali Keyvanfara, Muhd Zaimi Abd Majida, Arezou Shafaghata, Aliyu Muhammad Maganab, Hasan Lawanc, Saeed Balubaida.2015. "Assessment of Cost Escalation factors for Building and Civil Engineering Projects in Nigerian Construction Industry: a Multiple Regression Approach". Ali Keyvanfar et al. / Jurnal Teknologi (Sciences & Engineering) 74:4, 85–91. (2015).

[15] Nasiru, Zakari Muhammad, Kunya Sani Usman, and Abdurrahman Mutawakkil. "Assessment of Factors that Affect Cost Control by Nigerian Construction Contractors". Journal of Engineering and Applied Sciences. 4. (2012).

[16] Leavitt D, Ennis S, McGovern P. "The cost escalation of rail projects: using previous experience to re-evaluate the cal speed estimates". California high speed rail series, April working paper; (1993).

[17] Chabota Kaliba *, Mundia Muya, Kanyuka Mumba, "Cost escalation and schedule delays in road construction projects in Zambia". International Journal of Project Management 27, 522–531. (2009).

[18] Peter Morris and William F. Willson, "Measuring and Managing Cost Escalation" published in AACE International Transactions. (2006).

[19] Nashwan N. Dawood and William Bates, "A Decision Support System Specification for Cost Escalation in Heavy Engineering Industry" , J. of Computer-Aided Civil and Infrastructure Engineering, Vol 17, Issue 5, pages 342–357. (2002).

[20] Anderson, S., Molenaar, K., and Schexnayder, C. "Guidance for cost estimation and management for highway projects during planning, programming, and preconstruction." Transportation Research Board, Washington, D.C., 574. (2007).

[21] Anderson, S., Molenaar, K., and Schexnayder, C. "Guidance for cost estimation and management for highway projects during planning, programming, and preconstruction." Transportation Research Board, Washington, D.C., 574. (2007).

[22] Skitmore, R.M. and Ng, S.T. "Forecast Models for Actual Construction Time and Cost" Building and Environment 8(8) :pp. 1075-1083. (2003).

[23] Fredrick .S and Mariam.A. (2018). "Importance Level of On-Campus Student Housing FacilitySpaces: Perception of Postgraduate Students" Department of Construction Management and Quantity Surveying, Cape Peninsula University of Technology, South Africa, pp. 181-190.

[24] Salman Ahmed, Aftab Hameed Memon, Noor Ahmed Memon, Abdul Nasir Laghari, Muhammad Akram Akhund and Hafiz Usama Imad (2018). Commmon Factors of Cost Escalation in Construction Industry of Pakistan. Engineering, Technology & Applied Science Research, Volume 8, Issue 6, pp. 3508-3511.

[25] Akram M., Memon N.A., Ali T.H., Siddiqui F., " Developing an Expert System for Controlling Cost and Time Overrun (ESCCTO) in Construction Projects", 7 th International Civil Engineering Conference ointly Organized by IEF & NED University at IEP Convention Centre, Karachi, 12-13 June, 2015.

BIM Implementation of Reinforced Concrete Sandwich Panels

Shahid Ali Khan[1,a], Saddiq Ur Rehman[1,b], Muhammad Shoaib Khan[1,c] ,Mohammad Adil[2,d]

[1]Researcher, Department of Civil Engineering, UET Peshawar

[3]Assistant Professor, Department of Civil Engineering, UET Peshawar

Email address: [a] shahidalikhan414@gmail.com , [b] 15pwciv4335@uetpeshawar.edu.pk [c] muhammadshoaib5308@gmail.com and [d]adil@uetpeshawar.edu.pk

Abstract--- AEC industry has made considerable efforts to enhance the mechanical and thermal properties of buildings. Various types of material with its different proportion are used for construction including sandwich panel. Several experimental and theoretical studies were performed to find out behavior of sandwich panel under different conditions. Due to development and understanding of the software technologies and numerous tools, the construction industry has shifted towards the numerical studies. This paper presents the study of the behavior of reinforced concrete sandwich panels using Building Information Modeling (BIM). Autodesk Revit 2017 is used to model a small Residential building whose walls and slab are made of Reinforced concrete sandwich panel. Quantity takeoff and cost estimation is performed on the model which results in more economical construction.

Keywords-- Sandwich panel, BIM, Revit, Quantity takeoff, cost estimation, residential building.

1. BACKGROUND

Sandwich panel is a structural engineering product composed of three layers, a low density insulated core and a high density thin skin layer bonded to each side of the insulated core. It has relative characteristic of light weight, high stiffness, strength and thermal insulation, water proof, sound insulation and its ability to be designed in different geometry, due to these characteristic its use in structural application is considerably increasing e.g. in weight sensitive structures in which higher flexural rigidity is required [1,2]. To achieve a specific performance target various types of core materials are introduced to the structure. The behavior of these structures depends on the strength and stiffness of the sandwich panels. Various analytical and experimental studies have been performed to study the structural behavior of sandwich panel using different core materials.

Gara et al. (2012) determined the flexural behavior of sandwich panels having reinforced concrete in-filled Wythe's core and found that their strength increases with increase in thickness of core [3]. Kumar & Suman (2013) carried out experimental studies to determine the effect of different material and their core thickness on energy performance of sandwich panels and concluded that panels having Expended polystyrene Sheet (EPS) with a thickness of 70mm satisfies Energy conservation building code (ECBC) [4]. Asim Abbas et al (2019) studied experimentally the structural behavior of reinforced concrete sandwich panels (RCSPs) under the blast loading and concluded that RCSP panel was able to absorb and dissipate the blast energy and were also stable against the fragmentation relative to other buildings [5]. Most of the researchers performed either experimental or analytical study to find out the behavior of sandwich panel. There is very small portion of work done numerically which is required to

compare the result obtain from other two types of studies and develop a product which can help in modeling the phenomena or condition before it can actually happen.

This paper aims to study the behavior of sandwich panel numerically using Building Information modeling (BIM). BIM is a process that comprises generating and managing of digital characterization of physical and functioning characteristic of a system. Numerical modeling of mud and reinforced sandwich panel building will be carried out separately in Autodesk Revit and its detailing and quantity takeoff will be performed.

2. BIM TOOLS

Small and big construction companies e.g. AEC sectors use Building information modeling (BIM) software for different engineering challenges. BIM has develop various products for different challenges which has narrow down the path for choosing the most suitable software solution for a challenge. Now a day the BIM software is leading the construction management and building work to more efficiency and more transparency. BIM system use is not only limited to computer-aided design (CAD) but exceeds this limit to construction. Using all features of BIM will accurately help in reducing cost, detect and solve errors before it occurs on the implementation stage and also accelerated the construction time and schedule. Most of the BIM softwares used are provided by the Autodesk Company e.g. Revit, Naviswork, Archicad, Infraworks etc.

3. REVIT FAMILY

Revit is BIM software which has different features for architectural design, construction, structural Engineering and MEP. Revit families are the building unit for all the projects created in the Revit. All the projects in the Revit are made of combination of different Revit families and these families are made of group of different elements which possess same properties known as parameters. There are two types of families in Revit, system families and loadable families. System families are the ones which create the main building elements e.g. walls, roof, floors, stairs etc. while loadable families are the external RFA files which can be loaded into the Revit project e.g. Doors, Windows, Column etc. Revit families are further composed of material families. These material families are differentiated on the basis of its appearance and its thermal and physical properties. Material can be provided to some families e.g. walls, floors, roofs in multilayers, each layer can be made of specific thickness requires for modeling.

4. REINFORCED CONCRETE SANDWICH PANEL

The significance uses of reinforced concrete sandwich panels are increases due to their excellent thermal or heat insulation properties. In reinforced concrete sandwich panels Wythe's are separated to each other by expanded polystyrene sheet (EPS). In concrete reinforced sandwich panels the insulation material should be such that it causes less absorption of water from fresh concrete. Their strength is determined by constituent materials and the corresponding thickness of panel increases compressive strength capacity of reinforced concrete sandwich panel. various researchers observed the suitability of light

weight concrete to be used as a infilling material because they are found very stable during placing and handling [6].Shear connectors which are made from fiber reinforced polymer(FRP) or steel are used to enhance flexural strength of sandwich panels by increasing composite actions between outer cores [7].In this case the outer cores is considered as structural Wythe because sufficient resistance to loads are provided by panels in this case [8]. When the two outer cores of concrete behaves as a single unit then the panel is acting as a composite section where shear connectors transfers longitudinal shear which results in a linear distribution of bending stresses and strain across the whole thickness of the panel [8]. Concrete sandwich panels are considered as privacy product for weight and heat sensitive structures. Their failure is caused either by crushing of concrete or buckling. if the sufficient rigidity is not provided by shear connectors then buckling load governs over crushing load [8].
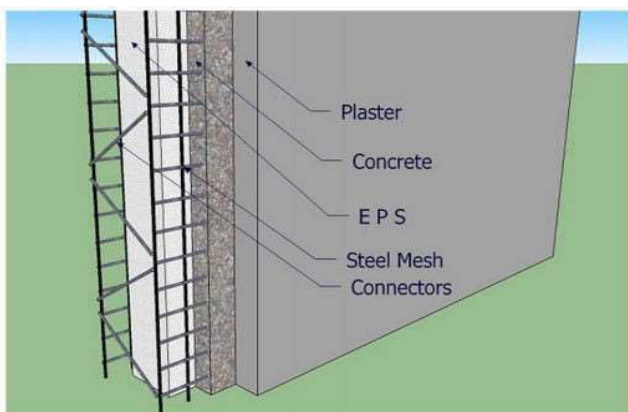
Figure 1 Reinforced concrete sandwiched panel [5]

5. RCSP REVIT FAMILY

Revit families for stabilized mud and reinforced concrete sandwich panel are created separately by using the concept of multi material layers. In both families polystyrene is used as insulated material in the center layer or core. The thickness of this polystyrene layer is 4 inches and its thermal and physical properties are assigned to it using Autodesk source i.e. the polystyrene material is already present in the Revit material library and its properties are assigned to the central layer of both sandwich panels.
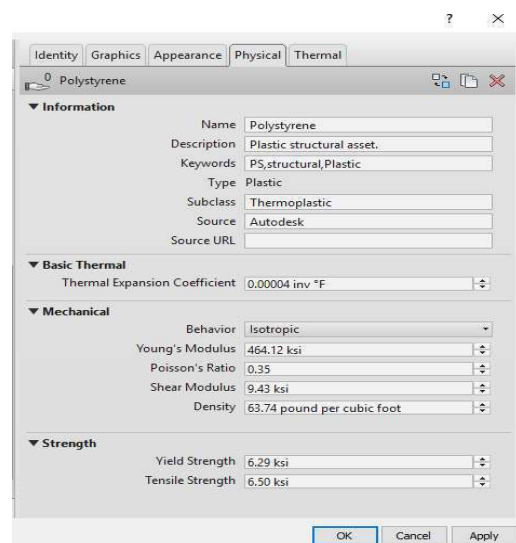
Figure 2 Thermal properties of polystyrene
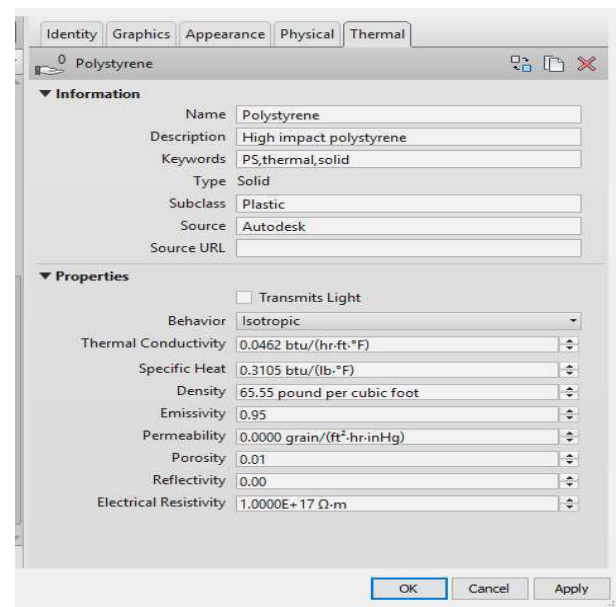
Figure 3 Physical properties of polystyrene

For concrete sandwich panel two outer layers of thickness 2.5 inches are created on each side of central core and then properties of 3.5 ksi concrete are assigned to these layers which are by default present in the Autodesk Revit. Thermal and physical properties are shown in Fig (5) and Fig (6) respectively.
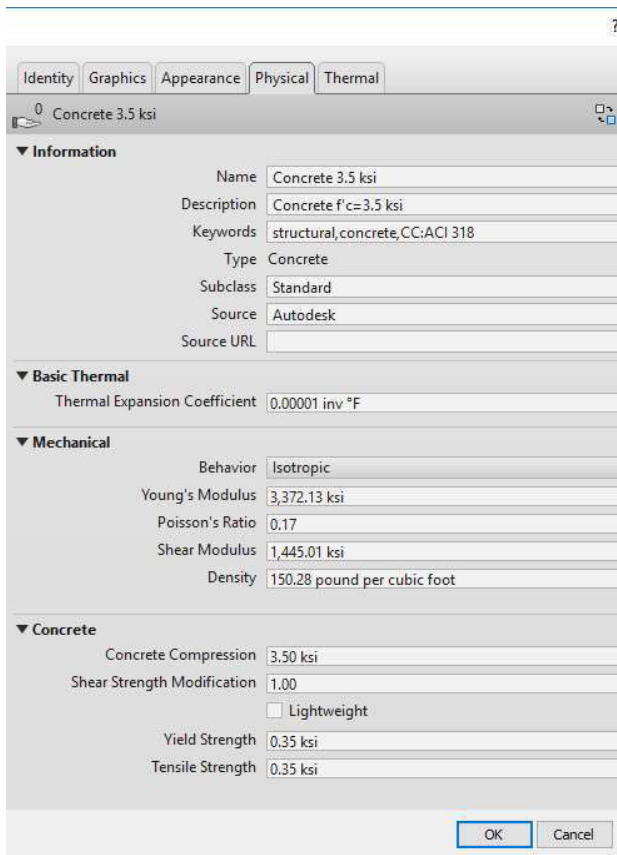
Figure 4 Thermal properties of concrete Wythe's
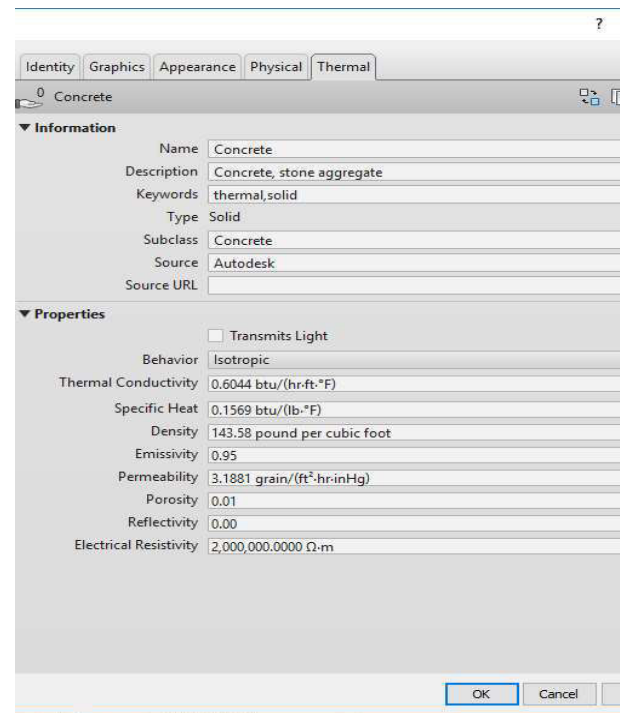
Figure 5 physical Properties of concrete Wythe's

6. RESIDENTIAL BUILDING BIM MODEL
Single storey residential building is selected for study in this paper. Autodesk Revit 2017 is used for BIM modeling of a Residential building whose walls and slab are made of three different layers i.e. concrete reinforced sandwich panel.

Figure 6. 3D BIM Model

Figure 6 is the 3D view representation of simple residential model in which expanded polystyrene is used as an intermediate core of walls and slab system and concrete of 3.5 ksi strength is used in outer cores. Reinforcement is provided only in the bottom portion of slab.
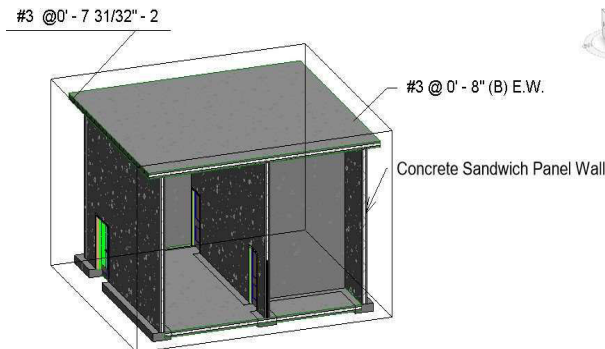

Figure 7. 3D BOX Section

The box section is shown in figure 7 represents the perspective and interior view of model showing expanded polystyrene in the walls in the form of white sheet.

East west and north south section shown in figure 8 and 9 are the levels detail and also detailing for rebar in the slab portion. Single story residential building has been developed presented here.
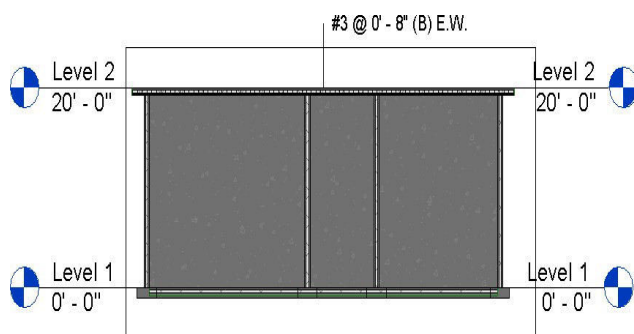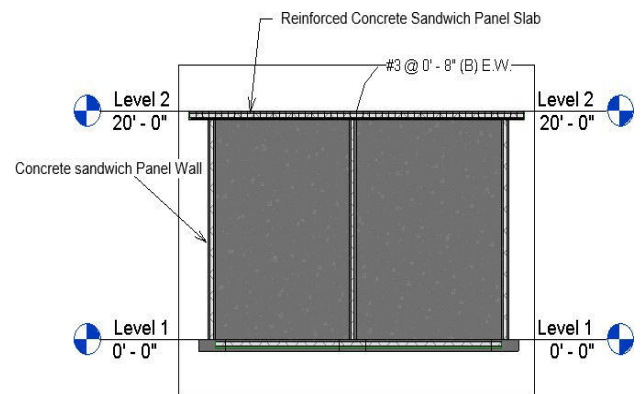

Figure 8. East West Section

Figure 9. North South Section

<Wall Material Takeoff>					
A	B	C	D	E	F
Material: Name	Family	Family and Type	Material: Cost	Material: Volume	Total cost
concrete 3.5 ksi					
concrete 3.5 ksi	Basic Wall	Basic Wall: Reinfor	110.00	407.06 CF	44776.30
concrete 3.5 ksi	Basic Wall	Basic Wall: Reinfor	110.00	240.63 CF	26468.75
concrete 3.5 ksi	Basic Wall	Basic Wall: Reinfor	110.00	386.51 CF	42516.15
concrete 3.5 ksi	Basic Wall	Basic Wall: Reinfor	110.00	234.61 CF	25807.03
concrete 3.5 ksi	Basic Wall	Basic Wall: Reinfor	110.00	109.48 CF	12043.28
concrete 3.5 ksi	Basic Wall	Basic Wall: Reinfor	110.00	362.93 CF	39922.27
concrete 3.5 ksi	Basic Wall	Basic Wall: Reinfor	110.00	109.48 CF	12043.28
concrete 3.5 ksi	Basic Wall	Basic Wall: Reinfor	110.00	108.41 CF	11925.16
Polystyrene					
Polystyrene	Basic Wall	Basic Wall: Reinfor	0.00	325.65 CF	0.00
Polystyrene	Basic Wall	Basic Wall: Reinfor	0.00	192.50 CF	0.00
Polystyrene	Basic Wall	Basic Wall: Reinfor	0.00	309.21 CF	0.00
Polystyrene	Basic Wall	Basic Wall: Reinfor	0.00	187.69 CF	0.00
Polystyrene	Basic Wall	Basic Wall: Reinfor	0.00	87.59 CF	0.00
Polystyrene	Basic Wall	Basic Wall: Reinfor	0.00	290.34 CF	0.00
Polystyrene	Basic Wall	Basic Wall: Reinfor	0.00	87.59 CF	0.00
Polystyrene	Basic Wall	Basic Wall: Reinfor	0.00	86.73 CF	0.00

Figure 10. Wall Quantity Takeoff

Quantity from wall has extracted using scheduling technique. That quantity is then used to determine the cost of parameters. Mainly two type of materials is extracted here (a) concrete (b) polystyrene.

<Floor Material Takeoff>				
A	B	C	D	E
Material: Name	Family and Type	Material: Volume	Material: Cost	Total cost
concrete 3.5 ksi	Floor: Floor 1	600.23 CF	110.00	66025.78
Polystyrene	Floor: Floor 1	480.19 CF	0.00	0.00
concrete 3.5 ksi	Floor: Floor 1	774.07 CF	110.00	85147.52
Polystyrene	Floor: Floor 1	619.25 CF	0.00	0.00

Figure 11. Floor Quantity Takeoff

Floor quantities determined using same procedure as in walls but in addition to polystyrene and concrete, rebar quantity and cost also calculated.

<Rebar Schedule>					
A	B	C	D	E	F
Family and Type	Reinforcement Vol	density	mass	Cost	total cost
Rebar Bar: #3	3948.58 in³	503.00 lb/ft³	1149.38 lbm	51.00	58618.52
Rebar Bar: #3	3914.11 in³	503.00 lb/ft³	1139.35 lbm	51.00	58106.89

Figure 12. Rebar Schedule

7. CONCLUSION AND RECOMMENDATION

i. Building information modelling (BIM) is a very quick way of linking 3D files to cost related information.

ii. Concrete infilled sandwich panels are easily developed and quantity extracted using BIM

iii. From the quantity estimation of concrete sandwich panels it was concluded that they are very cost effective and economical one.

iv. Concrete sandwich panels are also energy efficient and capable of insulating heat results in sustainable building.

v. BIM provides most accurate and predictable methods of project estimate and cost analysis

vi. Various scenarios of construction and design has explored by linking Real time model to quantity estimation using BIM

vii. Bill of quantity (BOQ) preparation is greatly dependent on cost and quantity information extracted from BIM model.

AKNOWLEGMENT

Reference

[1]. Garrido, M., Madeira, J. F. A., Proença, M., & Correia, J. R. (2019). Multi-objective optimization of pultruded composite sandwich panels for building floor rehabilitation. *Construction and Building Materials*, *198*, 465-478.

[2]. Lee, J. H., Kang, S. H., Ha, Y. J., & Hong, S. G. (2018). Structural Behavior of Durable Composite Sandwich Panels with High Performance Expanded Polystyrene Concrete. *International Journal of Concrete Structures and Materials*, *12*(1), 21.

[3]. Gara, F., Ragni, L., Roia, D., & Dezi, L. (2012). Experimental behavior and numerical analysis of floor sandwich panels. Engineering Structures, 36, 258-269

[4]. Kumar, A., & Suman, B. M. (2013). Experimental evaluation of insulation materials for walls and roofs and their impact on indoor thermal comfort under composite climate. Building and Environment, 59

[5]. Abbas, A., Adil, M., Ahmad, N., & Ahmad, I. (2019). Behavior of reinforced concrete sandwiched panels (RCSPs) under blast load. *Engineering Structures*, *181*, 476-490.

[6]. Lakshmikandhan, K. N., Harshavardhan, B. S., Prabakar, J., & Saibabu, S. (2017, August). Investigation on Wall Panel Sandwiched With Lightweight Concrete. In *IOP Conference Series: Materials Science and Engineering* (Vol. 225, No. 1, p. 012275). IOP Publishing.

[7]. Hamed, E. (2017). Load- carrying capacity of composite precast concrete sandwich panels with diagonal fiber-reinforced-polymer bar connectors. *PCI JOURNAL*, 34-44.

[8]. Poluraju, P., & Rao, G. A. (2014). Behaviour of 3D-Panels for Structural Applications Under General Loading: A State-of-the- Art. *International Journal of Research in Engineering and Technology*, *3*(16), 173-181.

Identification of Critical Flaws in National Drainage Project Right Bank Outfall Drain-II (RBOD-II)

Fazal Qadir Kandhro[1,a] , Tauha Hussain Ali[2,b] , Nafees Ahmed Memon[3,c]
Muhammad Aslam Leghari[4,d] , Shabir Hussain Khahro[5,e]

[1] Military Engineer Services (MES),Taxila Cantt
[2] Mehran U.E.T, Jamshoro,Sindh
[3] Mehran U.E.T, Jamshoro,Sindh
[4] NESPAK Consultancy, Hyderabad, Sindh, Pakistan
[5] Mehran U.E.T., Jamshoro Sindh

E-mail address: [a] fazalqadir626@gmail.com , [b] Pvc@admin.muet.edu.pk ,
[c] nafees.memon@faculty.muet.edu.pk , [d] leghariaslam@gmail.com, [e] shkhahro@gmail.com

Abstract—Water logging is an extremely important and necessary by-product for the irrigation channel system. If there is not a sudden stoppage or proper handling, it causes permanent losses of the cultivation of forming land. After construction of barrages at Gaddu, Sukkar and Kottri, water logging and salinity has developed. To control it, mega construction drainage projects were designed to dispose off into the Arabian Sea. Right Bank Outfall Drain (RBOD) project was aimed to alleviate the problem of drainage waste water from irrigated lands, effluent of lands and factories. It was divided in to three parts, namely RBOD-I, RBOD-II and RBOD-III. This study identifies the critical flaws in RBOD-II project. Based on extensive literature review and unstructured interviews fifty flaws were highlighted. Questionnaire survey was carried out with an aim to rank the identified flaws in terms of importance. Top sixteen factors having mean value equal or greater than 3.5 were selected as main factors affecting outcome of RBOD-II project. Improper calculation of indication cost during Project Cost-1, land acquisition problem, litigation caused due to land acquisition at some locations, slow financial flaw from federal government were ranked significantly higher among identified flaws affecting project outcome.

Keywords— Water logging, National Drainage Program, Right Bank Outfall Drain Project, Critical Flaws.

1 Introduction

After the construction of Sukkar Barrage in 1932, the possibility for drainage in the vicinity determined. The planner and executors were strongly recommendate that assured irrigation supply depends on the ground water table conditions which would change with the cultivate lands, because exact requirement for dispose off could not be predicated. Hence, at that time the project of Main Nara Valley Drain (MNVD) presently known RBOD was conceived in three stages in the western side of the area. MNVD was constructed in 1960 and later on linked with Manchar Lake in 1976 [1]. The complete area has not been developed for drainage and various local drains are yet to be connected with MNVD therefore, only that effluent is being disposed in to Manchar, which is presently connected. Further, the disposal of all the effluent of other two components namely RBOD-I & RBOD-III will carrying by RBOD-II and disposed off in to Arabia Sea. To save the command area of Kotri Barrage[2].

1.1 LEFT BANK OUTFALL DRAIN (LBOD)

In this connection, on the left side of Indus River, a drainage Project LBOD was started and completed component wise. The LBOD project was conceived to control water logging of 1.27 Million Acres in the left Bank of Indus River through a network of open surface drain [3].

12 RIGHT BANK OUTFALL DRAIN (LBOD)

Toward the west bank of the Indus River almost the same specific plan. The Right Bank Outfall Drain (RBOD) begins for the development of 4.40 Million Acres land. The Right Bank Outfall Drain is a surface drain project and carries drain from Balochistan through Sindh's various districts and outfall in to the Arabian Sea. RBOD was aimed to alleviate the problem of drainage waste water from irrigated lands, effluent of lands and factories. It was divided in to three component, RBOD-I (173 Km), RBOD-II (273 Km) and RBOD-III (185 Km) [4].

2 AIM OF THE STUDY

The aim of the study is to identify the critical flaws in on-going National Drainage Project (RBOD-II).

3 LITERATURE REVIEW

Success of construction projects depends mainly on success of performance. By many previous researches had studied the performance of construction projects remarked that one of the basic reasons for the construction industry's poor performance [5]. The main performance Criteria of construction projects as financial stability, progress of work, procurement system, standard of quality, health and safety, resources, relationship with clients, consultants, sub contractors, reputation and amount of sub contracting [6]. The failure of any construction project is mostly related to the performance problems and there are many reasons and factors which are contributed to such problems as; shortage or inadequacies in industry infrastructure, problem caused by clients and consultants and caused by contactor's incompetence [7]. Regarding project success, as each client will have their own idea of success. One client may be willing to sacrifice features for a quicker delivery, another may be happy to extend the time line to add in additional features. In both cases, the project did not deliver on time and on budget [8]. Each project has a different set of requirements, limitation, challenges and opportunities that affect a projects cultural, environmental and technological contents. The contractor and the owner pay for the extra charge for the completion of the project due to delay in large construction project. When the completion time of the construction project exceeds the agreed completion time, it is known as construction project delay [9].

Problems arises everyday on construction projects. This is not unusual or unexpected; indeed, the entire design and construction process involves resolving challenges and managing the risks inherent in project. However, certain problems go beyond the expectations and risks initially accepted by parties [10]. In order to improve the outcome of ongoing RBOD-II project, it is necessary to identify critical flaws. The identification of critical flaws affecting project outcome will also help in improving the strategy for future drainage projects.

4 METHODOLOGY

The flaws in national drainage project RBOD-II were identified with the help of literature review of international drainage projects, field survey and unstructured interviews. Further the experts' opinion was sought and 50 flaws were finalized. A questionnaire was designed to identify the

critical flaws having and adverse effect over project outcome.

5 DESIGN OF QUESTIONNAIRE

There were mainly two parts of the questionnaire, part one and part two. Part one asked about the respondent's demographics i.e personal information. Part two asked about the information related to significance of identified in affecting outcome of RBOD-II project. It was arranged in the order of priority scale from least important (1) to most important (5).

5.1 DATA COLLECTION AND ANALYSIS

One hundred fifty nine questionnaire proforma were distributed to clients, consultants and contractors. Ninety fully filled questioners were received from concerned stakeholders. The results obtained from the feedback of the questionnaires were analyzed by using SPSS version 17.00 (Statistical Package for the Social Sciences) software to obtain mean and rank of the factors. Identified flaws have mean value equal or greater than 3.5 were given significantly more importance for taking up further research towards identification of necessary measures for improving the outcome of RBOD-II project. Table 1 presents the mean and rank of identified flaws.

Mean and Rank of Identified Flaws		
Rank	*Factors*	*Mean*
1	Improper calculation of indication cost during PC-I	4.1770
2	Land acquisition problems.	4.0660
3	Litigation due to land acquisition at some locations and deferred payments	4.0660
4	Slow financial flow from federal government.	4.0660
5	Delays in decisions making by client	4.0550
6	Lack of coordination among client, consultant and	3.9220

	contractor.	
7	Impact of cost escalation on project cost.	3.9220
8	Lack of coordination among experts, stake holders and related organization to work together in harmony	3.9000
9	Reluctant of sub contractors to re-mobilize on old rates	3.8000
10	Variation in project cost due to inflations.	3.7880
11	Slow financial flow from Sindh Government.	3.6550
12	Lack of monitoring and feed back.	3.6330
13	Pending Claims	3.6000
14	Lack of Knowledge management	3.5440
15	Inadequate planning and scheduling	3.5220
16	Poor degree of consultants or designer involvement due to which frequent changes in drawing/specification.	3.5000
17.	Improper selection of sub-contractors by main contractors.	3.4660
18.	Improper evaluation of bids.	3.4000
19.	Prolonged or delayed vetting process.	3.3770
20.	Incomplete drawings, specifications and technical instructions provided by the consultant.	3.3220
21.	Inadequate internal quality audits.	3.1880
22.	Lack of disaster management plan.	3.1660
23.	Improper distribution of work to sub-contractors.	3.1000
24.	Changes in government's rules / regulations	2.8770
25.	Poor site management and supervision by project manager	2.8660
26.	Damage of public's basic infrastructures.	2.8440
27.	Lack of Risk identification.	2.8110
28.	Improper selection of Human Resources.	2.7660

29.	Improper consideration of actual site conditions	2.7220
30.	Ineffective role by project manager to deal with risk and uncertainty.	2.6770
31.	Political or community influence.	2.6650
32.	Improper consideration for disposal of effluent to Sea.	2.6550
33.	Frequent changes in the scope of work.	2.6000
34.	Poor specification or unclear/unsuitable specification.	2.6000
35.	Improper construction methods.	2.5770
36.	Improper assessment of project impact.	2.5660
37.	Material shortage at site due to main contractor.	2.5440
38.	Community dissatisfaction related to output of the project.	2.5440
39.	Lack of environmental impact assessment.	2.5330
40.	Lack of consideration of high tide flows in coastal areas	2.5220
41.	Lack of motivation / incentives to workers	2.5110
42.	Lack of the project integration.	2.5000
43.	Improper document and data control.	2.4440
44.	Improper quality Control of material supplied product.	2.4440
45.	Major and Minor Revision in designing.	2.4330
46.	Inadequate planning of equipment utilization and management.	2.3770
47.	Poor labour productivity	2.3330
48.	Delay due to non-availability of special equipment.	2.2220
49.	Lack of constructability.	2.1880
50.	Lack of inspection and testing.	1.9440

6 CONCLUSION

Under master drainage plan (MDP) the project RBOD will facilitate to protect Indus River water from pollution. RBOD-II project has been significantly delayed. In order to assess and improve the outcome of RBOD-II

project, this study identified fifty flaws. Further a questionnaire survey was carried out to rank the identified flaws. Top ranking flaws as identified in this study include: Improper calculation of indication cost during PC-I, land acquisition problem, litigation caused due to land acquisition at some locations, slow financial flow from federal government, delays in decisions making by client and lack of coordination among main stake holders of the project. Critical flaws identified in this study have an adverse effect over the outcome of RBOD-II project. Due attention of concerned stakeholders will help in avoiding further shortcomings in project outcome. The findings of this study will also help in improving the outcome of similar nature projects in Pakistan. No doubt that, RBOD-II project is said to be properly design and point of its final disposal was properly selected. Careful operation and proper maintenance will make the project successful and fruitful for the people of Pakistan.

REFERENCE

[1] Report Ministry of water and power development authority, (2002).

[2] Qureshi, A. S., McCornick, P. G., Qadir, M., & Aslam, Z. (2008). Managing salinity and waterlogging in the Indus Basin of Pakistan. Agricultural Water Management, 95(1), 1-10.

[3] Halepoto, 2003, "Experimenting with the lives of poor, case study on ADB funding for LBOD Project in Pakistan"

[4] Chandio, 2004, "Right Bank Outfall Drain Scheme in Sindh, Pakistan New Study on RBOD.

[5] Naeem Ejaz, J. H., Shabbir, F.,Shamim, M. A., Naeem, U. A., Tahir, M. F., Ahmad, N., & Farooq, Q. U. (2013). Assessment of most critical success factors for mega construction projects in Pakistan. Life Science Journal, 10(10s).

[6] Thomasen, (2008). Program management. Construction Management Association of America (CMAA).

[7] Ogunlana, S., Lim, J., & Saeed, K. (1998). Desman: A dynamic model for managing civil engineering design projects. Computers & structures, 67(5), 401-419.

[8] Saqib, M., Farooqui, R. U., & Lodi, S.

[9] H. (2008, August). Assessment of critical success factors for construction projects in Pakistan. In First International Conference on Construction in Developing Countries (ICCIDC-1), Advancing and Integrating Construction Education, Research and Practice, Karachi, Pakistan, August (Vol. 4, No. 5).

[10] Kumaraswamy, M. M., & Chan, W. M. (1999). Factors facilitating faster construction. Journal of Construction Procurement.

[11] Qureshi, A. S., McCornick, P. G., Sarwar, A., & Sharma, B. R. (2010). Challenges and prospects of sustainable groundwater management in the Indus Basin, Pakistan. Water resources management, 24(8), 1551- 1569.

Biocompatible Nano-Hydroxyapatite reinforced Titanium-Nickel Based Composites

Syed Abbas Raza[1,a], M. Imran Khan[1,b], Muhammad Umair[1,c], Ahmed Kathia[,d], Sohail Khan[1,e], M. Waqas Afridi[1,f], Tauheed Shahbaz[1,g]

[1]*Ghulam Ishaq Khan Institute of Engineering Sciences and Technology, Topi, 23640, KPK.*

[a)]gmm1846@giki.edu.pk; [b)]imranfmse@gmail.com; [c)]umairnaseer21@gmail.com; [d)]ahmedgcck@gmail.com; [e)]pcsohail@gmail.com; [f)]waqas.afridi@giki.edu.pk; [g)]tauheed@giki.edu.pk

Abstract- *Equi-atomic NiTi alloy composites reinforced with 2, 4 and 6 vol.% of Hydroxyapatite were synthesized using Conventional Sintering. Equitatomic NiTi pre-alloyed powder and nano- hydroxyapatite powder were mixed in Planetary ball Mill for 3 hrs. before being cold compacted at 40 MPa to form Pellets which were sintered in Horizontal Tube Furnace in Ar-Atmosphere in custom cycle but up to 3 hours at peak temperature of 1323 K. Increase in volume of nano-hydroxyapatite addition showed improved corrosion resistance in the composites by Tafel interpolation and increase hardness albeit with increasing porosity but due to the formation of different phases.*

Keywords--- *Nitinol; nano-Hydroxyapatite; Powder Metallurgy; Hardness; XRD; Corrosion; MMCs*

I. INTRODUCTION

TiNi based materials have been the forefront of Smart material innovation since their discovery by buehler in 1963[1]. The binary TiNi alloy compositions particularly equiatomic and Nickel-rich owing to their excellent corrosion behavior, biomedical properties[2], [3], superelastic properties[4]–[6] which make them ideal for biomedical applications. An enormous amount of work as already been done on the determination of biomedical properties of binary TiNi alloys as well higher order alloys[1], [7]–[9]. In addition, the effect of Hydroxyapatite has been well studied as biomaterial for implant synthesis.
TiNi biomedical alloys have focused mostly on the use of binary alloys for implant making as well as ternary and quaternary addition to determine their biomedical properties and biocompatibility while composites have been less profoundly studied. Previous research have focuses on the use of SiC[10], TiC[11], Ti_2AlC[12] among others for improving the mechanical properties of these alloys but not going beyond further to examine their more expanded use. The function of this study has been to evaluate the use of Nano-HAP on the phase dissolution and the electrochemical behavior essentially of the alloys which have been processed through powder metallurgy route so in that sense the presence of porosity plays an important role on its electrochemical behavior. Nano sized particles have been selected due to their superior biological and mechanical properties in comparison with larger sized (micron) particles and the fact that it allows for sintering at lower temperatures to achieve more dense structures comparatively. Additionally, this accounts for the fact that the use of Nano scale reinforcements owing to their high surface-to-volume ratio has allowed for finer control of properties and more homogeneity in distribution of themselves and properties associated with them.

II. EXPERIMENTAL WORK

The experimental details are as follows:

A. Preparation of Composites

Pre-Alloyed powder of Nitinol in the size range of 5-10 micron and Hydroxyapatite in the size range of 80-120 nm was obtained. Various composition of precipitates with 2%, 4% and 6% Hydroxyapatite were added to the pre-alloyed nitinol powder and mixed in planetary ball mill (PM 400) for 3 hours at 200 rpm followed by cold compaction at 400 MPa and the pressure was maintained for up to 12 seconds and the die walls were lubricated with ethanol to prevent sticking of the pellets with the Die wall. The sintering at a customized cycle to peak temperature of 1323K for 3 hours with the entire sintering cycle of the green pellets being carried out in quartz tube in an Argon atmosphere. The theoretical density was calculated using rule of mixtures and the green density was calculated using relative density measurements. The densification of the sintered pellets was measured using Archimedes principle.

B. Microstructure and Composition determination

The as prepared samples were grinded using Buehler grinding paper from the range of 220 to 2000 grade and then fine polished on 1um diamond polishing cloth. They were subsequently cleaned with distilled water before each stage of grinding & polishing to prevent and transfer of impurities and dried in air to perform optical microscopy analysis. EDX using TESCAN Mira electron microscope which was also used for characterizing composition of the structure.

C. Electrochemical Evaluation

Corrosion results were performed in 0.9% NaCl solution with Ag/AgCl reference electrode and platinum Counter electrode. Tafel interpolations were carried out against open circuit potential, which was carried out for 30 minutes, in order to determine the corrosion rate in addition to Potentio dynamic (Tafel) test to determine the corrosion behavior of the samples in the environment. The scan was carried out at the range of -0.3 V to 1.5 V at a sweep rate of 1 mV/s. The tests were performed in Ringers solution under aerated condition (Table 1).
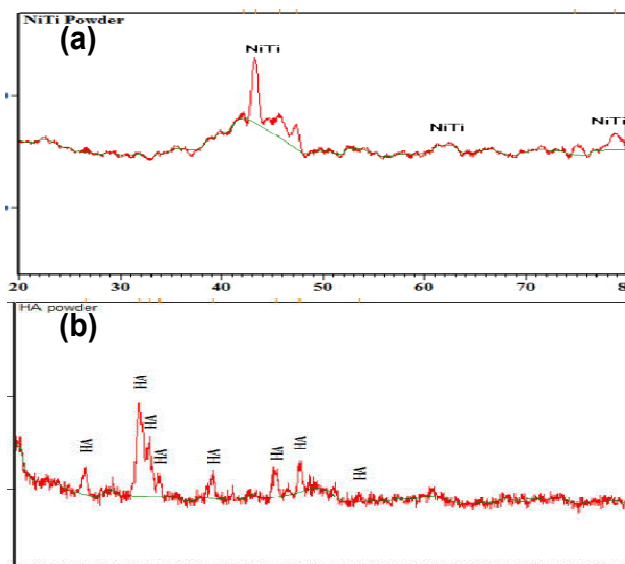

Fig. 1 shows the XRD of (a) Nitinol powder, (b) HAP powder

Table 1 Shows the composition of Ringer solution prepared

S.no	Chemical	Concentration (g/L)
1	NaCl	8.6
2	KCl	0.3
3	$CaCl_2.H_2O$	0.33

III. RESULTS AND DISCUSSIONS

A. Precursor Materials

XRD results showed that the Titanium Nickel powder showed different indexed peaks consisting of both B2 (*JCPDS no 03-065-7711*) and B19' (*JCPDS no 03-065-0365*) Monoclinic Phase as well. The peaks corresponded to higher intensity belong to B2 whereas lower intensity of B19' phase is also present in addition to Nickel-Titanium Oxide (*JCPDS no 01-072-0443*) which shows the deviation from stoichiometric composition. XRD pattern of Hydroxyapatite shows the presence Hexagonal structure corresponding to *JCPDS no 01-084-1998*[13], [14].

B. Microstructure and Pore Analysis

The optical microscopy results show that the reinforcement of Nitinol with Hydroxyapatite led to dissociation of the Nitinol into non-
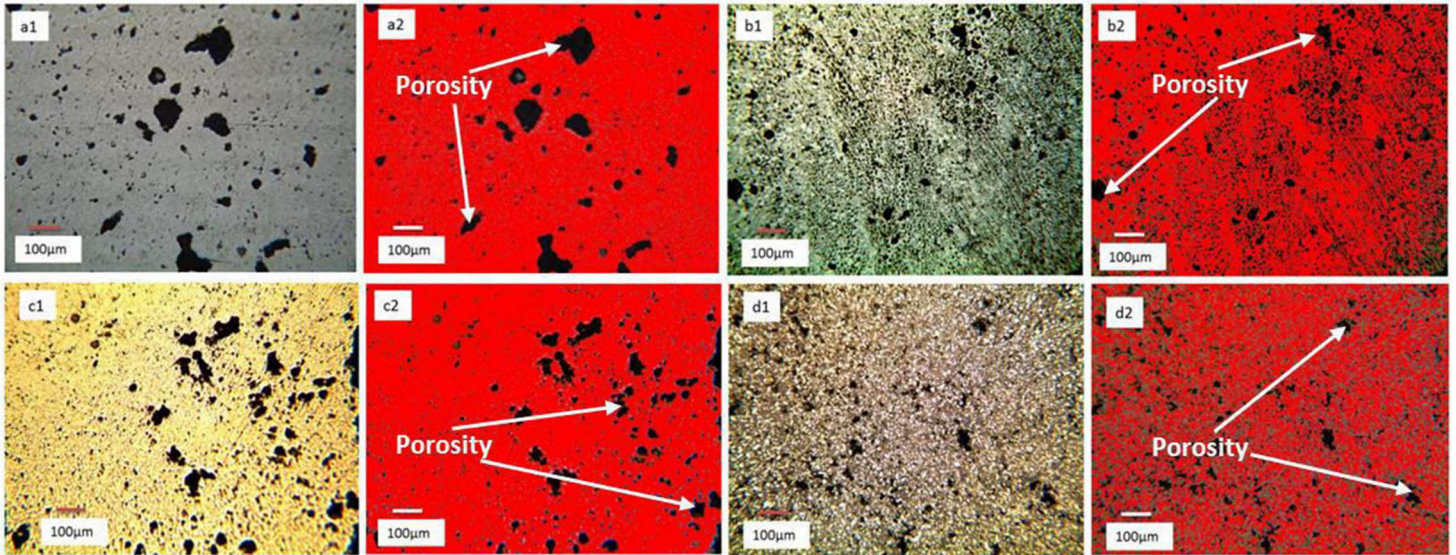
Fig. 2 shows the XRD of (a1-a2) Pure TiNi sample, (b1-b2) 2% vol. reinforced HAP, (c1-c2) 4% vol. reinforced HAP and (d1-d2) 6% vol. reinforced HAP.

stoichiometric phases as well as the fact that it lead to a decrease in the density of the samples as observable from the increasing pore quantity in the composite samples[4], [15]. The particles size of the hydroxyapatite mentioned to be in the nanoscale range effectively pins the diffusion of grains thereby hindering effectively the diffusion of particles along the grain boundary junctions thereby increasing the porosity of the area so they act as pinning sites. Furthermore, the addition of nano-HAP also increases the precipitation rate of the B2 phase into $TiNi_3$ and other constituent phases which exhibit stability at higher temperatures. Furthermore, the mixing of HAP with TiNi powder could have increased the dislocation density of the particles to allow for the more presence of precipitate nucleation site. The porosity itself changes orientation in the material as observable from the optical micrographs in fig.2 which shows that the porosity shifts from more closed-cell porosity (fig. 3) to open cell porosity[15]. The interconnected form of species has arisen due to
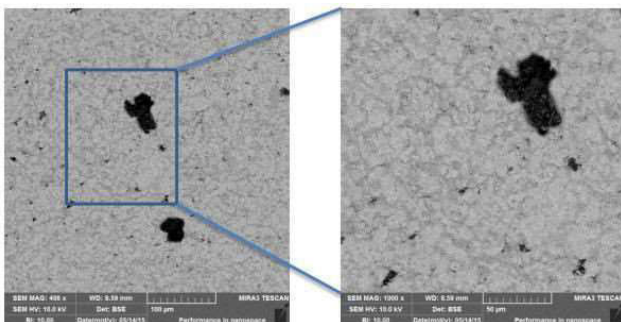

Fig. 3 shows SEM image of pure sintered Nitinol sample

the effective pinning of phase diffusion and particle diffusion during the sintering process and their pinning of grain boundary regions to effectively produce interconnected pore networks.

C. Phase Dissolution and Composition

The associated aspect of addition of HAP leading to increasing phase dissolution can be seen from EDX line analysis of the 2% and 4% vol. reinforced samples. It can be seen from the result that the increasing addition of the nano-HAP resulted in non-stoichiometric phase formation[10], [13] which can be seen from the out of phase wave pattern shown by line scan as well as the intensity of the Ti and Ni content. Furthermore some detection of Ca, P and H were detected confirming to the uniform distribution of the nano-HAP particles as observed by the lower end fluctuation of the line scan and the greater intensity of the nickel element in the scan shows increasing percentage of the nickel rich phase but the dominating aspect remains of the Titanium rich phase in the matrix (fig. 4).

D. Electrochemical Analysis

The tafel plots show that an interesting correlation between the sample and the solution and the effect of nano-HAP on the substrate. The tafel analysis show an improved resistance to corrosion behavior of the HAP reinforced
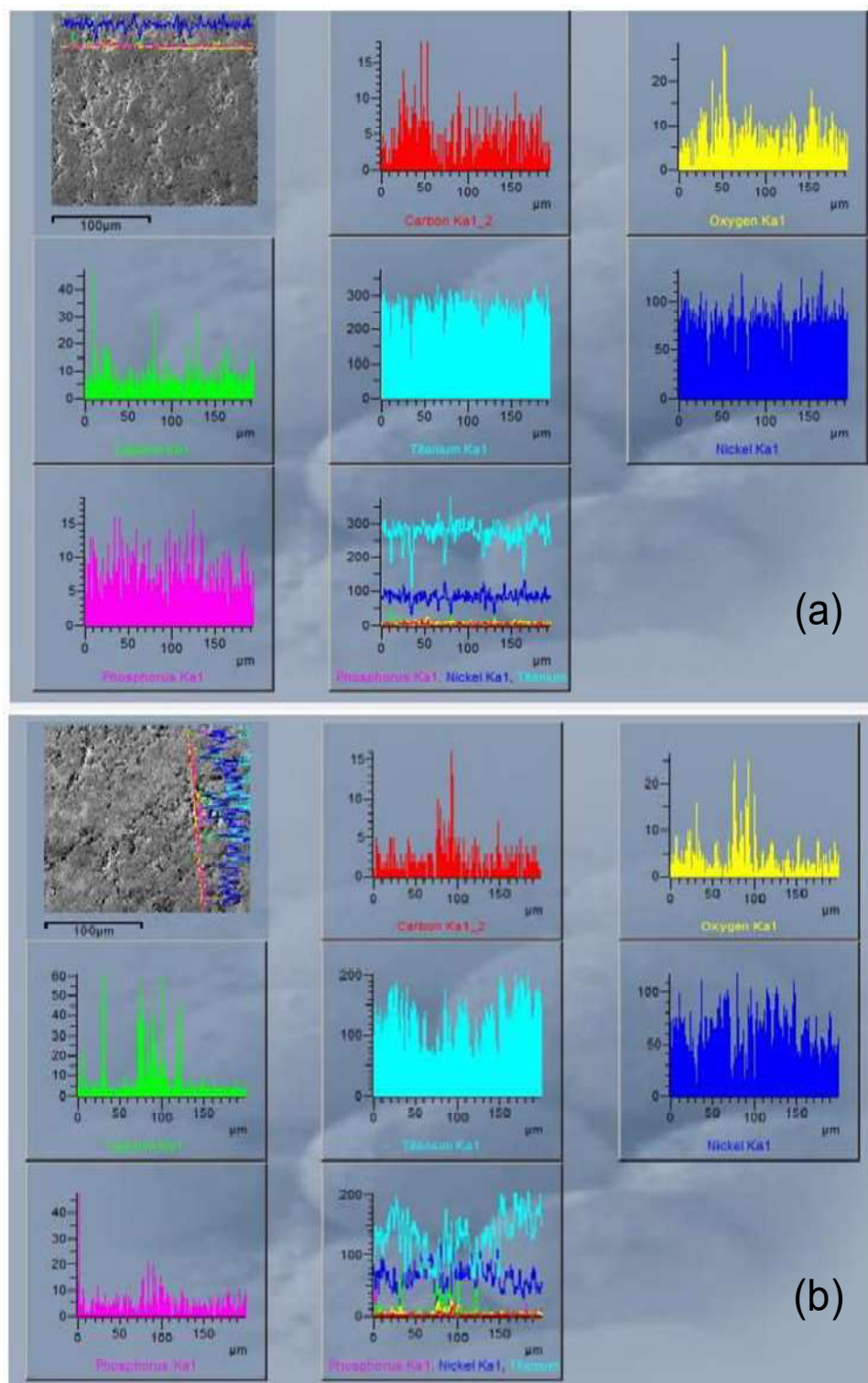
Fig. 4 shows EDX line analysis of the (a) 2% vol. reinforced TiNi, (b) 4% vol. reinforced TiNi.

samples. The corrosion rate decreases from 60.65 mpy to 2.991 for 4% reinforcement but however it increases to values of up to 236 mpy approximately for the 6% vol. reinforcement. It can be seen from the previous analysis and correlated with the tafel plot that increasing reinforcement up to 6% vol. led to the transformation of the products porosity type from closed cell to open cell porosity which accounts for greater penetration of fluid within the composite. The resulting increased penetration of the fluid shows the increasing formation of metastable pits[16] which are healed due to the formation of TiNi based oxide layer over the pitting area due to the aerated condition of the solution. With increasing
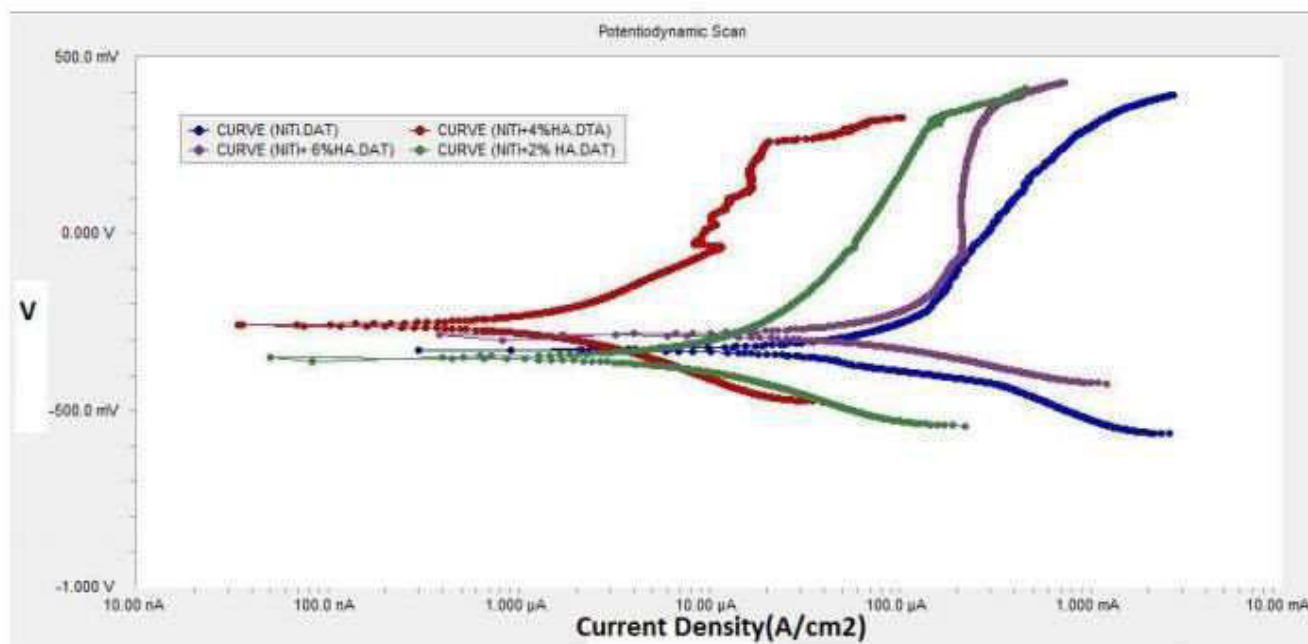
Fig. 5 shows the potentiodynamic plot of the composite materials

formation of protective coating over the alloy as a result of Titanium-rich[17] phase formation the pitting recovery takes place albeit at the cost of nobility of the alloy (Table. 2) in the solution which is affected by the increased surface area as well as the increasing content of the nickel-rich phase formation with increasing content of the TiNi$_3$ type phase promoting dissociation of Nickel into the solution.

Table 2 Show the selective values from tafel plot

S.no	HA Content (%)	Ecorr (mV)	Jcorr (µA/cm2)	Corrosion (mpy)
1	0	-330	64.5	60.65
2	2	-354	0.96	1.484
3	4	-259	3.63	2.991
4	6	-286	153	236.4

ACKNOWLEDGEMENT

REFERENCES

[1] J. Mohd Jani, M. Leary, A. Subic, and M. A. Gibson, "A review of shape memory alloy research, applications and opportunities," *Mater. Des.*, vol. 56, pp. 1078–1113, 2014.

[2] N. S. Manam *et al.*, "Study of corrosion in biocompatible metals for implants: A review," *J. Alloys Compd.*, vol. 701, pp. 698–715, Apr. 2017.

[3] J. Briceño, A. Romeu, E. Espinar, J. M. Llamas, and F. J. Gil, "Influence of the microstructure on electrochemical corrosion and nickel release in NiTi orthodontic archwires," *Mater. Sci. Eng. C*, vol. 33, no. 8, pp. 4989–4993, 2013.

[4] B. Yuan, X. P. Zhang, C. Y. Chung, M. Q. Zeng, and M. Zhu, "A comparative study of the porous TiNi shape-memory alloys fabricated by three different processes," *Metall. Mater. Trans. A Phys. Metall. Mater. Sci.*, vol. 37, no. 3, pp. 755–761, 2006.

[5] C. Bewerse, L. C. Brinson, and D. C. Dunand, "Materials Science & Engineering A Microstructure and mechanical properties of as-cast quasibinary NiTi – Nb eutectic alloy," *Mater. Sci. Eng. A*, vol. 627, pp. 360–368, 2015.

[6] I. H. Abidi, F. A. Khalid, M. Umer, M. A. Hussain, and A. Maqbool, "Tailoring the

pore morphology of porous nitinol with suitable mechanical properties for biomedical applications," *Mater. Lett.*, pp. 2–5, 2015.

[7] C. Li, Y. F. Zheng, and L. C. Zhao, "Electrochemical corrosion behaviour of Ti44Ni47Nb9alloy in simulated body fluids," *Mater. Sci. Eng. A*, vol. 438–440, no. SPEC. ISS., pp. 504–508, 2006.

[8] M. Es-Souni, M. Es-Souni, and H. Fischer-Brandies, "Assessing the biocompatibility of NiTi shape memory alloys used for medical applications," *Anal. Bioanal. Chem.*, vol. 381, no. 3, pp. 557–567, 2005.

[9] D. Mantovani, "Shape memory alloys: properties and biomedical applications," *Jom*, vol. 52, no. 10, pp. 36–44, 2000.

[10] H. J. Jiang, S. Cao, C. B. Ke, X. Ma, and X. P. Zhang, "Nano-sized SiC particle reinforced NiTi alloy matrix shape memory composite," vol. 100, pp. 74–77, 2013.

[11] C. Ma, D. Gu, D. Dai, M. Xia, and H. Chen, "Selective growth of Ni4Ti3precipitate variants induced by complicated cyclic stress during Laser additive manufacturing of NiTi-based composites," *Mater. Charact.*, no. March, pp. 0–1, 2018.

[12] L. Hu, A. Kothalkar, G. Proust, I. Karaman, and M. Radovic, "Fabrication and Characterization of NiTi/Ti3SiC2 and NiTi/Ti2AlC Composites," *J. Alloys Compd.*, 2014.

[13] M. Akmal, A. Raza, M. M. Khan, M. I. Khan, and M. A. Hussain, "Effect of nano-hydroxyapatite reinforcement in mechanically alloyed NiTi composites for biomedical implant," *Mater. Sci. Eng. C*, vol. 68, pp. 30–36, 2016.

[14] M. Farvizi *et al.*, "Microstructural characterization of HIP consolidated NiTi-nano Al2O3composites," *J. Alloys Compd.*, vol. 606, pp. 21–26, 2014.

[15] O. Scalzo, S. Turenne, M. Gauthier, and V. Brailovski, "Mechanical and microstructural characterization of porous NiTi shape memory alloys," *Metall. Mater. Trans. A Phys. Metall.*

Mater. Sci., vol. 40, no. 9, pp. 2061–2070, 2009.

[16] N. D. Alqarni, J. Wysocka, N. El-Bagoury, J. Ryl, M. A. Amin, and R. Boukherroub, "Effect of cobalt addition on the corrosion behavior of near equiatomic NiTi shape memory alloy in normal saline solution: Electrochemical and XPS studies," *RSC Adv.*, vol. 8, no. 34, pp. 19289–19300, 2018.

[17] S. A. Fadlallah, N. El-Bagoury, S. M. F. Gad El-Rab, R. A. Ahmed, and G. El-Ousamii, "An overview of NiTi shape memory alloy: Corrosion resistance and antibacterial inhibition for dental application," *J. Alloys Compd.*, vol. 583, pp. 455–464, 2014.

Development of ECG Data analyzer and recorder workstation with Portable USB DAQ for researchers and learners

Osama Malik, M. Faris, Sumaiya Sohail Rana, Jhanzaib Siraj Khatri and Hussain Kaizar Ali
Department of Biomedical Engineering
Faculty of Engineering, Science and Technology,
Hamdard University Karachi, Pakistan

Email address: osamamalik124@outlook.com, mfaris26@gmail.com, sumaiyarana123@gmail.com, jhanzaibkhashtri@outlook.com and Hussain.kaizar7@gmail.com.

Abstract—Electrocardiogram (ECG) is one of the vital diagnostic parameters of human body and provides crucial details of heart's electrical activity. It is among the key tools to diagnose various cardiovascular diseases. Traditionally, ECG is interpreted by the physicians. However, a lot of research is going on towards the development of systems to analyze features of ECG signal, detect abnormalities and diagnose diseases from it automatically. A system, therefore, is needed that can acquire the ECG signals from the body in its original state which can be used for the diagnostic purposes. The Propose of this endeavor is to develop a complete system capable of acquiring ECG signals from twelve Leads, displaying them as well as storing them for future use in research. The proposed system comprises of signal acquiring hardware consisting of buffers, instrumentation amplifiers (IA), analog filters to refine and extract noise free signals. The NI USB 6009 is the data acquisition device used to digitize the signals which are then processed, refined and displayed in real time in Graphical user interface developed in NI LabVIEW software.

Keywords—twelve leads ECG, Electrocardiogram, Instrumentation, LabVIEW, processing, DAQ.

I. INTRODUCTION

Bio-signals are produced by activity in nerve and muscle cells with their cell membrane potential being the primary originating source [1]. The widely utilized bio-signals for diagnosis of various diseases are Electrocardiogram (ECG) and electroencephalogram (EEG). ECG represents heart's electrical activity over a period of time. Electrodes are placed over the skin to detect the electrical signals. These electrical signals are essentials for ECG recording [2], represented in "Fig. 1".

ECG delivers significant information of the state and condition of heart to the medical personnel for the diagnosis and treatment of heart diseases and also for further research [3].

In this proposed system, ECG system is designed for researchers and learners that are working on bio signals.

Making this system portable and noise less keeping the knowledge of basic design and components selection accordingly.
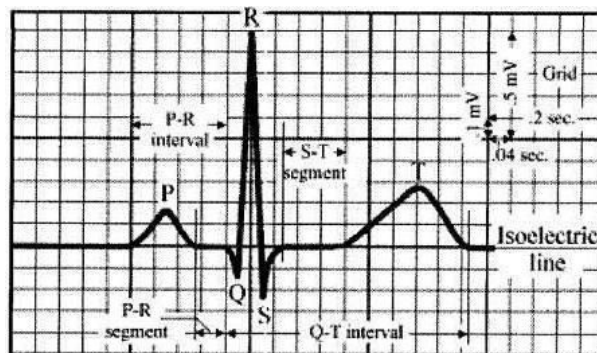

Fig. 1. ECG waveform

Results are in the form of real time display of the acquired ECG and is stored with necessary details in excel file format. It is readable in many software and can be used for analysis, simulation and testing of algorithms.

II. LITERATURE REVIEW

In this proposed system, an ECG monitoring system is developed with the help of LabVIEW and DAQ PCI card with 12 bit resolution. No such hardware description is included. Using a DAQ PCI card make it unportable device as PCI is supported only in desktop systems which means this design is specific for one desktop computer. Amplification stage is designed by using instrumentation amplifier AD623 which can be done through other low-cost instrumentation amplifier with better specifications, hence better results. With this designed system results are not justified as for diagnostic application [4].

The system is designed for Telemedicine application and measures physiological parameters such as ECG, photoplethysmogram and body temperature Our focus is on the ECG circuitry and its digital results. The ECG circuit lacks the Right Leg Driven circuit and frequency ranges of bandpass filters is not thoroughly discussed. Moreover, Arduino is used for data acquisition by utilizing its built-in analog to digital converter (ADC) which has low resolution of 10-bits and is not preferred for medical data acquisition. Additionally, Results are also not proper upon comparison with standard outputs [5].

The technique presented here is well designed, in which a single channel 3-lead ECG is designed with different ranges of filters. Filters ranges are different for clinical and diagnostic purpose as in this technique mentioned ranges are 0.028-160Hz and 0.03-106Hz. For analog to digital conversion NI DAQ is used which is good for medical data

acquisition. Results are displayed on LabVIEW front panel which are quite clear and proper [6].

This proposed system is microprocessor based ECG Monitoring technique, here Heart electrical activity is recorded digitally with the help of MATLAB based software. Using MATLAB means results are not in real time. Acquired ECG results are first saved and then processed into MATLAB. Before digital filtering pre-filtering is applied for clear line noise and artifacts, selection of band pass frequency ranges are very poor. This system's results are noisy and unclear for diagnostic or clinical purpose [3].

III. DESIGN APPROACH

An ECG's circuitry job is to amplify the small signal measured from the heart as well as to filter outside and internal noise. In this study, the amplification is implemented through a instrumentation amplifier whereas filtering is completed through common and differential mode filtering. There is a Right Leg Drive circuit which decreases noise and provides suitable grounding as shown in "Fig. 2".

A. Hardware Design

Electrodes selection is crucial for picking any bio-signal [2]. For any bio-signal acquisition, electrodes impedance must be same or with minimum differences. In this study disposable electrodes are used keeping their impedance matching in mind.
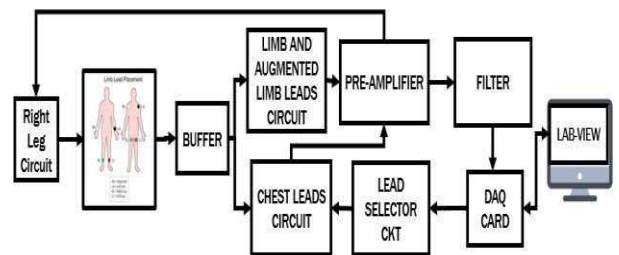

Fig. 2. Block Diagram

The ionic potentials are transmitted into unity gain buffers through the help of electrodes. Buffers are constructed using LM741 which are used to give strength to signals so that signals should have the capability to be fed into three different circuits [7].

Stabilized signals now can be differentiated using AD620 which is a low-cost instrumentational amplifier with excellent ac and dc specifications such as low noise, low input biasing current and lower power consumption making it well suited for medical applications. In this study, gain is kept 1000 for instrumentation amplifier [8]. Gain equation is shown in Eq 1.

$$R_G = \frac{49.4k\Omega}{G-1} \qquad (1)$$

G is the gain we need where R_G is the gain resistor.

Medical devices are preferred for its safety claims. In this system, protection is made using the "Right leg driven circuit".

This system is using Filters to remove unwanted signals as working with respect to selective band of frequencies. For Human ECG our required band is 0.02 to 150Hz [1], for which we used LM324 to make an active Butterworth band pass filter configuration. Resistors and capacitors for band pass are calculated using Eq 2.

$$Low\ Cutoff\ Frequency = \frac{1}{2\pi R_2 C_2} \qquad (2)$$

$$High\ Cutoff\ Frequency = \frac{1}{2\pi R_1 C_1} \qquad (3)$$

$$Gain = -\frac{R_2}{R_1} \qquad (4)$$

Results after filters are digitized using National Instrument Data Acquisition (NI DAQ) card as analog to digital converter. NI DAQ is a 12 bit resolution card which makes it a preferred choice for medical purposes [9].

This study is working for 3 channel 12 leads ECG with three different PCB boards. Lead I-III are easily acquired as well as augmented outputs are directly fed into DAQ. But for selection of 6 outputs of chest, a lead selector switch is used. DAQ card have digital output pins through which Lead selector switch is derived.

B. Software Approach

The software program in this project is used to perform the Channel selection, digital filtering, future calculations, and to display the ECG waveform on the monitor's screen as shown in Fig. 3.

In this system design, NI DAQ is used which is interfaced using LabVIEW VI (Virtual Instrument).

DAQ assistant VI is used in this system to measure and acquire signals from the ECG circuitry to the computer. DAQ assistant also work for signal generation to control analog and digital output pins.

Programmable output pins of DAQ card are used for switching in chest board, from V1-V6. In this system Boolean switches are used. through which we completely acquire 12 leads of ECG trace and display it on the front panel as shown in Fig. 4.
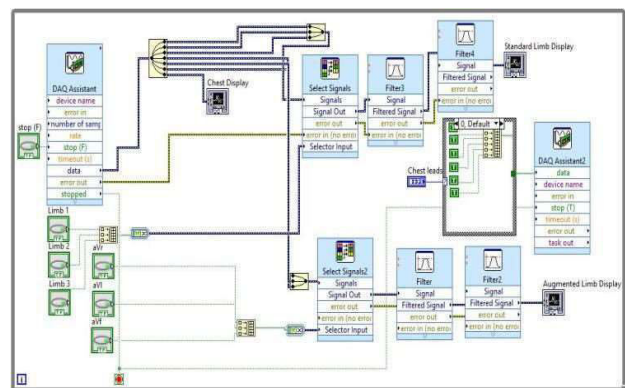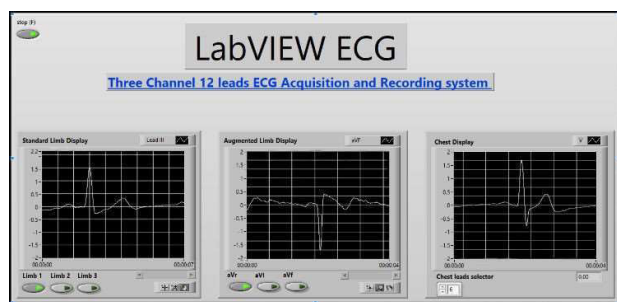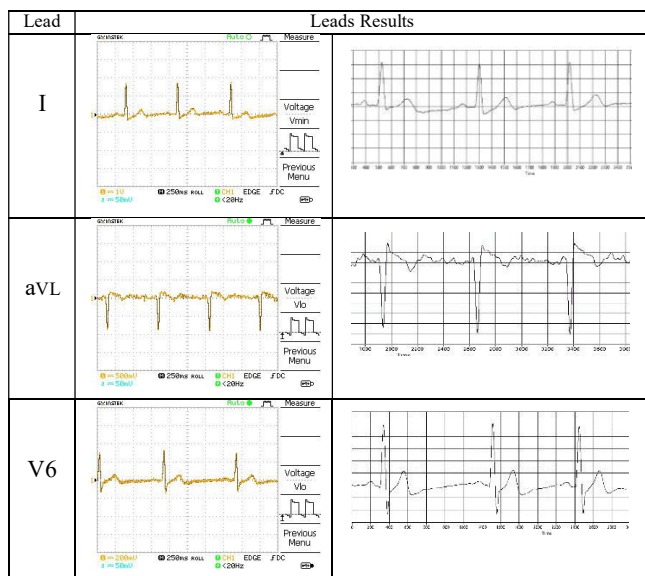

Figure 3 LabVIEW Block Diagram

Figure 4 Front Panel

Figure 5 Analog and digital filtered result of three selected lead.

IV. RESULTS

The final results obtained from our ECG hardware are significantly noise free and include all the required segments of ECG waveform. In Fig. 5, the comparison between the analog filtered output and the final output after digital filtering is shown.

CONCLUSION

In this proposed ECG system design results are clear and proper for diagnostic and clinical levels. Acquired digital raw data can be transfer and interpreted and used for Different simulation application.

REFERENCES

[1] Khandpur, Raghbir Singh. Handbook of biomedical instrumentation. Tata McGraw-Hill Education, 1994.

[2] Webster, John G. Medical instrumentation application and design. John Wiley & Sons, 2009.

[3] Rosli, Khairul Affendi, Mohd Hafizi Omar, Ahmad Fariz Hasan, Khairil Syahmi Musa, Mohd Fairuz Muhamad Fadzil, and Shu Hwei Neu. "Development of Electrocardiograph Monitoring System." In MATEC Web of Conferences, vol. 150, p. 01013. EDP Sciences, 2018.

[4] Han, Jun, Hao Yu, and Hongli Yang. "ECG-Analyzing Experimental System Based on Virtual Instrument." In 7th Asian- Pacific Conference on Medical and Biological Engineering, pp. 626-628. Springer, Berlin, Heidelberg, 2008.

[5] Bhatti, Anam, Asad Ali Siyal, Adeel Mehdi, Huma Shah, Hinesh Kumar, and Muhammad Ali Bohyo. "Development of cost-effective tele-monitoring system for remote area patients." In Engineering and Emerging Technologies (ICEET), 2018 International Conference on, pp. 1-7. IEEE, 2018.

[6] Jamil, MM Abdul, C. F. Soon, A. Achilleos, M. Youseffi, and F. Javid. "Electrocardiograph (ECG) circuit design and software-based processing using LabVIEW." Journal of Telecommunication, Electronic and Computer Engineering (JTEC) 9, no. 3-8 (2017): 57-66.

[7] Instruments, Texas. "Lm741 operational amplifier." LM741 datasheet, May (1998).

[8] Devices, Analog. "AD620 Datasheet." Low cost, Low Power Instrumentation Amplifier (1999).

[9] Bitter, Rick, Taqi Mohiuddin, and Matt Nawrocki. LabVIEW: Advanced programming techniques. Crc Press, 2006

3D Modeling of Ground Water Effect on Physical Properties of Rock

Engr.Bushra Nawaz[1, a], Dr.Noor Muhammad[1,], Zahid-Ur-Rehman[1,] and Khaleeq Ahmed[2,]

[1]Department of Mining Engineering, University of Engineering & Technology Peshawar,
25120, University Campus Peshawar
[2]Pakistan Institute of Engineering & Applied Sciences

Email address: [a] bushranawaz3@gmail.com

Abstract— Ground water is one of serious problem in underground mining operations. Water in rocks effect the index properties of rock and hence cause serious hazards like mine collapse. Therefore, to investigate the effect of water absorption on physical properties of rock, tests were conducted in laboratory on phosphate /dolomite specimens of Tarnwai Area. Results obtained from test were analyzed using regression analysis and standardized residual analysis. Relationship between the physical properties was develop using these analyses and quantified the water affect by 3D Modelling using XLSTAT. It will lead to a better understanding of water effect on rock mass properties.

Keywords— ground water, physical properties, water absorption, underground mining, 3D modelling

I. INTRODUCTION

Due to the sedimentary nature of phosphate/dolomite rock they are very porous. The porous nature of these rocks makes them highly vulnerable to moisture and water absorption. The influence of water is quite important for the inherent safety and stability of underground structures or projects. Water is the 'enemy' in most engineering problems (Michael, D.J., 1982).In many sedimentary rocks, water absorption & moisture cause a wide range of problems.[1]. Among the many factors influencing rock properties, moisture is one of the most important[2]. Apart from that, mine water continues to be a major concern to both operating and abandoned mines (Reddish, D.J., 1994). In a word, there has been no doubt that moisture can affect the properties of various rock types, particularly sedimentary rocks [3][4].

Therefore, it is necessary for underground workings to investigate the physical properties of rock for better understating of water effect.

In this paper, the effect of water is modelled and investigated using regression analysis. The relationship between different physical properties is compared by 3D modelling using XLSTAT.

II. EXPERIMENTAL METHODOLOGY

A. Procedure

First, the specimens are prepared for density, porosity, water absorption, moisture content and slake durability test. The specimens having the standard weight of 40-60gm were confirmed for test utilizing the standard procedure for test of ASTM (2001) Standard Test Method C97-83 [5][6].

B. *Moisture Content*

According to ASTM (1998) [6] [8] Standard test method for laboratory determination of water (moisture) ''Water content/ Moisture Content (w)'' is defined as

$$w = M_w / M_s \qquad (1)$$

where M_w = mass of pore water and M_s = mass of grain (solid component of the specimen).

C. *Water Absorption*

According to ASTM (2001) [5] ''Water absorption''(A_w),also known as ''absorption'' or ''total water absorption,'' is given by

$$A_w = (M_{sat} - M_{dry})/ M_{dry} *100 \% \qquad (2)$$

where M_{sat} = mass of saturated-surface-dried test sample in air and M_{dry} = mass of oven-dried test sample in air.

D. *Porosity*

According to ASTM (2001) [9] [10] "Porosity (n)" is given by

$$n = (V_v/V)*100\% \qquad (3)$$

where

$$V_v = (M_{sat} - M_{dry})/ density. water \qquad (4)$$

III. EXPERIMENTAL RESULTS & DISCUSSIONS

A. *Regression Analysis*

Data from laboratory experimental tests were obtained for these physical properties. Using eq (1), (2), (3), (4) physical properties are calculated and results are shown Fig. IIIA-III-1. Exponential/power relationship is developed and regressed for observing the correlation of properties

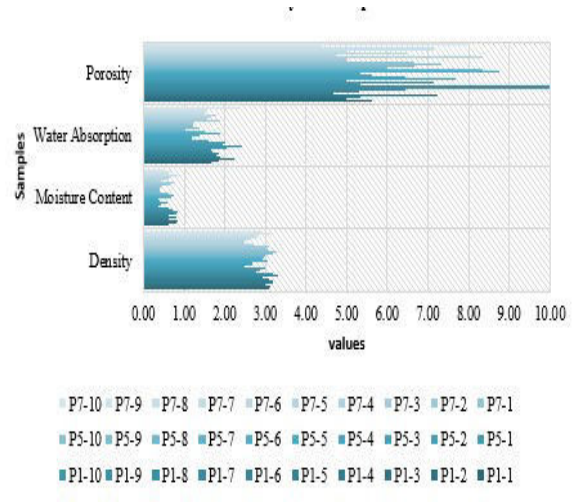Fig. IIIA-(2,3,4,5) are demonstrating the regression analysis for physical properties of rock.

Figure IIIA-1 Test Results of Physical Properties

Fig. IIIA-2 is showing the regression analysis of Moisture content by Density. The regression value obtained from this analysis is $R^2 = 0.823$. Confidence interval for mean of 95% is plotted along with the confidence interval of observed 95% of values.

Similarly, Fig. IIIA-3 is showing the regression of Porosity by Water Absorption. The regression value obtained from this analysis is $R^2 = 0.801$. Confidence interval for mean of 95% is plotted along with the confidence interval of observed 95% of values. Figure IIIA-4 is demonstrating the regression of Porosity by Moisture Content. The regression value obtained from this analysis is $R^2 = 0.840$. Fig. IIIA-5 is representing the regression of Water Absorption by Density. The regression value obtained from this analysis is $R^2 = 0.820$.
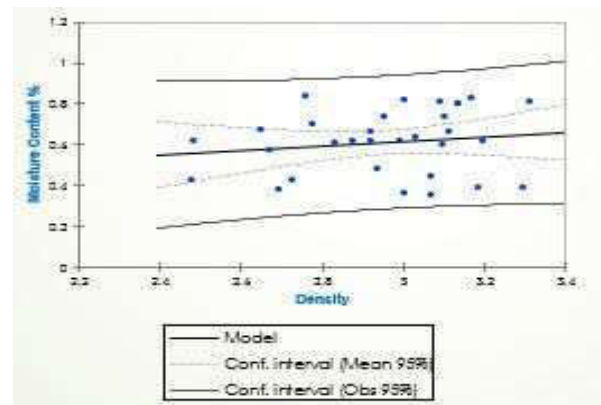

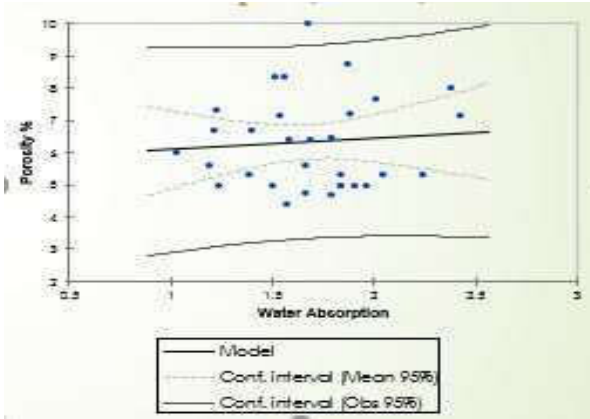*Figure IIIA-2 Regression of Moisture Content by Density*

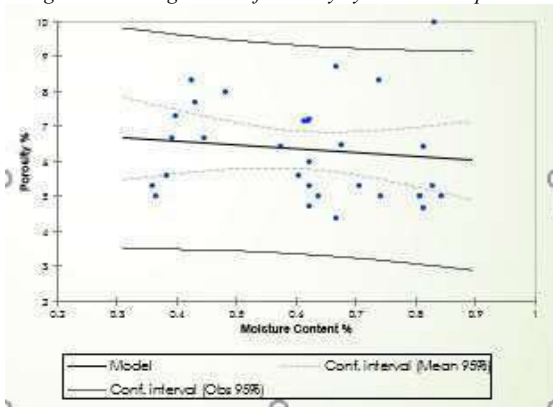*Figure IIIA-3 Regression of Porosity by Water Absorption*

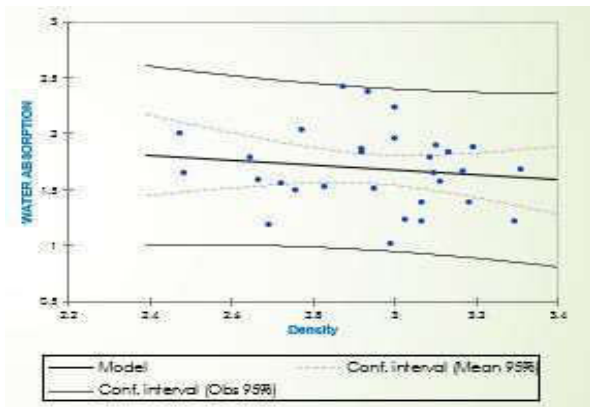*Figure IIIA-4 Regression of Porosity by Moisture Content*

Figure IIIA-5 Regression of Water Absorption by Density

B. 3D Modelling of Physical Properties

Physical properties are modelled in 3D using XLSTAT. This modeling is giving an understating of water absorption behavior with respect to physical properties

Fig. IIIB-1 is showing the 3D Modelling of Density & Moisture content by Water absorption. Color of the graph is quantifying the water absorption over density and moisture

content. Similarly, Fig. IIIB-III-2 is showing the 3D Modelling of Porosity & moisture Content by Water absorption. Fig. III-3 3D Modelling of Density & Porosity by Water absorption.
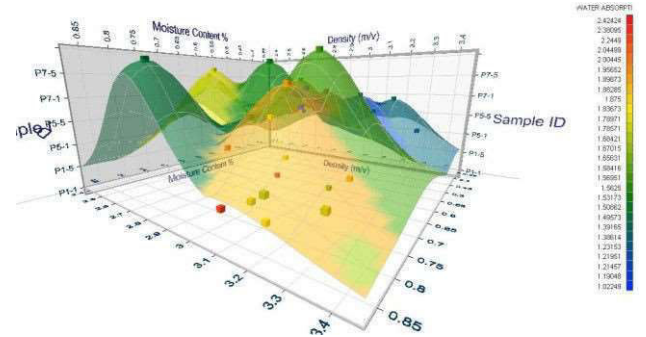

Figure IIIB-1 3D Modelling of Density & Moisture content by Water absorption
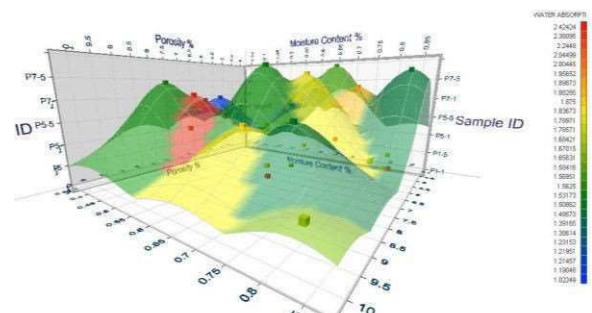
Figure IIIB-2 3D Modelling of Porosity & moisture Content By Water absorption
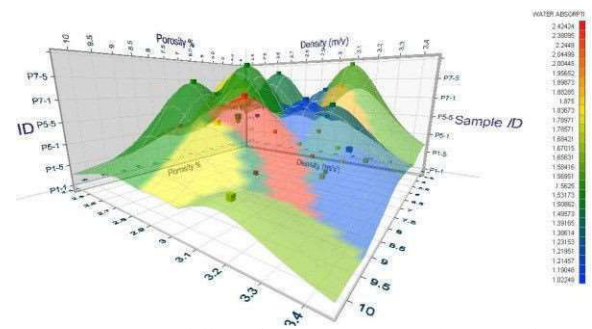
Figure IIIB-3 3D Modelling of Density & Porosity by Water absorption

C. Conclusions

The experimental results, regression analysis and 3D modelling of the physical properties presented in this paper show that water has a predominant effect on physical properties of rock. As the density of rock sample is decreasing than it is cause more water to accumulate into rocks. Porous nature of rock is also causing the rock to penetrate more the

water into pores and hence endangering safety and stability of underground workings.

Furthermore, water has weakening effect due to affecting the physical properties. As with physical properties, water has great effect on mechanical properties of rock so further work is being undertaken for studying groundwater effect on rock strength.

ACKNOWLEDGMENT

. The authors wish to express special thanks to Dr Noor Muhammad for her generous help and good intension and many thanks to Engr. Zahid-ur-Rehman & Engr. Sajjad Department of Mining Engineering, University of Engineering & Technology Peshawar, for their directions during the test and helpful discussion concerning this work.

REFERENCES

[1] Broch, E. 1974. The influence of water on some rock properties. Proc. 3rd ISRM Congr., Denver, Vol. 2A: pp.33-38

[2] Rao, K.S., Venkatappa Rao, G. & Ramamurthy, T. 1987. Strength of sandstone in saturated and partly saturated conditions. Geotechnical Engineering 18: pp.99-126

[3] Aughenbaugh, N.B. & Bruzewski, R.F. 1973. Investigation of the failure of roofs in coal mines. Final report on Bureau of Mines Contract HO111462

[4] Aughenbaugh, N.B. 1974. Effect of moisture on shale, Proc.23rd Annual Soil Mechanics and Foundation Engineering Conference, Recent Development in Geotechnical Engineering, Kansas City

[5] ASTM (2001) Standard test method for density, relative density (specific gravity),

and absorption of coarse aggregate. In: Annual book of ASTM standards, p 6

[6] ASTM (1998) Standard test method for laboratory determination of water (moisture) content of soil and rock by mass. American Society for Testing and Materials, Philadelphi

[7] Brown ET (1981) Rock characterization, testing & monitoring: ISRM suggested methods. Pergamon Press, Oxford, pp 81– 89

[8] Burshtein LS (1969) Effect of moisture on the strength and deformability of sandstone. Sov Min 5(5):573–576

[9] Borrelli E (1999) ARC laboratory handbook: porosity, vol 2. ICCROM, Rome, pp 12–13

[10] Silva RM, Schroeder C, Verbrugge J-C (2008) Unsaturated rock mechanics applied to a low-porosity shale. Eng Geol 97(1– 2):42–52

[11] Berg, C.R. 1995. A simple, effective- medium model for water saturation in porous rocks. Geophysics 60(4): pp.1070- 1080

[12] Bell, F.G. 1981. A survey of the physical properties of some Carboneate rocks. Bull. of the Int. Assoc. Eng. Geol. 24: pp.105- 110

[13] Hadizadeh, J. & Law, R.D. 1991. Waterweakening of sandstone and quartzite deformed at various stress and strain rates. Int. J. Rock Mech. Min. Sci. & Geomech. Abstr. 28(5): pp.431-439

Synthesis and Characterization of CNT based Nanocomposites

for Biomedical Applications

Nayab Jamal[1,a], M. Imran Khan[2,b], Hamza Alam[3,c], Rohan Riaz[4,d], Abbas Raza[5,e]

[1]*Ghulam Ishaq Khan Institute of Engineering Sciences and Technology, Topi, 23460, KPK.*

a) nayab.jamal@giki.edu.pk, b) imrankhan@giki.edu.pk , c) alamhamza181@gmail.com , d)rohan.riaz@hotmail.com
e)gmm1846@giki.edu.pk

Abstract— *In this present study an approach to the synthesis of the nanocomposite has been shown with Carbon nanotubes (CNT) and a metal. A nanocomposite can have a matrix, reinforcement or both in the nano range. In this particular composite CNT and the metal reinforcement are both in the nano range. CNT acts as a matrix while Copper and Manganese nanoparticles are the reinforcements. A bottom up chemical reduction method is used for the synthesis of these nanocomposites. For the reduction sodium borohydtrate has been used as the reducing agent.*

After the synthesis, nanocomposites are characterized using characterization techniques such as AFM and SEM to conduct the morphological analysis. The purpose of the characterization is to make sure that the synthesis of the required nanocomposite has been achieved. AFM provides the surface morphology where we can see individual atoms and there locations on the surface. AFM gives a very high resolution image and helps in determining the structure of the material. The SEM images obtained give a very clear image of the structure of the CNTs and the metal nanocomposites. It can be seen clearly that the CNTs act as a matrix for the Copper and Manganese nano particles. Two SEM images for both Manganese and Copper have been obtained in micro and nano range.

To observe the conduction of the nanocomposite a simple test was prepared to observe the conductivity of the materials. Theoretically the material should be highly conductive because of two reasons. Firstly CNTs and copper both are conductive and secondly they are in the nano range enhancing the conductivity due to increased surface area. The test comprises of a simple setup of a series LED connected to the nanocomposite solution in de ionized water. The solution was connected to a source of voltage and the overall setup was grounded to make a path for current to pass. When the voltage was applied the series of LEDs were illuminated. **This test helped assure the conducting nature of the nanocomposite.**

Keywords— *Nanocomposites, nanosensing, nanosynthesis, biomedical, CNT-Mn, CNT-Cu*

I. INTRODUCTION

Nanotechnology is the manipulation of matter on the atomic scale. It deals with engineering nanostructures ranging from 1-100nm in size in at least one dimension, and involves manufacturing or modifying different materials or devices within that size [1]. By reducing the size of a bulk material to micro and nano regime its physical and chemical properties change drastically. Size reduction of the crystalline structures will eventually result in the characteristic features of tiny individual atoms or molecules neglected in the bulk [2]. Nanocomposite is a matrix of nanomaterial in which two or more nano sized particles are incorporated. This results in a drastic improvement in electrical conductivity, mechanical strength, toughness, and optical properties. This is due to the combined properties of the matrix and the reinforcing nanomaterial. [3] Nanocomposites are widely being used as functional material for the sensors for detection and measurement of different analytes. Due to their faster response time nanocomposites have put quite a mark in the field. Nanocomposites due to their very small size have large surface areas and large surface energies due to which they are able to react very quickly to the analytes. [4]

Biosensing is a hottest field in which analytical devices like nanosensors are used to convert the response of bioanalyte into an electrical signal. It must be very specific, sensitive, and not dependent on physical parameters such as temperature and pH. It should be recyclable. [6]. Uric acid and ascorbic acid are one of the major biomolecules in human cell. The level of these biomolecules are of essential importance. Increase or decrease in the level of uric acid is also related to several disorders such as gout, hypertension, obesity, diabetes, high cholesterol and heart diseases. [5].

Nanosensors are sensors whose active elements include nanomaterials. Nanomaterials-based sensors have several benefits in sensitivity and specificity over sensors made from traditional materials. Nanosensors can have increased specificity because they operate at a similar scale as natural biological processes, allowing functionalization with chemical and biological molecules, with recognition events that cause detectable physical changes. Enhancements in sensitivity stem from the high surface-to-volume ratio of nanomaterials, as well as novel physical properties of nanomaterials that can be used as the basis for detection, including nanophotonics. Nanosensors can also potentially be integrated with nanoelectronics to add native processing capability to the nanosensor. [7] Nanosensors are recently used in plant biology, defense system, marine biology, and clinical sector [8, 9]Graphene or other carbon nanostructures combined with metal nanostructures are widely used as a nanosensors that show excellent performance in biosensing due to enhancement in their structure, chemical, mechanical, optical and novel electronic properties. [10]

II. EXPERIMENTAL WORK

A. Chemical Reagents

The chemical reagents involved in the synthesis of the Manganese doped CNTs and Copper doped CNTs are

1. Carbon Nanotubes (CNTs)
2. polyethyleimine
3. Methanol
4. Copper Chloride
5. Menganese acetate
6. Sodium Borohydrate

Carbon nanotube is the matrix. Copper Chloride and Manganese acetate are reduced to form Copper and Manganese nanoparticles. Sodiumm Borohydrate is used for the reduction of Copper Chloride and Manganese Acetate to Copper and Manganese nanoparticles. Methanol is used as a solvent to produce a colloidal solution.

B. Synthesis of CNT-Cu

For the preparation of CNT-Cu nanocomposite 0.03 g of CNTs was weighed. The weighed CNTs were then dispersed in polyethyleimine which was prepared by dissolving 334 μl into 5 ml of methanol. The solution of polyethyleimine and the CNTs was then placed on a magnetic stirrer to be stirred for two hours while maintaining at room temperature. To remove excess Polyethyleimine the solution was kept at room temperature for 12 hours to settle. The excess Polyethyleimine that comes to the top was then removed. To make a stable colloid the remaining CNTs were re-dispersed in 40ml of methanol. Now to make a nanocomposite, 0.1 M solution of $CuCl_2$ was prepared using methanol. This solution was then added to the stable colloid of CNTs and stirred vigorously for half an hour to completely dissolve the solution. For the reduction of the nanocomposite 10ml of Sodium borohydrate is used. It is added drop wise and stirred for 10 mins for effective reduction. The solution was then centrifuged and rinsed with 5ml of methanol and dried under vacuum at 50 °C.

C. Synthesis of CNT-Mn

For the preparation of CNT-Mn nanocomposite 0.03 g of CNTs was weighed. The weighed CNTs were then dispersed in polyethyleimine which was prepared by dissolving 334 µl into 5 ml of methanol. The solution of polyethyleimine and the CNTs was then placed on a magnetic stirrer to be stirred for two hours while maintaining at room temperature. To remove excess Polyethyleimine the solution was kept at room temperature for 12 hours to settle. The excess Polyethyleimine that comes to the top was then removed. To make a stable colloid the remaining CNTs were re-dispersed in 40ml of methanol. Now to make a nanocomposite 0.5 M solution of Manganese acetate was prepared using 100ml methanol. This solution was then added to the stable colloid of CNTs and stirred vigorously for half an hour to completely dissolve the solution. For the reduction of the nanocomposite 30ml of Sodium borohydrate is used. It is added drop wise and stirred for 10 mins for effective reduction. The solution was then centrifuged and rinsed with 5ml of methanol and dried under vacuum at 50 °C.

IV. RESULTS AND DISCUSSION

A. SEM Results

SEM images were obtained for CNT-Cu nanocomposite. It clearly shows Copper nanoparticles embedded in the CNTs. Particles at the front are brighter and display a more metallic look than the

particles at the back. This is due to the maximum reflection of electrons from the surface of the particles at the front. The nanocomposite shows the presence of mono dispersed Cu NPs having an average diameter of 5-7 nm.
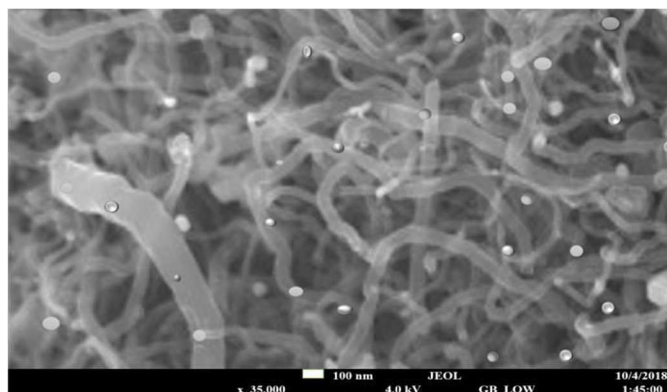

Fig 1: Zoomed SEM image of CNT-Cu nanocomposite

Fig 2: SEM image of CNT-Cu

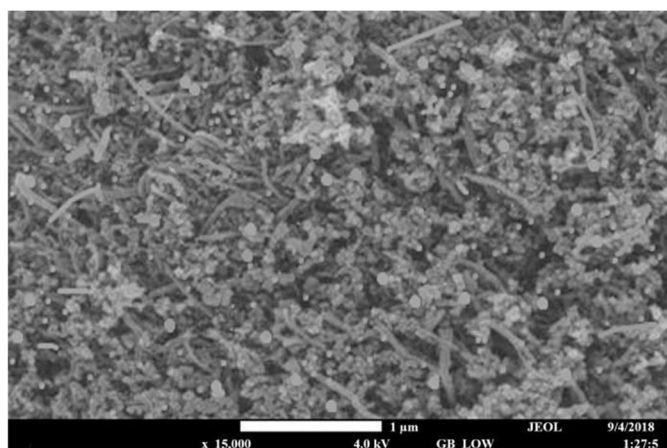Mn nanoparticles can be clearly seen in the SEM images (fig 3 and fig 4) being embedded in the CNTs network. Since the number of Mn nanoparticles reduced were more than the Cu nanoparticles we clearly see that Mn nanoparticles have agglomerated making it hard to identify CNT matrix beneath them. The size range of Mn nanoparticles is less 50 nm and these NPs enhance the surface availability of CNT.
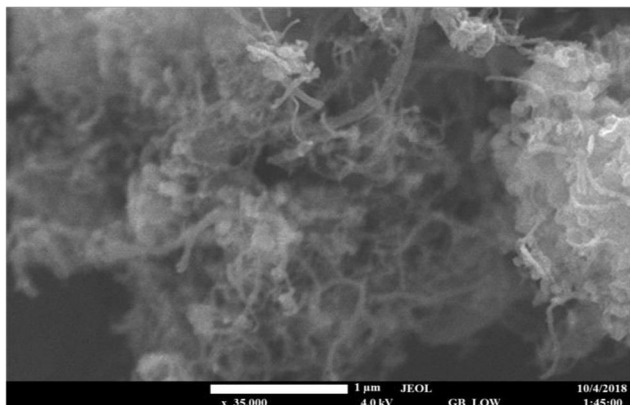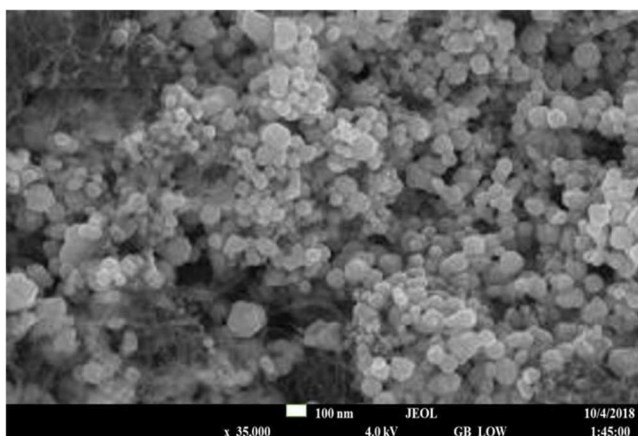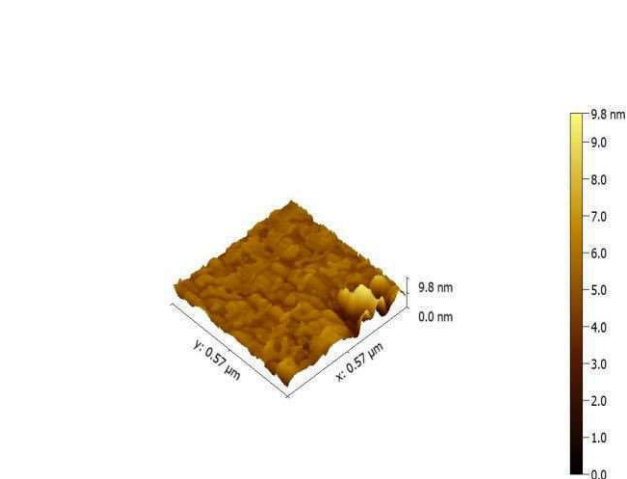
Fig 3: SEM image of CNT-Mn

Fig 5: FEM image of CNT-Cu

Fig 4: Zoomed SEM image of CNT-Mn

Fig 6: AFM image of CNT-Mn

C. Conductivity tests

Electrical Circuit is designed to compare the electrical potential of both solutions

1 • Preparation of solution of nanocompostei n deionized water

2 • Ultrasonication

3 • Circuit preparation
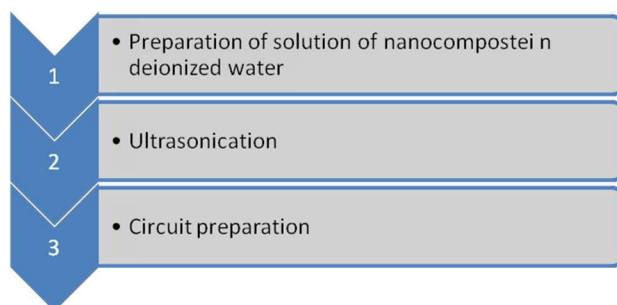
Fig 7: Conductivity test process flow diagram

For the conductivity test, 0.1M solution of both CNT-Cu and CNT-Mn was prepared in de-

B. AFM Results

The AFM images of CNT-Cu nanocomposite show a surface topography for the synthesized nanostructure. The particle size may only be approximated using these images due to lack of individual particle resolution. The CNTs are not clearly visible as the magnification of AFM is much larger than the dimensions of the CNT. Another AFM image for the CNT-Cu nanocomposite was taken from a different raster scan of the glass slide sample. The following image shows presence of nano-sized CNTs.

ionized water to make sure there was no conductivity due to the water. This solution was then sonicated for 30 minutes to obtain a homogenous mixture. A circuit was designed to observe if the solution conducted enough electricity to illuminate a series of LED bulbs.

The experiment was successful

Equipment
- Digital Multi Meter
- Bread Board
- 15 V power supply
- conducting wires

Following is the illustration of the circuit
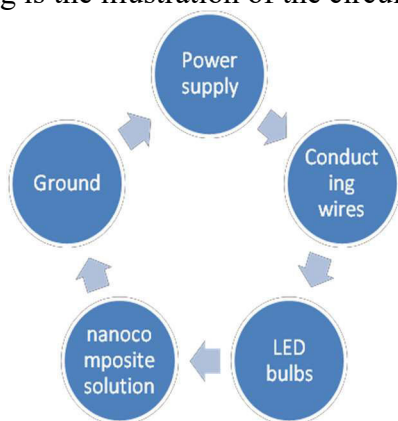
Fig 8: Circuit daigram

The circuit starts with connection from the 15 volt power supply on the breadboard. The wire is then connected to one end of a series of LED bulbs. The other end of the LED bulb is placed first in CNT-Cu and then CNT-Mn nanocomposite solution. In the solution another wire from the ground is placed to make a connection through the solution. As long as both the wires in the solution are not short we can observe the illumination of the LED bulbs due to the conduction of the solution.

Fig 9: Conduction test CNT-Mn
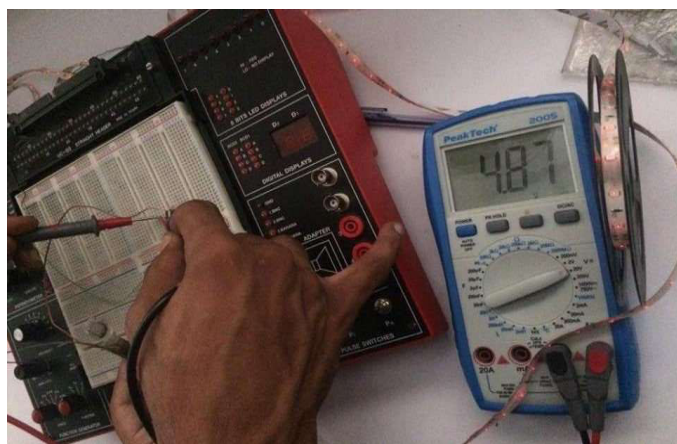
Fig 10: Conduction test CNT-Cu

Since, De Ionized water is non conductive in nature, the addition of Nanocomposite increases the conductivity of the solution. CNT-Cu showed a better conductivity and decreases the resistance of the solution more efficiently as compare to CNT-Mn nanocomposite.

The conductive behavior of CNT-Cu results in the higher value of voltage due to Copper being a better electrical conductor than Manganese.

Following are the results of the voltages compared with the de-ionized water

Solution	Value
De-ionized water	0.12 V
CNT-Cu solution in De-ionized water	4.87 V
CNT-Mn solution in De-ionized water	4.74 V
Direct Connection without Solution resistance	10.91 V

Fig 10: Conduction value table

IV. CONCLUSION

The synthesis of CNT-Cu and CNT-Mn with chemical reduction methods was successful. The CNT served as active reaction sites for the nucleation of metallic nanoparticles. The high surface area to volume ratio of the CNTs combined with the reactive nature of metal nanoparticles gives us a bio-sensory material.

The AFM images confirmed the presence of nanoparticles but not necessarily the entire nanocomposite due to resolution defects. The CNT-Cu nanocomposite was clearly observed through the SEM images. The CNT-Mn nanocomposite, on the other hand showed a greater agglomeration.

V. ACKNOWLEDGMENT

VI. REFERENCES

[1]   F. Sanchez and K. Sobolev, "Nanotechnology in concrete–a review," Construction and Building Materials, vol. 24, pp. 2060-2071, 2010.

[2]   H. S. Nalwa, Handbook of Nanostructured Materials and Nanotechnology, Five-Volume Set: Academic Press, 1999.

[3]   A. C. Balazs, T. Emrick, and T. P. Russell, "Nanoparticle polymer composites: where two small worlds meet," Science, vol. 314, pp. 1107-1110, 2006.

[4]   K. E. Drexler, "Drexler and smalley make the case for and against'molecular assemblers'," Chemical & Engineering News, vol. 81, p. 1, 2003.

[5]   H. Khadri, M. Alzohairy, A. Janardhan, A. P. Kumar, and G. Narasimha, "Green synthesis of silver nanoparticles with high fungicidal activity from olive seed extract," Advances in Nanoparticles, vol. 2, p. 241, 2013.

[6]   D. R. Thévenot, K. Toth, R. A. Durst, and G. S. Wilson, "Electrochemical biosensors: recommended definitions and classification," *Biosensors and Bioelectronics,* vol. 16, pp. 121 - 131, 2 001.

[7]   "Nanotechnology-Enabled Sensing". *National Nanotechnology Initiative.* 2009. pp. 4–10. Retrieved 2017-06-22.

[8]   Y. Lu and J. Liu, "Fluorescence based biosensor," ed: U.S . Google Patents, *20100151579* 2011.

[9]   A. Ibraheem and R. E. Campbell, "Designs and applications of fluorescent protein - based biosensors," *Current Opinion in Chemical Biology,* vol. 14, pp. 30 - 36, 2010.

[10]   J. Gong, T. Zhou, D. Song, and L. Zhang, "Monodispersed Au nanoparticles decorated graphene as an enhanced sensing platform for ultrasensitive stripping voltammetric detection of mercury (II)," Sensors and Actuators B: Chemical, vol. 150, pp. 491 - 497, 2010.

Fabrication of Tips for Scanning Tunneling Microscopy using Electrochemical Etching and Mechanical Shearing

Saad Naeem[,1], Hamza Jamil[2] Munib Asim [3]

[1&2]*Ghulam Ishaq Khan Institute of Engineering Science and Technology*
[3]National Centre for Physics
Email address: [a)]saadlk33@gmail.com and [b)]hamzajamiltrd@yahoo.com

Abstract— Probe tip for scanning tunneling microscope (STM) is the most important part. The quality of image is strongly dependent on tip sharpness and shape. A tip with uniform conical shape and apex sharpness of only few nanometers is required to produce atomic scale images of sample surface. Tips for STM were fabricated using electrochemical etching and mechanical shearing. Parameters for electrochemical etching such as voltage, molarity of solution and etching cycle were varied to find conditions which produced good quality tips. Efficient and accelerated two step method was implemented to achieve upto 50% higher fabrication rates. Tips were produced using three different types of wires; Stainless steel, Remanium steel and Tungsten alloy. Shape and sharpness of tips were observed under optical microscope after etching. The quality of tips was further investigated by running STM scans on a gold thin film using the produced tips. Best quality images were obtained with tips etched at lower voltage of about 3.5V. Tungsten tips produced good resolution at 500nmx500nm scan area due to better sharpness and uniform shape. Mechanically produced tips were also able to give good STM images at higher scan area but failed to resolve objects below 2000nmx2000nm scan area. Approximate sizes of defects and grains on gold surface were also calculated using line profile graphs.

Keywords—Tips, STM, Probes, Electrochemical Etching

I. INTRODUCTION

The tip of the probe is the most critical part of the Scanning Tunneling Microscopy (STM). The resolution and quality of image is directly related to how sharp the tip is. Ideally, the apex of the tip should be made up of a single atom. The tip is made of a very thin conducting metallic, usually Tungsten or Platinum/Iridium, wire which has been processed to obtain a single atom thick apex. There are two most common methods used to produce the sharp tips; mechanical shearing and electrochemical etching. Etching of the wire occurs when a potential difference is applied to the tip of the wire inside the electrolyte solution. The fastest rate of etching is at the meniscus due to high concentration of OH ions. The OH ions tend to move towards the wire (anode) and are higher in concentration just below the meniscus [1]. The rate of etching is lower below the meniscus level because the produced metal ions tend to form a protective layer around lower part of the wire [1],[2]. A thermoplastic polymer sleeve is also used to insulate dipped wire to impede etching on the lower part. Etching requires an aqueous base due to the consumption of OH ions [1],[2]. The etching occurs till weight of the wire below the meniscus is equal or lower then tensile strength of the wire. Once the weight exceeds the tensile strength of wire the bottom part detaches and falls into the solution [1-3] .This is called drop off.

Experimental Setup for Electrochemical Etching

A. Experimental Setup

The wire was insulated by a polymer sleeve. Polymer sleeve was cut nearly perpendicular to its longitudinal direction to align it with meniscus level. The sleeve was heated and pressed to encapsulate wire in it. Graphite rod and wire were washed by acetone followed by distilled water before the reaction. Graphite rod and wire were dipped in 100ml solution containing NaOH in distilled water. Electrolyte solution was prepared by adding weighed amount of NaOH pallets on electric weight balance. The solution was stirred until it became clear. The solution was further ultrasonicated for 20 Minutes. AC supply was used connected with Digital Multimeter to check Voltage. The reaction was stopped as drop off occurred to prevent over etching of upper tip. After etching, SS tips were washed using Iso-Propanol and Distilled water. Due to higher etching times and rigorous etching, contaminations were seen on SS wires. Tungsten wire was etched very quickly and subtly, so no washing was required.

Three different materials of wires were used. They were tested at following parameters. The washed tips were observed under the optical microscope to analyze their shape and sharpness. All the images taken from optical microscope were at same magnification i.e. 160X. Common sample Gold was used for each wire to compare the results.

Table 2.3 Parameters tested on different wire materials

Material	Wire Diameter	Parameters
Stainless Steel	0.3mm	Molarity, Voltage
Tungsten	0.2mm	Molarity, Voltage
Remanium(Ni-Co) Stainless steel	0.35mm	Molarity, Voltage

B. *Mechanism for Variable step voltage*

The rate of etching is governed by voltage. Higher the voltage, more rigorous and fast will be the etching reaction. Instead of using constant optimal voltage, various steps of voltages were used. First fast etching was done using higher voltages, then voltage was decreased in steps as the necking proceeded. Fast etching rate is called course etching. It is done to achieve initial neck faster. After the neck is achieved, the voltage is decreased in steps to keep slow etching rate to improve sharpness and shape of the tip. This step is called fine etching as it decides the final sharpness of the tip. Variable step process saves time and produces sharp tips.[4].

II. RESULTS AND DISCUSSIONS

A. 3.1 Stainless Steel Wire

The wire used for first set of trials was as received Stainless steel. The composition of wire was unknown. The wire conductivity was also not known. The wire of diameter 0.3mm was of appreciable strength which was not easy to bend.

Table 3.1: Results of Experiments Conducted on SS Wire using Different Parameters.

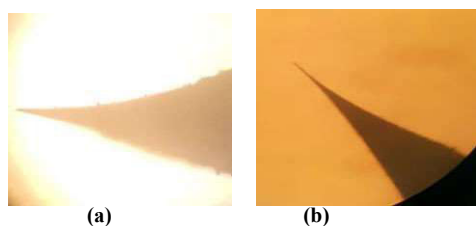| Molarity (M)	Voltage (V)	Drop off Time (mins)
2	4.5	210
2	7V(72min)->6V(122min)->8V(30min)	224
2	7.8(20 mins)->7V(53min)->7.8V(90mins)	163
2	7.5(90min)->6(30min)->5.5(60 min)->5(42min)->4(5min)	225
3	7.5(90min)->5.5(40min)->4.5(30min)->3.5	160
3	7.5(90min)->5.5(40min)->4.5(30 min)->3.5	160
3	7.5(90min)->5.5(40min)->4.5(30min)->3.5	160
3	6.3V(90min)->5.5(30min)->4(10min)->3.5	135
3	7.5(90min)->4.5(30min)	120

Fig 3.1.1 Optical microscope image for tips using SS wire in (a) Experiment 4 (b) Experiment 5

Higher the molarity, faster and rigorous was the rate of etching. By increasing the molarity of the solution the reaction time was decreased [4]. No significant effects on tip shape or sharpness were observed due to change in molarity. A difference of 47 minutes was observed between experiment 1 and 3 by applying variable voltage method. The results showed sharper tips by applying low voltage close to point of drop off.

B. *Remanium (Ni-Co) Stainless Steel*

Remanium is a orthodontic stainless steel alloy product from company named Dentaurum ®.

Table 3.2: Results of Experiments Conducted on Remanium SS Wire using Different Parameters.

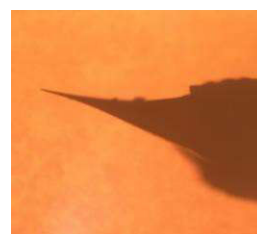| Molarity (M)	Voltage (V)	Drop off Time (min)
2.73	5(30min)->4.5(60min)->4(30min)->3.2	120
2.73	6V(30min)->7(15 min)->-4V(45min)	90
2.73	7(40 min)->3.5(20 min)	60

Fig 3.2.1 Optical microscope images for tip using Remanium SS wire Experiment 11

All three experiments were done on constant molarity i.e. 2.73 M. Only variable voltage method was applied. Different voltages were used for different time period and significant change in total time was observed. Total 60 minutes of time decreased between experiment 10 and 12(Table 3.2).

C. *Tungsten Wire*

The wire was tungsten alloy with unknown exact composition and least diameter.

Table 3.3: Results of Experiments Conducted on Tungsten Wire using Different Parameters.

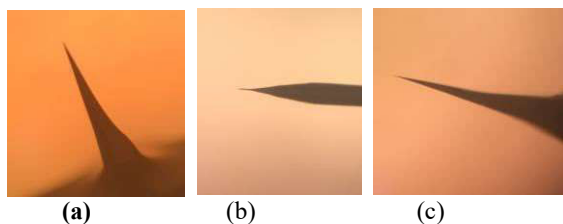| Molarity (M)	Voltage (V)	Drop off Time (min)
2	7(10 sec)->3.5(6sec)	0.26
2	3.5	2
2	3.5	1.6
1	3.6	3.8
1	3.6	3.9
1	3.6	3.9
1	3.6	3.1
1	3.6	3
1	3.6	3
1	3.6	3
1	3.6	3
1	3.6	3
1	3.6	3

Fig 3.3.11 Optical microscope images for tips using Tungsten wire in
(a) Experiment 14 (b) Experiment 15 (c) Experiment 17

Tungsten wire, due to its material characteristics etched very quickly. The quality of tips were also very good. In order to control reaction time and sharpness of tip, molarity of the solution was decreased from 2M to 1M. 4 out of 7 experiment were done at 1M solution.

Decrease in molarity resulted in increase in total reaction time i.e. total 2 minutes and 13 seconds of time difference was observed between experiment 15 and 16. The quality of tip was also enhanced by the change.

D. Effect of Wire Materials on Tip Fabrication

Tip material is one of the most important factor for STM imaging. As mentioned above, 3 different types of wire materials were used. The electrolyte solution was kept same for all three wires i.e. NaOH.

Stainless Steel wire took longest time to etch. If we keep all parameters constant, the SS wire was the slowest etching wire. On average it took more than 120 minutes to complete the reaction. The SS wire produced lowest quality of tips in terms of sharpness. Only 2 or 3 tips produced were sharp enough to conduct STM imaging.

Remanium (Ni-Co SS) wire etching time was in between SS and Tungsten wire. On average, Remanium wire took 90 minutes to etch. On optimum voltage settings it only took 60 minutes to etch. The quality of the tips were better as compared to SS. Most of the tips were sharp enough for imaging. The wire was mechanically very stable. The strength of this wire was highest compared to other two. It was straighten using two pliers before using. It also took a lot of time to straighten the wire.

Tungsten wire was the fastest to etch. Keeping constant settings, on average the wire etched only in 1.8-2 minutes. This shows that tungsten have highest reactivity with NaOH electrolyte. Tungsten tips were of best quality. Every produced tip was sharper than other two wires. Each tip was sharp enough for imaging. But, tungsten wires seem to be bent earlier than other wires during imaging. Mechanical strength of this wire was in between SS and Remanium.

The reasons behind etching times of each wire and their characteristics could be further explored. Composition of each wire was unknown. Spectroscopy data could be done to find out more about the properties of the wires and their behavior. The study on wire materials and characteristics were not conducted in this study.

E. STM Imaging

Only tungsten wire was used for sample imaging. Tungsten tips highlighted best quality as compared to other two wires. Remanium wire was unable to achieve optimum tunneling

due to oxide layer formation on the tip. The SS wire also resembled Remanium in terms of imaging. At higher scan areas i.e. 5000nm or 4000nm, macro surface defects like scratches and depressions were seen. The Fig. 3.5.1 shows a macro indent on the surface of gold sample at scan area of 5000nm.
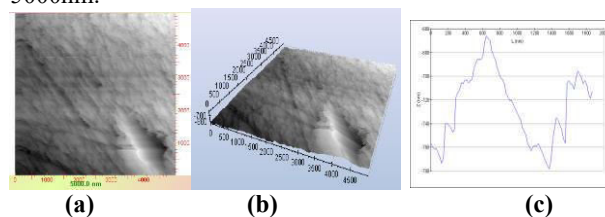

Fig 3.5.1: STM 2D (a) and 3D (b) image of depression in gold sample using tungsten tip at 5000nm. (c) Line Profile for depression at 5000nm.

The abrupt decrease in vertical distance Z towards more negative value in the line profile confirms the presence of indent. The approximate width of indent can be seen to be 800nm and a depth of about 60nm.

Another surface defect was observed when sample position was changed. In Fig 3.5.2, a micro crack was seen at 3000nm scan area. Multiple scratches can also be shown in the image. These surface defects give an indication of poor sample preparation, storage or handling.

Fig 3.5.2 STM 2D (a) and 3D (b) image of a scratch in gold sample using tungsten tip at 3000 nm. (c) Line Profile for scratch at 3000 nm.

The line profile of the crack was not unlike the depression discussed above. The approximate width of the crack is about 300nm and depth is 40nm.

Decreasing the scan area to about 1000nm, the grains were resolved. The image clearly shows grains aligned in a particular orientation and direction.

Fig 3.5.3 STM 2D (a) and 3D (b) image of grains in gold sample using tungsten tip at 1000nm. (c) Line Profile for 3 adjacent grains at 1000nm.

The above line profile was generated using three adjacent grains. The graph clearly shows the crests of three grains and depressions in each grain. The average grain size is 75nm. More zoomed grains can be seen in 500 nm area.
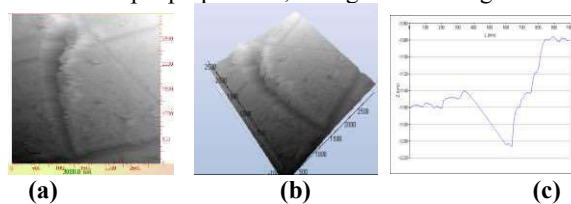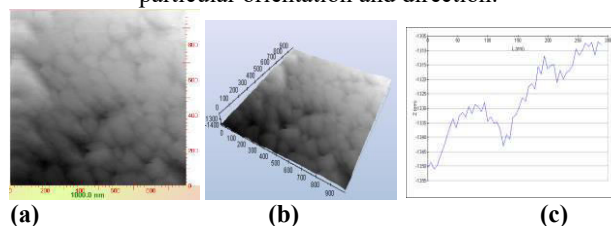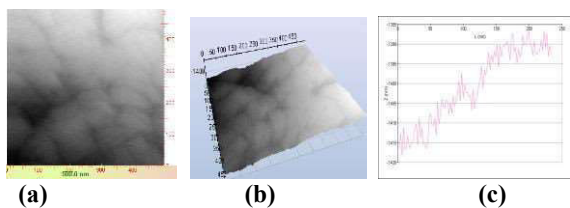
Fig 3.5.4 STM 2D (a) and 3D (b) image of grains in gold sample using tungsten tip at 500 nm. (c) Line Profile for grains at 500 nm.

The line gives information about two adjacent grains. The crest and troughs depict the changes in height profile. The grain, shows increase in Z. The distance between grains is below the surface, and hence appears darker in the image. The darkness in the image is translated as decline in the line profile. The approximate average grain size is 100nm.

a) *Mechanical Shearing*

The mechanical method was executed to gain insight of this process and to compare it with previous method.
Mechanical tips were fabricated using thin 0.2mm Tungsten wire and were tested for imaging.
The method is rather simple [7]. Tungsten wire was first straightened and then cleaned using acetone. One end of the wire was held using a straight plier and other was pulled using a wire cutter at an angle of 45 [8][1]The pulling action at angle of 45, is assumed to produce a point which can be used as tip for STM scanning.
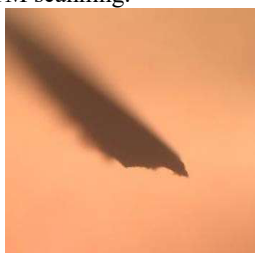

Fig 3.61: Optical microscope images of mechanically produced tip using 0.2mm tungsten wire.
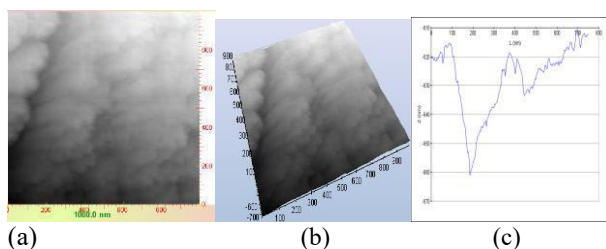
Fig 3.6.3: STM 2D (a) and 3D (b) image of a defect and grains in gold sample using tungsten tip at 2000nm. (c) Line profile of the defect.

.

Acknowledgement

References

[1]. A. N. Chaika, N. N. Orlova, V. N. Semenov, E. Yu. Postnova, S. A. Krasnikov, M. G. Lazarev. 17 January2014. "Fabrication of tungsten tips for High Resolution Scanning Tunneling Microscopy." Scientific Reports. Bernal, Rodrigo. 2008. "Reproducible Fabrication of STM Tips." 6.
[2]. Bing-Feng Ju, Yuan-Liu Chen, and Yaozheng Ge. 28 January 2011. "The art of electrochemical etching for preparing

tungsten probes with." AIP 9.
[3]. J. P. Ibe, P. P. Bey Jr., S. L. Brandow, R. A. Brizzolara,N. A. Burnham, D. P. DiLella, K. P. Lee, C. R. K. Marrian. 1990. "On the electrochemical etching of tips for scanning tunneling

microscopy." JVSTA.
[4]. D.Z. Joe, 1999. "Scanning Tunneling Microscopy (STM)." Mathur, Andra. August 2011. "Tungsten Tip Preparation." 4.
 [5]. Schaefer, Roland. 1989. Design and Constrution Of Scanning Tunneling Microscope. Pennsylavania: Carnegie Mellen. Valencia, Victor A. 2015. "Preparation of Scanning Tunneling Microscopy TIps." eCOMMONS

Comparative Analysis of DDOS Attacks Types With Attack Strategy

Mujahid Shah[1,a], Sheeraz Ahmed[2,b], Atif Ishtiaq[3,c], Malik Taimur Ali[4,d], Muhammad Junaid[5,e], Aasma Khan[6,f]

[1,2,3,4,6]Iqra National University, Peshawar, Pakistan
[1,2,5]Career Dynamics Research Centre, Peshawar, Pakistan
[2,5]Hajvery University, Lahore, Pakistan

email address: [a] mujahidshah51@gmail.com, [b] sheerazahmed306@gmail.com, [c] cray15@hotmail.com, [d] maliktaimur@hotmail.com, [e] engr.panwar@hotmail.com, [f] aasmakhan794@gmail.com

Abstract — **There is no doubt that the frequency and sophistication of DDOS attacks focused on numerous industries around the globe is in all likelihood to accelerate within the near destiny. DDOS attacks get the maximum attention while a firewall fails, carrier outage occurs, a website goes down or customers complain, however the upward thrust of quick, sub-saturating attacks introduces in addition dangers which shouldn't be disregarded or underestimated. Hackers have grown to become to this attack method as they can deliver larger and more state-of-the-art attacks, with little or no effort. In this paper, we display that which DDOS attack types use what sort of attack strategy to breakdown the target servers, service and network.**

KEYWORDS: **DDOS, BOTS, HTTP**

I. INTRODUCTION

Today's DDOS attacks are some distance greater deceptive and common than the existing ones. Indeed, the cyber danger has become more and more state-of-the-art and companies continue to be susceptible to DDOS due to the fact that various conventional protection infrastructure merchandise, which include firewalls and IPs, are not enough to mitigate current attacks. Proactive DDOS protection is a critical part in proper cyber security safety in opposition to lack of carrier and the capability for superior, multi-modal attack techniques. The arena WWW was designed in 1989. The first-ever website was developed in 1991. Currently there may be 1.2 billion web sites, huge wide variety and type of

online programs and web services are incorporated with one-of-a-kind web services like e-commerce, online banking, online buying, on line training, e-fitness care and crucial infrastructure business control structures (ICS) and so forth. Those day's industries are relying on and lot extra on internet linked devices and on-line internet program. Now a day the cyber attacker is particular professional and nicely equipped to convey a success attack of a very excessive stage on corporations and governments. Cyber-crime is big commercial enterprise now and the extent of information being stolen is massive. There are greater than 430 million specific classes of malware. It is a massive risk to authorities, organizations, customers and initiations around the arena.

Mainly, there are 3 varieties of DDOS attack.

1) Volume Based Attacks

These consist of ICMP floods, UDP flood and spoofed-packet flood. The attack's intention is to saturate the bandwidth of the attacked, is measured in bits per second (Bps).

2) Protocol Attacks

Consists of fragmented packet attacks, SYN floods, ping of death, SMURF DDOS and

additional. This kind of attack consumes real server sources, or those of intermediate conversation devices, collectively with firewalls and load balancers, and is measured in packets per second (PPs).

3) *Application Layer Attacks*

Includes low-and-gradual attack, get/post floods, attacks that focus on apache, windows or open BSD vulnerabilities and more. Comprised of seemingly legitimate and innocent requests, the motive of these attacks is to crash the internet server, and the importance is measured in Requests per second (RPs).
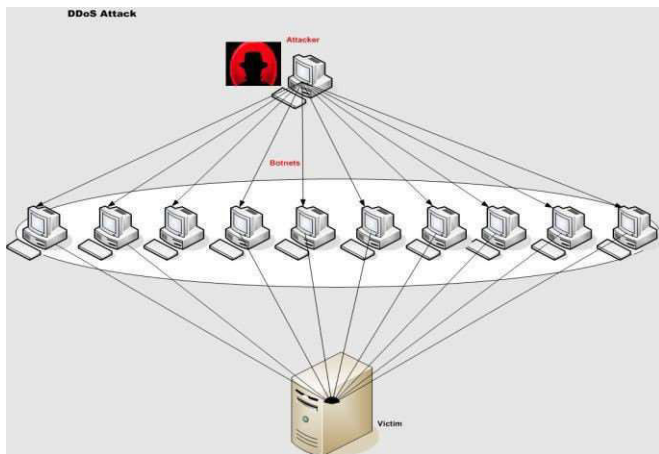
Fig 1 Distributed Denial of Service Attack

II.   LITERATURE REVIEW

In [1] the researchers focused to gain insights into the present day research on the detection of these attacks with the useful resource of comprehensively analyzing the selected primary research to reply a predefined set of studies questions. This survey also discusses numerous demanding situations that want to be addressed,

and informs readers with recommendations for possible destiny research commands.
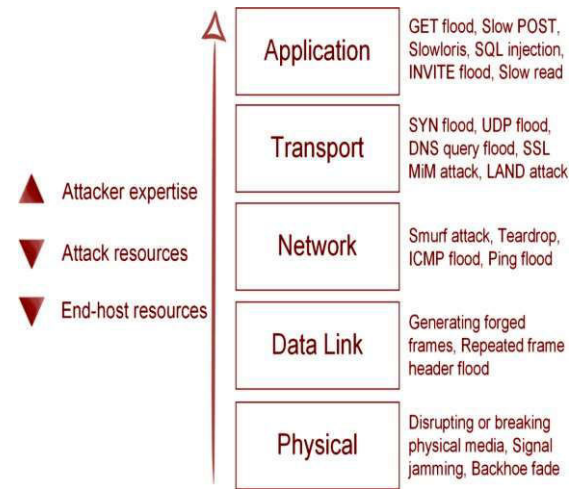
Fig 2 DoS attacks at different layers of network stack.

In [2] authors symbolize and evaluate the famous DDOS attack equipment and trace mills utilized by the attackers nowadays. The technical info provided would sincerely help the researchers to handpick the correct DDOS attack device and track generator for designing their real experiments so that their proposed DDOS defense techniques may be confirmed in a better way.
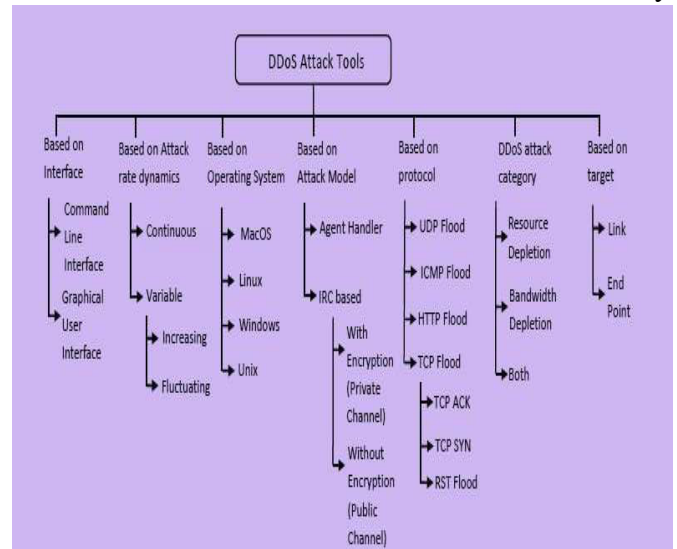
Figure 3: Taxonomy of DDOS attack tools

In [3] authors evaluated using the prevailing intrusion detection and prevention device to determine whether or not it is the super set of guidelines to mitigate the DDOS attacks on a network environment.

In [4] authors proposed the idea of auto encoder is accomplished, this is one of the deep mastering based totally fashions that learn deep useful abilities within the software program application layer DDOS attack dataset. The stacked auto encoder deep gaining knowledge of shape, is aimed to collect immoderate level competencies
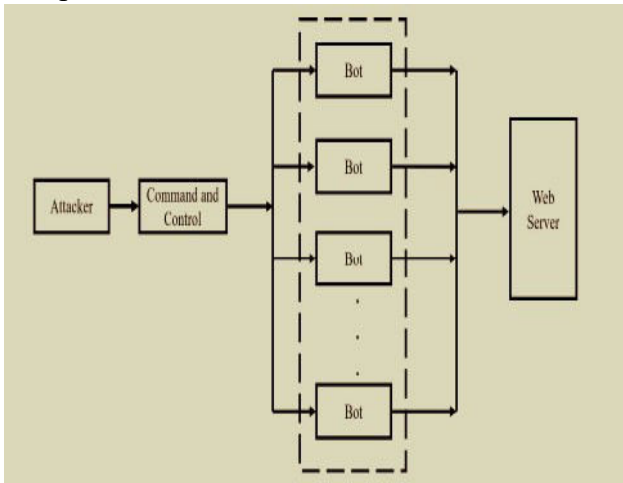
Fig. 4 Launching of AL-DDOS Attack

In [5] the authors developed an ontological framework to classify the proposed mitigation methods under three layers of protection-in-intensity prevent, come across and respond. Research executed each of these three pillars are further conceptualized primarily based on underlying layout and protection principles. The paper additionally proposes trade category schemes based on placements of goal additives, while supplying

qualitative analyses on research sports on DDOS
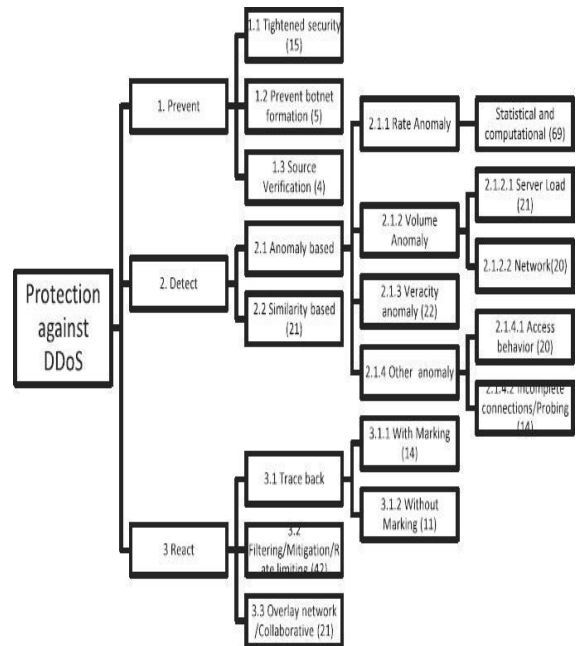
Fig. 5 Classification of DDOS Countermeasures

In [6] The researchers comprehensive survey of preventing DDOS attack recognize by data mining techniques with the use of identifying DDOS attack patterns and analyze patterns by machine learning algorithms. There are some leading machine learning algorithms used to recognize the DDOS attack such as k-nearest neighbor's algorithm (KNN), support vector machines (SVM), random woodland as well as naïve base. The paper also highlights open troubles, studies demanding situations and viable solutions on this place. The end result suggests the very best accuracy rate of preventing DDOS attack recognizing by way of records mining algorithms.
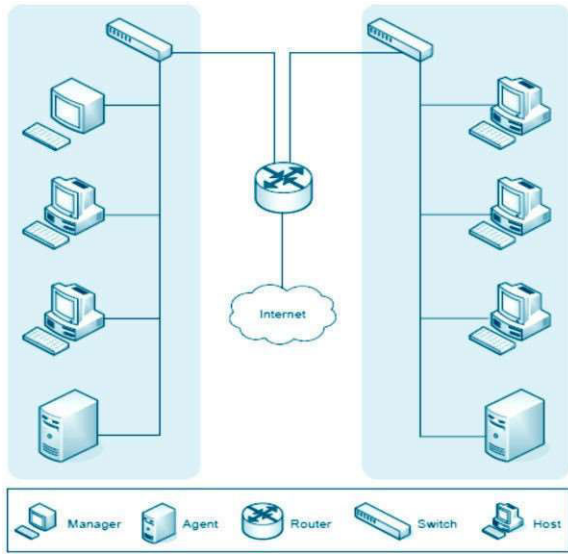
Fig 6 Increase of network traffic

In [7] the researchers used rank correlation measures, specifically, spearmen rank correlation (src) and partial rank correlation (%) to discover low-charge DDOS attacks. those measures are empirically evaluated the usage of three actual-lifestyles datasets. experimental outcomes show that each measures can electively discriminate valid trace from attack hint that P.C plays better than SRC in detection of low price DDOS attacks in terms of spacing between malicious and legitimate hint

In [8] authors presented recent techniques in coping with allotted denial of service attacks. DDOS attack is the fairly new sort of attack to cripple the supply of internet provider and resources. in the course of in the final decade, anomaly detection has drawn to the eye of many researchers to conquer the weak point of signature-primarily based is ids inside the detecting novel attacks, and KDD cup 'ninety nine is the commonly broadly used facts set for the

assessment of these structures.
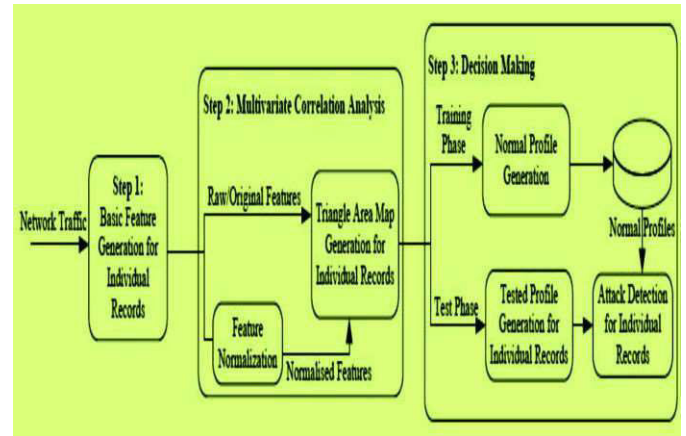
Fig 7 Framework of the proposed denial-of-service attack detection system

In [9] authors targeted on mitigating complicated gradual inquiring for http-DDOS attacks that focus on the PS. An evidence-of concept prototype is applied with simplified countermeasures and tested demission to.
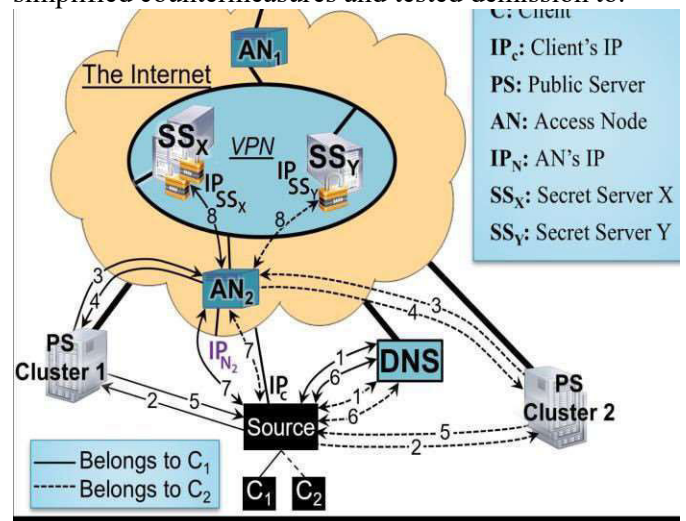
Fig 8 Architecture of the proposed method

In the [10] the writers http/2 implements novel compression techniques to reduce bandwidth, find out this compression technology to imparting know-how on its danger from DDOS, especially in http/2 to http/1 proxy deployment.

In the [11] the writers have been matching the risk resemblances between a cyber-attack, the DDOS, and

the mathematical prototypical of opportunity, levy walks. This contrast turned into goals to determine the validity of levy walks as a prototypical just like the DDOS probability features. This research bolstered the sminov revamp, for making fake gaining knowledge of with the related mathematics properties of actual strolls. This framework for simulated studying age may be applied for making abnormal supported likelihood thickness features. The smirnov alter turned into acclimated settled a cyber-indicated relate increasing ZCR price due to the fact the segment beneath examination suggests a much bigger movement.

In [12] authors experimented with green spoofed mitigation scheme (ESMS) which uses the TCP probing approach at the aspect of the bloom clean out take delivery of as real with version.
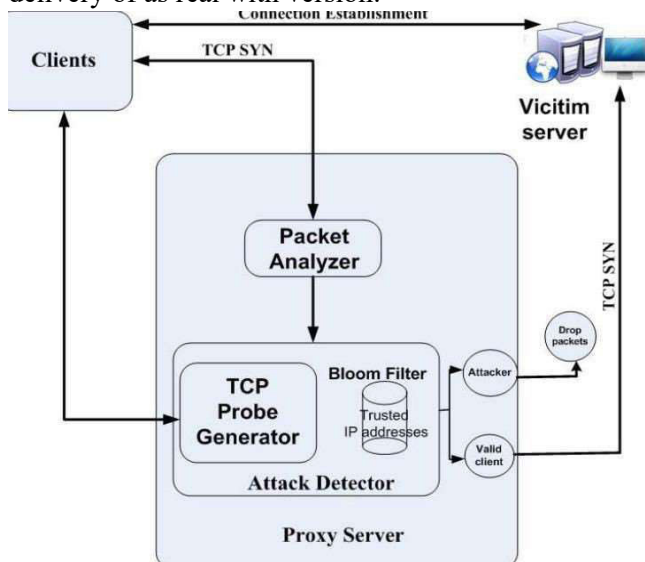
Fig. 9 Framework of the Efficient SYN spoofing Detection and Mitigation Scheme (ESDMS)

In [13] the researches proposed a technique that does not anticipate the cumulative bizarre returns to be normally distributed, as a substitute use the empirical distribution for checking out purposes. In most cases find no widespread effect on the stock returns however in cases wherein a DDOS attack creates an interruption within the offerings supplied to the consumer, we find a large bad effect.

III. Conclusion

In this paper, know DDOS attack type as associating with specific attack strategy the purpose is to show that which attack types using what kind of attack strategy to breakdown the target servers, services and network. In this research DDOS attacks are categorized based on attack type and attack strategy. We have mentioned that the different detection techniques focused different type of attack as highlighted in table 1 below. Some techniques consider attack strategy and some has missing. This paper will be a short introduction to the researchers that the understand attack strategy who want to work further in this area.

REFERENCES

[1] Singh, Karanpreet, Paramvir Singh, and Krishan Kumar. "Application layer HTTP-GET flood DDOS attacks: Research landscape and challenges." *Computers & Security* 65 (2017): 344-372.

[2] Behal, Sunny, and Krishan Kumar. "Characterization and Comparison of DDOS Attack Tools and Traffic Generators: A Review." *IJ Network Security* 19, no. 3 (2017): 383-393.

[3] Jiang, Muhui, Chenxu Wang, Xiapu Luo, MiuTung Miu, and Ting Chen. "Characterizing the Impacts of Application Layer DDOS Attacks." In *Web Services (ICWS), 2017 IEEE International Conference on*, pp. 500-507. IEEE, 2017.

[4] Yusof, Mohd Azahari Mohd, Fakariah Hani Mohd Ali, and Mohamad Yusof Darus. "Detection and Defense Algorithms of Different Types of DDOS Attacks." *International Journal of Engineering and Technology* 9, no. 5 (2017).

[5] Yadav, Satyajit, and Selvakumar Subramanian. "Detection of Application Layer DDOS attack by feature learning using Stacked AutoEncoder." In *Computational Techniques in Information and Communication Technologies (ICCTICT), 2016 International Conference on*, pp. 361-366. IEEE, 2016.

[6] Stefanidis, K., and D. N. Serpanos. "Countermeasures Against Distributed Denial of Service Attacks." In *Intelligent Data Acquisition and Advanced Computing Systems: Technology and Applications, 2005. IDAACS 2005. IEEE*, pp. 439-442. IEEE, 2005.

[7] Bandara, K. R. W. V., T. S. Abeysinghe, A. J. M. Hijaz, D. G. T. Darshana, H. Aneez, S. JKaluarachchi, K. V. D. L. Sulochana, and Mr DhishanDhammearatchi. "Preventing DDOS Attack Using Data Mining

Algorithms." *International Journal of Scientific and Research Publications* 6, no. 10 (2016): 390.

[8] Ain, Arindom, Monowar H. Bhuyan, Dhruba K. Bhattacharyya, and Jugal K. Kalita. "Rank Correlation for Low-Rate DDOS Attack Detection: An Empirical Evaluation." *IJ Network Security* 18, no. 3 (2016): 474-480.

[9] Devare, Avinash, Monika Shelake, Varsha Vahadne, and Pratibha Kamble4 Banu Tamboli. "A System for Denial-of-Service Attack Detection Based on Multivariate Correlation Analysis." *International Research Journal of Engineering and Technology (IRJET)* 3, no. 04 (2016).

[10] Eid, Mohamad Samir A., and Hitoshi Aida. "Secure Double-Layered Defense against HTTP-DDOS Attacks." In *Computer Software and Applications Conference (COMPSAC), 2017 IEEE 41st Annual*, vol. 2, pp. 572-577. IEEE, 2017.

[11] Beckett, David, and Sakir Sezer. "HTTP/2 Tsunami: Investigating HTTP/2 proxy amplification DDOS attacks."

In *Emerging Security Technologies (EST), 2017 Seventh International Conference on*, pp. 128-133. IEEE, 2017.

[12] Gonzalez, Jesus David Terrazas, and Witold Kinsner. "Zero-crossing analysis of Lévy walks for real-time feature extraction: Composite signal analysis for strengthening the IoT against DDOS attacks." In *Cognitive Informatics & Cognitive Computing (ICCI* CC), 2016 IEEE 15th International Conference on*, pp. 143-153. IEEE, 2016.

[13] Kavisankar, L., C. Chellappan, S. Venkatesan, and P. Sivasankar. "Efficient SYN Spoofing Detection and Mitigation Scheme for DDOS Attack." In *Recent Trends and Challenges in Computational Models (ICRTCCM), 2017 Second International Conference on*, pp. 269-274. IEEE, 2017.

Table 1: DDOS attack Type and attack Strategy

Attack	DDOS Type	Attack Strategy
In [3] Application Layer	Volume Based Attacks	Slowloris
In [4] Network Layer	Protocol Attacks & Volume Based Attacks	Not mention
In [5] Application Layer	Protocol Attacks	Asymmetric
In [7] Network Layer	Protocol Attacks & Volume Based Attacks	Not mention
In [8] Network Layer	Protocol Attacks & Volume Based Attacks	low-rate and High rate
In [10] Application Layer	Application Layer Attacks	low-rate and High rate
In [11] Application Layer	Application Layer Attacks	Not mention
In [13] Network Layer	Protocol Attacks	Not mention

A Comprehensive Survey on Demand Side Management Techniques for Home Appliances Scheduling

Ali Raza[1,a], Sheeraz Ahmed[2,b], NajeebUllah[3,c], Asif Jan Marwat[4,d], Abdul Hanan[5,e]

[1,3,5]*CECOS University, Peshawar, Pakistan*
[2,4]*Iqra National University, Peshawar, Pakistan*

email address: [a] aliraza.edu@gmail.com, [b] sheerazahmed306@gmail.com, [c] najeeb@cecos.edu.pk,
[d] asifjanwarwat@yahoo.com, [e] hanan@cecos.edu.pk

Abstract -- To improve the appliances' energy control management, energy consumption reduction, balancing the electricity demand and supply in real time, reducing the expenditure of electricity infrastructure and enhance the feasibility of distributed energy resources and storage, Demand Side Management (DSM) is considered as a very important energy management tool within a smart grid. In order to achieve energy balancing or additional services, DSM is a way to take advantage of demand elasticity. DSM could offer significant environmental, economical, and reliability benefits. Taking clients into consideration, DSM facilitates them by decreasing electricity charge by effective as well as preservation techniques. Further improvement in cooperation to client satisfaction as well as DSM could very well be accomplished through establishing Distributed Energy Storage (DES), along with Distributed Energy Generation (DEG), as well as Distributed Energy Generation and Storage (DEGS) systems.

Keywords— Demand Side Management, Appliances Scheduling, Peak-to-average ratio, Energy Management

I.   INTRODUCTION

Electricity acts as a major concern in one's lives, unfortunately for Pakistan the problem is out there, since more than one decade it is affecting the development and economical growth of Pakistan. Pakistan is spending billions of dollars every year by importing oil to meet the energy generation requirements. 1% of the energy is generated with two sources which are solar, wind power, hydel whereas for non-renewable resource nuclear, fossil fuels (Furnace oil, natural gas, charcoals) are used [1]. In order to satisfy all energy demand from customers, the grid capacity should be designed in such a way that it satisfy the customers peak power demand rather than their average power demand which leads to installing new power generation and transmission infrastructure. DSM offered through controlling user's energy consumption by means of aiming to minimize Peak-to-Average Ratio (PAR).

The purpose of PAR is to measure how much energy is used and how it effects the system when it comes to efficiency and reliability. The energy used at peak time decrease the efficiency of electricity generation of the system, and vice versa. A number of SG readings revealed substantial drop-off through DSM with respect to cost. Such drop off results in reducing the overall capital cost investments, improved usage of SG resources, and constant decline in user's bills for electricity [2]. Thus,

1

DSM is the key component of future SG which helps in controlling the energy consumption used by the customer. Electric Power Research Institute introduced DSM in the mid-eighties looking at it now it is more used due to the integration of information and communications technology in the form of Smart Grid.

With the development of new efficient low cost storage devices, user is able to efficiently store electricity for long periods of time. Furthermore, by using such devices, users can charge energy for their energy storage devices at low demand periods, and then use that energy to supply for home devices at peak electricity consumption periods [3]. As an involvement, of such storage equipment at residential unit turn out to be the major sources in uttermost load reduction and saving energy for upcoming SG.
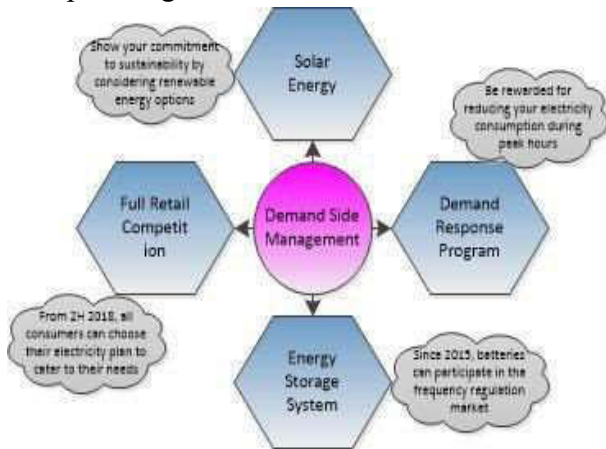
Figure 1: Demand Side Management (DSM)

Although, people know DSM, it can also be known as Demand Side Response (DSR) is somewhat modification of different methods like financial incentives, or behavioral changes from educational point of view. In a smart grid, DSM is a mechanism, to make more informed decisions about reducing their bills by allowing producers to reduce peak loads by encouraging consumers [4]. The main purpose of DSM is to

enable and encourage the consumers to use less energy in peak hours and more at off-peak time such as night time and weekends thus it does not meant consumer should not use energy at peak time but to reduce the usage, for example a new DSM application to help the operators to save energy at off-peak time and use the same saved/stored energy at peak time by balancing the intermittent generation from wind and solar units. It is illustrated in the Figure 1 that how the consumers manage the power usage.

To make better utilization of available generating power capacity, DSM programs are implemented, without installing new power generation infrastructure [5]. The process is defined in two methods: the first method of DSM is that the consumer can reduce the power usage by scheduling the usage of electricity whereas the second method is the consumer can shift the energy that is stored and will be able to use it at peak to non-peak hours.

DSM helps in reducing the overall load on the electric network. DSM contains of all those activities that administer time of energy usage so as to suspend investment in new electrical installations [6]. DSM brings many benefits; it enables consumers to store power for longer period of time. User will be able to store energy at off-peak time which then can be used at peak time resulting in reduction in expense and for the management side reduction of dependency on expensive imports or energy resources making environment cleaner. This will encourage consumer to shift the usage of their high energy consumption devices to off-peak hours by making schedules on energy consumptions.

DSM usually incorporate programs being implemented through services which can be used to schedule the electricity usage of clients. This can be performed either by controlling the load

2

contracts or indirectly by incentive programs. A further consideration, regarding minimization in bills of electricity as well as behave like alternate power supplier in situations of power disruption from power plants is low-cost battery storage systems [2]. In DSM, the estimating components and direct control methodologies are utilized by the vitality providers to influence buyers' utilization practices and reshape the aggregate load. The season of-utilization valuing methodology sets diverse costs among the day to urge buyers to move their request to off-top hours. Like the season of-utilization estimating, the basic pinnacle valuing applies a prespecified high cost among the assigned basic pinnacle time frames. The continuous valuing receives the time-fluctuating cost by the discount cost of power and the cost of energy age to empower purchasers to alter their request in light of supply. It is by and large the adjustment of shopper's request of power through different strategies, for example, money related impetuses and customer instruction.

Whether it be investments in transmission or distributed networks DSM plays a huge role. It completely works on electricity that the control system provides which is cost effective and also beneficial to the environment. DSM works like a control unit in the smart grid to balance the course of energy demand and supply between energy suppliers and users. In order to establish the efficient and real-time connection between energy suppliers and users, such balance is implemented by merging the energy management with reliable communication [7]. The main purpose of using DSM is to enable consumers to use electricity at off-peak time also store it which helps in usage of that same energy which is stored in peak hours.
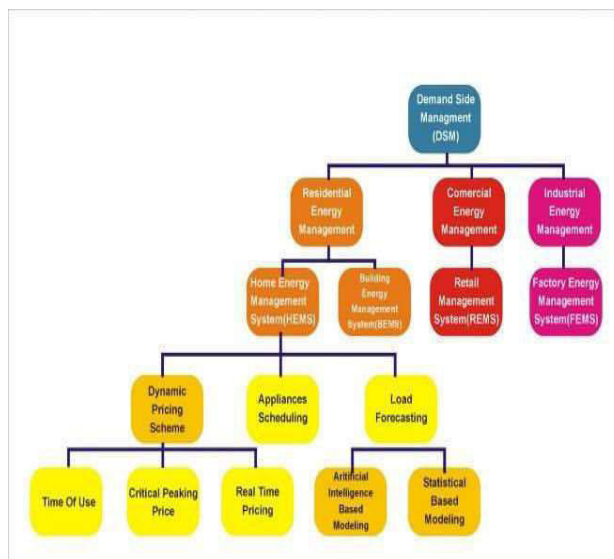
Figure 2: DSM Techniques

II. TECHNIQUES OF DSM

Many people are working on the technique of DSM for home appliances scheduling to reduce the energy cost as shown in the Figure 2. In the recent past years, a lot of work has been done on DSM. So some of the popular techniques, we have considered, which are going to be presented in the following section.

2.1 Distributed Energy Storage on GA[8]

In this, approach known as a distributed energy storage planning based on Game Algorithm (GA) in DSM is proposed. For DSM smart grid is an important component as it provides control energy supply and demand process in smart grid between energy supplier and user. To enable DSM, first there is a need of construction of reliable and efficient communication infrastructure in smart grid based on cognitive radio technology. Many connecting nodes over an entire region need to be cover by smart grid communication infrastructure. Different studies showed that for efficient DSM schemes method known as game theory can be applied. In various studies, the

3

main focus is on storage units and scheduling of distributed energy generation. In a proposed model several consumers are considered having a cognitive radio based smart grid communication system. As communication is bi-directional so from smart appliances information of load can be collected in forward direction and after that it sends them to the destination. Similarly, information can be send back to smart appliances. For scheduling consumption of energy, every consumer have a smart meter (SM) for exchanging information with the central units. If one day is divided into H slots and H = 24, means 1 time slot = 1 hour, N = set of users, n = numbers of users, $g_\square^h$ = amount of energy generated, $s_\square^h$ = amount of energy stored and the total user load id given by the formula

$$l_\square^h = \sum_{a \in A_n} e^h + s_{\square,\square}^h - g_\square^h$$

Maximum and minimum energy of appliance is express by the given formula

$$e_{min,n,a} \leq e^h_{n,a} \leq e_{max,n,a.}$$

Where maximum and minimum power of storage device is shown by the formula

$$S_{min,n} \leq \sum_{t=0}^{h} s^t_n \leq S_{max,n} \qquad \forall h \in \{0, \dots, H\},$$

Distributed storage unit may be considered as power producer and power consumer. In the given game theory model, Nash equilibrium is achieved by adjusting energy consumption which not only reduce the peak load in grid but also helpful for user's privacy and their interest. So result shows that the technique is more efficient than previously presented techniques.

2.2 Load Management Algorithm[9]

In this technique, authors have proposed scheduling scheme by means of load management algorithm. Many existence schemes are unable to handle these large

appliances. For connection permission, a request is send by the appliances to DSM controller and within each time slot and through minimization problem entire pattern is provided. The proposed technique is applied on hostel where residential region consist controllable appliances more than 600 having 8 types and different power rate. Result proved that, cost is minimized due to such technique. Hence, this technique is efficient for managing huge quantity of controllable loads.

2.3 Energy Consumption Scheduling[10]

For enabling DSM in future smart grid, energy consumption scheduling is presented by the authors. Here communication is bi-directional via LAN. Every user has a smart meter and users can interact with each other, in smart meters ECC units are set in. The intend behind this technique is to cut customer's electric bill which is possible through changing appliances operation to off-peak time. Without thinking about peak time, consumer may use appliances any instant and ECC unit recommends a suitable time to the customer. So the proposed technique reduces peak demand and cost of energy.

2.4 DSM Algorithm[11]

DSM algorithm is proposed by the authors using GA, which is a load shifting scheme. Basic aim is to reduce total cost and to minimize Peak to Average Ratio (PAR). Smart grid is one of the well-known system because of its distinctive features and dynamic pricing. Time of Use (TOU), Extreme Day Pricing (EDP), Real Time Pricing (RTP) and Day Ahead Pricing (DAP) are some pricing schemes used in DSM. As nature of electricity is irregular so on different time slot, RTP signal may vary but having constant value at that particular slot. For

4

minimizing user's electricity bill and PAR formula is given as follows.

$$\sum_{t=1}^{24}\sum_{a=1}^{n}\sum_{b=1}^{m} X_{ab}(t)*E_{ab}(t)*E_p(t)$$

$$\sum_{t=1}^{24}\sum_{a=1}^{n}\sum_{b=1}^{m}X_b(t)*E_b(t)\leq P(t)$$

$$M_a = 24 - h_a$$

Results show that the technique reduces PAR, total cost and efficiently control loads in commercial, industrial, and residential areas. Moreover, reliability is increased due to low load demand during peak time.

2.5 Comparison of DSM Techniques[12]

In this paper, two DSM techniques have been compared, proposed by two different authors. One has presented daily and other has presented hourly mechanism. Both appliances and power grid is connected with Energy Consumption Scheduler (ECS). For reducing cost, each ECS runs an algorithm for scheduling local consumption. Here every user has to give part of full amount proportional to energy consumed per day. Individual bills are minimizes iteratively by every ECS. Then load information is pass on to the system and all further updates about load are given to all ECS. Consumer's constraints are given by the formula.

$$\sum_{h\in H}{}_{na}^{h} = E_{na,} \ \forall \alpha \in A_n$$

In hourly billing method cost is divided between users according to load at this particular time. Formula is given below.

$$b_{\square}^{HP}(x_{\square},x_{-n}) = \sum_{h\in H}\frac{_{-n}^{-h}}{\sum_{m\in N}\frac{m}{\square}}\mathcal{C}\ (l^h)$$

According to the simulation results as compare to other techniques, hourly mechanism has three times less fairness indicator and small loss of efficiency has no effect.

2.6 EHEMC Technique[13]

In this research, authors have presented an efficient home energy management controller (EHEMC) method for minimizing peak to average ratio and electric cost. Now a days demand response (DR) is considered as a crucial DSM activity. DR is a plan for user so that users can consume energy in response to energy cost. Architecture of presented HEMS consists of smart meter, in-home display, utility, advanced metering infrastructure (AMI), and market pricing. EHEMC system is responsible for scheduling energy utilization profile. Total appliances consumption of one day is represented by the formula.

$$E_{c,T_l} = \sum_{t=1}^{T}(\sum_{j=1}^{N} E_{(aj,l)})\forall \ t \ \varepsilon \ T, \alpha \epsilon A$$

Home appliances are divided into three types. First type of appliances is those which are regularly operated and energy utilized in one day is represented as:

$$\delta R_s, T_l = \sum_{t=1}^{T}(\sum_{R_a\in A_n} \delta^t R_a * \delta(t))$$

Second type is shiftable appliances and energy consumption formula is given as:

$$\delta S_a, T_i = \sum_{t=1}^{T}(\sum_{S_a\in A_n} v_{\square}^t * \delta(t))$$

Elastic or flexible is a third type of appliances their energy profile are adjustable. Formula is give below.

$$\delta\varepsilon_a, T_l = \sum_{t=1}^{T}(\sum_{\varepsilon_a\epsilon A_n} \mu_{\square}^t * \delta(t))$$

As primary goal is to minimize cost, results proved that the technique has achieved its goal by reducing cost as compare to its unscheduled cost.

5

2.7 Game Theoretical Framework for DSM[14]

It is essential to set up new power generation and communication infrastructure to satisfy the peak demand. For solving such problem DSM programs have presented. Devices which are more efficient can stock up more electricity. Furthermore, users can use the stored electricity during peak utilization time. In this game theoretical framework is applied to model DSM problem. Moreover, pricing approach is used by the providers, by which customers can shift power consumption to low demand time.

Furthermore, there are three cases in which load profile of each user is divided. First case with no DSM program, second case is DSM without battery and third case is DSM with battery. Results show that during third case reduction of peak load is more as compare to second case. Furthermore, in presented algorithm optimal solution is considered for scheduling. This paper showed that PAR can be reduced using DSM and can be beneficial for smart grid system but it is not mentioned that how this method is good for larger systems. Secondly, in first model user cannot sell back energy to the providers.

2.8 Optimization for Scheduling[15]

In this paper, for building demand response authors presented mechanism in which data structure, machine learning and optimization are merged together. By dividing appliances into three different groups demand response is developed on the bases of proposed mechanism. For residential houses home heating, ventilation, and air conditioning (HVACs) is considered initially for reducing electric bill cost. Optimization formula is given below.

$$C = \sum_{i=1}^{24} pi \cdot Q_i$$

$$0 \leq Q_i \leq Q_{max}, T_i^{min} \leq T_i \leq T^{max}, i = 1, \ldots, 24$$

Whereas for HVAC with fixed load demand response is given as

$$C = \sum_i pi \cdot (Q_i^{HVAC} + Q^{fixed}) \leftrightarrow C$$

$$= \sum_i pi \cdot Q_i^{HVAC}$$

Formula obtained after considering all types of loads is given as

$$Minimize: \quad c = \sum_i pi \cdot (Q^{HVAC}_i + Q^{fixed}_i + Q^{deferrable})$$

$$Subject\ to: \quad 0 =\leq Q^{HVAC}_i \leq Q^{max}, T^{min}_i \leq T_i \leq T^{max}_i$$

Algorithm proposed, showed the generation of optimal DR policy and learning process of HVAC power consumption. Results obtained through proposed technique showed that presented learning based DR system is most optimal and efficient as compared to other DR techniques.

2.9 DSM for Cost Reduction[16]

In this research, authors have proposed a DSM system for decreasing electric cost and increasing comfort level of consumers. The technique comprised of new logarithmic cost function along with the facility of selling back the excess electricity to the grid. The presented technique is developed by converting the problem from constrained version to unconstrained version through segmentation based penalty process. In the presented model consumer's electric needs are obtained. Local area network (LAN) is a medium of communication between consumers and utility company where as through wide area network (WAN) communication take place between utility company and wholesale market. Smart meters are used for transferring of data and for

6

activities like monitoring, controlling and managing of appliances. For scheduling energy consumption scheduler is used. The main aim of presented method is to get solution which is socially optimal. So optimization formula is given as:

$$\min_{Y} J^{glob}(Y) = \sum_{k \in K} J_k(y_k) \; s.t., 1 \leq Y \leq u,$$
$$q \leq BY \leq b, r \leq AY \leq e, o \leq SY \leq d$$

Next constrained global minimization problem is converted to unconstrained version for solving DSM through diffusion approach. Formula for optimization problem is given below.

$$\min_{y_k, k \in K} j^{glob}(Y) \triangleq \sum_{k=1}^{K} J_k(y_k),$$
$$s.t. \; y_1 \in \aleph_1, \dots, y_K \in \aleph_K$$

So the load demand curve obtained

through implementing proposed technique showed that fluctuation is minimized and PAR is reduced 29% per day.

2.10 DSM and Power Utilization for Appliances[17]
The main focus of authors in this research is on demand side energy and power utilization scheduling for different appliances (shift able, throttle able and essential). As compared to traditional grid system, SG distributes information and electricity automatically in two way flow. So objective of proposed method is, for each kind of appliances, optimal response should be attained. For reducing cost, optimal response in initiated which also Figure out operation time for shift able appliances and power consumption for throttle able appliances. For collecting preference details, customer's demand and distribution of electricity, every customer is facilitated with a smart meter. For essential appliances such as lamps and TV's, power

supply is continuous whereas operation time can be delayed for shift able appliances and for throttle able devices at time of fixed operation energy utilization can be adjusted. For load demand description power consumption can be defined by the following three scheduling vectors:

$$e_{n,i} \triangleq [e_{n,i}^1, \dots, e_{n,i}^t, \dots, e_{n,i}^T],$$
$$e_{n,8} \triangleq [e_{n,8}^1, \dots, e_{n,8}^t, \dots, e_{n,8}^T],$$
$$e_{n,r} \triangleq [e^1, \square, \cdot, e^t, \cdot, \square, e^T], \square,$$

Optimization problem is solved for n consumers using formula

$$\min_{e_n \in E_n} \frac{1}{2} e_n' Q_n e_n$$
$$s.t. \; A_n e_n \leq b_n$$

Where as its dual function is given as:

$$q(\mu) = \inf_{e_n \in E_n} \left\{ \frac{1}{2} e_n Q_n e_n + \mu'(A_n e_n - b_n) \right\}$$

Obtained results show that presented distributed algorithm is efficient for reducing cost. Total price can also be reduced by power adjustment of throttle able appliances and through scheduling shift able appliances.

III.   CONCLUSION

DSM is a vital instrument for permitting extra productive usage of energy resources available for country. Like, DSM coupled to power lattice could lessen energy crunches, minimizing blackouts and increase lattice unwavering quality, reduce imports dependency on expensive fuels, diminish cost of electricity, and undermine ecological discharges. Comparable benefits could be achieved through DSM techniques, when attached to various categories of energy utilization. In this manner, DSM offers critical economic as well as environmental benefits.

7

REFERENCES

[1] Said, GulNabi, Sheeraz Ahmed, Kashif Ali Awan, and AmjadKhattak. "Electrical Energy Regulation and Load Management for addressing Power Crisis in Pakistan."In Proceedings of 2nd International Multi-Disciplinary Conference, vol. 19, p. 20. 2016.

[2] Shaaban, M. F., A. H. Osman, and M. S. Hassan. "Day-ahead Optimal Scheduling for Demand Side Management in Smart Grids." In Modelling Symposium (EMS), 2016, European, pp. 124-129.IEEE, 2016.

[3] Nguyen, Hung Khanh, Ju Bin Song, and Zhu Han. "Demand side management to reduce peak-to-average ratio using game theory in smart grid." In Computer Communications Workshops (INFOCOM WKSHPS), 2012 IEEE Conference on, pp. 91-96. IEEE, 2012.

[4] Wijaya, Tri Kurniawan, Thanasis G. Papaioannou, Xin Liu, and Karl Aberer. "Effective consumption scheduling for demand-side management in the smart grid using non-uniform participation rate." In Sustainable Internet and ICT for Sustainability (SustainIT), 2013, pp. 1-8. IEEE, 2013.

[5] Rasheed, Muhammad Babar, Nadeem Javaid, Ashfaq Ahmad, Mohsin Jamil, Zahoor Ali Khan, Umar Qasim, and Nabil Alrajeh. "Energy optimization in smart homes using customer preference and dynamic pricing." Energies 9, no. 8 (2016): 593.

[6] Gaur, Gaurav, Nishtha Mehta, Rin tu K hann a, and SandeepKaur. "Demand side management in a smart grid envir onment." In Smart Grid and Smart Cities (ICSGSC), 2017 IEEE International Conference on, pp. 227-231. IEEE, 2017.

[7] Wang, Kun, Huining Li, Sabita Maharjan, Yan Zhang, and Song Guo. "Green Energy Scheduling for Demand Side Management in the Smart Grid." IEEE Transactions on Green Communications and Networking 2, no. 2 (2018): 596-611.

[8] Ullah, M. N., Nadeem Javaid, I. Khan, Anzar Mahmood, and M. U. Farooq. "Residential energy consumption controlling techniques to enable autonomous demand side management in future smart grid communications." In Broadband and Wireless Computing, Communication and Applications (BWCCA), 2013 Eighth International Conference on, pp. 545-550. IEEE, 2013.

[9] Gaur, Gaurav, Nishtha Mehta, Rintu Khanna, and Sandeep Kaur. "Demand side management in a smart grid environment." In Smart Grid and Smart Cities (ICSGSC), 2017 IEEE International Conference on, pp. 227-231. IEEE, 2017.

[10] Wang, Kun, Huining Li, Sabita Maharjan, Yan Zhang, and Song Guo. "Green Energy Scheduling for Demand Side Management in the Smart Grid." IEEE Transactions on Green Communications and Networking 2, no. 2 (2018): 596-611.

[11] Rajarajeswari, R., K. Vijayakumar, and Ashutosh Modi. "Demand side management in smart grid using optimization technique for residential, commercial and industrial load." Indian Journal of Science and Technology 9, no. 43 (2016).

[12] Jacquot, Paulin, Olivier Beaude, Stéphane Gaubert, and Nadia Oudjane. "Demand side management in the smart grid: an efficiency and fairness tradeoff." In Innovative Smart Grid Technologies Conference Europe (ISGT-Europe), 2017 IEEE PES, pp. 1-6. IEEE, 2017.

[13] Safdarian, Amir, Mahmud Fotuhi-Firuzabad, and Matti Lehtonen. "Optimal residential load management in smart grids: A decentralized framework." IEEE Transactions on Smart Grid 7, no. 4 (2016): 1836-1845.

[14] Ma, Jinghuan, He Henry Chen, Lingyang Song, and Yonghui Li. "Residential load scheduling in smart grid: A cost efficiency perspective." IEEE Transactions on Smart Grid 7, no. 2 (2016): 771-784.

8

[15]   Yue, Siyu, Di Zhu, Yanzhi Wang, and Massoud Pedram. "Distributed load demand scheduling in smart grid to minimize electricity generation cost." In PES General Meeting| Conference & Exposition, 2014 IEEE, pp. 1-5. IEEE, 2014.

[16]   Rahim, Muhammad Hassan, Adia Khalid, Ayesha Zafar, Fozia Feroze, Sahar Rahim, and Nadeem Javaid. "A Hybrid Technique for Residential Load Scheduling in Smart Grids Demand Side Management." In International Conference on Emerging Internetworking, Data & Web Technologies, pp. 1007-1017. Springer, Cham, 2018.

[17]   Zhang, Dong, Shuhui Li, Min Sun, and Zheng O'Neill. "An optimal and learning-based demand response and home energy management system." IEEE Transactions on Smart Grid 7, no. 4 (2016): 1790-1801.

9

Packet Size Optimization Techniques and Challenges for Wireless Body Area Networks

Sheeraz Ahmed[1,a], Muhammad Saqib[2,b], Muhammad Aadil[3,c], Mukhtar Ahmed[4,d], Muhammad Junaid[5,e]

[1,2,3] *IQRA National University, Peshawar, Pakistan*
[1,5] *Hajvery University, Peshawar, Pakistan*
[4] *Islamia College University, Peshawar, Pakistan*

email address: [a)] sheerazahmed306@gmail.com, [b)] saqibbcsian@gmail.com, [c)] m_aadil@hotmail.com,
[d)] mukhtaricp@gmail.com, [e)] engr.panwar@hotmail.com

Abstract—In WBANs, longer packets may encounter higher misfortune rates because of unforgiving channel conditions. Then again, shorter packets may experience the ill effects of more prominent overhead. Thus, the ideal packet size must be selected to different execution measurements of WBANs. According to the latest research, numerous methodologies have been suggested to decide ideal packet size in WBANs. Literature discussed in this paper primarily focuses on packet size optimization in a particular application or sending condition. This paper discusses the current trends and practices on packet size optimization for wireless body area networks to encourage the researchers for more investigation in that particular area. The objective of this paper is to give a superior comprehension of packet size streamlining methodologies and applications utilized in WBAN, it will likewise present some research issues that are still open for researchers and complications related to those issues.

Keywords— Energy proficiency, network reliability, Cross-layer design, packet size optimization, wireless body area network

1. INTRODUCTION

Wireless Body Area Networks (WBANs) are being used in numerous application extents, for example, armed forces, business, astronomical, graphic observation, horticulture, logistics and many more [1], [2], [3]. WBAN comprises of various sensors implanted on the body and sent to detect useful parameters in a field [4]. Those sensors are dependable from getting estimations on body on which they are implanted and passing on the information towards the sink hub that gathers, filters and aggregated data is sent to the central server for further processing on the data. As the nodes have restricted power supply, each part of WBAN ought to be composed with most extreme care to scatter the constrained vitality to augment the system lifespan [5],[6]. Generally, wireless sensor networks have been classified in four wide classes as per the sending situations: Wireless Underground Sensor Networks (WUSNs), Terrestrial WSNs (TWSNs), Underwater WSNs (UWSNs), and Body Area Networks (BANs). Every one of the classification has its unique and interesting attributes because of the kind of condition that is utilized for information transmission and has extra difficulties due to their questionable and variable divert qualities in various proliferation situations.

In the literature discussed in this paper, packet size optimization concentrates on a particular application area or surroundings in which it is deployed. The fundamental attributes of BAN are energy proficiency, Quality of Service (QoS) provisioning, flexibility and scalability [7]. These features are discussed in literature with several methodologies in their specific area of application.

The vast majority of research is done to lessen power consumption and to alleviate the critical network conditions to encounter the prerequisites of BAN application areas that have specific nature of administration necessities, for example, throughput, vitality efficacy and delay. Prerequisites for BAN area in which they are deployed is not quite the same as each other, since a portion of the BAN applications require high vitality effectiveness, for example, military observation frameworks, while on the other hand application areas like health care and disaster management, require low inertness. In this way, packet size optimization methods need to fulfill the criteria of these BAN applications.

WBANs have significant difficulties in communication, information processing and administration. These difficulties are the tight asset limitations, flexible system design, powerfully evolving data transfer capacity, range, and computational power capabilities. [8]. Power utilization is the most troublesome asset requirement to be fulfilled for BANs among the difficulties mentioned earlier. Subsequently, numerous energy-aware procedures are intended for giving force to preserve and manage the power on both link layer and network layer. Despite the fact that energy is devoured by means of the sensors while detecting, communication, and transmitting the information on the way to the sink, correspondence control utilization is the predominant term in BANs [8]. Latest investigations in the area demonstrate that bundle of measures directly affects the execution of correspondence between sensor nodes. It is notable that due to severe network disorders longer packets observe higher data loss, whereas packets with shorter size basis greater data overhead. To regulate the trade-off between network dependability and vitality proficiency, numerous methodologies are anticipated to decide the ideal packet measure in

BANs. Figure 1 presents a run of the mill link-layer bundle arrange in sensor networks [9]. Packet format has three basic parts (i.e. trailer, header and payload). The header contains information related to current section number; adds amount of fragments and source along with destination nodes. Trailer field includes parity bits to control the error. Payload incorporates data bits. Length of Header, Trailer, and Payload are represented as LH, LT, and LPL respectively.
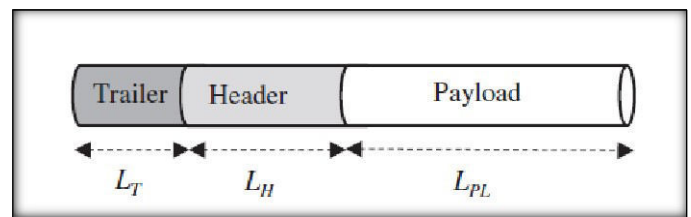
Figure 1:Link-layer packet arrangement in BANs

Packet size can be improved agreeing to several networking criteria [10-21]. Several measurements for example, output proficiency and the vitality effectiveness, are utilized for execution criteria for optimization of packet size. For example, energy productivity is utilized as an optimization metric [10] to decide the settled ideal packet length for expanding the energy proficiency.

The fundamental target of the research is to give a superior comprehension of packet size optimization methodologies utilized in WBAN to present unaddressed issues and difficulties in this research area.

2. LITERATURE REVIEW

BANs are implanted inside the body of humans or located outside the body to collect useful parameters of the body. A large portion of the BAN uses are identified with medicinal services for nonstop observing of patients who have interminable maladies. There are likewise different applications where BANs are generally utilized, for example,

crisis reaction, disaster management, and execution assessment of the athletes [10-13]. Besides, sensor nodes utilized in BANs have additionally unique operational attributes and network qualities for in and on body situations [14]. Human developments and dynamic proliferation conditions make acknowledgment of dependable and energy-efficient BANs a testing undertaking. Furthermore, the body shadowing, which happens when the flag way between the sensor nodes implanted and the transceiver is hindered, is likewise another testing issue for BANs correspondence [15]. Energy utilization is the most basic issue in BANs [16, 17].

Optimal packet size for BANs is examined to increase the energy [18]. Distinctive error control mechanisms including Automatic Repeat Query (ARQ), Forward Error Correction (FEC) square codes, for example, Bose–Chaudhuri–Hocquenghem (BCH), RS, and FEC convolutional codes broke down. Hop-length expansion method with FEC square codes is connected. Major separations can be addressed by the FEC square codes with the hop-length expansion method, since the procedure broadens the broadcast extend for a similar communication power.
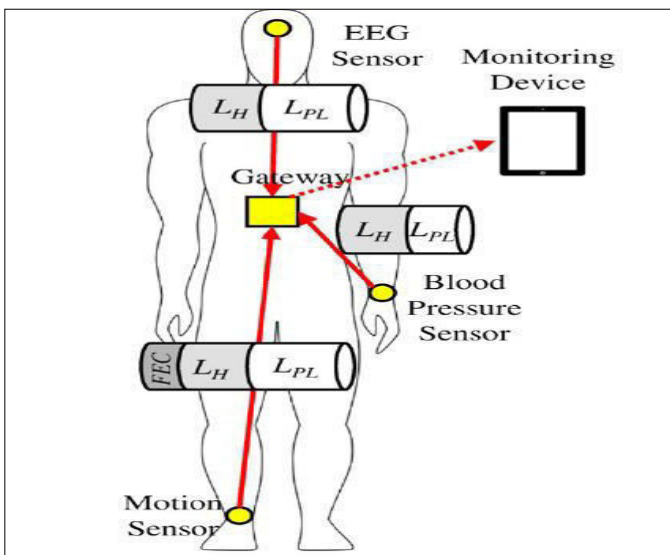

Figure 2: Packet size optimization for a typical BAN; EEG = electroencephalogram.

Figure 2 shows the results, in which three nodes are deployed to screen electroencephalogram, movement, and circulation of blood in the body. The mounted nodes pass on the obtained information to focal passage node which is then checked by a portable observing gadget, (for example, an advanced cell). As the space between mobile node and central node is greater, so by utilizing a FEC component, lengthier distances can be come to with less mistakes; henceforth, longer packets are supported for such situation. Then again, sensor nodes dont utilize a FEC component; consequently, smaller packages are utilized.

Remote health care monitoring shows such kind of a research study. In this regard, the physical conditions of a man are examined with implanted and mounted nodes, after which the gathered parameters are transmitted through gateway via single-hop transmission. At that point, this information flows through a monitoring station by the access point. In this research, ideal packet size along with energy efficiency are planned with various plans for error controlling for in and on-body planted nodes.

Simulations are done by considering diverse situations for implanted and mounted propagating conditions. Statistical assessments are done to demonstrate energy effectiveness execution for the ARQ and FEC codes. Initially, effects of modulation schemes, for example, on-off keying (OOK) and BPSK on the BER for on and in-body systems are investigated due to the distance between the gateway and body surface get extended. Line-of-sight (LOS) and non-line-of-sight (NLOS) divert modeling techniques are utilized for reforms. Non-line-of-sight displays more way misfortune than LOS demonstrate, along these lines, bring down hop-length augmentations are supported by the NLOS models. It has been observed that BPSK has the

ability to broaden the hop-length more as compare to OOK for a particular BER value and for all NLOS and LOS direct models in both implanted and mounted nodes. Moreover, packet size streamlining has the effects on the energy proficiency for to control error, for example, ARQ and convolutional code with Rc = 1/2 are researched using various BER esteems i.e. 10 to 3 and 10 to 5. The energy efficiency is supposed to be greater whereas decay dejects with the growth of packet payload for both implanted and mounted systems. This is obvious that on-body sensing systems are influenced with variety of fading. Subsequently, ideal packet payload lengths are gotten for both systems (in and on-body) as per the distinctive BER standards. Outcomes demonstrated that packet size is smaller for mounted sensing systems than the implanted sensing systems in view fading impacts. Moreover, it is additionally demonstrated, the ARQ conspire gives more vitality proficiency as soon as payload length increases than the convolutional code with Rc = 1/2 for both systems (in and on-body). Furthermore, energy proficiency becomes down as soon as the payload length increase with FEC square codes, for both implanted and mounted systems. It has been learnt from this research that FEC square codes offer more energy efficacy as compare to other error control plans. In the event where the payload of length k square code builds, the ideal packet size and energy efficiency increases equally.

Medium access control (MAC) outlines are advanced to build the vitality proficiency in IEEE 802.15.6 ultra-wideband (UWB) BANs. For accomplishing the objective, the likelihood of packets recognition and effective gathering of the packets are reckoned in two QoS manners: the default approach and high QoS approach, of UWB. The default approach uses BCH (63, 51) code for

FEC and on-off motioning for wide-ranging WBAN applications.

While, the other high QoS approach is utilized for greater needs and health related facilities and exploits type II hybrid ARQ with differential signaling. In the current research, the energy production is displayed by consolidating vitality utilization expenses of uplink and downlink channels and gathering and communicating energies. The anticipated framework demonstrates, IEEE 802.15.6 UWB physical layer Protocol Data Unit (PPDU) is utilized. Physical layer convention information unit comprises of 3 sections, i.e., physical layer benefit information component, a physical layer header (PHR) and a synchronization header (SHR). Packet identification and synchronization information is given by SHR. Details are done keeping in view end goal to discover the likelihood of fruitful packet recognition (PSHR), the likelihood of effective gathering of PHR (PPHR), and the likelihood of achievement of transferring of packets (PPPDU). Hypothetical outcomes remain contrasted and the reproduced effects for default approach and high QoS approach as per SNR increments. Accordingly, it has been discovered, that the base SNR esteems must be in range of 15.5 to 9.8 dB to make 99% of packets progress likelihood (PPPDU) for vitality identification by using the default approach and for autocorrelation with high QoS approach, separately. Besides, vitality productivity is estimated for different frame lengths and bit error probabilities Packet measure advancement for a regular BANs [19, 20, 21] 7.3×10^{-2}, 1.2×10^{-2}, 8.8×10^{-3}, 5.2×10^{-3}, and 3.4×10^{-3} as the frame size get increased. Outcomes demonstrated that ideal package size estimate increments as soon as bit error probability reduces. For example, the ideal package measure is about 300 octets when the bit error

probability is $5.2 \times 10-3$ for default approach, and becomes the 76 octets as the bit error is $1.2 \times 10-2$. At long last, ideal frame size to boost vitality effectiveness in IEEE 802.15.6 UWB BASNs is additionally found by a shut shape articulation for the default approach.

An adaptable non-layered and solicitation-oriented role-based engineering for WBANs has been displayed [22]. Different situations, for example, health services, crisis case, game, and battlefield are being noted as important area of applications for WBAN. Observing developments of expecting mothers, individuals with mental issues can be noted as cases of social insurance situation. Moreover, continuous information exchange is vital for crisis cases, for example, fire and disaster management events. In this situation, BAN system can provide important information as state, area, and damage of casualties and soldiers. Gaming frameworks have been transformed by utilizing wearable sensors. These days, players are more interfaced with games, a portion of the amusements enable clients to regulate and control their character with their own body parts with the help of wearable sensors. Gamer drives its control instructions to framework over BAN. In the Battle filed situation, officer insurance is finished by observing fighter's crucial signs and sends those readied information to medicinal individual via BAN. In light of the perception that prerequisites of each BAN application is not quite the same as the other, the proposed design consists of 3 parts that are essential , particular parts, and specific parts. Essential parts incorporate context-aware data part, QoS part, directing part, error-free conveyance part, security and fragmentation role and protection part. Then again, applications, which are under a similar situation, share the particular parts and the specific parts, independently. Part information of use is put

into the part headers and can be utilized by alternate applications. In this way, different parts don't should be embedded and the system stack diminishes with the part determination. Moreover, throughput proficiency of error control plans, for example, ARQ, BCH (127, 20, 1), and convolutional code Rc = 1/2, are assessed to implement role-based engineering.

Ideal package measures used for every one of these inaccuracy control strategies are additionally establish to build the throughput execution. Example of which is the ideal packet estimate, that expands throughput effectiveness of 211 bits for ARQ plot with $10-3$ BER. Assessments demonstrated that suggested design which is role-based beats conventional layered design as far as throughput productivity is concerned. Moreover, the throughput productivity execution of the anticipated role-based design conspire and additionally assessed with a similar error control plot in different BER esteems (i.e., 0.001 and 0.00001) as the payload increases its length. After validation it has been proven that throughput effectiveness and the ideal payload length increment with the diminishing of BER. Also, throughput proficiency with a smaller length of payload, for example, 350-2000 bits are estimated as the separation increments with a similar error control plans for both implanted and mounted sensors networks by means of LOS network model and attached body sensor systems by means of NLOS network display. Observation was made that the bigger loads gives more throughput productivity (e.g., throughput increases to 12.8% as the payload length reaches 2000 as compare to 350 bits). Additionally, it has been demonstrated that proficiency of throughput for the error control plans is great as the load estimate increments. This is also experienced that FEC square codes joined by means of hop-length expansion procedure and BPSK

regulation accomplishes most elevated throughput by means of the ideal packet size estimation.

The way out of keeping overcrowding issue in BANs is displayed via indicating ideal package measure that limits retransmission endeavors when fault circumstances occur [13]. In BANs, sensor hubs are implanted in body of human beings for medicinal services or battle field uses. Crucial signs are gathered from the body of human with the help of these implanted nodes which are then sent to the base station In any case, high BERs happen in BANs due to lossy connections, clamor, impedance, and blurring. Moreover, congestion happens amid the crisis circumstances when the system stack is high, that diminishes a quality of a network and vitality proficiency which results in expanded communication suspensions. Those issues are ought to be tackled by means of taking care of the clog issue for productive information transmission in a crisis circumstance. By way of solution for those situations, impacts of shifting pack magnitudes for the execution of BANs in various BERs are explored and assessed by reproductions via considering package conveyance proportion, deferral at each end, total retransmissions, overhead, add up to package delivered, and got after some period. Outcomes demonstrated that package transfer ratio weakens, delay at both ends and the amount of retransmissions grows as soon as elongated package measure are utilized in high BER conditions due to conflict happening at high movement. Then again, utilizing the packets of small size can result in immense measure of overheads in low BER circumstances. The ideal packet measure of 640bits is come to be good for such issues. To this end, the execution of armed services and medicinal services, utilizing BANs stands expanded in anticipating congestion.

In view of these current investigations, which are outlined, and thought about in Tables 1 and 2, from BANs viewpoint, it has been noted that ideal package measure altogether alterations as indicated by BAN application prerequisites and furthermore differs between the topology and the strategy. Hence, application prerequisites (e.g. high throughput, high vitality effectiveness, or little delay at both ends) need to be take care of before determining ideal package measure. As per a brief outline, ideal package sizes in light of prerequisites of particular WBAN applications are presented in Table 3.

Table 1: Packet size optimization practices in WBAN

Enviro nment	Technique	Purpose	Performance metrics
BASNs	Study of package measure to optimize the BANs and using hop-length extension scheme for FEC block codes [18]	Finding most legitimate error regulating plan to Increment vitality adequacy with the perfect payload package measure.	Vitality Proficiency
	An adaptable non layered and application-oriented based design for BANs [22]	Expanding the vitality productivity with the error control plans for an ideal bundle estimate.	Vitality Proficiency
	Preventing overcrowding issue in BANs [13]	Reducing re-transmission efforts via defining ideal pack size.	typical delay , Packet delivery ratio, no. of re-transmissions and overhead

Table 2: Comparison of packet size optimization techniques based on their environments

Enviro-nment	Study	Energy efficiency	Relia-bility	Network lifespan	Latency
BANs	[18]	Yes	Yes	No	No
	[20]	Yes	Yes	No	No
	[22]	No	Yes	No	No
	[8]	No	Yes	No	Yes

Table 3: Optimal package measure conferring to BAN applications

WBANs application	Requirement	Optimum packet size
Battle field and medicinal area	Greater vitality competence & faultless communication	640 bits 69
combat zone observing, mechanical process control, environmental and safety purposes.	Greater energy effectiveness	50 bits 31
Battlefield, industrials uses, and environment defense uses & industrial process control, security	Greater vitality proficiency	456 bits with no use of BCH codes & 1888 bits with the use of BCH codes 34
Automation systems, logistics, environment, and fiasco situations and unavoidable database frameworks	Greater throughput	2048 bits 27

3. KEY UNDEVELOPED RESEARCH PROBLEMS

The greater part of this study is in the direction of deciding perfect package measure in BANs for the vitality effectiveness, low latency, and high throughput. Though, such investigations confront numerous difficulties as a result of particular application prerequisites and proliferation attributes of organization situations. In forthcoming section, we feature these research problems which are still open for researchers for deciding the ideal package measure for BANs.

3.1 SERVICE PROVISIONING:

QoS prerequisite for every BAN area differs application to application. Subsequently, the packet size optimization strategy must fulfill the particular application area necessities (e.g. vitality efficiency, little delay). Although indicating ideal package measure, remote network settings essentially well-thought-out to create sensible arrangements. Besides, the ideal packet size can be balanced by the type of traffic; this may be real and non-real time. Real-time packages require shorter delay, along these lines; little packet size can be utilized. Then again, packet sizes of greater length can be favored for non-real-time and best effort packets.

3.2 TRANSMISSION POWER CONTROL:

Power utilization is an essential issue because of restricted battery for sensor nodes. Numerous investigations outline space to decide ideal packet size to expand the energy effectiveness. The wide are of works in literature utilize the little package measure for diminishing communication control. In any case, if the transmission is controlled by the network condition, the ultimate package measure can be discovered precisely.

3.3 CROSS-LAYER DESIGN:

Outline of a total cross-layer come closer commencing the physical layer to the application

layer for optimization of packet size in BAN which has not been addressed in literature for various BAN areas. For instance, different antenna models e.g. omni-directional or directional radio wires at physical layer or diverse MAC conventions (e.g. TDMA, CSMA, and half and half) at the connection layer be reflected to decide the ideal package measure.

3.4 RELIABLE COMMUNICATION:

Error control is a basic problem in WBANs, as the quantity of re-transmission diminishes once the error free communication is accomplished. In literature discussed earlier, some error control components, for example, ARQ, FEC, and half and half strategies, are applied to get the ideal packet size. But, the performance measurement of these systems hasn't been fully compared for various WBAN applications to get the comparing ideal packet size.

3.5 ENERGY-HARVESTING WBANs:

Energy Harvesting (EH) might improve execution of WBANs by means of its own charging ability. Accessible vitality from surroundings, for example energy from sun, thermal, magnetic can be rummaged to control remote sensors. Though, current package measure methods for WBANs can't be straightforwardly applicable to EH-BANs. This is on account of the existing vitality that changes with time, rather than monotonically diminishing in energy-harvesting WBANs. To this end, ideal packet size arrangements are required for energy-harvesting WBANs to adjust the trade-off between energy utilization and QoS.

4. CONCLUSION

Packet measure is a vital constraint to expand the execution of BANs. Several optimization methods are anticipated by the specialists to enhance the system execution as far as the energy effectiveness, throughput, and delay are concern (among other execution measurements). These methodologies are grouped into various scientific categorizations.

Meanwhile several of these suggest using the package of fixed length or the dynamic package length, whereas others suggest utilizing different package arrangements or optimization systems. Optimization methods for package length are investigated in terms of WBANs. We reviewed the latest optimization schemes for package length to meet the necessities of particular application area to decide the ultimate package length. At last, we expressed the primary undeveloped research issues in the zone of package length optimization for forthcoming studies.

REFERENCES

[1] Prasad, Poonam. "Recent trend in wireless sensor network and its applications: a survey." Sensor Review 35, no. 2 (2015): 229-236.

[2] Barcelo-Ordinas, Jose M., Jean-Pierre Chanet, K-M. Hou, and J. García-Vidal. "A survey of wireless sensor technologies applied to precision agriculture." In Precision agriculture'13, pp801-808. Wageningen Academic Publishers, Wageningen, 2013.

[3] Seema, Adolph, and Martin Reisslein. "Towards efficient wireless video sensor networks: A survey of existing node architectures and proposal for a Flexi-WVSNP design." IEEE Communications Surveys & Tutorials 13, no. 3 (2011): 462-486.

[4] Akkaya, Kemal, and Mohamed Younis. "A survey on routing protocols for wireless sensor networks." Ad hoc networks 3, no. 3 (2005): 325-349.

[5] Yildiz, Huseyin Ugur, Sinan Kurt, and Bulent Tavli. "The impact of near-ground path loss modeling on wireless sensor network lifetime." In Military Communications Conference (MILCOM), 2014 IEEE, pp. 1114-1119. IEEE, 2014.

[6] Kurt, Sinan, and Bulent Tavli. "Path-Loss Modeling for Wireless Sensor Networks: A review of models and comparative evaluations." IEEE Antennas and Propagation Magazine 59, no. 1 (2017): 18-37.

[7] Fulara, Yogesh Kumar. "Some aspects of wireless sensor networks." International Journal on AdHoc Networking Systems 5, no. 1 (2015): 15-24.

[8] Rahimi, Mohammad, Rick Baer, Obimdinachi I. Iroezi, Juan C. Garcia, Jay Warrior, Deborah Estrin, and Mani Srivastava. "Cyclops: in situ image sensing and interpretation in wireless sensor networks." In Proceedings of the 3rd international conference on Embedded networked sensor systems, pp. 192-204. ACM, 2005.

[9] Sankarasubramaniam, Yore, Ian F. Akyildiz, and S. W. McLaughlin. "Energy efficiency based packet size optimization in wireless sensor networks." In Sensor Network Protocols and Applications, 2003. Proceedings of the First IEEE. 2003 IEEE International Workshop on, pp. 1-8. IEEE, 2003.

[10] Bächlin, Marc, Kilian Förster, and Gerhard Tröster. "SwimMaster: a wearable assistant for swimmer." In Proceedings of the 11th international conference on Ubiquitous computing, pp. 215-224. ACM, 2009.

[11] Chenji, H., A. Hassanzadeh, M. Won, Y. Li, W. Zhang, X. Yang, R. Stoleru, and G. Zhou. "A wireless sensor, adhoc and delay tolerant network system for disaster response." Technical Report LENSS (2011).

[12] Gao, Tia, Christopher Pesto, Leo Selavo, Yin Chen, JeongGil Ko, JongHyun Lim, Andreas Terzis et al. "Wireless medical sensor networks in emergency response: Implementation and pilot results." In Technologies for Homeland Security, 2008 IEEE Conference on, pp. 187-192. IEEE, 2008.

[13] Yigit, Melike, H. Ugur Yildiz, Sinan Kurt, Bulent Tavli, and V. Cagri Gungor. "A survey on packet size optimization for terrestrial, underwater, underground, and body area sensor networks." International Journal of Communication Systems31, no. 11 (2018): e3572.

[14] Yigit, Melike, H. Ugur Yildiz, Sinan Kurt, Bulent Tavli, and V. Cagri Gungor. "A survey on packet size optimization for terrestrial, underwater, underground, and body area sensor networks." International Journal of Communication Systems31, no. 11 (2018): e3572.

[15] Cotton, S. L., A. McKernan, A. J. Ali, and W. G. Scanlon. "An experimental study on the impact of human body shadowing in off-body communications channels at 2.45 GHz." In Antennas and Propagation (EUCAP), Proceedings of the 5th European Conference on, pp. 3133-3137. IEEE, 2011.

[16] Yang, Guang-Zhong, and Guangzhong Yang. Body sensor networks. Vol. 1. London: Springer, 2006.

[17] Zhang, Yanqing, Fan Zhang, Yousef Shakhsheer, Jason D. Silver, Alicia Klinefelter, Manohar Nagaraju, James Boley et al. "A Batteryless 19μ W MICS/ISM-Band Energy Harvesting Body Sensor Node SoC for ExG Applications." IEEE Journal of Solid-State Circuits 48, no. 1 (2013).

[18] Domingo, Mari Carmen. "Packet size optimization for improving the energy efficiency in body sensor networks." ETRI Journal 33, no. 3 (2011): 299-309.

[19] Oto, Mert Can, and Ozgur B. Akan. "Energy-efficient packet size optimization for cognitive radio sensor networks." IEEE Transactions on Wireless Communications 11, no. 4 (2012): 1544-1553.

[20] Yigit, Melike, H. Ugur Yildiz, Sinan Kurt, Bulent Tavli, and V. Cagri Gungor. "A survey on packet size optimization for terrestrial, underwater, underground, and body area sensor networks." International Journal of Communication Systems31, no. 11 (2018): e3572.

[21] Holland, Matthew, Tianqi Wang, Bulent Tavli, Alireza Seyedi, and Wendi Heinzelman. "Optimizing physical-layer parameters for wireless sensor networks." ACM Transactions on Sensor Networks (TOSN) 7, no. 4 (2011): 28.

[22] Domingo, Mari Carmen. "Throughput efficiency in body sensor networks: A clean-slate approach." Expert Systems with Applications 39, no. 10 (2012): 9743-9754.

Design and analysis of the structure of a drill rig

Kamran Mahboob [1,2, a], Ayaz Ahmad[2, b] Umar Mushtaq[2, c], Muhammad Muneeb Aslam[2, d],
Abdul Qaddus[2, e], Farman Ali [2, f]

[1]University of Engineering and Technology, Lahore

[2]Chenab College of Engineering and Technology, Gujranwala

Email address: [a] mahboobccet@gmail.com [b] ayazccet@gmail.com [c] umarmushtaqccet@gmail.com

[d] muneebaslamccet@gmail.com [e] aqaddusccet@gmail.com [f] farmanaliccet@gmail.com

Abstract—**World is becoming hungrier for the energy with every passing day. A major portion to meet world's energy demand depends upon the Fossil fuels extraction especially Petroleum. In Pakistan like many other countries in the world, a major portion of the electricity is produced from petroleum products. The extraction of these petroleum products from several feet beneath the earth surface requires certain techniques like drilling the well using a drill rig. In this paper, an effort is made to design a drill rig. First, a 3d model is designed using CAD software. Three different types of structures are modelled by varying the cross section of the structures. Then these structures are analyzed using CAE software. A comparison of all three structures is presented and an optimum structure with minimum deformation is suggested.**

 Keywords—Drill rig oil, Mast structure, Simulation, CAE

I. INTRODUCTION

Drilling the well is one of the basic operation in extraction of oil from beneath the earth in both on and off shore [1] [2] operations. Drill rigs are designed and developed for drilling holes within the surface of the earth. Drill rig is a huge system used to drill a well of water, well of oil, or natural gas wells. They can be small to extent that these can be taken by a person auger [3]. Drill rigs can be used to sample mineral resources, take a look at rock, soil and groundwater characteristics, and additionally may be used to put in sub-surface fabrications, along with facilities, special equipment's, tunnels or wells [4]. A drill rig is a cell system mounted on the top of vehicles, tracks or trailers, or land. Oil and natural gas drill rigs are not only handiest to discover earth's resources but additionally to drill holes that permit the oil or natural fuel to be extracted from the reservoirs. Broadly speaking in onshore oil fields, a well is drilled and then drill rig is moved off the place. A smaller rig is constructed for convenience. Small drill is moved directly to the well and set properly on line [5]. This frees up the previous drill rig to drill hole at other place and operation is streamlined bearing in mind specialization of sure offerings, i.e., completions vs. drilling[6].

Fig. 1. Land rig [7]

II. DEVELOPMENT

Drilling rig is split into the subsequent most important systems. Following are the major systems of drill rig oil.

A. Hoisting system

Hoisting System consists of pulley system, used for lowering and rising of the travelling block via large pulley and wires system. It is used for elevating and lowering of the drill pipes. It consists of the components shown in Figure 2. Draw works is huge gyratory drum with metal wire wrapped around it. The drum is further connected to the motor and gearing system. The movement of the drill hook and travelling block in or out of the well is controlled by draw works drum. The metal wire or drill line received over a pair of sheaves at the top of the tower of drill rig, commonly known as crown block and similarly wrapped over sheaves at the bottom known as travelling block with a suspending drill hook.

The elevator which is connected to the travelling block is used to pull out the drill string or casing from the hole. However, the drill line is received over the sheaves at top and bottom, it is connected with the reverse drum through dead line anchor so it can`t move. The other end attached with draw works drum of the drill line, known as fast line.
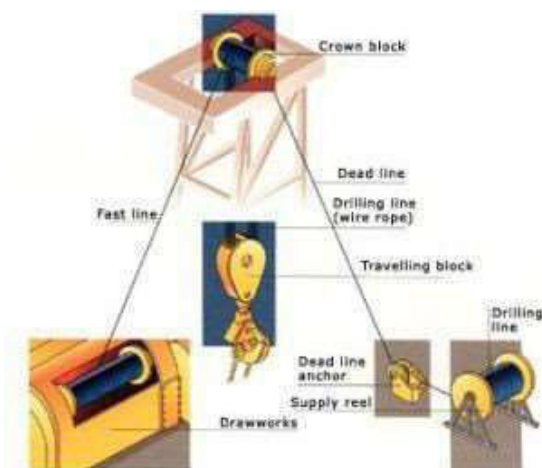

Fig. 2. Hoisting System [8]

Fig. 3. Rotating System [9]

B. Rotary system

The drill rig rotary system is used to revolve the drill string and also drill bit at the bottom. It is used to provide rotary electricity to drill bit for cutting. The equipments included in this system are shown in Figure 3, which is mainly rotary house, swivel, Kelly, rotary drives, drill string and drill table [10].

Swivel is connected with the kelly house and hook, which makes a robust joint, because it offers the pressure seals and endure the overall weight of the drill string.

The Kelly is hexagonal in cross-section, provides rotational motion to the drill string. It is made of treated steel to prevent from unnecessary wear caused by braking connections.

C. Circulating System

The Circulating equipment consists of the following components; flow lines, nozzles, mud pumps, tanks and mud pits. The mud is impelled by the mud pump with the help ofsand pipe and rotary hose into drill string. The mud travels down through the drill string to drill bit, where it is sprayed by nozzles at the lowermost of hole.

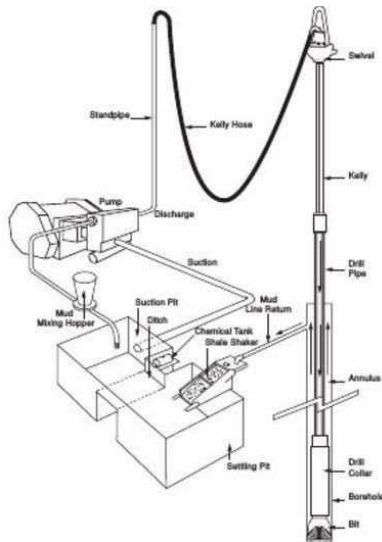Drill rig oil includes the following sub components.

Fig. 4. Circulating System [11]

1) Centrifuge

It is a system used to separate fine slits and soil from the drill mud.

2) Solids Control

It is a system that is used to prepare drill mud for the process of drilling.

3) Chain tongs

It is wrench with a segment of chain that is wrapped around anything that is to be tightened or loosened.

4) Desander/Desilter

It incorporates hydro cyclones that remove sand and silt from the drill mud.

5) Degasser

It is a tool that is used to remove air and gas from the drill mud.

6) Draw works

It is the segment consists of the spool, which has a primary feature to move in and out of the drill line to elevate or move down the travelling block.

7) Drill Bit

It is a tool at the end of the drill string, which tears apart the rock that is to be drilled. It incorporates highly pressurized fluid at its exits.

8) Elevators

It is a tool that grips the drill pipe and moves it in or out of the drilled hole.

9) Mud motor

It is a hydraulically powered tool located simply at the top of the drill bit that spins the drill bit.

10) Dust pump

It is a reciprocal kind of pump that is used to drill mud into the system.

11) Mud tanks

It is frequently known as mud pits, which are used to store the drill mud.

12) Rotary desk

These are used to rotate the drill string which is connected to gears and bit at side.

13) Shale shaker

It is used to filter the slits from mud after cutting before pumping it back to the hole being drilled.
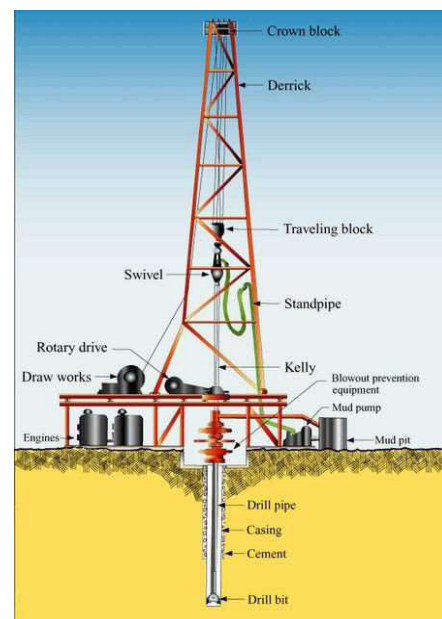

Fig. 5. Drilling system overview[12]

III. WORKING

Drilling a hole with drill rig oil includes following techniques.

A. Drilling a well

The group set the rig and starts the process of drilling. From the start, the group drills a hole down to a determined depth that is little above the oil lure [13] [14]. Following are the fundamental steps in drilling:

1. Locate the drill bit, drill pipe and collar within the hole.

2. Connect turntable and Kelly, and start operating.

3. During drilling, drill mud moved in and out of the hole with rocks that are cut.

4. As the hole gets deeper and deeper more drill pipes are entered and fitted in it.

B. Cement the hole

When they attain the targeted depth, they have to cement the casing- region, casing-pipe sections are fitted into the hole to save it from collapsing. The spacers are provided with the casing pipe to keep it still in the hole. The casing team fits the casing pipe in the hole after that cement team pumps cement down the casing pipe and allows it to be hardened.
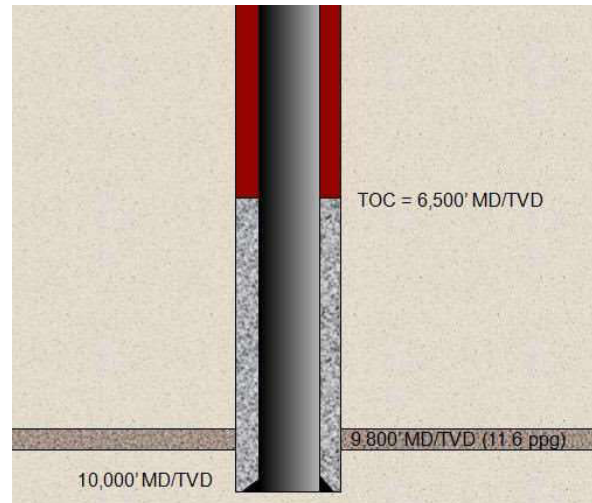

Fig. 6. Drilling system [15]

Fig. 7. Cementing the hole [16]

C. Testing for oil

Drilling process progresses and the team drills the hole, then put in casings and cements it, then drills again. When the oil appears with the rock cuttings, it means the drilled hole has reached the oil reservoirs.

At this point, group participants remove the drilling equipment from the hole and carry out numerous checks to verify this finding:

- Properly logging – a sensor is lowered down into the hole to test the rock formation.

- Drill-stem checking out – a device is lowered into the hole to check the pressure.

- Centre samples - samples of rock are taken to search for traits of resource rock.

D. Oil well

After the final depth is reached, the perforating gun is lowered down into the hole. It contains explosives that are used to create a small hole in the casing to allow the flow of oil or gas up the hole after the casing is perforated

and the tube is fitted in the hole with packers to seal it from outside. Ultimately, they set up a Christmas tree that regulates the flow of the oil or gas out of the well.
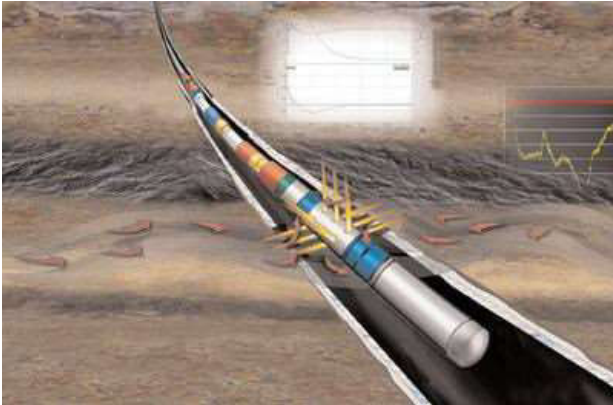

Fig. 8. Drilling perforation [17]

E. Oil Extraction

After the drill rig is removed, the team places a pump at the head of the well. Inside the pump system, motor drives an equipment field that is acting as a lever. The lever pushes and pulls a bladed rod up and down. The bladed rod is connected to a sucker rod that is connected to a pump. This device creates a pressure that causes the oil or gases to flow upward.

F. Enhanced oil recovery

In a few instances, when the oil is too heavy to drift, another hole is drilled into the reservoir and steam is injected into the reservoir under high pressure. The steam heat then causes the oil to get thin and the pressure push it up the well. This process is known as enhanced oil recovery.
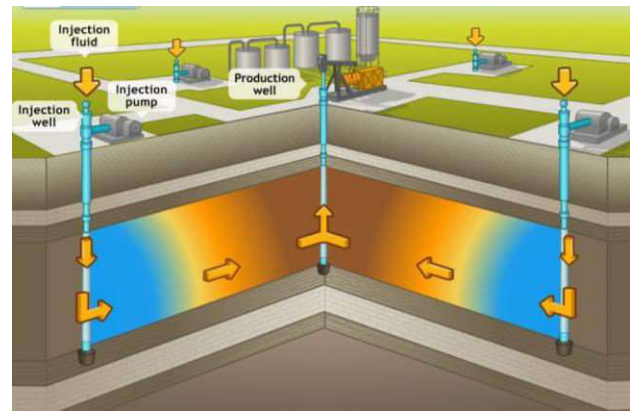

Fig. 9. Oil extraction [18]

Fig. 10. Enhanced oil recovery [19]

IV. DESIGN

Three variants of the structure are designed having different cross section area. CAD models are developed for all variants. The geometrical details of these structures are as follows:

A. Cross-section's dimensions

The cross section used in all three structures is of I beam cross section of different dimensions.
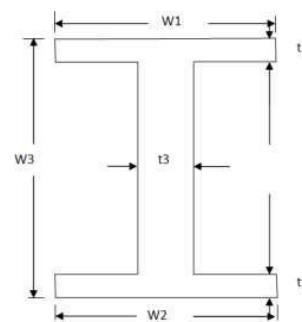

Fig. 11. Cross Section of the structure

Cross section dimensions such as width and thickness of flanks are enlisted in Table I.

TABLE I – WIDTH AND THICKNESS OF FLANKS

Model No.	W1(m)	W2(m)	W3(m)	T1(m)	T2(m)	T3(m)
1	0.3	0.3	0.6	0.03	0.03	0.03
2	0.1	0.1	0.2	0.01	0.01	0.01
3	0.15	0.15	0.3	0.015	0.015	0.015

B. Mast model dimensions

Height = 44.8 m

Width across shoes = 7.6 m

Length from front to rear shoe = 6.6 m

Top crown width = 3.3 m

V. MAST MODEL AND ANALYSIS

A. Model

Pre-processing of the structures are carried out in ANSYS. The coordinates of the nodes of the structure are calculated from the CAD file and compiled. These are then imported in ANSYS Design Modular to create the nodes points. The mast structure is created by joining these node points through line. Then cross section is assigned to complete the design as shown in figure 12.
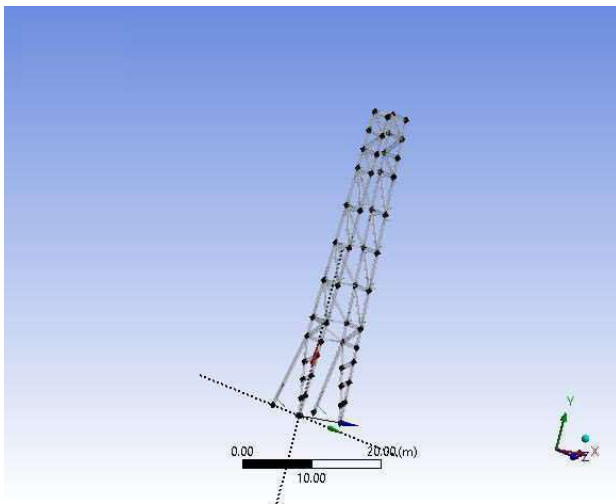

Fig. 12. Points of structure

B. Analyis

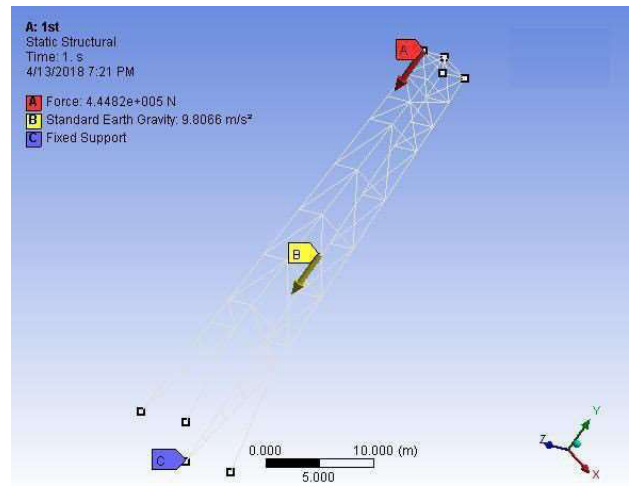In this section steps about the analysis procedure carried out on the structure model are discussed.

Fig. 13. Boundary conditions

1) Meshing

First step involves the meshing of the structure.

2) Boundary conditions

Following boundary conditions are applied on the model.

a) Fixed support

Structure is fixed at the base as shown in the figure 13.

b) Standard Earth's gravity

Earth's gravity is applied on the structure downward to incorporate structure weight as it is shown in the figure 13.

c) Hook load

A hook load of 444820 N is applied at the top in –y direction as shown in the figure 13.

VI. RESULTS

The analysis results which include the total deformation, axial forces, total shear force and total bending moment are enlisted in the Table II. The analysis results of total deformation and total bending moment are shown as follows:

A. Deformation

The total deformation of all three structures is plotted as shown in figure 14 for the structure 1, figure 15 for the structure 2 and figure 16 for the structure 3.
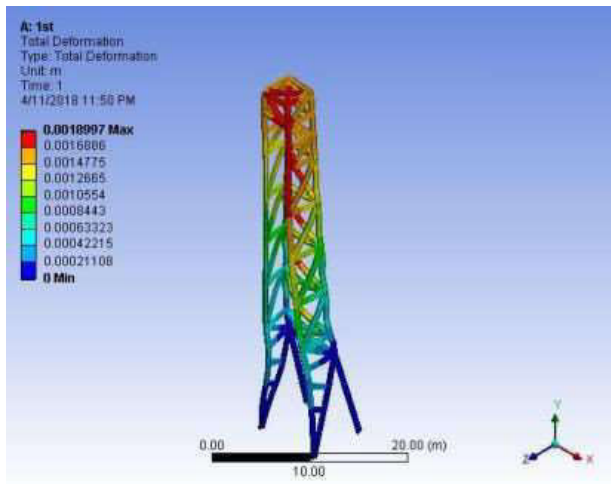

Fig. 14. Total deformation in structure 1

Fig. 15. Total deformation in structure 2

Fig. 16. Total deformation in structure 3

B. Bending moment

The total bending moment results of all three structures are plotted as shown in figure 17 for the structure 1, figure 18 for the structure 2 and figure 19 for the structure 3.
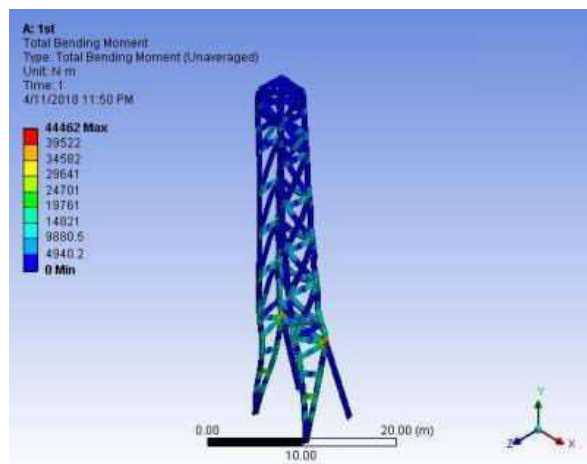

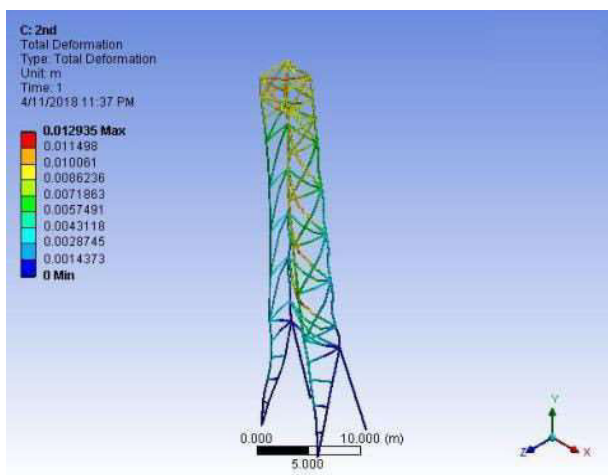Fig. 17. Total Bending Moment in structure 1
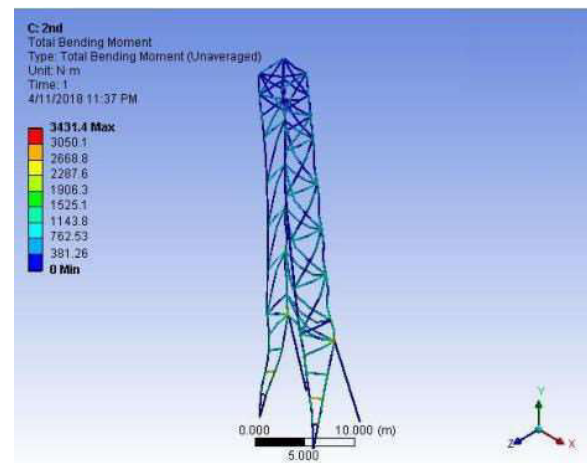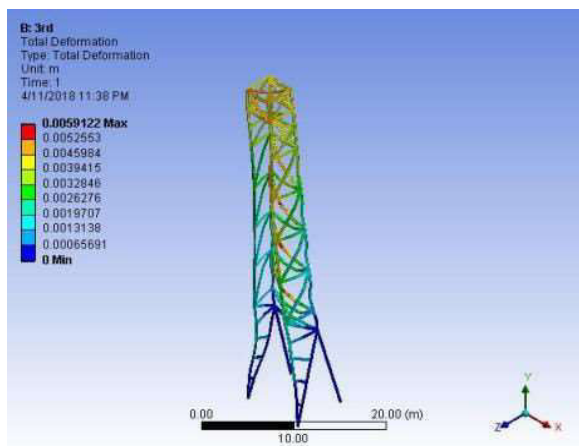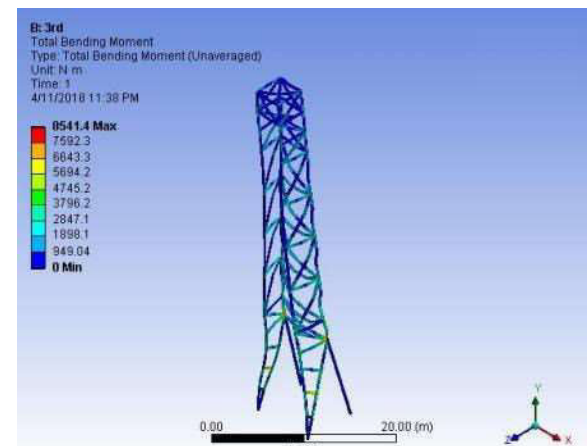

Fig. 18. Total bending moment in structure 2

Fig. 19. Total Bending Moment in structure 3

TABLE II. RESULTS OF ALL STRUCTURES

N o.	Hook Load (N)	Total Deformati on (m)	Axial Force (N)	Total Shear Force (N)	Total Bending Moment (Nm)
1	444820	0.0018997	31854	28519	44462
2	444820	0.012935	3186.4	2970	3431.4
3	444820	0.0059122	7398.8	6929	8541.4

VII. COMPARISON CHARTS

The comparison charts of total deformation and bending moment are plotted as follows;
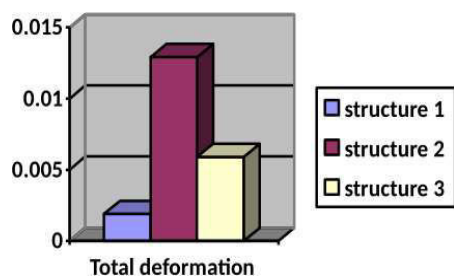
A. Total Deformation

Fig. 20. Comparison chart for total deformation

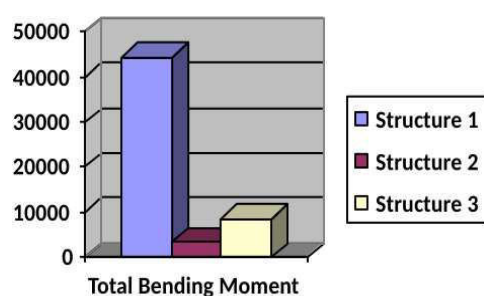### B. Total Bending Moment

Fig. 21. Comparison chart for total bending moment

IX. CONCLUSIONS

1) It is clear from the above mentioned results that the structure 1 is best among the structures under study as it exhibit minimum deformation.

2) The max defection is at the side of the structure, so we recommend that the cross links should be used to reduce the deformation.

3) Maximum bending moment is present at the base of the tower and we can add reinforcement.

4) Extra elements can cause increase in deflection due to increased weight, therefore, an optimum number of element should be used.

ACKNOWLEDGMENT

REFERENCES

[1] S. C. Geekiyanage, D. Sui, and B. S. Aadnoy, "Drilling Data Quality Management: Case Study With a Laboratory Scale Drilling Rig," in *ASME 2018 37th International Conference on Ocean, Offshore and Arctic Engineering*, 2018, pp. V008T11A010-V008T11A010.

[2] C. Craig and M. Islam, "Integrated power system design for offshore energy vessels and deepwater drilling rigs," *IEEE Transactions on Industry Applications,* vol. 48, pp. 1251-1257, 2012.

[3] T. Beebe, J. H. Vazquez, J. Rousseau, L. Samuelsson, P. Cunnion, and C. Coan, "Alternative Operation Scheme for a Jackup Drilling Rig to Meet Target Soil Bearing Pressure Requirements," in *Abu Dhabi International Petroleum Exhibition & Conference*, 2018.

[4] S. Tudor, G. Marin, G. Stoianovici, and C. Bălan, "Borehole Drilling Rig and step-by-step Movement of a Stationary Drilling Installation," *Electrotehnica, Electronica, Automatica,* vol. 66, pp. 186-193, 2018.

[5] A. Austefjord, S. Blaylock, I. Forster, M. Sheehan, and C. Wright, "Small-Scale Drilling Test Rig For Investigation of Axial Excitation On The Drilling Process," in *MATEC Web of Conferences*, 2018, p. 16001.

[6] S. Soe, C. Lagat, B. Evans, M. Mostofi, and S. Fox, "The Coiled Tubing Drilling Rig for Mineral Exploration," in *SPE/ICoTA Coiled Tubing and Well Intervention Conference and Exhibition*, 2018.

[7]   Contrelec. (2019, 02/07/19). *Land Rig PCR*. Available: http://www.contrelec.co.uk/pages/case-study-5

[8]   welldrillingbasicinfo. (2019, 02/07/19). *Hoisting system*. Available: https://welldrillingbasicinfo.wordpress.com/2013/05/03/hoisting-system/

[9]   Petroprophet. (2019, 02/07/19). *The Rotary System*. Available: https://www.petroprophet.com/the-rotary-system/

[10]   Y. Tetsuo, E. J. Cargill, T. M. Gaynor, J. Hardin Jr, R. T. Hay, I. Akio*, et al.*, "Robotic controlled drilling: A new rotary steerable drilling system for the oil and gas industry," in *IADC/SPE Drilling Conference*, 2002.

[11]   Jack. (2019, 02/07/19). *DRILLING RIG CIRCULATING SYSTEM*. Available: http://www.oilngasdrilling.com

[12]   F. Bu and J. Dykstra, "Indirect adaptive robust controller design for drilling rotary motion control," in *ASME 2014 Dynamic Systems and Control Conference*, 2014, pp. V001T09A001-V001T09A001.

[13]   J. R. Hasle, U. Kjellén, and O. Haugerud, "Decision on oil and gas exploration in an Arctic area: case study from the Norwegian Barents Sea," *Safety science,* vol. 47, pp. 832-842, 2009.

[14]   B. S. Aadnøy and K. Andersen, "Design of oil wells using analytical friction models," *Journal of petroleum Science and Engineering,* vol. 32, pp. 53-71, 2001.

[15]   S. Energy. (2019, 02/07/19). *Drilling*. Available: https://www.studentenergy.org/topics/drilling

[16]   D. Formulas. (2019, 02/07/19). *Cement Transition Period in The Oil Well Can Cause Well Control Situation*. Available: http://www.drillingformulas.com/cement-transition-period-in-the-oil-well-can-cause-well-control-situation/

[17]   Rigzone. (2019, 02/07/19). *How does well completion work*. Available: https://www.rigzone.com/training/insight.asp?insight_id=326

[18]   N. Olabi. (2019, 02/07/19). *Shutterstock.com/Thaiview*

Report Offers No Clues Into What Caused Explosion at Oil Well Near Windsor. Available: https://www.westword.com/news/windsor-explosion-report-provides-no-new-answers-from-extraction-oil-and-gas-10064153

[19]   2b1. (2019, 02/07/19). *EOR*. Available: https://www.2b1stconsulting.com/eor/

Selection of drive system for heliostat of concentrated solar thermal power plant

Kamran Mahboob[1,4,a], Momen Rasool[2,b], Umair[2,c], Muhammad Qasim Nawaz[2,d], Abdul Rehman Sajjad[2,e] and Tabish Fawad[2,3,f]

[1] Dept. of Mechanical Engineering, University of Engineering and Technology Lahore, Pakistan
[2] Dept. of Electrical Engineering, Chenab College of Engineering and Technology Gujranwala, Pakistan
[3] Dept. of Electrical Engineering, FEAS Riphah international University Islamabad, Pakistan
[4] Dept. of Mechanical Engineering, Chenab College of Engineering and Technology Gujranwala, Pakistan

Email address: [a] mahboobccet@gmail.com , [b] momen.rasool@yahoo.com and [c] umairccet@gmail.com
[d] qasimccet@gmail.com [e] moon.ccet@gmail.com [f] tabishfawad666@gmail.com

Abstract—With the advancement in the domain of science and technology, we witness a lot of development in energy harnessed from sun. Concentrated solar thermal technologies are frequently used as a source for modern day power generation. Past decade has shown huge development in solar power tower technologies. As we know, heliostat is building block of solar thermal tower power plant and efficiency of the plant depends upon how accurately it reflects the light on receiver placed on the top of the tower. In this research, an effort is made to select the drive system for tracking system of the heliostat. In the start, a review of different tracking system is presented. Advantages and disadvantages of all these systems are enlisted. Based on this review, it is concluded that hybrid stepper motor is best drive system for tracking the heliostat of the solar thermal power plant.

Keywords—tracking system, heliostat, solar tower power plant, drives

I. INTRODUCTION

A rise in the global economy and modern life style is much dependent upon the conventional energy resources. These resources are depleting at rapid pace as well as we can see global warming on the rise[1]. This has forced the world to shift away from fossil fuel technology towards renewable energy technologies [2] like wind, solar etc. Solar technologies vary from small household installation to very large solar power plant. Solar concentrating technologies are mainly used for larger power plants [3] and we can see that number of solar tower power plants is increasing amongst newly installed solar thermal power plants [4].

In solar tower power plant, we have a central tower on which receiver is placed [5, 6]. A large number of mirrors are placed all around the tower known as heliostat field that reflects the light on the receiver placed on the top of the tower [7]. In order to track the sun all day long, a tracking system is placed under heliostat that places it in such a way that rays of sun after striking the heliostat concentrate to the receiver all day long [8]. In order to track the sun accurately special efforts are required by the tracking system [9]. The efficiency of solar tower power plant directly depends upon the efficiency of the optical field [10].

Fig. 1. Solar Thermal power plant[11]

Fig. 2. Heliostat in Solar Thermal power plant[11]

The concentrated light on the receiver heats the High Temperature Fluid (HTF) [12] [13]. Many types of HTF are used depending upon plant design and its operation like molten salt, liquid sodium [14] etc. This HTF transfers heat from the receiver to the exchanger to generate steam. Direct steam can also be generated depending upon the plant design. A storage can also be designed to keep plant operational during no sun [15] [16]. The generated steam runs the turbine and electricity is generated [17].

A. Heliostat

Heliostats is the main component of concentrated solar tower power plant that reflects the sun rays to the receiver mounted on top of the tower [18] by placing itself at bisecting angle to target and sun.

The heliostat has following main parts as shown in figure 3 [19].

1. Mirror surface

2. Support structure

3. Pedestal

4. Control system

5. Drive system

II. TRACKING SYSTEM OF HELIOSTAT

A tracker is a system or structure on which mirrors are mounted, that can track an object or something else which will be defined in its controlling mechanism. It can change its position to track that thing or object, if the object is sun the tracker is known as sun tracker. A tracker may be automatic or manual depends upon its design. A manual tracker usually contains only controller and a driving mechanism. In addition to manual system, a tracker usually requires sensors for its automation. Here we discuss only driving mechanism of tracker. The driving mechanism of tracker uses electric motors, actuators or their coupling with gears, pulley belt system to move or rotate the facet and actually define the degrees of freedom of the tracker.

Fig. 3. Parts of Heliostat [19]

Fig. 4. High precision solar tracking drive [20]

Fig. 5. Zomeworks, Passive Tracker, UTRF-064 [21]

There are two type of coupling mechanism used in tracker's drive system: Series Coupling and Parallel Coupling. In series coupling, motors or actuators are connected in series to increase the degree of freedom of structure, while in parallel, they are connected in parallel.

Solar trackers are categorized as active and passive on the bases of drive methods.

A. Passive Trackers

In these trackers, a volatile fluid is compressed in containers, which is attached to both ends of the rack. The solar radiation creates pressure inside the container which makes the system imbalance and tends the system to move accordingly.
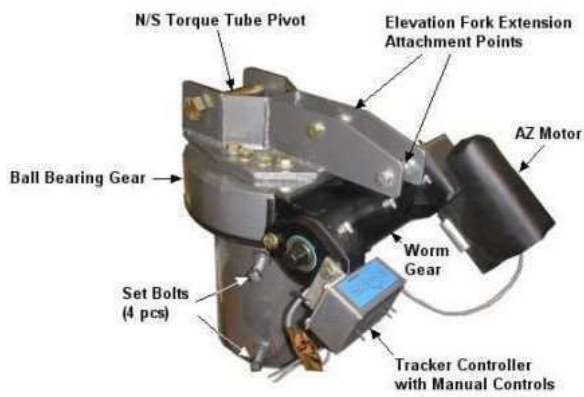

Fig. 6. Dual-Axis, Active Solar Trackers Passive Tracker [22]

This non-precise orientation makes it unsuitable for concentrating PV collector or tower solar concentrating system. However, it works better in mono or poly crystalline PV panel system. The system does not use any gear and motor for rotation hence, the power is not required.

B. Active Trackers

In these trackers gears and motors are used to drive the panel rack. The control circuit (microcontroller, Programmable Logic Controller (PLC), Personal Computer (PC), etc.) sends command to the motor to rotate – in order to track the sun. Since the motors consume energy, they could be used only once required. Different types of actuators and motors are used in Active Tracking Strategy i.e. Stepper Motors, Servo Motors, Linear Actuators, Linear Servos, Brushless DC Motors etc.

III. REVIEW OF DRIVE UNITS FOR TRACKING SYSTEM

Drive unit is responsible for movements in the tracking system. Some commonly used drive systems are as follows:

    A. Brushed DC Motor

    B. Brushless DC Motor

    C. Hybrid Stepper Motor

    D. Servo

    E. Electric Actuator

Fig. 7. DC Motor [23]

A. Brushed DC Motor

The conversion mechanism of electrical energy into mechanical energy is done by DC motor. William A Lynch [24] used two electro optic sensors with small and cost effective electronic control circuit. Tracking resolution of control circuit was within 0.1 degree. Soteris A Kalogirou [25] used three LDRs to track the sun position, DC motor feedback element sensor gives deviation from zero is 0.2 and 0.05° with 100 and 600 Wm^{-2} solar radiation respectively. Salah Abdullah [26] used two PLC drivers, first for joint rotating and second for east-west tracking. On the fixed surface that is tilted at 32 degree toward south, energy collected was measured and compared. The two axis triangular surfaces have collected 41.34% of solid surface. P. Roth [27] used a rectangular pyrheliometer to detects the position of the sun and operating the motor. This system calculates the position of the sun and control the movement under cloudy conditions. Kosuke Aiuchi [28] used photo sensor refracting telescope with an equatorial mount. With the cloud sensor, the heliostat operated stably within an error of 10 mrad in cloudy weather.

Fig. 9. Polar tracking system [30]

DC motor can be rotated in both directions by inverting the direction of the supplied current. The most effective way to achieve this is the so-called H-bridge [31]. Adrian Catarius used four PV sensors, microcontroller processes, two H-Bridges for the two DC motors two worm gear assemblies and four LED. Nader Barsoum [32] used a gear motor, PIC16F84A microcontroller and photocells. Single-axis freedom increase 20% energy output and double-axis freedom increase more than 40%.

Fig. 8. Brushed DC motor[29]
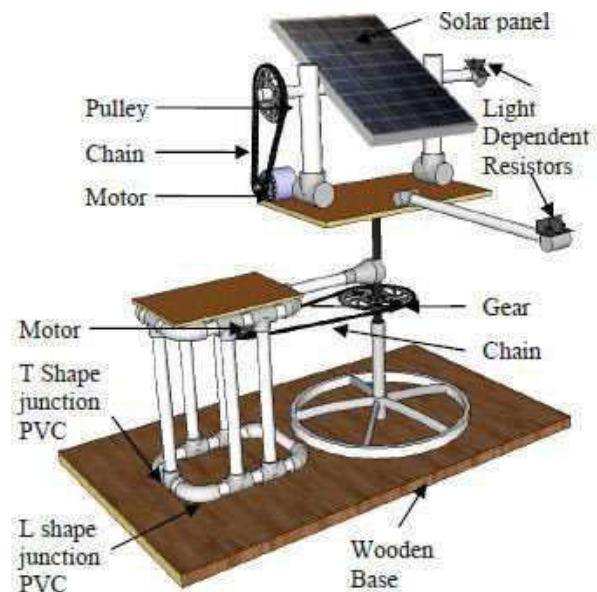
Fig. 10. Two DoF solar tracker [32]

1) Advantages

- Initial cost is low
- Reliability is high
- Simple logic to control motor speed

2) Disadvantages

- Maintenance is high i.e. regularly replacing or cleaning of brushes, commutator and springs
- Life span during high intensity use is low

B. Brushless motors

The brushless motor is a DC motor that works without a mechanical brush and a traditional brush motor switch. It has different chara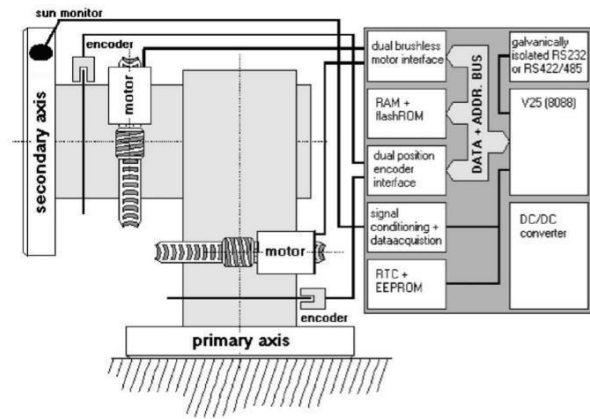cteristics of the brush motor that is more affordable in the long term, granting the fundamental cost is high. In 2003, A. Georgiev [33] used three Eppley pyrheliometers settled on the INTRA unit that is connected with automatic registering system and UV components used with RTC and RAM powered by power source. Between the radiations the concurrence difference of about 60W/m2 i.e. about 6% of 1000W/m2. The instrument must be sequential against cavity radiometer for successful measurement with this installation.

Fig. 11. Brushless DC motor [34]

Fig. 12. Block diagram of INTRA sun tracker [33]

1) Advantages

- Life span is long
- Low maintenance requirements
- Efficiency is high

2) Disadvantages

- Initial cost is high
- Motor speed controller is complicated

C. Hybrid Stepper Motor

Hybrid stepper motor is combination of variable resistance (VR) and permanent magnet (PM) stepper motors. Just like PM motor, it contains a permanent magnet in the rotor teeth. There are two arrangements of the teeth called glasses ring the rotor. One of these rings is South Pole, and other ring is North Pole. Hybrid stepper motor has stator poles just like VR motor. The stator poles in hybrid motor are some of the times called teeth. Steve Schell [35] used a hybrid stepper motors. These motors are incredible fit for the application since they are economical, require no position input sensor and give high torque and low speed yield, which diminishes the measure of fundamental rigging decrease. For a more straightforward proportion of heliostat execution, beam portrayal

framework is introduced that focuses on the pinnacle Image Processing of beam anticipated onto these objectives gives estimations of the beam shape just as the pointing exactness.
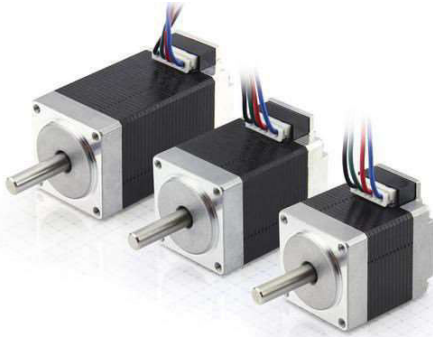

Fig. 13. Hybrid stepper motor [36]

Stepper motor is a type of DC brushless motor that equally divides 360 degree in number of steps. The motor uses open loop mechanism but still a controller is required to command the spindle to move or hold at one of these steps. The main disadvantage of these motors is that their torque is decreased with increase in its speed. These motors are used in devices requires high accuracy like 3D Printers etc. Dong Il Lee [37] proposed an optimal real time design for solar tracking of heliostat using illuminance sensor (CdS) and Simulink program for maximizing the efficiency of solar absorption in receiver. The maximum error was calculated using simulation which is within 1° between 8:00 am and 5:00 pm. Francisco Duarte [38] developed an open loop dual axis sun tracking mechanism based upon solar astronomical data with which exact position of the sun can be predicted for certain location to move the structure accurately. Stepper motors are used for each axis. The system cost and power usage is low as compared to traditional trackers due to simple hardware. According to several studies, the production is approximated to be increased by 40% using dual axes solar tracking mechanism.

Fig. 14. Stepper motor [39]

1) Advantages

- Precise Positioning
- Quite rugged
- Construction is simple
- Little maintenance required and reliable
- At low speeds gives high torque
- No need for position or velocity

2) Disadvantages

- At high speeds torque is diminished
- Noise and resonance
- Current consumption is high
- Suitable for speeds under 1,000 rpm

D. Servo Motors

A servo motor is linear or rotatory actuators used for precise control of velocity, acceleration or position both angular and linear of an object using closed loop mechanism. It uses a potentiometer for its position feedback and need a controller for its operation. They are usually used where high torque is required with increase in speed. They are usually used in automated manufacturing and robotics. P. Roth [27] built a hybrid solar tracking electromechanical system using pyrheliometer and four-quadrant photo detector for feedback and centred instrument using servo motor. If the sun is undetected due

to clouds in sky, a predefined algorithm calculates the position of sun using astronomical formulas and controls the system, until the sensors can again sense the sun. Ching-Chuan Wei [40] proposed a novel method for sun tracking by tracking the brightest region of sky using camera. It is logical to assume that the brightest region of sky represents position of sun. The method is cost effective, real time and accurate in sunny days and building shelters. However, in thick cloudy weather, sun position is possibly far from actual sun centred.
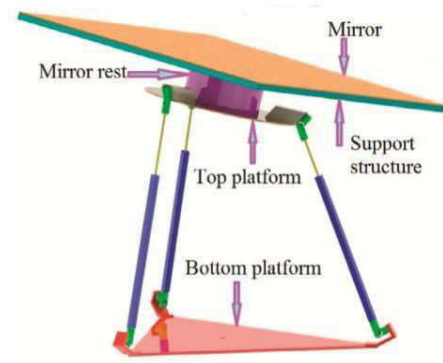
1) *Advantages*

- Relative to motor size higher output power

- Vibration and resonance free operation

- Higher efficiency

- High speed and torque operation

Disadvantages

- Stabilize feedback loop tuning required

- Complex Structure

- Encoder is required

- Motor cooling is poor

- Sustained overload can damage the motor

Fig. 15. Servo motor [41]

(a) CAD model of the 3-UPU wrist

Fig. 16. 3 UPU heliostat and its joints [42]

E. Actuator

A linear or prismatic actuator is an electromechanical device used to change the circular motion of an electric motor into linear motion. Linear Actuators have disadvantages sometime because of their non-constant holding force. They are capable of driving larger structures using their slow drive. James Larmuth [43] shows if we use Helio-40, there will be as small effect on cost on selection of tracking algorithm, but have a large effects on packing ratio, optical performance and control of the heliostat. R.B Ashith Shyam [42] proposed a 3-UPU, three degree of freedom parallel manipulator to use electronically reconfigureable 3-UPU and redundancy to achieve Azimuth-Elevation and Target-Aligned configurations and thus achieve the advantage of both. The serial mechanism has less tracking accuracy as compared to parallel manipulators. A prototype is used and numeric results are validated.

1) *Advantages*

- Components can work in complex configuration

- Flexibility of motion control

- High efficiency

- High torque operation is possible

- Low operation and maintenance cost

2) Disadvantages

- Can be used for moderated speeds only

- High purchase cost

IV. CONCLUSIONS AND RECOMMENDATIONS

Different drives of tracking system for heliostat of solar tower power plant are discussed in detail in this article. Advantages and disadvantages of different type of drives for tracking systems are enlisted. Based on this review, it is concluded that hybrid stepper motor is best suited for heliostat of solar tower power plant. Hybrid stepper motor is selected due to following reasons,

1. Hybrid stepper motor is quite precise and precise tracking of the heliostats is required so that maximum efficiency of the heliostat field can be achieved.

2. Hybrid stepper motor has to operate in harsh desert conditions and it is best suited for these types of conditions due to its rugged nature.

3. Due to large size of heliostat, there is requirement of system with higher torque and hybrid stepper motor supports higher torque under low speeds.

4. Their reliability makes hybrid stepper motor the selection for this application as a system with greater reliability is required.

Following are recommendations:

1. Proper selection of the control system for these drives is required.

2. A control system along with sensors can be constructed to increase the reliability and accuracy.

3. A prototype is to be developed to check all the parameters of the tracking system using hybrid stepper motor

V. FUTURE WORK

A literature survey for different sensors and controls will be carried out that can be selected alongside these drives.

VI. ACKNOWLEDGMENT

The authors would like to thank Chenab College of Engineering and Technology Gujranwala for providing technical facilities and support throughout the course of this work.

REFERENCES

[1] K. Mahboob, S. Tanveer, F. Ali, F. B. Naeem, H. Khalid, and A. Khan, "A review on types of renewable energy technologies and its effect on environment in Pakistan," in *2018 International Conference on Renewable, Applied and New Energy Technologies(ICRANET)Air University Islamabad*, 2018, p. 180140.

[2] K. Mahboob, M. M. Aslam, A. Qaddus, A. Ahmad, U. Mushtaq, and A. Khan, "Design and Analysis of Tower Structure for Solar Thermal Power Plant," in *2018 2nd International Conference on Energy Conservation and Efficiency (ICECE)*, 2018, pp. 30-36.

[3] E. Carra, J. Ballestrín, J. Polo, J. Barbero, and J. Fernández-Reche, "Atmospheric extinction levels of solar radiation at Plataforma Solar de Almería. Application to solar thermal electric plants," *Energy,* vol. 145, pp. 400-407, 2018.

[4] R. Chen, Z. Rao, and S. Liao, "Determination of key parameters for sizing the heliostat field and thermal energy storage in solar tower power plants," *Energy Conversion and Management,* vol. 177, pp. 385-394, 2018.

[5] O. Farges, J.-J. Bézian, and M. El Hafi, "Global optimization of solar power tower systems using a Monte Carlo algorithm: Application to a redesign of the PS10 solar thermal power plant," *Renewable Energy,* vol. 119, pp. 345-353, 2018.

[6] K. Mahboob, M. Irfan, A. Ali, F. Ali, H. Mehmood, and A. Khan, "Design and Analysis of 50MW Solar Power Plant in Multan using Solar power tower technologies," in *2018 International Conference on Renewable, Applied*

and New Energy Technologies(ICRANET)Air University Islamabad, 2018, p. 180142.

[7]   M. J. Wagner and T. Wendelin, "SolarPILOT: A power tower solar field layout and characterization tool," *Solar Energy,* vol. 171, pp. 185-196, 2018.

[8]   P. Hu and W. Huang, "Performance analysis and optimization of an integrated azimuth tracking solar tower," *Energy,* vol. 157, pp. 247-257, 2018.

[9]   A. Kribus, I. Vishnevetsky, A. Yogev, and T. Rubinov, "Closed loop control of heliostats," *Energy,* vol. 29, pp. 905-913, 2004.

[10]   J. Spelling, A. Gallo, M. Romero, and J. González-Aguilar, "A high-efficiency solar thermal power plant using a dense particle suspension as the heat transfer fluid," *Energy Procedia,* vol. 69, pp. 1160-1170, 2015.

[11]   A. News. (2017, 02/10/2019). *Solar thermal power plant announced for Port Augusta 'biggest of its kind in the world'.* Available: https://www.abc.net.au/news/2017-08-14/solar-thermal-power-plant-announcement-for-port-augusta/8804628

[12]   W. Han, J. Hongguang, S. Jianfeng, L. Rumou, and W. Zhifeng, "Design of the first chinese 1 MW solar-power tower demonstration plant," *International Journal of Green Energy,* vol. 6, pp. 414-425, 2009.

[13]   N. Noor and S. Muneer, "Concentrating solar power (CSP) and its prospect in Bangladesh," in *Developments in Renewable Energy Technology (ICDRET), 2009 1st International Conference on the*, 2009, pp. 1-5.

[14]   A. Fritsch, C. Frantz, and R. Uhlig, "Techno-economic analysis of solar thermal power plants using liquid sodium as heat transfer fluid," *Solar Energy,* vol. 177, pp. 155-162, 2019.

[15]   A. Bayon, R. Bader, M. Jafarian, L. Fedunik-Hofman, Y. Sun, J. Hinkley*, et al.*, "Techno-economic assessment of solid–gas thermochemical energy storage systems for solar thermal power applications," *Energy,* vol. 149, pp. 473-484, 2018.

[16]   C. Prieto, A. Rodríguez, D. Patiño, and L. F. Cabeza, "Thermal energy storage evaluation in direct steam generation solar plants," *Solar Energy,* vol. 159, pp. 501-509, 2018.

[17]   K. Mahboob, F. Ali, H. Mehmood, M. Irfan, S. Tanveer, and A. Khan, "Design, analysis and optimization of 50MWe Solar Power Plant in Multan using CSP parabolic trough technology," in *2018 International Conference on Renewable, Applied and New Energy Technologies(ICRANET)Air University Islamabad*, 2018, p. 180610.

[18]   H. Price, E. Lupfert, D. Kearney, E. Zarza, G. Cohen, R. Gee*, et al.*, "Advances in parabolic trough solar power technology," *Journal of solar energy engineering,* vol. 124, pp. 109-125, 2002.

[19]   K. Mahboob, A. Qaddus, M. M. Aslam, A. Ahmad, U. Mushtaq, and A. Khan, "Structural Design of Heliostat for Solar Thermal Power Plant," in *2018 2nd International Conference on Energy Conservation and Efficiency (ICECE)*, 2018, pp. 23-29.

[20]   HENGTAI. (2019, 02/06/19). *Tower Heliostat Cycloidal Gear Reducer Solar Tracking Drive High Precision.* Available: http://www.helicalgearreducer.com/sale-3544594-tower-heliostat-cycloidal-gear-reducer-solar-tracking-drive-high-precision.html

[21]   Solaris. (2019, 02/06/19). *ZOMEWORKS PASSIVE TRACKER - UTR-064.* Available: https://www.solaris-shop.com/zomeworks-utrf-064-passive-solar-tracker/

[22]   WATTSUN. (2019, 02/06/19). *DUAL AXIS TRACKERS.* Available: https://www.altestore.com/store/solar-panel-mounts/active-solar-panel-trackers/wattsun-solar-trackers/wattsun-dual-axis-trackers-p5508/

[23]   M. Dynamics. (2019, 02/10/19). *DC straight motors.* Available: https://www.motiondynamics.com.au/g.p.g-90w-90mm-brushed-dc-motor-12v-or-24v-straight-shaft.html

[24]   W. A. Lynch and Z. M. Salameh, "Simple electro-optically controlled dual-axis sun tracker," *Solar energy,* vol. 45, pp. 65-69, 1990.

[25]   S. A. Kalogirou, "Design and construction of a one-axis sun-tracking system," *Solar Energy,* vol. 57, pp. 465-469, 1996.

[26]   S. Abdallah and S. Nijmeh, "Two axes sun tracking system with PLC control," *Energy conversion and management,* vol. 45, pp. 1931-1939, 2004.

[27]   P. Roth, A. Georgiev, and H. Boudinov, "Design and construction of a system for sun-tracking," *Renewable energy,* vol. 29, pp. 393-402, 2004.

[28]   K. Aiuchi, K. Yoshida, M. Onozaki, Y. Katayama, M. Nakamura, and K. Nakamura, "Sensor-controlled heliostat with an equatorial mount," *Solar Energy,* vol. 80, pp. 1089-1097, 2006.

[29]   n. n. a. r. lab. (2019, 02/10/19). *Brushed DC motor theory.* Available: http://hades.mech.northwestern.edu/index.php/Brushed_DC_Motor_Theory

[30]   C.-d. Lee, H.-y. Yeh, M.-h. Chen, X.-l. Sue, and Y.-c. Tzeng, "HCPV sun tracking study at INER," in *Photovoltaic Energy Conversion, Conference Record of the 2006 IEEE 4th World Conference on*, 2006, pp. 718-720.

[31]   M. M. Arturo and G. P. Alejandro, "High-precision solar tracking system," in *Proceedings of the World Congress on Engineering*, 2010, pp. 844-846.

[32]   N. Barsoum, "Implementation of a prototype for a traditional solar tracking system," in *Computer Modeling and Simulation, 2009. EMS'09. Third*

UKSim European Symposium on, 2009, pp. 23-30.

[33] A. Georgiev, P. Roth, and A. Olivares, "Sun following system adjustment at the UTFSM," *Energy Conversion and Management,* vol. 45, pp. 1795-1806, 2004.

[34] M. C. O. M. Team. (2019, 02/10/19). *Brushless DC Motor.* Available: https://www.motioncontrolonline.org/blog-article.cfm/Brushed-DC-Motors-Vs-Brushless-DC-Motors/24

[35] S. Schell, "Design and evaluation of esolar's heliostat fields," *Solar Energy,* vol. 85, pp. 614-619, 2011.

[36] NANOTEC. (2019, 02/10/19). *Hybrid Stepper Motors.* Available: https://en.nanotec.com/products/2263-hybrid-stepper-motors/

[37] D. I. Lee, W. J. Jeon, S. W. Baek, and N. T. Ali, "Optimal Design and Control of Heliostat for Solar Power Generation," *International Journal of Engineering and Technology,* vol. 4, p. 388, 2012.

[38] F. Duarte, P. D. Gaspar, and L. C. Gonçalves, "Two axes solar tracker based on solar maps, controlled by a low-power microcontroller," *Journal of Energy and Power Engineering,* vol. 5, pp. 671-676, 2011.

[39] Inventables. (2019, 02/10/19). *Stepper Motor.* Available: https://www.inventables.com/technologies/stepper-motor-nema-17

[40] C.-C. Wei, Y.-C. Song, C.-C. Chang, and C.-B. Lin, "Design of a solar tracking system using the brightest region in the sky image sensor," *Sensors,* vol. 16, p. 1995, 2016.

[41] CLR. (2019, 02/10/19). *What is servo motor.* Available: https://clr.es/blog/en/what-is-servo-motor-and-when-is-it-used/

[42] R. A. Shyam and A. Ghosal, "Path planning of a 3-UPU wrist manipulator for sun tracking in central receiver tower systems," *Mechanism and Machine Theory,* vol. 119, pp. 130-141, 2018.

[43] J. Larmuth, K. Malan, and P. Gauché, "Design and cost review of 2 m2 heliostat prototypes," *Port Elizabeth,* 2013.

Significance of Fly Ash on Compressive Strength of Concrete with Different Curing Techniques

Norheen Amina[1,a], Dr. Muhammad Arif Khan[2,b], Engr. Hira Ishtiaq[2,b]

[1]*Architectural Engineering, UET, Lahore, Pakistan*

[2]*Architectural Engineering, UET, Lahore, Pakistan*

[2]*Civil Engineering, UOL, Lahore, Pakistan*

Email Address: [a)]archiengg_noor@yahoo.com , [b)]chairmanaed@uet.edu.pk , [b)]hiraishtiaq10@gmail.com

Abstract—**In this research fly ash concrete has been investigated through experimental studies on various techniques of curing that is implemented to observe the strength gaining trend. For this purpose, curing techniques vary from conventional curing to modern technique of curing including self-curing. Self-curing is a process to hydrate the inside of concrete. Self-curing does not only increase the strength but also reduces the risk of autogenous shrinkage. Self-curing is only possible through materials which serve as internal water reservoirs to concrete.**

It has been proved in various studies that brick is one of the effective materials as aggregate replacement. This study explores the behavior of over burnt brick for self-curing concrete instead of normal brick. Furthermore, over burnt brick has not yet been much investigated for this particular reason.

Keywords—self-curing, curing techniques, over burnt brick ballast, fly ash mix concrete, compressive strength

I. INTRODUCTION

There are four main reasons of defects in concrete; 1-Insufficient reinforcement and concrete cover 2- Removal of Premature formwork 3-Speedy completion of work 4-Inexperienced workmen and lack of inspiration [1]. The success of building depends upon its performance that how it behaves against environmental effects. When building is designed properly and constructed according to design standards it will have specified design strength. Problems faced in reinforced concrete structures are not restricted to those where the concrete is not aimed for durability. It also comprises concrete structure which is not constructed for good performance and for durability. So the second reason of problems in reinforced concrete buildings is related to poor construction. In fact, many of the problems encountered today in reinforced concrete structures are related to inadequate construction practices [2]. The admixtures are added to achieve the targeted strength. Fly ash, silica fume and blast furnace slag are admixtures used in concrete not only to increase strength but also helps to develop a sustainable environment [3]. The admixtures not only reduce pollution by replacing cement but also reduce dumping issues of industrial waste [4].

One of the important characteristics effecting concrete strength is curing and it becomes critical when admixtures are added [3]. The use of self-curing techniques is useful to further enhance the strength of concrete and to resolve the problem of labor negligence. For this purpose, light weight aggregate can be used as replacement of coarse aggregate [5].

The use of Polyvinyl alcohol with optimum dosage of 0.48%, when measured by the weight

of cement, can serve as successful self-curing agent beyond this polyvinyl alcohol is not an efficient self-curing agent. It delivers higher compressive, tensile and flexural strength [6].

It can be concluded that, concrete with self-curing agent Poly Vinyl Alcohol (PVA) attain strength equal to normal curing concrete whereas concrete with agent Super Absorbent Polymer (SAP) does not [5].

II. EXPERIMENTAL PROCEEDURE

A. Cement

The physical properties of cement effect the setting time, strength of concrete, abrasion resistance, resistance to freeze thaw effect, resistance to acid and alkali's attack and rate of hydration [3]. Cement used in this research work was Pioneer Cement which is ordinary Portland cement (reside to category I cement according to ASTM) and manufactured locally.

B. Sand

Lawrancepure sand was used in this research as fine aggregate. Sieve analysis was performed on sand to find its grain size. Furthermore, bulk density, water absorption and specific gravity tests were performed on sand to analyze other physical properties.

C. Coarse Aggregate

Preliminary tests performed on aggregate were sieve analysis, bulk density, water absorption and specific gravity to find grain size, loose and compacted density and % pores present in it, amount of water absorbed and specific gravity respectively. In this research margalla crush was used with maximum size 20mm (3/4").

D. Over Burnt Brick Ballast

The properties of concrete that uses crushed bricks as partial substitute of natural aggregate shows better results. The experimental investigation shows that higher strength concrete can be achieved by using crushed brick aggregate [7]. It has been studied that even recycled brick can also be used as coarse aggregate in concrete [8]. Bricks investigated for this study were taken from brick kiln near kala khatai morr. Later these bricks were converted to brick ballast by following procedure.

Bricks were taken from brick kiln near kala khatai morr.

Compressive strength of over burnt bricks was checked. Then bricks were crushed in crusher to form aggregate.

Fig. 1. Preparation of over burnt brick ballast from over burnt bricks

Over burnt brick ballast then sieved manually to get maximum size 20mm.

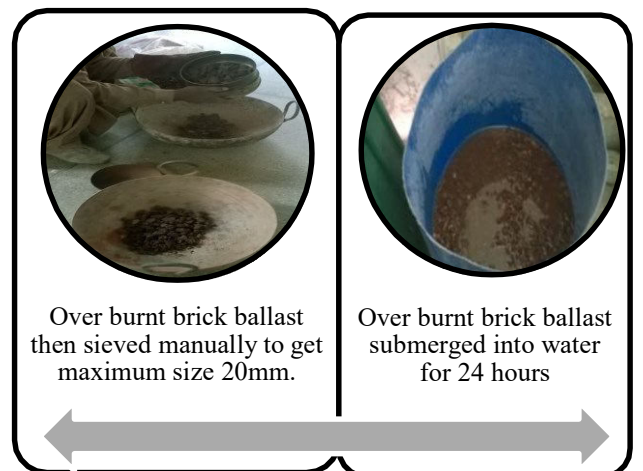Over burnt brick ballast submerged into water for 24 hours

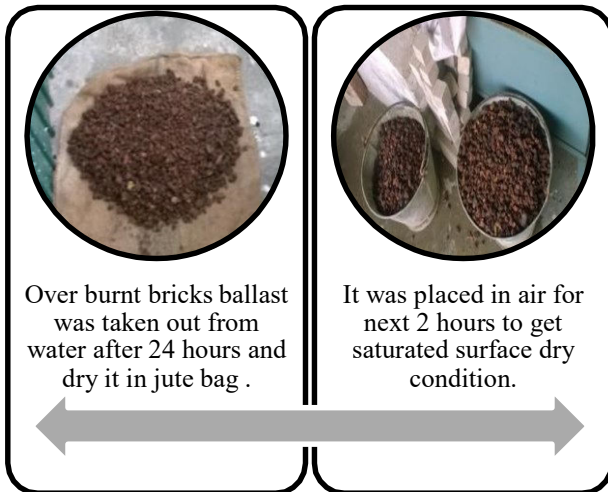Fig. 2.Preparation of over burnt brick ballast from over burnt bricks

Fig. 3.Preparation of over burnt brick ballast from over burnt bricks

Over burnt bricks or brick bat produced in kiln due to uneven temperature are waste bricks [8]

E. Fly Ash

Fly ash used in this study was obtained from ICI Pakistan Limited Jhelum. Fly ash was classified as F class according to ASTM C-618. Color of fly ash obtained was brown. Chemical composition of fly ash was also monitored.

F. Water

For mixing and curing of concrete tap water was used.

G. Preparation of Concrete Mixture

All the experimental work was performed in structure lab of Architectural Engineering Department UET Lahore. The experimental program was designed to investigate the compressive strength of fly ash in concrete and varying the curing techniques from conventional immersion to self-curing. For this purpose, nominal mix of M25 1:1:2 was selected with water to cement ratio as 0.4.

Concrete cubes of size 4" and cylinder 4"X8" were casted, cured and tested. To achieve maximum compressive strength fly ash was checked at 0%, 10% and 20% cement replacement by weight. Total nine cubes were casted consisting three cubes of each percentage. Percentage cement replacement of fly ash with maximum compressive strength was selected to prepare concrete mix. Concrete with fly ash and without fly ash were casted and cured at eight curing techniques. Self-curing technique was also included. For self-curing over burnt brick ballast was used as aggregate replacement. Compressive strength of over burnt brick ballast was checked at 0%, 25%, 50%, 75% and 100% aggregate replacement by weight. Total eighteen cubes were casted including three cubed for each replacement of aggregate. In experiments lawrancepur sand and margalla was used as aggregate. 28 days curing strength of compression was determined at 8 curing techniques. For each curing techniques four cubes for fly ash concrete and four cubes for concrete without fly ash were prepared. So total 64 cubes were prepared. 18 cylinders casted, 3 for each curing technique. Cylinders were casted only for three curing techniques i.e. ponding, air curing and internal external curing with external curing through ponding. Compressive strength of fly ash concrete was compared to ordinary concrete. Total 85 cubes and 18 cylinders were casted.

H. Curing Techniques/ Methods

The concrete samples (cubes and cylinders) were hydrated using eight different techniques until their compressive strength was determined at 28 days. The curing techniques that were applied are:

- Water Submerged Curing/Ponding (A): This involved the submersion of the

concrete cube and cylinders specimens in water according to ASTM C31 .

- Burlap Curing (B): This involved covering the concrete samples (cubes and cylinders) underneath burlap which was kept wet twice a day [9].
- Moist Sand Curing (C): This involved submerging entire concrete samples (cubes and cylinders) in wet sand which was kept moist by wetting the sand on daily basis [9].
- Air Curing (D): This served as the control. It involved no form of active curing by just exposing the samples to ambient air in the Laboratory.
- Polythene Curing (E): The specimens were covered with at least two layers of polythene sheet to prevent moisture movement from the concrete specimens (cubes) [9].
- Self-Curing (F): The specimens were prepared by using brick ballast as light weight coarse aggregate and curing by just exposing the specimens (cubes and cylinders) to ambient air in the Laboratory [6].
- Self-Curing with External Curing by Ponding (G): The specimens were prepared by using brick ballast as coarse aggregate and curing by just submerging the specimens (cubes and cylinders) in water.
- Self-Curing with External Curing by Polythene (H): The specimens were prepared by using brick ballast as coarse aggregate and curing with at least two layers of polythene sheet to prevent moisture movement from the concrete specimens (cubes).

Concrete was 0 % replacement of fly ash nominated as 2 and concrete with 10% replacement of fly ash named as 1.

III. PRELIMINARY TESTS

Following test was done on concrete or aggregate before casting to check the physical properties of concrete. Experimental investigation was carried out in structure lab, material and testing lab and soil lab.

- Sieve Analysis as prescribed in the ASTM C136
- Bulk density prescribed in the ASTM C-29
- Moisture absorption and Specific gravity as prescribed in the ASTM C128 and ASTM 127-04
- Slump test ASTM C 143

IV. RESULTS AND DISCUSSION

A. Comparison between Physical Properties of Gravel and Over Burnt Ballast

From preliminary tests to check the physical properties of gravel were compared with over burnt brick ballast.

TABLE 1. COMPARISON BETWEEN PHYSICAL PROPERTIES OF GRAVEL AND OVER BURNT BALLAST

Property		Gravel	Brick Ballast
Specific Gravity		2.805	0.505
Maximum Nominal Size (mm)		20	20
% Water Absorption		0.805	11.77
Bulk Density (kg/m³)	Loose	1376.76	590.9
	Compacted	1577.46	717. 17
% Voids		14.58	21.36

From test results it was concluded that specific gravity of gravel was greater than over burnt brick ballast. The maximum nominal size chosen was 20 mm so passing of ¾" sieve and

retaining of ¼" sieve was selected for experiments.

Water absorption of brick ballast was significantly greater than gravel. As water absorption of gravel was 0.805% and water absorption of over burnt brick ballast was 11.77%. Over burnt brick ballast absorbed greater quantity of water. Finally, bulk density of gravel both loose and compacted was greater than over burnt brick ballast and percentage of voids was greater for over burnt brick than normal gravel.

B. *Slump Test*

Slump test carried out on concrete to check the workability. Over burnt brick ballast was replaced with gravel by weight. For different percentage of over burnt brick ballast the slump was checked.
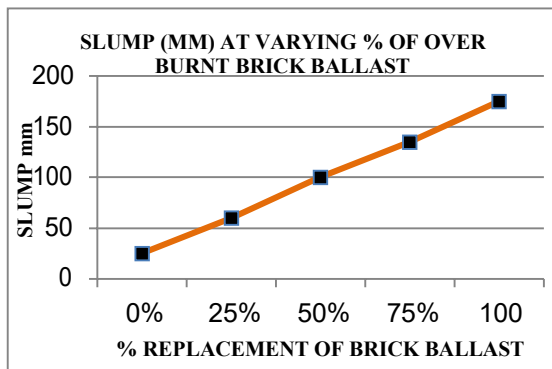

Fig. 4. Relationship between slump and % of over brick ballast as aggregate replacement in concrete

Workability increased with addition of over burnt brick ballast in concrete. At 0% replacement slump value was 25mm (1"). At 25% replacement, slump value was 60mm (2.3").

At 50% replacement slump value 100 mm (4"). In the same way 75% and 100%

replacement gave slump value as 135mm (5.5") and175 (6").

C. *Compressive Strength Test*

All the cylinders and cubes were removed from curing and tested for compressive strength. The test was carried out as prescribed in ASTM C-39. Compressive strength = load /area (N/mm^2)

Purpose of varying fly ash was to find out optimum value to form fly ash mix concrete. Cubes were taken out of water at day 7, dried properly; weighed accurately and compressive strength was checked in UTM at uniform loading 2N/sec.

7 days curing strength of small cubes were tested at 0%, 10% and 20% replacement of fly ash by weight of cement. The compressive strength was 30.88 N/mm^2, 35.88 N/mm^2 and 32.27 N/mm^2 respectively. Maximum compressive strength 35.88 N/mm^2 was obtained at 10% replacement of fly ash. Further increase in fly ash decreased the compressive strength.
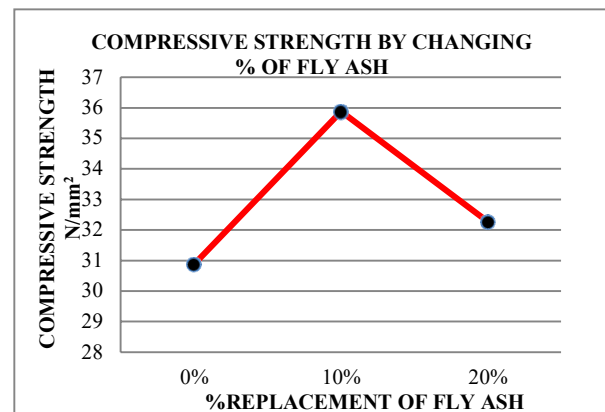

Fig. 5. Relationship between compressive strength and % replacement of fly ash as cement

Small cubes (100mmx100mmx100mm) with nominal mix of M25 (1:1:2) and 0.40 w/c were prepared using overburnt brick ballast as partial replacement of aggregate. 7 days curing

compressive strength of small cubes were tested at 0%, 25%, 50%, 75% and 100% replacement of crushed bricks by weight of coarse aggregate. The compressive strength was 30.88 N/mm^2, 39.13N/mm^2,36.82 N/mm^2, 33.83 N/mm^2, and 31.05 N/mm^2 respectively. Maximum compressive strength was 39.18 N/mm^{2}at 25% replacement. 25% replacement increased compressive strength 26.71% than 0% replacements of crushed over burnt brick. Further increase in crushed bricks decreased the compressive strength.
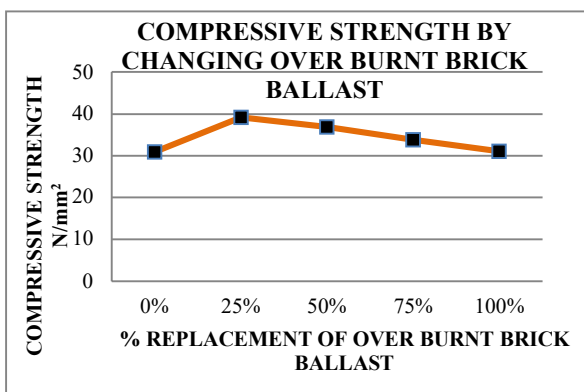

Fig. 6. Relationship between compressive strength and % replacement of brick ballast as aggregate

Concrete cubes of size 4" and cylinder 4"X8" with nominal mix of M25 (1:1:2), 0.40 w/c using 10% fly ash as partial replacement of cement and 25% over burnt brick ballast as partial replacement of coarse aggregate were casted, cured for 28 days and then checked for compressive strength in UTM. The results are as follows:

- G2 cubes got maximum compressive strength which is 54.9 N/mm^2 and D2 cubes got minimum compressive strength that was 39.46 N/mm^2 .So, increase in strength was 39.13%.

- A2 cubes gave good results, the compressive strength of concrete is 52.54 N/mm^2 there is 38.22% increase in

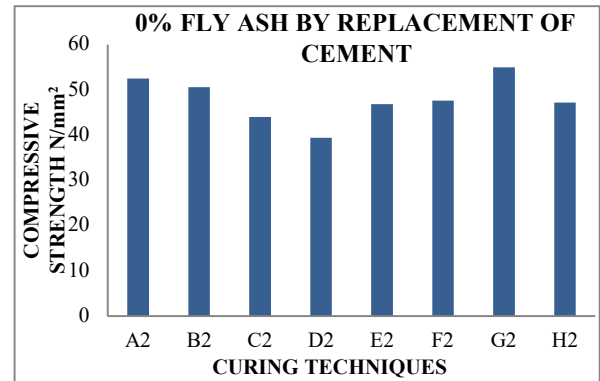strength than D2 cubes and 4.3% decrease in strength as compared to G2.

Fig. 7 Relationship between compressive strength of simple concrete and curing techniques /methods/ conditions

- B2, C2, E2 cubes showed compressive strength as 50.69 N/mm^2, 44.01 N/mm^2, 46.56 N/mm^2 respectively. The increase in strength was 28.46%, 11.53%, 17.99% than air cured concrete respectively.

- F2 cubes and H2 cubes revealed compressive strength as 47.67 N/mm^2 and 47.05 N/mm^2. The increase in strength was 20.8% and 19.2% than D2 respectively.
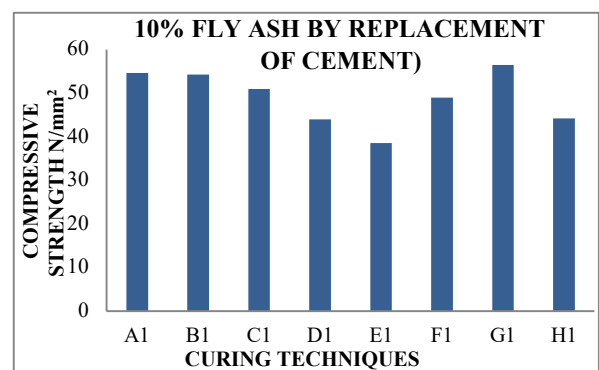

Fig. 8 Relationship between compressive strength of fly ash concrete and curing techniques /methods/ conditions.

- G1 cubes with developed maximum compressive strength which was

56.5N/mm^2 and D1 cubes got minimum compressive strength that was 44.09N/mm^2. So increase in strength was 27.22%.

- A1 cubes achieved the compressive strength of concrete as 54.705N/mm^2 there is 24.08% increase in strength than D1 cubes and 3.2% decrease in strength as compared to G1.

- B1, C1, cubes showed compressive strength as 54.26 N/mm^2, 50.98 N/mm^2, respectively. The increase in strength was 23.06%, 15.63%, 17.99% than air cured concrete respectively.

- E1 cubes showed compressive strength as 38.61N/mm^2 which was less than D1 cubes and % decrease was 12.42.
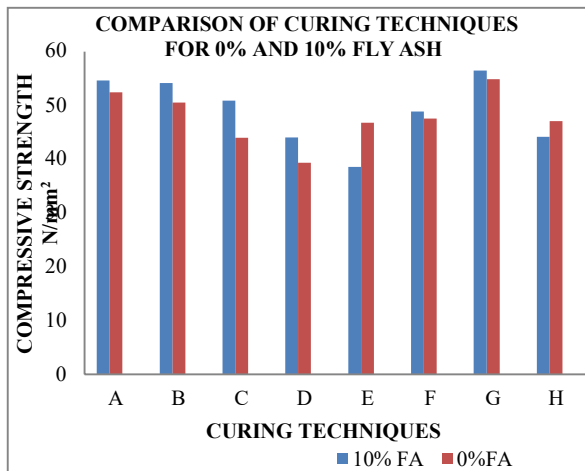

Fig. 9 Relationship between compressive strength of fly ash concrete and simple concrete at different curing techniques /methods/ conditions

- F1 cubes and H1 cubes revealed compressive strength as 48.98N/mm^2 and 44.28N/mm^2. The increase in strength was 13.38% and 2% than D2 respectively

- G1 cylinders also achieved maximum compressive strength which was

40.21N/mm^2 and maximum compressive strength of G2 cylinders is 36.47N/mm^2

- A1 cylinders achieved the compressive strength as 40.88N/mm^2. A2 cylinders got compressive strength 24.47 N/mm^2.

- D2 cylinders got minimum compressive strength that was 24.47 N/mm^2 while D1 cylinders got compressive strength 39.88 N/mm^2.

- Compressive strength of cylinder was less than compressive strength of cubes. Average % decrease is 28.15%.

V. CONCLUSIONS

Slump value increased with increasing value of brick ballast. At 0% replacement of crushed brick slump value is 25mm (1"). At 25% replacement, slump value is 60mm (2.3"). At 50% replacement slump value 100mm (4"). In the same way 75% and 100% replacement gave slump value of 135mm (5.5") and 175mm (6").

Compressive strength of concrete with 10% fly ash (replacement of cement) by weight was higher than concrete without fly ash. But Compressive strength decreased when quantity of fly ash increased beyond 10 % (replacement by weight of cement). Internal curing was an efficient way of curing. Because in this process concrete is hydrated from inner side and self-desiccation of concrete was unlikely to happen.

Over Burnt Brick ballast can also be used for internal curing of concrete. Brick ballast should be in saturated surface dry conditions. Otherwise, surface water contributes to the workability of concrete and targeted strength cannot be achieved.

Moreover, in this study E1 (Polythene Sheet Curing) concrete showed compressive strength as 38.61N/mm^2 which is less than D1 (air cured) cubes and % decrease was 12.42. So, this type of curing (impermeable covering) was not suitable for fly ash mix concrete.

The unit weight of lightweight concrete produced with brick ballast was less than concrete produced with aggregate. Max Density of concrete was 2513 Kg/m^3 and minimum density 2424 Kg/m^3. When brick ballast was added the density reduces from 2246 Kg/m^3 to 2189 Kg/m^3. The unit weight of lightweight concrete produced with brick ballast was less than concrete produced with aggregate. So, there was 10% reduction of density resulting reduction in dead load of structure. By using lightweight concrete, the dead load and as a result the weight of the building can be substantially decreased. So, it is possible to reduce the dimensions of the supporting structure to minimize the earthquake force on the building and economize the project.

VI.   RECOMMENDATIONS

- Self-cured concrete (using over burnt brick as aggregate replacement) should be used in multistoried buildings and vertical members where water submerged curing is inaccessible. It is highly recommended in areas like Lahore, Multan where hot climate is a major problem. It is also suitable in water scarce areas or where salinity of water is big issue like in different cities of Sindh.

- Compressive strength of concrete made of over burnt brick should further be studied at 56 or 90 days to find out ultimate strength of concrete.

- Durability aspect of concrete made of over burnt brick aggregate should further be checked for permeability and freezing thawing effect.

- Compressive strength of concrete made of over burnt brick should also be studied by changing different sand characteristics to find out ultimate strength of concrete.

- Self-curing properties should further be increased by replacing sand with surkhi to determine ultimate strength.

REFERENCES

[1] Femi, O. T. (2014). Effects Of Faulty Construction On Building Maintenance. *International Journal of Technology Enhancements and Emerging Engineering Research*, *2*(3), 73–79.

[2] Chahal, N., Siddique, R., & Rajor, A. (2012). Influence of bacteria on the compressive strength, water absorption and rapid chloride permeability of concrete incorporating silica fume. *Construction and Building Materials*, *37*(1), 645–651. https://doi.org/10.1016/j.conbuildmat.2012.07.029

[3] Neville A.M., (2000), "Properties of Concrete", Final Edition, pp.844.

[4] Anil, S., Reddy, K., & Reddy, K. C. (2015). Effect of Fly Ash on Strength and Durability Parameters of Concrete, *4*(5), 2013–2015.

[5] Kumar, P. M., Sastry, K. V. S. G. K., Student, M. T., Engineering, C., Reddy, G. P., College, E., & Pradesh, A. (2016). Strength Characteristics of Self Curing Concrete With Different Self Curing Agents, 16511–16517.

https://doi.org/10.15680/IJIRSET.2016.050
9143

[6] Evangeline, S. (2014). Self Curing
Concrete and Its Inherent properties.
*International Journal of Engineering
Research and Applications*, *4*(8), 66–71

[7] Cachim, P. B. (2009). Mechanical
properties of brick aggregate concrete.
Construction and Building Materials,
23(3), 1292–1297.
https://doi.org/10.1016/j.conbuildmat.2008.
07.023

[8] Kallak, F. S. (2009). Use Of Crushed
Bricks As Coarse Aggregate In Concrete.
Tikrit Journal of Eng. Sciences, *16*(3), 64–
70.

[9] Raheem, A. A., Soyingbe, A. A., &
Emenike, A. J. (2013). Effect of Curing
Methods on Density and Compressive
Strength of Concrete. *Cement and Concrete
Composites*, *3*(4), 55–64

A review of the types and applications of solar energy technologies and their effect on environment in Pakistan

Kamran Mahboob [1, 2, a], Abdul Qaddus [2, b], Muhammad Muneeb Aslam [2, c],
Farman Ali [2, d], Saad Bin Tanveer [2, e], Awais Khan [1, f]

[1]Dept. of Mechanical Engineering, University of Engineering and Technology Lahore, Pakistan

[2]Dept. of Mechanical Engineering, Chenab College of Engineering and Technology Gujranwala, Pakistan

Email address: [a] mahboobccet@gmail.com , [b] aqaddusccet@gmail.com , [c] muneebaslamccet@gmail.com, [d] farmanaliccet@gmail.com [e] saadccet@gmail.com [f]awais211@uet.edu.pk

Abstract— Greater dependencies on fossil fuels for power generation have damaged the global environment severely in past few decades. Effect of these climate changes are seen everywhere and more severely in South Asian region. Severe energy crisis in countries like Pakistan has pushed them more and more towards thermal power generation through fossil fuels. The use of fossil fuels has greatly disturbed the echo system and has increased local temperatures. Effects of these changes are evident from glaciers of Himalayas and indirectly these disturb all the river system across South Asia. In this article, an approach to harness the solar energy for power generation is discussed in detail. Different methods currently available for converting solar energy to electrical power are discussed. These covers mirror reflection and concentration technologies like solar tower thermal power plant, solar parabolic trough, enclosed trough, solar parabolic dish for steam and sterling engine applications, flat plate collector, fresnel technologies, linear fresnel reflector, solar updraft tower, photovoltaic and roof heating systems etc. Application of these systems as well as advantages and disadvantages of different methods are enlisted. Furthermore, their effect on climate is also discussed in detail. Also different regions across Pakistan are highlighted that are suited for each type of technology. This include sunshine, heat and radiation map, DNI etc. In the later part of this article, effects of solar energy on environment are discussed. It is concluded that direct solar power is useful all across Pakistan and concentrated solar technology is best suited for the southern region technically and both of these have positive effects towards environment.

Keywords—Environment, Solar thermal energy, Climate change, Power plant, Radiation Map of Pakistan

I. INTRODUCTION

As the population of Pakistan is growing and a migration to cities continues, electricity consumption is increasing. There exist a considerable gap between generation and demand causing longer hours of load shedding [1]. FY2017 showed consumption growth in Household and agriculture sectors in Pakistan [2].
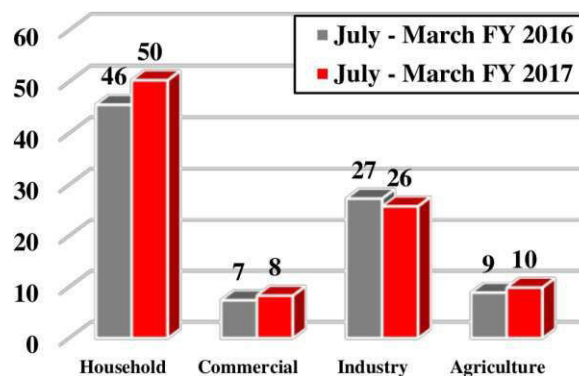

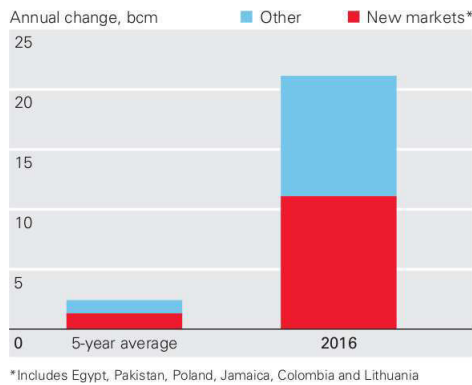Fig.1. Share of Electric Generation [2]

Fig.2. LNG Supply and Demand [3]

Due to increase in demand, new generation plants are under process. Majority of these are thermal in nature and will use LNG or coal as fuel. Bhiki power plant is operational from 2017 and uses gas for electricity generation. Sahiwal coal power plant, Bin Qasim coal power plant, Baloki, Haveli Bahadur Shah plants are all thermal power plants.

Renewables (other than hydro), which could diminish high cost powerlessness, contribute under 1% of the current sustainable power source blend. Pakistan has huge potential in renewable and an extensive effort is required to develop this area in Pakistan [4]. This will create cheap electricity without harming the climate.
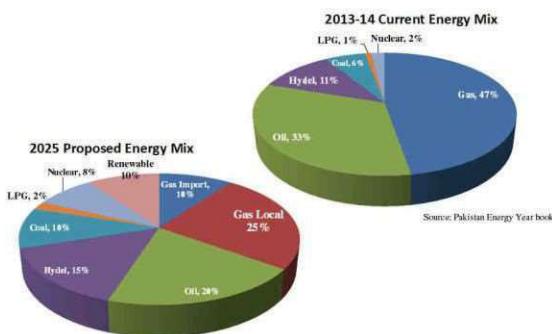

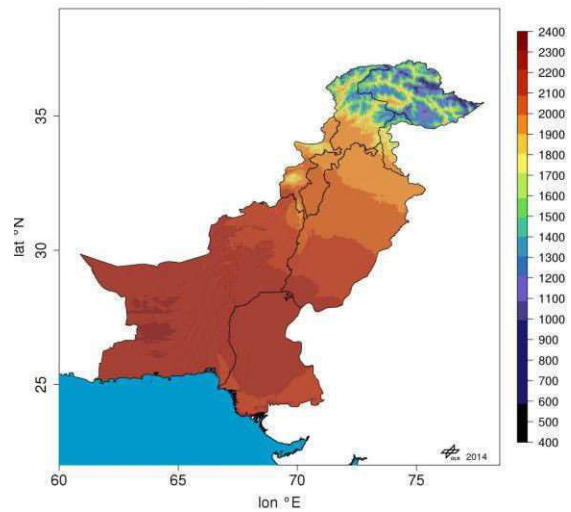Fig.3. Pakistan's Current and Proposed Energy Mix [5]

Fig.4. Global Horizontal Irradiance for Pakistan in KWh/m^2 [6]

A. *Global Horizontal Irradiance for Pakistan*

Renewable energy especially Solar can be used to cover the gap between capacity and demand of the power sector in Pakistan. Nearly 90% of land area in Pakistan has a Global horizontal irradiance (GHI) value above 1500KWH/m^2 and especially in southwest of Pakistan irradiation level is comparable to the best of the world. According to world bank estimation mean value of GHI annually is 2071KWh/m^2 for entire Pakistan [7].

II. SOLAR ENERGY TECHNOLOGIES

Solar energy technologies convert solar energy to other forms of energy like electrical, potential, heat etc., that can be used for household, commercial and industrial purposes [8]. Solar energy technologies (SET) can supply controllable power for varying demands that makes it unique amongst other renewable technologies [9]. An integrated storage like thermal, potential or electrical enables SET to supply the power even during non-production hours like night or cloudy day. Dispatchable and reliable nature of SET can enable them to form future low-carbon power grid and will support renewable energy technologies.
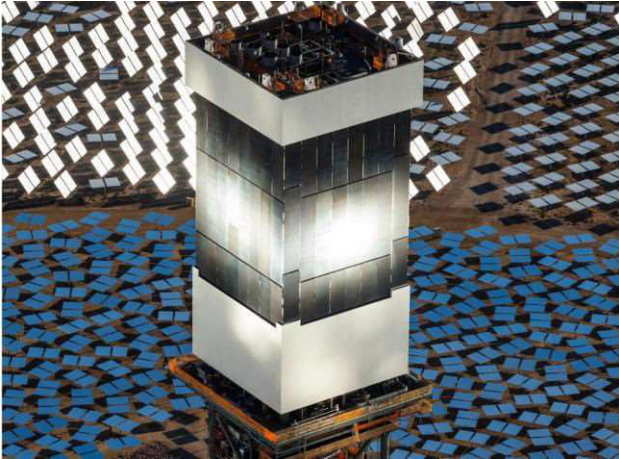
Fig.5. Ivanpah Solar Power Plant [10]

Solar thermal energy technologies can be categorized as follows;

    A. Concentrated solar energy technologies.

    B. Direct solar energy technologies.

A. Concentrated Solar Energy Technologies

Concentrated solar energy technologies (CSET) focus on the solar radiations using mirrors or reflective surfaces. Focusing radiations from large area to a small area produce high concentration that can be used for heat or power generation [11]

Concentrated solar energy technologies can be subdivided into following types:

1. Linear concentrating technologies

2. Solar tower power plant

3. Solar Parabolic dish technologies

4. Concentrated photovoltaic technologies

1) Linear Concentrating Technologies:

Linear concentrating technologies (LST) consist of long flat, rectangular or curved shape reflecting surfaces that focus the solar radiations to a long tube placed on the focus line. Around 95% of solar thermal based power plants are of LST.

LST can be subdivided into following types;

a) Parabolic trough

b) Enclosed trough

c) Linear fresnel reflectors

a) Parabolic Trough

Parabolic trough consists of a curved parabolic cross section trough having mirrored reflecting surface that focuses the solar radiations to an absorbing receiver placed on the focus line [12]. The receiver consists of a glass tube of larger length in which a fluid is flowing. Parabolic trough consists of one axis tracking system that positions the trough whole day so that radiations remain focused on the receiver regardless of sun's changing position. This incorporates daily variations whereas seasonal variations are neglected as one axis tracking is used. A vacuum is present between receiver and enclave glass tube that will reduce the heat losses due to convection considerably. As fluid flows through the length of the receiver, it becomes heated. Water, oil and molten salt are common fluids used in the receiver. Superheated steam is generated directly or using heat exchangers depending upon type of fluid flowing. This steam will run the turbine and electricity is produced. The fluid is recycled again and again in the receiver [13].

Fig.6. Solar Parabolic Trough [14]

Fig.7. Enclosed Trough [15]

b) Enclosed Trough

The Enclosed trough consists of a curved reflecting mirrors system that is enclosed in a glasshouse. This is greenhouse type enclosure and uses greenhouse effect to increase the efficiency of the system by increasing inside temperature, decreasing heat losses and protecting from other environmental effects [16].

Sun is tracked daily by one axis tracking system and light is converged to the receiver. The receiver is a steel pipe through which water/steam is flowing. This steam passes through a turbine to produce electricity. It can also be fed to oil wells for enhanced oil recovery process [17].

c) Linear Fresnel Reflectors

Fresnel reflector works on the same principle as parabolic trough. It consists of long, thin mirror strips placed such that they produce fresnel lens effect. These strips focus the light onto a receiver. Fresnel effect receiver is placed at small focal length and trough has larger aperture diameter. These reflectors are capable of concentrating the light to an intensity of 30 times the original. The main difference between parabolic trough and linear fresnel is that receiver is fixed above the mirror field [18]. Cost of fresnel reflectors is less compared to parabolic trough as their manufacturing is relatively easy [19].

Fig.8. Linear Fresnel Reflectors [20]

2) Solar Tower Power Plant:

Solar tower power plant is the most used technology for solar power generation after the parabolic trough plant. It consists of a large tower placed at the middle and large number of heliostat placed around it in a field [21]. Heliostat field reflect the light to the top of the tower on which receiver is placed [22]. Heliostat has two axis tracking system that tracks the sun and focuses the light to the tower all day long, over the span of complete year. The molten salt, oil or water is used as HT fluid and is pumped to the receiver placed on top of the tower [23]. In the receiver, it is heated and either converted to steam if water is used or heat exchanger produces superheated steam that drives the turbine and electricity is produced [24].

Fig.9. Ivanpah Solar Power Plant [25]

Fig.10. Solar Concentrator in Mohammed bin Rashid Al Maktoum Solar Park [26]

3) Solar Parabolic Dish Technologies:

The Solar parabolic concentrator is a concentrated solar power system that consists of a parabolic shape dish that concentrates light onto its focal point. It has two axis tracking system to track the sun all day long throughout the year. Parabolic dish concentrator consists of parabolic mirror facets that concentrate the solar radiations to a receiver. The receiver is mounted on the end of boom structure at the focal point of the mirrors. The receiver is either a stirling engine or steam generator [27]. The efficiency of solar parabolic dish is higher compared to other CSP technologies. The dishes of various ranges can be find, most of them generally ranges between 10 to 25 kW. Larger prototype model of 400 m^2 is now in process [28].

4) Concentrated Photovoltaic Technologies

This is a combination of solar concentration system and photovoltaic technologies. In this system, a concentrated beam is focused onto a receiver that is made up of high concentration photovoltaic material. This solar cell receiver convert the highly concentrated solar radiations to electricity. The electricity generation efficiency is higher at higher concentrations [29]. A portion of the converged radiation is converted to electricity and remaining energy can be used in other applications in the form of heat energy [30].

Fig.11. Concentrated Photovoltaic Cogeneration system [29]

B. Direct Solar Power Technologies

Direct solar power technologies can be subdivided into following types;

1. Flat plate solar collector technologies

2. Solar Updraft Towers technologies

3. Photovoltaic cells

1) Flat Plate Solar Collector:

Flat plate collector technologies consist of an absorber plate placed inside an insulated box having glass or plastic on the top. Solar radiations pass through the glass sheet and are absorbed by the plate. Tubes are attached to the plate through which fluid is circulating [31]. Flat plate solar collectors are usually used for household water heating systems. Their typical applications are for technologies ranging between 30-70 degree Centigrade.

Fig.12. Flat Plate Collector [32]

Fig.13. Solar Updraft Tower Prototype Manzanares [33]

2) Solar Updraft Towers Technologies:

A solar updraft tower consists of a large tower with a large greenhouse structure at its base. A turbine is placed at the base of tower. Air inside greenhouse structure is heated by the sun rays and it tries to go up through the tower. Turbine placed between base and tower is driven by upward movement of air and electricity is generated [34].

3) Photovoltaic Cells:

A photovoltaic (PV) cell is made up of semiconductor material that generates electricity when sun rays fall on it. Photon present in the light strikes the material and some of them are absorbed and liberate some of electrons to the top of surface. With more and more electron coming to the surface, a potential is created between up and down surface of the cell [35]. This will create a potential difference causing the current to flow and generate electricity. Efficiency of solar cells varies between 5-10%. They are quite useful for off grid applications.

Fig.14. Flat Photovoltaic Cells [36]

III. APPLICATION OF SOLAR ENERGY TECHNOLOGIES

Applications of solar energy technologies are as follows:

1. Main application of the solar technologies is to generate electricity. That ranges from small roof top PV unit to large solar parks, sterling engine units and solar thermal power plants.

2. Solar thermal energy can be used for heating the houses in the winter and solar air conditioning in the summer.

3. Solar energy technologies can be used for water cleaning and desalination process especially along the coastal belt and in areas where water is contaminated.

4. Solar energy technologies can be used in vehicles and transportation.

5. Solar energy technologies can be used to generate steam that can be used for different industrial processes like textile factories, paper mills, eatable cooking and packaging, fruits drying units and enhanced oil recovery.

6. Solar water pumping is very useful in off grid areas.

7. On a very small scale, we can see the use of photovoltaic systems to power household application like watches, calculators etc.

IV. ENVIRONMENTAL AND ECONOMICAL EFFECTS

Solar energy will have environmental and economical impacts. The advantages and disadvantages are discussed as follows:

A. *Advantages of Solar Energy Technologies*

The main advantages of solar energy technologies are as follows:

1. One of the biggest advantage of solar energy is that it is clean and environment friendly.

2. Solar energy does not have carbon emission as in case of fossil fuels and does not harm the environment.

3. No greenhouse effect as in the cases of fossil fuel technologies.

4. Solar energy does not emit dangerous pollutant that can damage the ground, river and ocean water.

5. Solar energy is quite predictable compared to other renewable technologies like wind power etc. If the storage is integrated, a consistent 24-hour power is obtained.

6. Existing plants, grids and other facilities can be integrated with solar energy technologies.

7. Running a solar energy power plant has a negligible running cost as no fuel cost involved.

B. *Disadvantages of Solar Energy Technologies*

The main disadvantages of solar energy technologies are as follows;

1. Some of solar power plants use water as liquid flowing inside plant. These plants are usually situated in desert or water deficiency areas. Greater use of water in the plant can disturb Eco system.

2. Concentrating power plant can affect wild life and birds if they come to the heat zone. In addition, some endangered species can be forced to move or harmed especially in desert areas.

3. Higher starting cost is a big issue in solar energy plants. Financing the project is also an issue due to higher start-up costs.

V. CONCLUSIONS AND RECOMMENDATIONS

This article has discussed solar energy technologies and their applications in detail. Pakistan is relying more and more on thermal power generation from fossil fuels which is increasing the cost per unit and harming the environment. With more and more burnt fuel particles in the air, rain is becoming acidic that in turn damage the ground, river and ocean water along with polluting the air and smog is quite common in cities near these plants. Pakistan has plenty of sunshine and solar angle to harness solar energy that will be clean and cost effective. In the previous section, advantages and disadvantages of solar energy technologies are discussed in detail and keeping them in view, solar energy is best solution to avoid greenhouse gases, contamination and have other benefits.

Following are recommendations;

1. PV panels should be installed all along Pakistan and special subsidy should be given by government in this regard. Dual way meter should be installed that will reduce the cost of batteries and will encourage greater house hold production.

2. Concentrated solar plant should be installed in southern Pakistan. Desert areas like Thar, Thal and vast areas of Baluchistan are best suited.

3. Solar heating and cooling should be encouraged and flat plate collector should be installed in the north of Pakistan for heating the homes and solar air conditioning in the south.

4. Solar desalination plant should be developed and installed all across the coastal region to get drinkable water.

5. As the PV market is growing, there is need to establish research facilities for enhancing the efficiency and production of in house cheap cells.

VI. ACKNOWLEDGMENT

The authors thank Chenab College of Engineering and Technology, Gujranwala for providing technical facilities and support throughout the course of this work.

REFERENCES

[1] H. A. Pasha and W. Saleem, "The impact and cost of power load shedding to domestic consumers," *The Pakistan Development Review,* pp. 355-372, 2013.

[2] F. D. Economic Adviser's Wing, Government of Pakistan,Islamabad,, "Pakistan Economic Survey," 2016-2017.

[3] B. P. Global, "BP statistical review of world energy June 2017," 2017.

[4] K. Mahboob, S. Tanveer, F. Ali, F. B. Naeem, H. Khalid, and A. Khan, "A review on types of renewable energy technologies and its effect on environment in Pakistan," in *2018 International Conference on Renewable, Applied and New Energy Technologies(ICRANET)Air University Islamabad*, 2018, p. 180140.

[5] HDIP, "Energy Year Book," Hydrocarbon Development Institute of Pakistan,Karachi2013-2014.

[6] S. C. Stokler S, "Solar Resource Mapping for Pakistan: solar modelling report. ESMAP," *Renewable Energy Resource Mapping Initiative. Washington, DC: World Bank Group,* 2015.

[7] W. B. G. International Finance Corporation, "A Solar Developer's Guide to Pakistan,," Jan 2016.

[8] K. Mahboob, A. Qaddus, M. M. Aslam, A. Ahmad, U. Mushtaq, and A. Khan, "Structural Design of Heliostat for Solar Thermal Power Plant," in *2018 2nd International Conference on Energy Conservation and Efficiency (ICECE)*, 2018, pp. 23-29.

[9] I. E. Agency, "Renewable Energy Technologies: Solar Energy Perspectives, OECD/IEA," Paris.

[10] BrightSource. (2019, 01/10/2019). *IVANPAH Solar Electric Generating System*. Available: http://www.brightsourceenergy.com

[11] A. Mittal and N. Mittal, "Review Paper On: Concentrating Solar Power with Mirrors," 2017.

[12] K. Mahboob, F. Ali, H. Mehmood, M. Irfan, S. Tanveer, and A. Khan, "Design, analysis and optimization of 50MWe Solar Power Plant in Multan using CSP parabolic trough technology," in *2018 International Conference on Renewable, Applied and New Energy Technologies(ICRANET)Air University Islamabad*, 2018, p. 180610.

[13] H. Price, E. Lupfert, D. Kearney, E. Zarza, G. Cohen, R. Gee*, et al.*, "Advances in parabolic trough solar power technology," *Journal of solar energy engineering,* vol. 124, pp. 109-125, 2002.

[14] TNEI. (2019, 01/10/2019). *Concentrated solar power*. Available: https://www.tneigroup.com/files/concentrated-solar-power

[15] G. Solar. (2019, 01/10/2019). *Glasspoint introduced the concept of an enclosed trough to EOR*. Available: http://www.wikiwand.com/en/GlassPoint_Solar

[16] B. Bierman, J. O'donnell, R. Burke, M. McCormick, and W. Lindsay, "Construction of an enclosed trough EOR system in South Oman," *Energy Procedia,* vol. 49, pp. 1756-1765, 2014.

[17] B. Bierman, C. Treynor, J. O'donnell, M. Lawrence, M. Chandra, A. Farver*, et al.*, "Performance of an enclosed trough EOR system in South Oman," *Energy Procedia,* vol. 49, pp. 1269-1278, 2014.

[18] D. Mills, "Advances in solar thermal electricity technology," *Solar energy,* vol. 76, pp. 19-31, 2004.

[19] N. El Gharbi, H. Derbal, S. Bouaichaoui, and N. Said, "A comparative study between parabolic trough collector and linear Fresnel reflector technologies," *Energy Procedia,* vol. 6, pp. 565-572, 2011.

[20] R. Bernhard, H. Laabs, J. de Lalaing, M. Eck, M. Eickhoff, K. Pottler*, et al.*, "Linear Fresnel Collector Demonstration on the PSA—Part I: Design, Construction and Quality Control," in *14th International SolarPACES Symposium, Las Vegas, NV, Mar*, 2008, pp. 3-7.

[21] K. Mahboob, M. M. Aslam, A. Qaddus, A. Ahmad, U. Mushtaq, and A. Khan, "Design and Analysis of Tower Structure for Solar Thermal Power Plant," in *2018 2nd International Conference on Energy Conservation and Efficiency (ICECE)*, 2018, pp. 30-36.

[22] J. Spelling, A. Gallo, M. Romero, and J. González-Aguilar, "A high-efficiency solar thermal power plant using a dense particle suspension as the heat transfer fluid," *Energy Procedia,* vol. 69, pp. 1160-1170, 2015.

[23] K. Mahboob, M. Irfan, A. Ali, F. Ali, H. Mehmood, and A. Khan, "Design and Analysis of 50MW Solar Power Plant in Multan using

Solar power tower technologies," in *2018 International Conference on Renewable, Applied and New Energy Technologies(ICRANET)Air University Islamabad*, 2018, p. 180142.

[24] W. Han, J. Hongguang, S. Jianfeng, L. Rumou, and W. Zhifeng, "Design of the first chinese 1 MW solar-power tower demonstration plant," *International Journal of Green Energy,* vol. 6, pp. 414-425, 2009.

[25] M. Strauss. (2019, 01/10/2019). *Take a Look at the World's Largest Solar Thermal Farm.* Available: https://www.smithsonianmag.com/science-nature/take-a-look-at-the-worlds-largest-solar-thermal-farm-91577483/

[26] khaleejtimes. (2018, 08/01/2018). *Solar concentrator.* Available: https://www.khaleejtimes.com/business/energy/a-new-era-beckons-for-solar-par

[27] A. Hafez, A. Soliman, K. El-Metwally, and I. Ismail, "Solar parabolic dish Stirling engine system design, simulation, and thermal analysis," *Energy Conversion and Management,* vol. 126, pp. 60-75, 2016.

[28] K. Lovegrove, G. Burgess, and J. Pye, "A new 500 m2 paraboloidal dish solar concentrator," *Solar Energy,* vol. 85, pp. 620-626, 2011.

[29] M. I. Hussain and G. H. Lee, "Parametric performance analysis of a concentrated photovoltaic co-generation system equipped with a thermal storage tank," *Energy Conversion and Management,* vol. 92, pp. 215-222, 2015.

[30] P. J. Verlinden, "Update on two-year performance of 120 kWp concentrator PV systems using multi-junction III–V solar cells and parabolic dish reflective optics," presented at the 33rd IEEE Photovoltaic Specialists Conference, , San Diego, CA, USA, 2008.

[31] F. Kiliç, T. Menlik, and A. Sözen, "Effect of titanium dioxide/water nanofluid use on thermal performance of the flat plate solar collector," *Solar Energy,* vol. 164, pp. 101-108, 2018.

[32] S. solar. (01/11/2019). *Flat Plate Solar Collectors.* Available: http://www.siliconsolar.com/flat-plate-solar-collectors.html

[33] S. B. Solar. (01/11/2019). *Solar updraft technologies.* Available: https://www.solar-updraft-tower.com/en/technical-concept/prototype-manzanares/

[34] N. Mehla, K. Kumar, and M. Kumar, "Thermal analysis of solar updraft tower by using different absorbers with convergent chimney," *Environment, Development and Sustainability,* pp. 1-19, 2018.

[35] R. Ferreira, N. J. van Rensburg, and A. Nel, "A study into the efficiency of embedded solar photovoltaic cells in double roman shaped roof tiles," in *2018 5th International Conference on*

Renewable Energy: Generation and Applications (ICREGA), 2018, pp. 301-304.

[36] NREL. (08/01/2018). *Photovoltaic*. Available: https://www.nrel.gov/workingwithus/re-photovoltaics.html

The use of virtual reality (VR) technologies in automotive design

Kamran Mahboob [1, 2, a], Malik Safi Ullah [2, b], Ahsan Naseem [2, c], Farman Ali [2, d],
Saqib Tanveer [2, e], Awais Khan [1, f]

*1Dept. of Mechanical Engineering, University of Engineering and Technology Lahore,
Pakistan*
*2Dept. of Mechanical Engineering, Chenab College of Engineering and Technology
Gujranwala, Pakistan*

Email address: [a] mahboobccet@gmail.com , [b] saficcet@gmail.com , [c] ahsannaseemccet@gmail.com,
[d] farmanaliccet@gmail.com [e] Saqib.ch946@gmail.com, [f] awais211@uet.edu.pk

Abstract—A major part of world mobility depends upon automotive sector development. Currently, we are witnessing the shift from fossil fuels towards electric automotive sectors. Last decade has shown sharp developments in the field of computer and IT. The application of CAD softwares in design and development is increasing with every passing day. The visualisation of the designed data in softwares plays a vital role during design. One major limitation is visualisation of 3D geometry on a 2D monitor display. In this paper, an effort is made to use the VR technologies for the visualisation of design models of automotive sector. This paper discusses different strategies and methods to visualise CAD models in VR. An interface is developed between desktop computer and android phone to perform visualisation while using VR. This paper also talks about the bidirectional control of visualisation in Computer and android mobile. Furthermore, the benefits and challenges associated with the use of VR in the visualisation of the CAD model is brought to light.

Keywords—Virtual Reality (VR); Automotive; Design; CAD; 3D technologies.

I. INTRODUCTION

VR is a computer generated and interactive experience that takes advantage of audio, visual, haptic and other types of feedback [1]. A VR scene is based upon simulation carried out using different computer algorithms; the rendering is also performed using different computer algorithms. The virtual environment created with the help of computer computations can sometime be captivating comparable to the real world. For instance the work of [2] mentions one such virtual environment. It is evident from the use of computer simulations in product development that it improves productivity, quality, reduces cost and development time to a great extent [3-7].

Augmented reality is also among new emerging technologies that layers the virtual data over a live camera feed [8]. These days VR is commonly available in the form of VR headsets which are widely available enabling a person to look around, manoeuvre about, and interact with the virtual artefacts of a virtual and computer generated world.

Fig.1. VR system inside CAVE [9].

Fig.2. Powerwall system and Hybrid HMD at John Deere [1].

A complete virtual reality hardware system may contain a visual display, tracking systems, handheld controllers and may also be a haptic devices [10].

Virtual reality can be used with different conceivable configurations that largely depend on the application at hand. For instance, VR facilities typically use one or more of the following, a large display (i.e. power wall), multiple walls connected together [11], desktop tracking and head-mounted displays (HMDs) [12] [13].
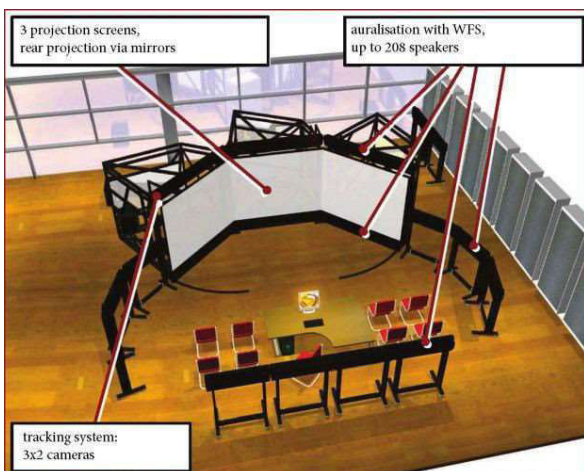
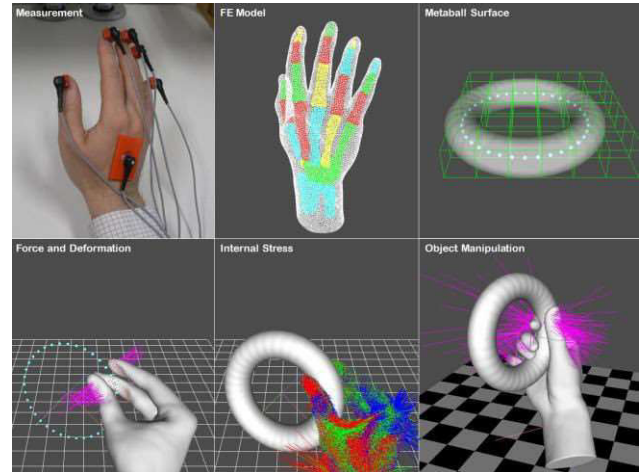Fig.3. Audio-visual stereoscopic projection system [14].

Fig.4. Interaction with virtual object using deformable hand [15]

An audio system can comprise of a headset, a speaker or a complete surround sound audio system. Sound localisation can also simulate moving sound from a location within a virtual environment [16].

Virtual environment interaction is critical in many applications of virtual reality, it traces various media systems (optical, magnetic, ultrasonic, inertial, etc.), enables the location and orientation of physical objects to be calculated in real time within physical space [17]. This becomes particularly valuable when calculating the correct display of user perspectives.

In addition to signal recognition algorithms, tracking systems allow natural body movements to be transformed into functional interaction techniques [18]. The portable console allows users to navigate and manipulate objects in the virtual world to enhance interaction.

II.   CAD MODEL DEVELOPMENT

The process of designing starts with the CAD modelling [19, 20]. Surface and solid modelling is carried out using different CAD softwares like CATIA, Solidworks etc. Assembly of model is performed to have a view of final product.
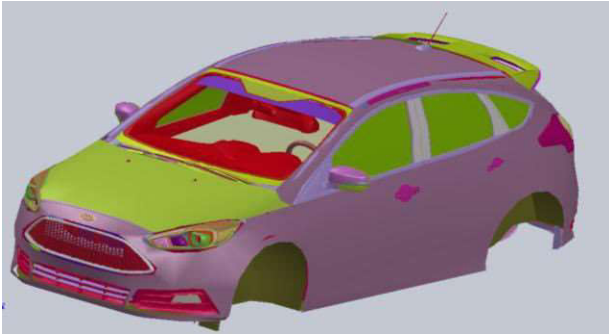
Fig.5. Automotive CAD model[1]

Different connections are applied during the assembly processes, which are useful in body kinematics and understanding body physics.

CAD model can be saved and converted into different formats like prt, STEP, IGES, msh, obj etc. depending upon the utility.
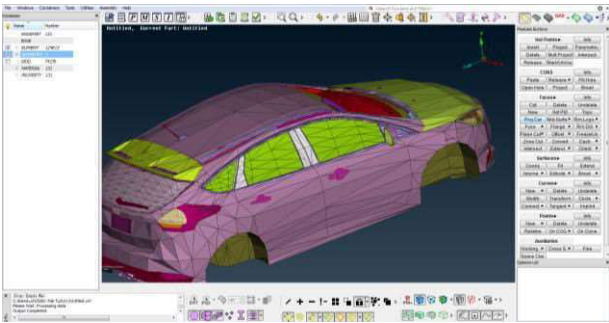

Fig.6. Automotive Obj model

III. CAD TO VR

The main challenge in performing VR visualisation is the model preparation. As a matter of fact, VR cannot render the native CAD geometries. The CAD model has to be first exported as an exchange format and later imported in VR. The choice of one particular exchange format depends upon multiple factors e.g. the data format, mesh size, geometry, animations, kinematic and dynamic relationship. Furthermore, each exchange format carries different information as outlined in the work of [21]. As our goal is to visualise a car in virtual reality, therefore, first VR model has to be prepared from the CAD geometry. This conversion process is described in next subsection.

A. Schematic of CAD model to VR conversion

As the model is in CAD software and it has to be transferred to VR (Unity) for virtual reality visualisation. Currently available VR softwares mainly support geometric exchange formats e.g. JT, OBJ, STL, VRML etc. In our application Unity is used as VR rendering software, the CAD model is first converted to OBJ model. After starting new project and setting the background environment inside Unity, the OBJ file is placed in the asset directory of the unity project. This file is then pulled in Unity for further processing. Fig. 7 briefly describes the overall conversion process.
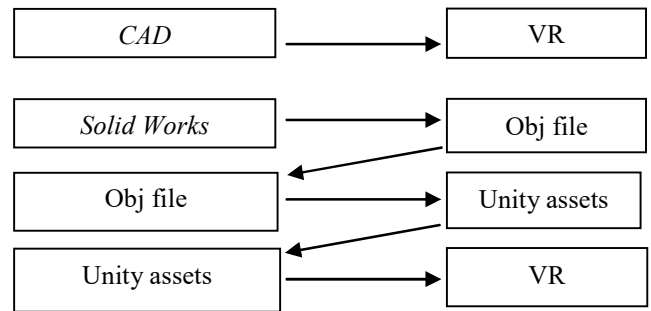

Fig. 7. CAD to VR conversion

B. Environment variable adjustments

After placing the imported model into new environment, different parameters need to be adjusted. Imported model parameters can be changed/adjusted e.g. material, colour, size, position etc. Also variables of the room or place where model is to be placed are adjusted accordingly. Light and camera effects related to visualisation in VR are also adjusted.
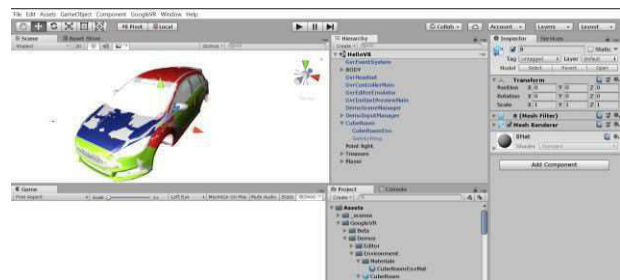

Fig. 8. Environment setting in Unity

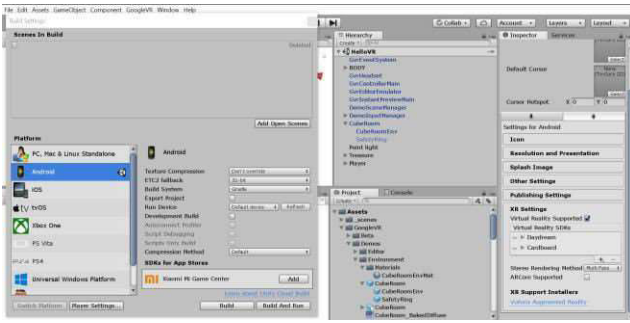[1] The geometrical model was obtained from GrabCAD.com

Fig. 9. Android settings in Unity

C. Android build settings in Unity

We want to use an android phone for the visualisation; it requires build settings in Unity to be changed to android platform. PC settings are changed to android and player settings are also changed. After finalizing the setting, app is pushed in the android mobile for visualisation. App push is performed by connecting the phone to computer and then by building the project in unity.

D. Visualisation of CAD model into VR

1) 2D visualisation

Initial visualisation of the model in the 2D environment can be seen in the camera rendering window by using "build and play" option inside Unity. Maximizing the window can help in better 2D visualisation.

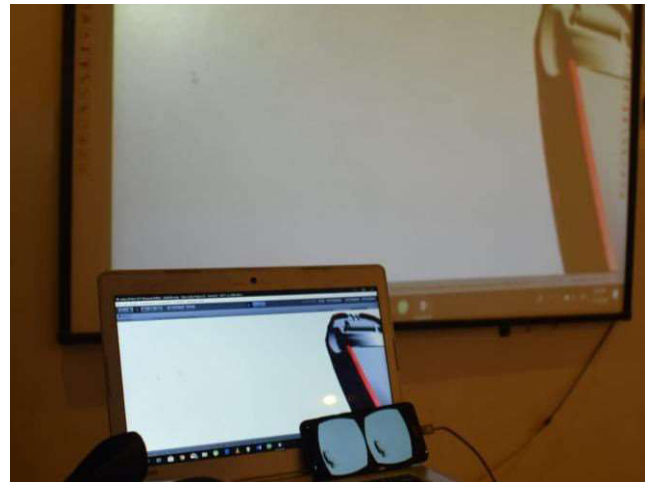Fig. 10. 3D VR headset visualisation

Fig. 11. Control through computer or mobile

2) 3D visualisation

For 3D visualisation, two different techniques can be used. First technique involves visualisation using 3D screen with polarized glasses e.g. in CAVE type VR system or in power wall. Other method is use of VR headset or Google cardboard. By placing the model in the VR better 3D visualisation can be achieved.

IV. VR CONTROL

Visualisation in the VR can be controlled using the input from computer key board, computer mouse or from attached android mobile.

A. Build and Run

In "build and run" computer push the program to a Smartphone. Smartphone is then placed in the VR headset and viewed by moving head in different directions for visualisation.
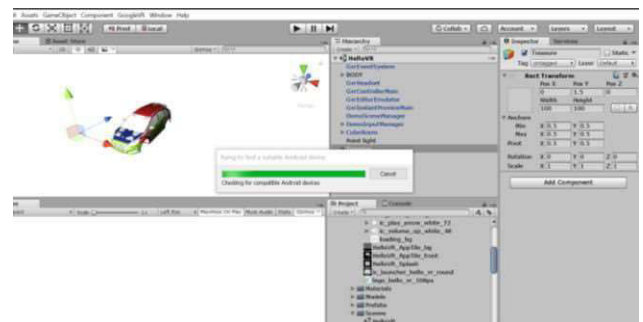

Fig. 12. 3D VR headset visualisation

B. Unity Remote

In instant preview, Smartphone is connected with computer and unity remote 5 android app is installed in the Smartphone. After that Smartphone automatically installs instant preview and visualization is started.

1) Computer control:

GvrEditorEmulator prefab from GoogleVRCore is used in unity to split the visualization screen in two parts. Computer control is turned on in Unity. By pushing the play button, project can be seen on the Smartphone and it is controlled through computer.

2) Smartphone control:

For Smartphone control GvrEditorEmulator is turned off and GvrControllerMain is turned on. In this case, the project data can be visualized on Smartphone and computer but it will only be controlled from Smartphone.
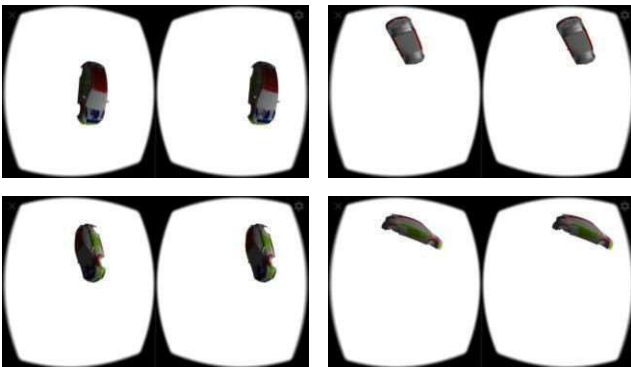

Fig. 13. Different views using unity remote

Fig. 14. 2D VR visualisation

V. MODEL VARIATION FOR VISUALISATION

Since geometric model is transferred from CAD to Unity, for quick visualisation model is rotated. This will help in visualizing the model from different point of views without incorporating the controls.

VI. CONCLUSIONS AND RECOMMENDATIONS

This article has discussed VR technologies and their applications in detail. It is evident from this research that VR technologies can be used effectively in the automotive design process. By using VR headset, a 3D method is developed that is quite cost effective. Moreover, visualisation using VR can render the scene quite closer to the reality. As quick transition from conventional to electronic automotive is happening, VR technologies will enhance the efficiency in designing process by reducing the errors that may arise during development and manufacturing. In the end it is concluded that future design and development processes can be reshaped by the use of the VR technologies. It is recommended that model finish should be of high resolution so that a perfect visualisation is to be achieved.

[1] The geometrical model was obtained from GrabCAD.com

VII. FUTURE WORK

The developed model will be extended to involve physical calculation.

VIII. ACKNOWLEDGMENT

REFERENCES

[1] L. P. Berg and J. M. Vance, "Industry use of virtual reality in product design and manufacturing: a survey," *Virtual Reality,* vol. 21, pp. 1-17, 2017.

[2] A. Mahboob, C. Weber, S. Husung, A. Liebal, and H. Krömker, "Model based systems engineering (MBSE) approach for configurable product use-case scenarios in virtual environments," in *DS 87-3 Proceedings of the 21st International Conference on Engineering Design (ICED 17) Vol 3: Product, Services and Systems Design, Vancouver, Canada, 21-25.08. 2017*, 2017, pp. 281-290.

[3] A. Mahboob, A. Liebal, S. Husung, C. Weber, and H. Krömker, "A method for efficient and task oriented configuration of Virtual Reality (VR) models for the analysis of technical systems," in *Engineering for a Changing World: Proceedings; 59th IWK, Ilmenau Scientific Colloquium, Technische Universität Ilmenau, September 11-15, 2017*, 2017.

[4] C. Weber, S. Husung, A. Mahnboob, H. Krömker, S. Hörold, and A. Liebal, "Benutzer- und aufgabenorientiertes virtuelles Modell für die Produktentwicklung," 2016.

[5] K. Mahboob, F. Ali, H. Mehmood, M. Irfan, S. Tanveer, and A. Khan, "Design, analysis and optimization of 50MWe Solar Power Plant in Multan using CSP parabolic trough technology," in *2018 International Conference on Renewable, Applied and New Energy Technologies(ICRANET)Air University Islamabad*, 2018, p. 180610.

[6] K. Mahboob, M. Irfan, A. Ali, F. Ali, H. Mehmood, and A. Khan, "Design and Analysis of 50MW Solar Power Plant in Multan using Solar power tower technologies," in *2018 International Conference on Renewable, Applied and New Energy Technologies(ICRANET)Air University Islamabad*, 2018, p. 180142.

[7] K. Mahboob, S. Tanveer, F. Ali, F. B. Naeem, H. Khalid, and A. Khan, "A review on types of renewable energy technologies and its effect on environment in Pakistan," in *2018 International Conference on Renewable, Applied and New Energy Technologies(ICRANET)Air University Islamabad*, 2018, p. 180140.

[8] M. Billinghurst, A. Clark, and G. Lee, "A survey of augmented reality," *Foundations and Trends® in Human–Computer Interaction,* vol. 8, pp. 73-272, 2015.

[9] J. Bergounhoux. (2017, 01/15/19). *At the heart of PSA's design process: from virtual reality to clay models.* Available: https://www.techviz.net/au-coeur-du-design-process-de-psa-de-la-realite-virtuelle-aux-maquettes-en-argile-lusine-digitale

[10] S. D. Laycock and A. Day, "A survey of haptic rendering techniques," in *Computer Graphics Forum*, 2007, pp. 50-65.

[11] C. Cruz-Neira, D. J. Sandin, and T. A. DeFanti, "Surround-screen projection-based virtual reality: the design and implementation of the CAVE," in *Proceedings of the 20th annual conference on Computer graphics and interactive techniques*, 1993, pp. 135-142.

[12] E. Larsen, F. Umminger, X. Ye, N. Rimon, J. R. Stafford, and X. Lou, "Methods and systems for user interaction within virtual reality scene using head mounted display," ed: Google Patents, 2018.

[13] Q. Huang, H. Song, and Z. Ren, "Optical magnifying combination lens, head-mounted optical display system and virtual reality display device," ed: Google Patents, 2018.

[14] A. Siegel, C. Weber, A. Mahboob, A. Albers, D. Landes, and M. Behrendt, "Virtual Acoustic Model for the Simulation of Passing Vehicle Noise," in *ASME 2016 International Design Engineering Technical Conferences and Computers and Information in Engineering Conference*, 2016, pp. V01BT02A055-V01BT02A055.

[15] K. Hirota and K. Tagawa, "Interaction with virtual object using deformable hand," in *2016 IEEE Virtual Reality (VR)*, 2016, pp. 49-56.

[16] O. Rummukainen, T. Robotham, S. J. Schlecht, A. Plinge, J. Herre, and E. A. Habels, "Audio Quality Evaluation in Virtual Reality: Multiple Stimulus Ranking with Behavior Tracking," in *Audio Engineering Society Conference: 2018 AES International Conference on Audio for Virtual and Augmented Reality*, 2018.

[17] D. A. Bowman, S. Coquillart, B. Froehlich, M. Hirose, Y. Kitamura, K. Kiyokawa*, et al.*, "3d user interfaces: New directions and perspectives," *IEEE computer graphics and applications,* vol. 28, pp. 20-36, 2008.

[18] S. Mitra and T. Acharya, "Gesture recognition: A survey," *IEEE Transactions on Systems, Man, and Cybernetics, Part C (Applications and Reviews),* vol. 37, pp. 311-324, 2007.

[19]   K. Mahboob, M. M. Aslam, A. Qaddus, A. Ahmad, U. Mushtaq, and A. Khan, "Design and Analysis of Tower Structure for Solar Thermal Power Plant," in *2018 2nd International Conference on Energy Conservation and Efficiency (ICECE)*, 2018, pp. 30-36.

[20]   K. Mahboob, A. Qaddus, M. M. Aslam, A. Ahmad, U. Mushtaq, and A. Khan, "Structural Design of Heliostat for Solar Thermal Power Plant," in *2018 2nd International Conference on Energy Conservation and Efficiency (ICECE)*, 2018, pp. 23-29.

[21]   M. Lorenz, M. Spranger, T. Riedel, F. Pürzel, V. Wittstock, and P. Klimant, "CAD to VR–a methodology for the automated conversion of kinematic CAD models to virtual reality," *Procedia Cirp,* vol. 41, pp. 358-363, 2016.

[1] The geometrical model was obtained from GrabCAD.com

Utilizing marble waste in building construction blocks by partial substitution of cement

Muhammad Nauman[1,a], Wajid Ali[1,b], Irfan Ahmed Khan[2,c], Muhammad Adnan Khan[1,d], Yaseen Muhammad[1,e], Khan Shahzada[3,f], and Muhammad Imran Ahmad[1,g,*]

[1]Department of Chemical Engineering, University of Engineering and Technology, Peshawar

[2]National Institute of Urban Infrastructure and Planning, University of Engineering and Technology, Peshawar

[3]Department of Civil Engineering, University of Engineering and Technology, Peshawar

Email address: [g,*]imran.ahmad@uetpeshawar.edu.pk

Abstract—The objective of this study is to investigate the feasibility of utilizing waste marble slurry in building blocks with partial substitution of cement. Another objective is to save the natural marble resources from wasting which are economically valuable. When marble rocks are processed in industry through different methods such as cutting and polishing about 20 % to 30% of material wasted in form of slurry and powder dust which results in serious environmental problems. For utilizing marble powder in building blocks samples with 0, 7, 10 and 15% substitutions were prepared and compressive strength test was conducted of samples at 7 and 28 days. Results show that compressive strength of 10% substitution in building construction blocks was better than conventional blocks.

Keywords—marble waste, industrial symbiosis, building blocks, compressive strength, sustainability.

I. Introduction

Marble industry during processing produces waste slurry which seems to be increasing due to the fact that number of marble production industries is increasing due to high demand of marble products. In general marble industry in Pakistan and specially in Khyber Pakhtunkhwa is growing rapidly. Natural marble reserves present in KP are major part of the total marble reserves present in Pakistan [1].

Due to large quantity of marble present in KP and their processing created ecological problems. Marble processing mainly causing water pollution and have negative impacts on surface water when thrown in clean water bodies. Marble slurry waste decreases the fertility of soil and alkalinity of soil becomes high [2].

During marble processing water is used as coolant for heat produced due to friction in marble cutting. When processing one ton of marble stone in gang saw or vertical saw used in marble industry about one ton of slurry is produced which has the composition of 70% water and 30% marble powder and then the slurry is dumped in rivers or other water bodies without treatment which is a nuisance for environment [3].

The main purpose of this study is the utilization of waste marble powder/sludge thereby reducing water pollution and air pollution. Utilizing waste marble powder/sludge may be used as raw material in the building construction blocks due to which its mechanical strength may also be improved.

II. Review of Marble Waste Utilization in Building Materials

Several research groups have studied the use of marble waste as partial substitution of cement in concrete and other building materials. In terms of mechanical performance, [4] demonstrated that 10% substitution of marble powder gives optimum results of compressive strength. [5] reported that when 20% of marble powder was added without substitution of cement, 15 % increase in compressive strength was observed. [6] reported that compressive strength with 5, 7, 10, and 15% substitution of marble powder, i.e. partial substitution of cement in concrete, decreased after 28 days. They also observed that with decrease in water ratio the compressive strength increased and also the porosity of concrete decreased with increase of substitution of marble powder. [7] showed that keeping the water ratio at 0.5 w/p, the compressive strength for 5 and 7% substitution of marble powder as partial substitution of cement increased while the compressive strength decreased at 15% substitution.

III. Materials and Method

The following materials were employed in experimental work:

Marble powder having 0.25 mm sieve size and specific gravity of 2.4. Sand having 4 mm size and specific gravity of 2.67. Gravel size was 3-5 mm with a specific gravity of 2.6. Portland cement having a specific gravity 2.82 and tap water.

Construction blocks were made out of the enlisted materials with specified amounts as shown in Table 1. It may be observed from Table 1 that while sand and gravel were kept constant at 3.256 kg and 5.5 kg respectively. The amount of cement was reduced from 1.627 kg to 1.383 kg by substituting it with marble powder.

TABLE I.   QUANTITY OF MATERIALS USED PER BLOCK

S.No	Quantity per block (kg)			
	Sand	Gravel	Cement	Marble
1	3.256	5.5	1.627	0
2	3.256	5.5	1.505	0.122
3	3.256	5.5	1.46	0.1627
4	3.256	5.5	1.383	0.244

Managing of marble waste is a big problem nowadays. The manufacturing of eco-blocks with a partial substitution of cement with marble powder gives high strength and less water absorption rate as compared to conventional building blocks. Samples of different percentage were produced with a water-cement ratio of 0.5. The cement substitution with marble powder was 7.5, 10, and 15% respectively. The chemical composition of marble sludge and ordinary Portland cement is shown in Table 2.

TABLE II.   CHEMICAL COMPOSITION OF WASTE MARBLE

Component	Cement	Waste marble powder
SiO_2	21.2	28.35
Al_2O_3	5.62	0.42
Fe_2O_3	3.24	9.70
CaO	62.94	40.45
MgO	2.73	16.25
Density (kg/cm^3)	3.10	2.80

It may be observed from Table 2 that waste marble dust is lighter than cement having lower alumina, and calcium oxides while higher silica, iron and magnesium oxides. The experimental procedure was as follows:

The received marble sludge from factory was air dried through heating and broken down into fine powder through hammer-mill. The powder was put into the sieve shaker to get a homogenous powder. The fine powder (7.5%) was mixed with the gravel of size (3-4 mm) in diameter. This mixture of gravel and marble powder was mixed with the required amount of cement in a mixer. Water was then added in the mixer and the mixture was mixed well. Finally this mixture was cast in moulds to form blocks as shown in Fig. 1.

The same procedure applied for the other samples (10% and 15% substitution of cement with waste marble dust). Conventional blocks (without marble powder) were also produced for comparison.

Fig. 1. Picture of mixture cast in mould

After natural strengthening and removal from the moulds, watering took place up to specified days. After drying these blocks were soaked. Tests were carried out to determine strength for 7 days and 28 days. Compressive strength test was carried out for the blocks through Universal testing machine (UTM) as shown in Fig. 2.

Fig. 2. Strength testing on UTM

IV.   RESULTS AND DISCUSSION

The chemical composition of cement and marble powder given in Table 2 shows that marble powder has 28% silica while cement has 21%, also marble powder has high percentage of iron and magnesium oxides. However, lime (CaO) being major component of cement

(62.94%) is lower in waste marble powder (40%). Alumina content in waste marble powder is also lower compared on ordinary Portland cement, so based on the properties of these oxides partial substitution of cement with waste marble powder may be suitable. The compressive strength of construction block samples for 7 days and 28 days are shown in Fig. 3. It may be observed from Fig. 3 that 10% substitution shows high strength of 2250 psi on 28 days as compared to 15% substitution. Moreover, it may be noticeable that as the number of days for curing increases strength of building blocks increases.
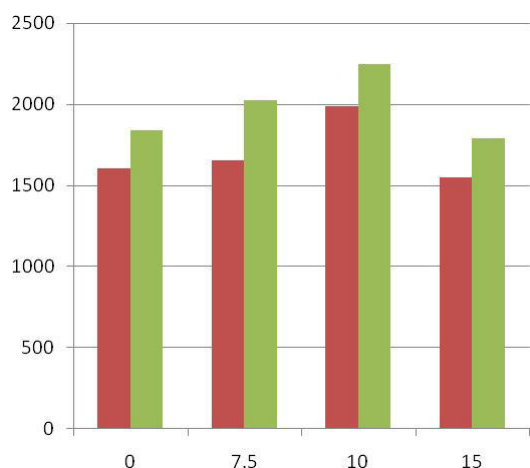

Fig. 3. Compressive strength (psi) of block samples

The compressive strength of construction block samples with 7.5 and 10% substitution of cement with waste marble dust is higher than conventional blocks for 7 days as well as 28 days. The construction block samples with 10% substitution of cement show highest strength at both 7 days and 28 days. However, further substitution of cement with waste marble dust (15%) reduces the strength at both 7 days and 28 days as compared to conventional blocks.

It may be worthwhile to note that compressive strength would need to be measured at 90 days for construction block samples produced substituting cement with waste marble dust to infer how the reactions proceed between 28 days and 90 days of curing.

V. CONCLUSIONS

This research work aims to investigate the feasibility of producing building construction blocks using waste marble powder to partially substitute ordinary Portland cement. The amount of cement in construction block samples was reduced through addition of waste marble powder up to 15%. The amount of sand and gravel was kept constant. The compressive strength for construction block samples was tested on 7 and 28 days and compared with conventional construction blocks, i.e. without any substitution. The results for 7 and 28 days show that 10% substitution of cement with waste marble dust gives higher compressive strength compared to conventional construction blocks. The compressive strength for 7.5 and 10% samples increased from 7 to 28 days. Further tests would be carried out to determine the strength at 90 days in comparison with conventional blocks. The results

obtained in this research imply that waste marble dust may be utilized in building construction blocks thereby reducing the cost, increasing the strength, and most importantly decreasing the environmental impacts associated with improper disposal of waste marble slurries.

REFERENCES

[1] A. Manan, Y.J. Iqbal, 'Phase, microstructure and mechanical properties of concrete' J. Pak. Mat. Soc. (2007) 1(2), 68-72.

[2] F. Akbar, 'Effect of marble industry effluent on seed germination, post germinative growth and productivity of Zea mays' Pak. J. Bio. Sci. (2007) 10(22).

[3] W. Shah 'Life cycle assessment of marble industry for cleaner production technology as a pollution prevention measure' PhD Thesis, University of Peshawar (2011).

[4] C. Vaidevi, 'Engineering study on marble dust as partial replacement of cement in concrete' Ind. J. Eng. (2013) (4), 9-11.

[5] A. Arshad, I. Shahid, U.H.C. Anwar, M.N. Baig, S. Khan, K. Shakir, 'The wastes utility in concrete' Int. J.Env. Res. (2014) 8(4), 1323-1328.

[6] A. A. Aliabdo, A. Elmoaty, M.A. Elmoaty, E.M. Auda, 'Re-use of waste marble dust in the production of cement and concrete' Constr. Build. Mat. (2014) 50, 28-42.

[7] A. Ergun, 'Effects of the usage of diatomite and waste marble powder as partial replacement of cement on the mechanical properties of concrete' Constr. Build. Mat. (2011), 806-812

Small Scale Design and Implementation of Computer Numerical Control Machine for Multi Tasking

Adeel Saleem[1]
School of Electrical and Electronics Engineering
North China Electric Power University, Beijing, China
Department of Electrical Engineering
The University of Lahore, Lahore, Pakistan
adeel.saleem@ee.uol.edu.pk

Adnan Sabir[2]
COMSATS Institute of Information Technology, Sahiwal.

Atif Iqbal[3]
School of Renewable Energy & Clean Energy
North China Electric Power University, Beijing, China
atifiqbal@ncepu.edu.cn

Adil hussain[4*]
School of Electrical and Electronics Engineering
North China Electric Power University, Beijing, China
1164200124@ncepu.edu.cn

Abstract— To minimize the time to market of a product design and development, rapid prototyping is extensively used. Understanding as well as better communicating the product design and rapid tooling, new systems are being utilized by the manufacturers. To manufacture small parts through small machinery could be very efficient, effective and also reduces the initial cost. In this paper a cost effective, productive, efficient, and user-friendly small scale 3 axis Computer Numerical Control (CNC) machine is introduced/develop, which monitor and control many tightly coupled machining tasks. The desired task is obtained by giving numerical inputs in the form of G code to the microcontroller. The microcontroller (Arduino Uno) interprets this program into corresponding electrical signal for inputs to the three-stepper motor. CNC motion generated by keeping Stationary tool/moving base. These motors are connected with Stationary tool/moving base that allows to move in 3 dimensional defined locations through a numerical code, which consists of coordinates.

Keywords— Computer Numerical Control (CNC), Arduino Uno micro controller

I. INTRODUCTION

Rapid and very fast development of technology, the current industry demands great precision, accuracy and excellent quality with the higher production rate as well as economical [1-2]. Among them all, most demanding aspects are dimensional correctness, high efficiency and higher production rate that can be achieved by the excellent machine tools [3-4].

The Computer Control Numerical (CNC) technologies are playing a vital role to fulfill these requirements of current industry now days [6-9]. Due to the advancement of CNC technologies, Nano scale products are being manufactured with the excellent precision and accuracy. Because of high precision, many industry products are manufactured by CNC machine tools, which help to build a strong foundation of industry also playing a key role for development level of country. Among of them products include mold, screw, automobile, mold, aerospace materials and precision of the parts entirely dependent upon manufacturing. There is a requirement of strict quality in some products such as, military, aerospace materials as well as semiconductors and so on. By these requirements of strict quality, high speed production and with excellent accuracy as well as precision is the main challenge and requirement for CNC machines [5], [10]. The ability to use CNC machines enables the manufacturing process in efficient way and depreciation of manufacturing time. This helps to reduce the manufacturing time and resultantly decrease of the production cost. Production of Nano scale products in a quiet fast way with the great precision as well as accuracy demands higher capabilities and more intelligent behavior of machine [11-15]. In this paper a user friendly and cost-effective CNC machine is implemented, that is capable to produce prototypes from huge variety of materials such as ploy-carbonate, wax, wood, aluminum and brass. The proposed prototype design is consisting of 3-axis desktop mill machine, which produce complex parts enriched of geometry.

II. METHODOLGY

Functional block diagram and circuit diagram of proposed system is shown in fig. 1 and 2. The proposed developed system comprise of three main components:

- Mechanical Hardware
- Electronics Hardware
- Control Software

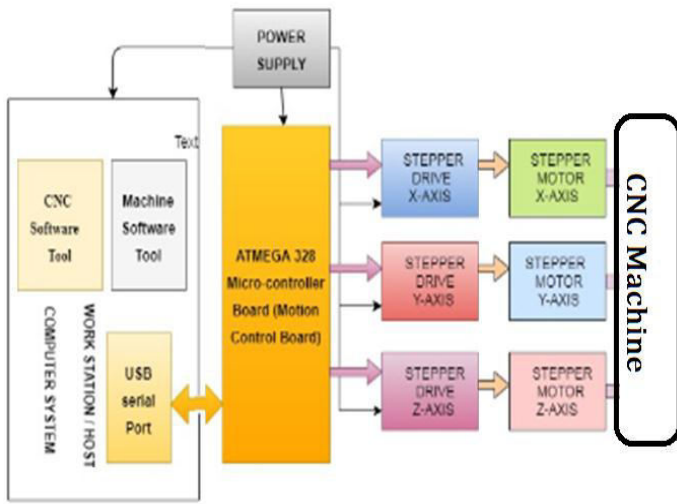A desired task is generated by CAD (Computer Aided Design) software such as open SCAD, Free CAD etc.

Fig 1: The block diagram of proposed CNC system

it is the use of computer system to help in the creation, modification and analysis or optimization of a design. CAD software generate desired task in the form of mesh file format having extension. STL because this file is easily read by CAM software. A CAM software tool used to translate CAD files (.STL file format) into desired set of G-code commands. The CAM package is used to define the appropriate tool paths taking into account, raw material size, tool diameter, tool length, feed rate, support tabs, tool type, and spindle RPM.
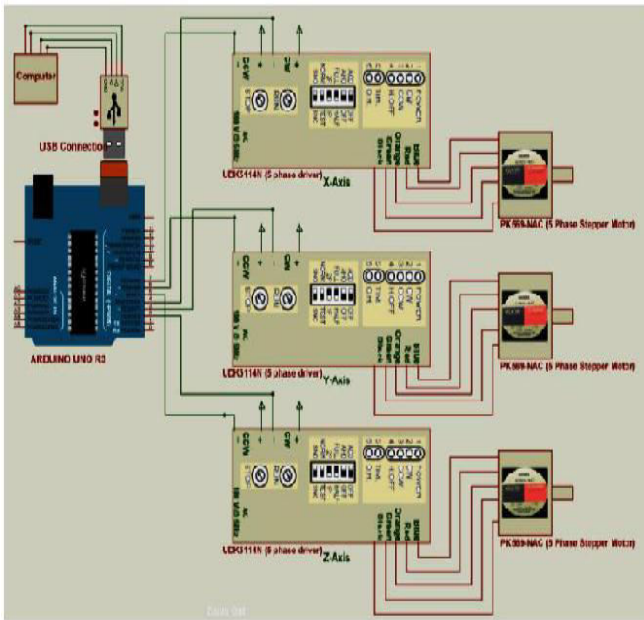

Fig 2: The circuit diagram of CNC machine

The G-codes are used to define motion behavior, reset or redefine coordinate origins and define measurement units. The resulting G-code controller is then passed into communicate with CNC controller hardware. Grb1 controller software served as interpretations which send G-code file to (atmega-328 controller) through USB serial port communication. The

micro-controller Atmega 328 generates desired electrical pulses which in result further sent to driver card of the stepping motors. Thus, controlling their movement along 3 axes. In order to start desire task just generate the G-code of the design and feed it to the sender software (Grbl Controller) and the machine will start to follow instruction to complete desired task. The desired task can be any like Etching PCBs and Engraving, Milling, Drilling wood and other soft materials used for the production of complex parts with geometry.

In order to overcome the vibration and make a machine cost effective, the spindle runs at the spindle used is of 30,000 rpms is capable of working on wood, plastic and thin sheet metal. Spindle motor has the low power as well as speed. So, the detached material volume per turn is decreased resultantly decrease in vibration.

III. DESIGN AND IMPLEMENTATION

A. Mechanical Design

Electromechanical hardware plays a key role in a multi axis CNC machine. The electromechanical components move a working tool to a defined location through numerical code consists of coordinates. In this design, CNC motion uses Cartesian coordinates for motion by keeping Stationary Tool/Moving Base. By keeping the Tool stationary (most active motions) give an extra advantage to increase cutting ability for harder material [16].

The material chosen for making the structure was iron due to its natural toughness and it provides sufficient strength to grip the parts with no effect of deformation. The structure is made of sheet metal of 6.35mm thickness. The rectangular tube is 3 inches by 2.5 inches in dimension. The overall sides of the base are 2.5ft each.
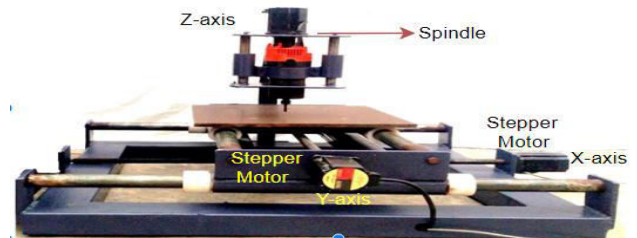

Fig 3: Complete Mechanical Portion of CNC Machine

B. Electronic Design

The electronics hardware act as a bridge between mechanical hardware and the driving computer.
The electronic hardware can be divided into four categories:

> Stepper Motors
> Motor drivers
> Arduino Uno Controller

A. Stepper Motor

As Stepper motors are used to drive the CNC machines mechanical system because these motors produce more torque

at low speed. The choice and selection of motors is done using following equations.

$$\text{Maximum angular speed } \omega_{max}$$
$$= 1.6(in/\text{sec})(10\ rev/in)(2\pi\ rad/rev) \qquad (1)$$

$$\text{Maximum angular rate } \alpha$$
$$= \omega_{max}/t_{acc1}\ (rad/sec^2) \qquad (2)$$

Where t_{acc1} is an acceleration time in sec Ball screw inertia J_B

$$= \frac{\pi * L * r^4 * p}{2 * g}\ (lb.in.sec^2) \qquad (3)$$

Here L = Ball screw length, r = Screw Radius while p = material density

Table 1: Specification For Motor

Frame Size	60mm
Type	Standard Type
Shaft Type	Double Shaft
Maximum Holding Torque	1.66N · m
Rotor Inertia J	560×10^-7kg · m^2
Basic Step Angle	0.72°
Rated Current	1.4A / Phase
Winding Resistance	1.7Ω / Phase
Mass: Motor	1.3kg

J_{L-m}: Load Inertial reflected to motor

$$= \frac{WL+WT}{g} * \frac{1}{\frac{2*\pi}{1*rev}*Ps}\ (lb.in.sec^2) \qquad (4)$$

Here,
W_L = Load weight
W_T = Table weight
P_s = Motor rev per inch
Inertia of rotor = 560×10^-7kg · m^2
$J_{total} = J_M + J_{L-M}\ (oz.in.sec^2) \qquad (5)$
where
1 oz = 0.06363 lb
$\tau_P = \tau_{acc} = J_{total} * \alpha\ (oz.in) \qquad (6)$ τ_{acc} acceleration torque at motor shaft due to reflected inertia from load and mechanism.
$Fg = (W_L + W_T) * \sin\Upsilon \qquad (7)$
Fg is a Gravity forces and Υ is the angle of the centre line with horizontal line. $\Upsilon = 0$ so, Fg = 0
$F_{fr} = \eta * (W_L + W_T) * \cos\Upsilon \qquad (8)$
Here η denotes coefficient of friction among sliding parts. η = 0.01

$$T_{L \to M} = (\frac{F_P + F_g + F_{fr}}{\frac{2\pi}{1rev}*P_s*e}) + T_p\ (lb.in) \qquad (9)$$

T_{L-M} is a load torque reflected to motor

Now total torque reflected to Motor can be calculated as: According to calculation the specification for motor is shown in Table 1 [17].

B.   Motor Drivers

The motor driver is another important part of the CNC machine. The motor driver used in this project is UDK5114N. conversion of power signals from driving signals based on TTL based is the main purpose of this part which is used for driving the motor. The complexities of the stepper motors drive system depend on the power requirements of the stepper motors being driven [18].

C.   Arduino Uno Controller

The Arduino Uno is used to connect the CNC stepper motor drivers to the computer. The computer sends data (tool coordinates and feed-rates) to electronics control board, which subsequently sends motor pulse commands to the individual stepper motor drivers which in turn drives each respective motor accordingly [19].
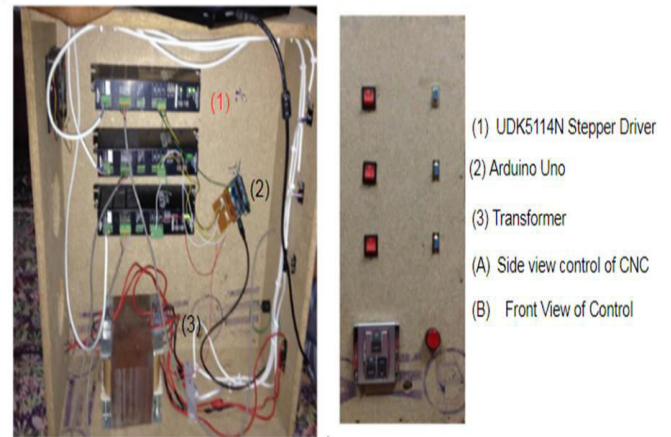

Fig 4: Control Structure of CNC machine

Arduino is being flashed with Grbl firmware which is a free, open source and high-performance software for interpreting Gcode and generating corresponding commands for steppers. To completely control one stepper, motor the Grbl firmware generates two signals. Of these two signals one is a level active signal whose high or low state determines the direction of the motor. The other signal is a pulse signal which keeps on switching between high and low levels. The frequency of this signal determines the speed of the stepper motor. This implies that in order to properly run 3 axes machine the Grbl firmware generates six signals.

D.   CAD, CAM and Motion Control Software (Grbl Controller)

The design of desired complex shape is generated by Computer Aided Design. Change and manipulate the parts with respect to parameters, is made easy by CAD tools. The

most widely used interchangeable mesh file format is exchangeable mesh file format.
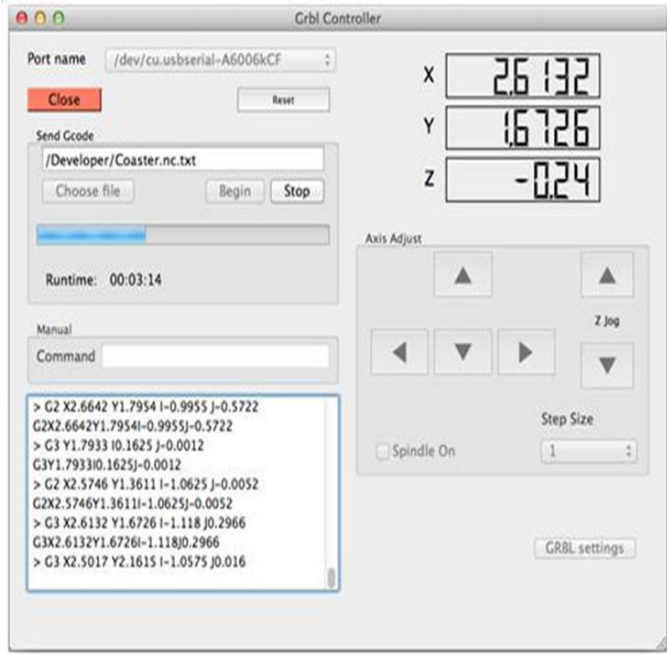

Fig 5: Grbl Controllers Graphical User Interface

STL is used to generate G-code through CAM tools. CAM is the next stage of CAD. A part created in CAD can be downloaded and manufactured. Translation of CAD files into a machine friendly format is carried out by the microcontroller.
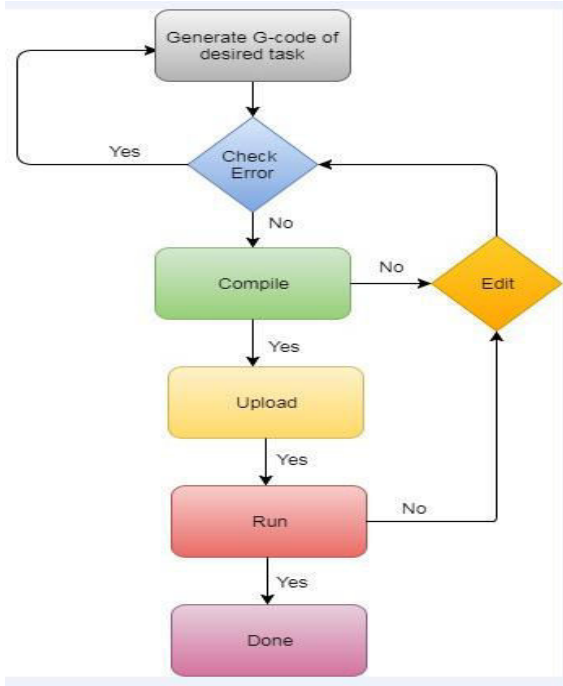

Fig 6: Flow chart of desired task implementation

The resulting G-code is then passed into software package that communicates with the CNC controller hardware. The G-code interpreter within the controller determines the distance between points and prescribes how many motor steps are required to generate the desired motion. Finally, the controller generates the stepper motor pulses that generate motor movement. The micro-controller Atmega 328 generates desired electrical pulses which in result further sent to driver card of the stepping motors. Thus, controlling their movement along 3 dimensional.

IV. RESULTS AND DISCUSSIONS

The final result exceeded expectation as the design of desired complex shapes on plywood was successfully created with expected accuracy.
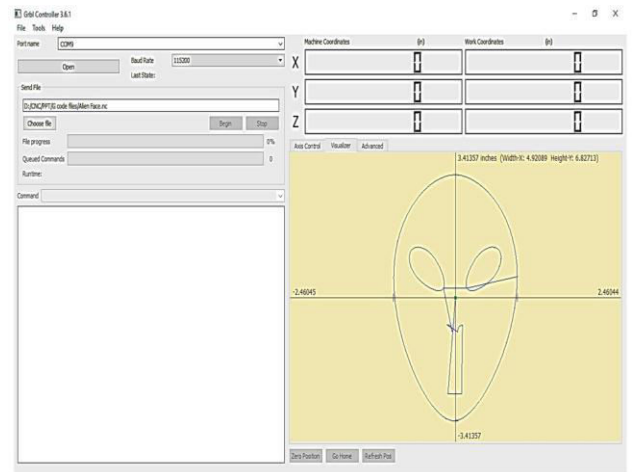

Fig 7: Code Running of Grbl Controller for desired task.

Machine has been used to create several shapes and patterns on plastic, paper, foam, polystyrene, wood, cardboard and thin sheets of iron and steel.

Fig 8: Finished designs on plywood

V. CONCLUSION

Increase in the demand of small-scale higher precision parts compels the rapid growth has been observed in this market. Fabrication of comparatively small parts requires smaller

manufacturing machines, thus resulting of reduced cost, high efficiency and great precision. Machine has been used to create several shapes and patterns on plastic, paper, foam, polystyrene, wood, cardboard and thin sheets of iron and steel. Machine will be less precise, because of manufacturing mistakes and imprecision of machine body parts. However, it will be adequate to create small features such as letters, shapes and graphs. Overall, the design of desired shapes was created and implemented successfully. Results pattern shows the satisfactory results and prove the supremacy of this machine. new design must be created after evaluation of prototype with respect to calibration and assembling. This could be very helpful in achieving more precise and efficient machine for the same amount of budget.

VI. APPENDIX

Parameter considered for the selection of stepper motor

Max velocity = 1.6 inches / sec

Time for acceleration (Ramp) =0.32 sec

Operates at maximum velocity for 5 seconds.

Time of ddeceleration = 0.32 sec

Friction Torque = 0.2 oz in

Acceleration Torque = 141.18 oz in

Weight of load and table (WL+WT) = 1000lb

REFERENCES

[1] Parenti P , Bianchi G , Cau N , Albertelli P ,MonnoM . A mechatronic study on amodel-basedcompensation of inertial vibration in a high-speedmachine tool. J MachEng 2001;11(4):91–104

[2] Altintas Y , Brecher C , Weck M , WittS . Virtual machine tool. CIRP Ann 2005;54(2):115–38

[3] Erkorkmaz K , Altintas Y , Yeung CH. Virtualcomputer numerical control system CIRPAnn 2006;55(1):399–402

[4] Yeung CH, Altintas Y , Erkorkmaz K . VirtualCNC system. Part I. system archi-tecture. Int J MachTools Manufacture 2006;46(10):1107–23 I .

[5] Yeung CH, Altintas Y , Erkorkmaz K . Virtual CNC system. Part II. Highspeed contouringapplication. Int J MachTools Manufacture 2006;46(10):1124–38 I .

[6] Kao YC, Chen MS. Anintelligent virtualmulti-axis machine tool remote service system. IEEE/ASME Int ConfAdv Intell Mechatronics2012:632–7

[7] Erkorkmaz K , Altintas Y . Highspeed CNC system design, Part I: jerk limited trajectory generation and quintic spline interpolation. Int J MachTools Manu-facture 2001;41(9):1323–45 I

[8] Tsai MS, NienHW , Yau HT. Developmentof integrated acceleration-decelera-tion look-ahead interpolation technique for multi-blocks NURBScurves. Int J Adv Manufacturing Technol 2011;56(5):601–18 I

[9] Koren Y . Cross-coupled biaxialcomputer control for manufacturing system. J Dyn Syst, MeasControl 1980;102(4):265–72.

[10] Kima MS, Chung SC. A systematic approach to designhigh-performance feed drive systems. Int J MachTools Manufacture 2005;45:1421–35.

[11] Kamalzadeh A . Precision control of highspeed ball screw drives Doctorthesis of Department MechanicalEngineering, WaterlooUniversity;2008.

[12] Yeh SS, Hus PL. Analysis and designof integrated control for multi-axis motion systems. IEEE Trans Control Syst Technol 2003;11(3):375–82 .

[13] DingG , Zhu S , Yahya E , Jiang L , MaS , Yan K . Prediction of machining accuracy based ona geometric error model in five axis peripheral millingProcess. Pro.of Inst MechEng, Part B 2014;228(10):1226–36.

[14] Srinivasan K , TsaoTC. Machine tool feed drives and their control-a survey of the state of the art. J ManufacturungSci Eng 1997;119:743–8.

[15] Tang W, Yan G , Xu X , Yu D , Wang Z , Chu H . A research on NC machining cutting parameters optimization.In: International conferenceon information sci-ences, machinery, materialsand energy (ICISMME); 2015. p. 1791–7

[16] JEREMY VAILLANT, 2013, ANALYSIS, IMPLEMENTATION AND EDUCATIONAL IMPACT OF DIGITAL FABRICATION TECHNIQUES USING DESKTOP MACHINES

[17] https://www.orientalmotor.com.sg/products/st/list/detail/?product_name=PK569B&brand_tbl_code=ST&series_code=G001&type_code

[18] http://www.mechatronics4u.com/product/1596734/5-phase,-stepping-motor,-super-vexta,-udk5114n,-1.4a-oriental-motor.html

[19] https://www.arduino.cc/en/Main/ArduinoBoardUno, (November-2015)

Post CPEC Infrastructure Requirements of Peshawar

Rafiullah Jan Cusit[1, a], Hamza Iqbal Cusit[2, b] and Eng. Dr.Mehboob Alam[3, c]

[1]City University Peshawar
[2]City University Peshawar
[3]City University Peshawar

Email address: [a]rafiullahjan819"gmail.com, [b]hamza.iqbal3030@gmail.com [c]hodcivil@cusit.edu.pk

Abstract— China Pakistan Economic Corridor is the way of tremendous growth of trade between the two countries and the increasing volume of imports and exports is associated with increased infrastructural requirements for the population of Peshawar. The study analyzes social and economic impacts on Peshawar in face of CPEC projects. Identification of service industry like vehicles for good transportation, people and goods being transported were carried out. The study focuses on transportation sector of greater Peshawar region. The study analyzes the available capacity of different resources e.g. diesel storage, parking lots and maintenance facilities along their locations. Finally a feasibility study is performed to chosen the needs of greater Peshawar region in facilitation of the cargo transport of CPEC.

Keywords— CPEC, Impacts, Transportation Sector, Trade trucks, Infrastructural needs.

I. INTRODUCTION

China Pakistan Economic Corridor is the gateway of development of both countries through trade. It is a route that will connect the central Asian countries, Afghanistan, Iran and India to European countries to china and Pakistan through Gwadar sea port and the maritime Silk Road. The whole corridor is composed of different types of mega projects i.e. energy, infrastructure, railway network, industrial zones, Gwadar development industrial zones, fiber optic and others. The whole scenario is categorized to be completed in different time phases. This aims for a significant rise of trade between Pakistan and China in a short term and long term future prospect. It also accounts for urbanization of the cities of Pakistan because job growth will attract the jobless peoples from surrounding and far areas to the main cities of the country that will have an ultimate impact on the population growth. Industrialization has a positive impact on urbanization because jobs are created in the job market with migration of peoples towards cities increasing the population. Besides this, the social and economic impacts (Socio-economic impacts, CPEC CoE) shall arise due to CPEC Portfolio. Unemployment will force the labor force, technical, the skilled and unskilled towards the major cities like Lahore, Faisalabad, and Karachi as well as towards the node cities like Gilgit, Peshawar, Islamabad, Multan, Sukker, Quetta, Hyderabad, Dera-Ismail Khan and Gwadar [1].

The increase in trade volume will be needed to incorporate high number of trade trucks for imports and exports through CPEC. This amount of cargos will be in need of different infrastructural needs poster to CPEC in its service. Thus identified service industries i.e. vehicles that are being used in the trade, peoples that are involved in the whole system and the goods that are being transported are the target industries. To provide the required infrastructure needed for vehicle, it needed technical truck information, existing filling stations and maintenance services from greater Peshawar region with their elite locations to calculate more needs to make it comfortable for cargos to avail the services easily.

By this study, the impacts due to CPEC projects will be determined for the greater city of Peshawar keeping in mind the different variables. The impact analysis will be statistical

study using different parameters. A trade truck needs various kinds of services that will be identified, located and calculated for a specific amount of trade cargos in the future of corridors trade. A model will be developed which will be composed of all services that is needed for a trade cargo. These services will be provided all in one place at different feasible locations in Peshawar. The model area will be designed along with a sustainable green infrastructure that shall be very environment friendly.

II. LITERATURE REVIEW

This research study is composed of two different areas, one is impact of CPEC projects on the face of the greater region of Peshawar and the infrastructural needs of the cargo trade trucks that enter to Peshawar coming from Khunjerab pass in their future prospect at the completion of the CPEC short term and long term projects.

Dealing with the impacts of CPEC, it is a wide study not only to Peshawar but the whole country. We will code the work done in this area by the center of excellence regards the impacts of CPEC projects on the country. The CoE (Centre of Excellence) has conducted an excellent work by carrying the statistical work as impacts on the region. The main areas covered under their study are population growth and their relativity to the job market, increase of jobs due to CPEC projects and the percentage of hiring national and international skilled and unskilled labor force i.e. the Pakistani and Chinese side. According to it, the road projects in the infrastructure projects 93% (47000) domestic workers from Pakistan side and 7% (3,780) foreign workers from Chinese

side [2]. The projects included different road sections across the country with skilled and unskilled workforce. The skilled labor required for the road projects included Senior executives, Business process managers, Construction managers, Building specialist, Surveyors, Project managers, Quality engineers, Civil- Engineers, Prime movers operations and construction professionals along with Technical side. Figure I show the total job statistics [2].

The greater region of Peshawar is not directly involved in CPEC but is amongst one of the important node cities of CPEC. The amounts of trade trucks from Khunjerab pass to Pakistan is our basic thesis requirement for research completion and that is the point of interest which will have impact and infrastructural needs in Peshawar. In this study, impacts on Peshawar due to CPEC projects was analyzed using the statistical approaches and great rises and falls have been recorded.

The second area of our research which is of our main concern is to determine and calculate generally and technically the need of infrastructure that shall have to be provided for the trade trucks coming to Peshawar in the future after the long term projects completed in CPEC. It first needed to identify the service industry that will be incorporated in the CPEC trade. The identified service industries were vehicles that will be incorporated in the trade, peoples that will be hired directly and indirectly in the CPEC and the goods that is being transported to Pakistan in this trade. Taken into account the vehicle service industry because it will need infrastructure which is of our main concern to identify and calculate. This also needed to identify the existing facilities in the

Figure 1 Total Jobs created under road related infrastructure projects
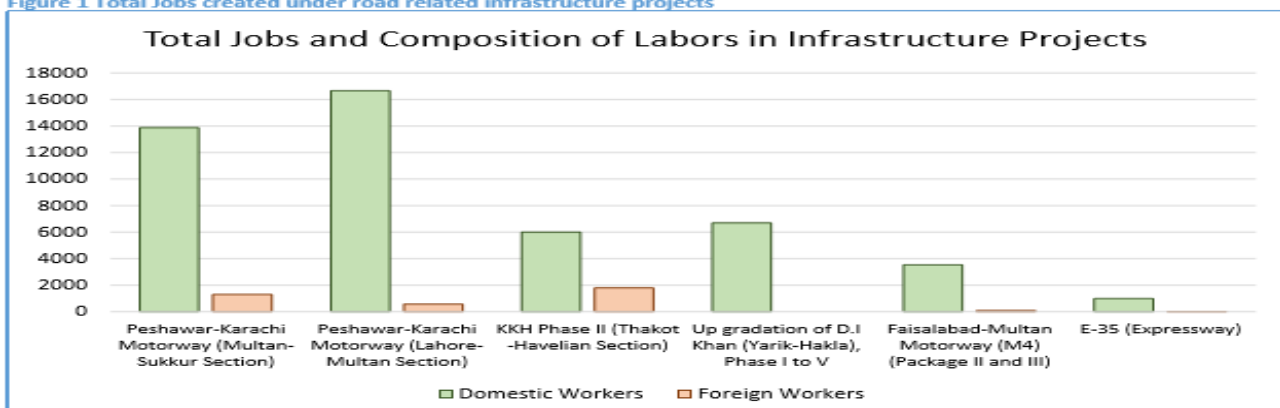
greater region of Peshawar i.e. total number of filling stations and their monthly sale with locations, total number of truck servicing workshops with their locations and to locate their most feasible location along the technical truck information was needed. This data collection is aimed for to calculate the infrastructure needs for a specific amount of trade trucks. These infrastructure will be composed of further filling stations needed, workshops needed, parking lots, residential areas and others along with a proper location.

The above needs were determined by conducting a feasibility study. The amount needed is calculated and shown in the results. At last, a model is designed that is composed of having all the required infrastructure needs of trade trucks in one place and it will be assumed that this model will be provided at all places with a specific distance from other model area and with a proper location as required for the trade truck from Khunjerab pass to greater Peshawar region. It shall be also composed of a sustainable green environment friendly system. A system that improves environmental conditions such as a rain garden. A rain garden is not a water garden nor a pond or a wetland and it is dry most of the time. It typically holds water only and during and following a rainfall event. They prevent the breeding of mosquitoes because it drains in 12-48 hours.

III. METHODOLOGY

- Field surveys were conducted in the main city and attached areas of Peshawar. Some questioners and collection sheets were made for asking and collecting the statistical data.
- To analyse the CPEC impacts in the Peshawar region, questions were asked from peoples related to different industries and also the labours working with different departments and private sector agencies.
- The existing number of filling stations in Peshawar region was measured by visiting to each of them asking for its

monthly sale of diesel in litres and noting the locations. This was carried for all different companies i.e. P.S.O, TOTAL PARCO, Shell, Attok etc.

- The number of workshops in the Peshawar regions was measured with their locations.
- Numbers of parking lots were measured with their locations.
- These all were located on maps and the most feasible and nearest services to the G.T Road of Peshawar were considered amongst the total facilities.
- The area for the parking lots required by trade trucks was calculated using the single area acquired by a truck multiplying to the total number of trade trucks that enters the greater city of Peshawar. This was determined for all the types of trucks and the different types of trucks with their technical information i.e. axle load, oil tank capacity, mobile oil capacity and make by company were collected by visiting the truck measuring units, motorway interchanges and drivers.

IV. RESULTS

- The number of filling stations were determined in the same manner as in Table I for the rest of companies and the total sale of diesel in Peshawar regions was recorded as 95,78000 litres/month. These results were utilized to calculate the additional number of filling stations in Peshawar.
- The technical truck information was collected to find the consumption of trucks.

For example, number of trucks enters to Peshawar are 100000 per month. The truck type

is HINO 14 Axle with tank capacity of 500 liters. Then;

$$diesel\ required\ (per\ month) = 100000 \times 500$$
$$= 50000000\ liters\ /\ month$$

$$diesel\ required\ (per\ day) = \frac{100000 \times 500}{30.5}$$
$$= 1639345\ liters\ /\ day$$

But if it is considered that the truck fills the tank only once in Peshawar during 1 trip, then;

$$\frac{1639345}{2} = 819673\ liters\ /\ day$$

Table I

#	Company	Location	No. of Stations	Total Sale (liters/month)
1	P.S.O	Greater Region of Peshawar	39	55,00000
2	SHELL	do	17	18,68,000
3	ATTOCK	do	7	700000
4	TOTAL PARCO	do	18	15,10,000
	TOTAL		81	95,75000

Area need for Trucks:

$$No\ of\ Trucks\ enters\ Peshawar\ (per\ month) = 100000$$
$$then, the\ area\ reqyured\ for\ this\ amount\ will\ be;$$
$$area\ of\ a\ 14\ Axle\ HINO\ truck = 2.85 \times 10 = 28.5\ m^2$$
$$Area\ required = 28.5 \times 100000 = 2850000\ m^2$$

The same calculations and results are applied for other types of trade trucks.

Mobile Oil need of truck:

$$14\ Axle\ HINO\ needs\ 17\ US\ Quarts\ as\ total\ mobile\ oil\ capacity$$
$$then, for\ 100000\ trucks\ of\ same\ kind\ will\ need;$$
$$Mobile\ oil\ needed = 100000 \times 17 = 1700000\ Quarts$$
$$consumption\ of\ truck = Rs\ 8\ per\ kilometer$$
$$then\ consumption\ of\ total\ trucks\ will\ be;$$
$$= \frac{1700000}{1000}$$
$$= 1700\ \frac{Quarts}{meter}\ for\ total\ trucks$$

V. CONCLUSION

Impacts due to CPEC projects can be analyzed socially and economically. Trends were recorded in job growth from 2015-2017.there

would be more job growth and opportunities in the future.

The trade trucks identified as vehicle industry amongst the trade and people need infrastructure for its services i.e. filling, parking lots and maintenance services which are analyzed, identified, located and calculated to be provided in the future at the greater Peshawar region at most feasible sites.

VII. AKNOWLEDGMENTS

VIII. REFERENCES

[1] Adnan Khan, Dr Saleem Janjua, Mudassar Saleem, "Urbanization Dynamics in Pakistan: Pre and Post CPEC analysis" A publication of CPEC Centre of Excellence.

[2] Dr Shahid Rashid, Muhammad Muzammil Zia, Shujaa Waqar, "Employment Outlook of China Pakistan Economic Corridor: A Meta-Analysis" A publications by CPEC Centre of Excellence.

Approximation of the Masses and other properties of Unknown Hyperons in Standard Model

Imran Khan

Department of Physics, University of Science and Technology,
Bannu 28100, Pakistan

Email address: immarwat@yahoo.com

Abstract—In particle physics, study of the symmetry and its breaking play very important role in order to get useful information about the nature. The classification and arrangements of subatomic particles is also necessary to study particle physics. Particles which are building blocks of nature are quarks, gluons and leptons. Baryons and Mesons composed of quarks were arranged by Gell-Mann and Okubo in their well- known Eight-Fold way up to SU(3) symmetry. Standard model of particles is composed of these particles. Particles in SU(4) also make some beautiful patron. These make some multiplets. but all the baryons with spin $J^P = 3/2^+$ in these multiplets have not been observed till date. In this paper the SU(4) multiplets have been organized and studied in an easy and new way. As a result we obtained some clues about the masses and other characteristics of the unknown hyperons. These approximations about the characteristics of the unidentified baryons have been recorded in this article. Mass formula for the baryon SU(4) multiplets have been obtained.

Keywords—Baryons, SU(3), SU(4), Hyperons, Standard Model, Mass Formula.

I. INTRODUCTION

Baryons are made of three quarks (qqq). The three flavors up u, down d, and strange s, imply an approximate flavor $SU(3)$, which requires that baryons made of these quarks belong to the multiplets on the right side of the „equation" $3 \otimes 3 \otimes 3 = 10_S \oplus 8_M \oplus 8_M \oplus 1_A$ .Here the subscripts indicate symmetric, mixed symmetry, or anti-symmetric states under interchange of any two quarks [1].These were classified and arranged by Gell-Mann and Okubo in De-Couplets ($J = 3/2$, $l = 0$) and Octets ($J = 1/2$, $l = 0$) with +1 parities [2–4]. The Gell-Mann / Okubo mass formula which relates the masses of members of the baryon octet is given by; [2–4]

$$2(m_N + m_\Xi) = 3m_\Lambda + m_\Sigma \qquad (1)$$

While mass formula for De-couplets consists of equal spacing between the rows. The spaces are equal to an average value $-151 \mathrm{MeV/c^2}$.

$$M_\Delta - M_{\Sigma^*} = M_{\Sigma^*} - M_{\Xi^*} = M_{\Xi^*} - M_\Omega \quad (2)$$

Gell-Mann used this formula and predicted the mass of the Ω^- baryon in 1962, equal to $M_\Omega = 1685 MeV/c^2$ [2]. Whereas the actual mass of the Ω^- is 1672 MeV/c^2 which was observed in 1964 [4]. Their mass difference is only 0.72 %, or in other words it was 99% true guess.

Now let"s move towards baryon types made from the combination of four quarks, i.e. up u, down d, strange s and charm c. These belong to $SU(4)$ multiplets. The $SU(4)$ multiplets numerology is given by

$$4 \otimes 4 \otimes 4 = 20_S \oplus 20_M \oplus 20_M \oplus 4_A \; [5].$$

We are interested in twenty particles having spin 3/2 and even parity +1 forming one of the $SU(4)$ multiplets. These particles are in their ground states, that is with $l = 0$. Their masses and other properties are listed in the Table 1.

Since the mass splitting due to strangeness is typically of order 151 MeV/c^2 in the de-couplet, which is an effect of about 13% of the masses it contains. The splitting due to charm in the $SU(4)$ particles multiplets is expected to be

larger [6]. The ratio $\dfrac{m_2}{m_1} = \dfrac{m_4}{m_3}$ indicates the direction of the increasing mass in the Strangeness, or Charm-ness planes in $SU(3)$ and $SU(4)$ multiplets respectively. It gives the mass symmetry breaking ratio for the multiplet [6]. In the $SU(3)$ framework the Gell-Mann / Okubo relation for the $J^P = 1/2^+$ Octets, Eq. (1) and the equal spacing rule for the $J^P = 3/2^+$ de-couplets, Eq. (2) work so nicely that we cannot abandon linear mass formulae for baryons [6]. Using the above relation for baryons of $J^P = 3/2^+$ de-couplet of $SU(3)$ gives a mass symmetry breaking ratio of order 1.0.

Table 1. List of the spin $J^P = 3/2^+$ particles formed from three quarks combinations (qqq) of four quarks u, d, s and c [5].

| S.#	Particle Name	Symbol	Quark contents	Rest Mass (MeV/c^2)
1	Delta $^{++}$	Δ^{++} (1232)	uuu	1232±2
2	Delta Plus	Δ^+ (1232)	uud	1232±2
3	Delta Zero	Δ^0 (1232)	udd	1232±2
4	Delta Minus	Δ^- (1232)	ddd	1232±2
5	Sigma Plus	Σ^{*+} (1385)	uus	1382.8±0.4
6	Sigma Zero	Σ^{*0} (1385)	uds	1383.7±1.0
7	Sigma Minus	Σ^{*-} (1385)	dds	1387.2±0.5
8	charmed Sigma $_{++}$	Σ_c^{*++} (2520)	uuc	2517.9±0.6
9	charmed Sigma $^+$	Σ_c^{*+} (2520)	udc	2517.5±2.3
10	charmed Sigma Zero	Σ_c^{*0} (2520)	ddc	2518.8±0.6
11	Xi Zero	Ξ^{*0} (1530)	uss	1531.80±0.32
12	Xi Minus	Ξ^{*-} (1530)	dss	1535.0±0.6
13	charmed Xi $^+$	Ξ_c^{*+} (2645)	usc	$2645.9^{+0.5}_{-0.6}$
14	charmed Xi Zero	Ξ_c^{*0} (2645)	dsc	2645.9±0.5
15	Omega Minus	Ω^- (1672)	sss	1672.45±0.29
16	charmed Omega Zero	Ω_c^{*0} (2770)	ssc	2765.9±2.0
17	double charmed Xi $^{++}$	Ξ_{cc}^{*++}	ucc	Unknown
18	double charmed Xi $^+$	Ξ_{cc}^{*+}	dcc	Unknown
19	double charmed Omega $^+$	Ω_{cc}^{*+}	scc	Unknown
20	triple charmed Omega $^{++}$	Ω_{ccc}^{*++}	ccc	Unknown
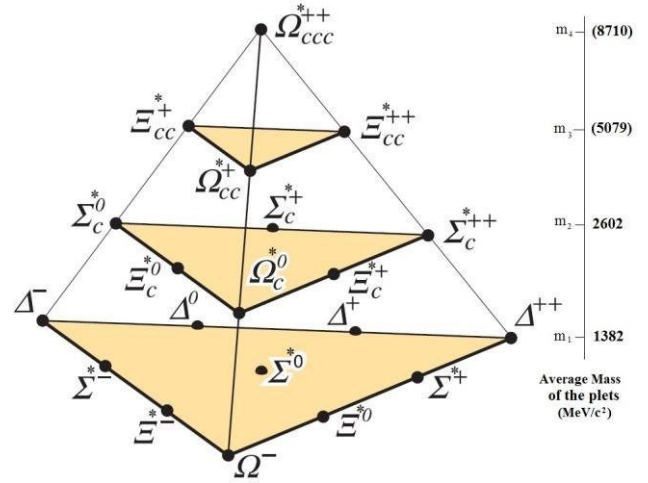
Fig. 1. $SU(4)$ 20–plet of Baryons ($J^P=3/2^+$) made of u, d, s and c quarks, with an $SU(3)$ de-couplet at the bottom [5].

II. METHOD

There are four particles in the Table 1, whose masses are unknown. Let''s try to make some predictions about the unknown masses of the Ξ_{cc}^{*++}, Ξ_{cc}^{*+}, Ω_{cc}^{*+}, and Ω_{ccc}^{*++} hyperons. Let the particles listed in Table 1 may be grouped in pyramid shape of increasing charm number from $C = 0$ to $C = 3$ as shown in Fig. 1 [5]. Masses of the particles are expressed in round numbers. The bottom of the „Pyramid" is the $SU(3)$ de-couplet of $J^P = 3/2^+$ particles at $C = 0$. Average masses written on the right side of the Fig. 1 are discussed later in the text.

We can expand this 20–plet given in Fig. 1 in the shape as shown in Fig. 2, with increasing Charge Number from bottom to top. Also there becomes a beautiful pattern of Isospin numbers, I of the particles. We can treat it as follows:

Adding masses of the Δ^{++} and Δ^+ in the first row of Charm Number $C = 0$, gives 2464 MeV/c^2, which is 54 less than the mass of the Σ_c^{*+} (2518) particle in 2nd row of Charm Number $C = 1$. Hence approximately equal to its mass. Similarly Adding masses of Δ^+ and Δ^0 particles gives 2464 MeV/c^2, which is 55 less than the mass of the Σ_c^{*0} (2519) particle in 2nd row of Charm Number $C = 1$. Same can be done

for other particles. It gives approximate mass of the particle in the adjacent row with higher

charm-ness.
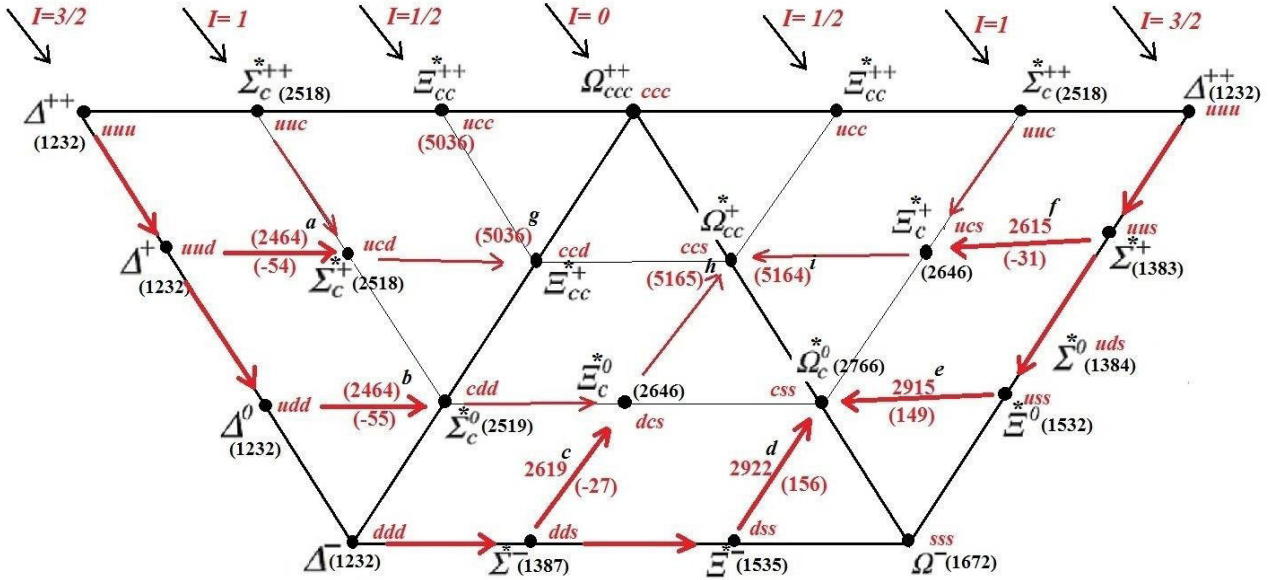

Fig. 2. *SU*(4) 20–plet of Baryons (*J*^{P}=3/2$^+$) made of *u*, *d*, *s* and *c* quarks, arrows represent lines of the addition of particles masses. Indexed with *a-e* (See Table 2), and numbers beneath the arrows are mass difference between theoretical and experimentally observed masses of the particles.

II   MASSES OF THE Ξ_{cc}^{*+} AND Ξ_{cc}^{*++}

Assuming the same behavior of the masses, we can sum up masses of two particles in 2nd row of Charm Number $C = 1$, and get mass of the particle in 3rd row with charm Number $C=2$.

Sum of the masses calculated in such a manner are indexed from (*a*) to (*i*) in Fig. 2; and are listed in Table 2. Masses of the Particles in 3rd row of charm Number $C = 2$ are unknown. Using this method the masses of these unknown particles Ξ_{cc}^{-} and Ω_{cc}^{-} have been obtained and are equal to 5036 *MeV*/*c*^{2} and 5164 *MeV*/*c*^{2} respectively, as can be seen in Table 2.

Since Ξ_{cc}^{*+} and Ξ_{cc}^{*++} are two different states of same particle, i.e. their Iso-spin equal to ½, therefore both will approximately have equal masses, equal to 5036 *MeV*/*c*^{2}. If we see Fig. 2, values of Iso-spin numbers are decreasing from $I = +3/2$ to $I = 0$ by –½, from left to right, and then increasing by +½ till +3/2. Similarly, value of the third component of Iso-spin, I_z, decreases for particles of same

Isospin quantum number, at upper horizontal row to particles at lower horizontal row by 1.

Table 2. Calculations of masses of the particles from sum of other particles, indexed in Fig. 2.

S#	In dex	Particle 1 (m$_1$)	Particle 2 (m$_2$)	m$_1$ + m$_2$ (MeV/c^2)	Resultant Particle (m)	$(m_1+m_2)-m$
1	*a*	Δ^{++} (1232)	Δ^{+} (1232)	2464	Σ_c^{*+} (2518)	-54
2	*b*	Δ^{+} (1232)	Δ^{0} (1232)	2464	Σ_c^{*0} (2519)	-55
3	*c*	Δ^{-} (1232)	Σ^{*-} (1387)	2619	Ξ_c^{*0} (2646)	-27
4	*d*	Σ^{*-} (1387)	Ξ^{*0} (1535)	2922	Ω_c^{*0} (2766)	156
5	*e*	Σ^{*+} (1383)	Ξ^{*0} (1532)	2915	Ω_c^{*0} (2766)	149
6	*f*	Δ^{++} (1232)	Σ^{*+} (1383)	2615	Ξ_c^{*+} (2646)	-31
7	*g*	Σ_c^{*++} (2518)	Σ_c^{*+} (2518)	5036	Ξ_{cc}^{*+} (??)	??
8	*h*	Σ_c^{*0} (2519)	Ξ_c^{*0} (2646)	5165	Ω_{cc}^{*+} (??)	??
9	*i*	Σ_c^{*++} (2518)	Ξ_c^{*+} (2646)	5164	Ω_{cc}^{*+} (??)	??

Therefore Ξ_{cc}^{*++} will have $I_z = \frac{1}{2}$, since it lies at upper row, while Ξ_{cc}^{*+} will have $I_z = -\frac{1}{2}$ due to its place at lower row.

Mass of the double charmed Xi +, Ξ_{cc}^{+} (probably with $J^P = \frac{1}{2}^+$) is approximately equal to 3519 MeV/c^2 [5]. We can compare this value with the theoretical mass of the Ξ_{cc}^{*+} particle with $J^P = 3/2^+$, we extracted i.e. 5036 MeV/c^2. Percentage difference between these two masses is $\frac{5036 - 3519}{3519}$, which is equal to 43%. It is in agreement with the percentage mass difference between masses of proton/ neutron and delta resonances (having same quark contents, but different spins) $\frac{1232 - 938}{938}$ equal to 31%. It is acceptable, and hence we can take 5036 MeV/c^2 as approximate mass of the Ξ_{cc}^{*+} and Ξ_{cc}^{*++} particles with some uncertainty equal to its square root, given by ± 71 MeV/c^2.
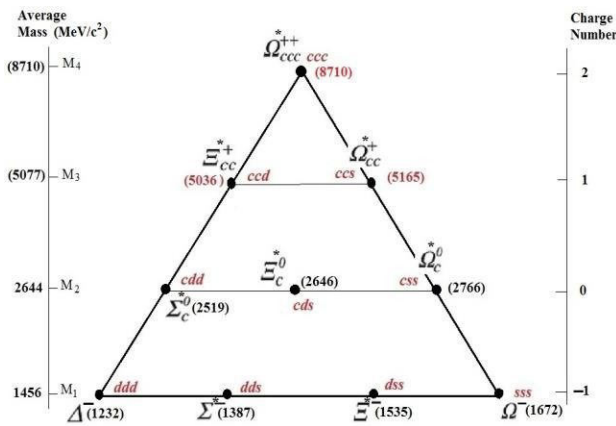
Fig. 3. A portion of the *SU*(4) Multiplets, with increasing Mass, Charge number and Charmness from bottom to top.

III   MASS OF THE Ω_{ccc}^{++} PARTICLE

Mass of the Ω_{ccc}^{++} particle can be estimated using Fig. 3. Taking average mass value of first three rows i.e. rows with $C = 0, 1, 2$ and finding their difference may lead us to the mass of the particle at the top, with $C = 3$.

M_1 (Average mass of row with $C = 0$) = 1456 MeV/c^2

M_2 (Average mass of row with $C = 1$) = 2644 MeV/c^2

M_3 (Average mass of row with $C = 2$) = 5100 MeV/c^2

M_4 = mass of Ω_{ccd}^{++} particle.

Table 3. Predicted masses and other properties of the unknown particles in Standard Model of *SU*(4).

| S.No. | Particle | Mass (MeV/c^2) | Iso spin | | Parity (P) | Spin and Total angular Momentum (s, J) | $I (J)^P$ |
			I	I_z			
1	Ξ_{cc}^{++}	5036 ± 71	$\frac{1}{2}$	$+\frac{1}{2}$	+1	$\left(\frac{3}{2}, \frac{3}{2}\right)$	$\frac{1}{2}\left(\frac{3}{2}\right)^+$
2	Ξ_{cc}^{+}	5036 ± 71	$\frac{1}{2}$	$-\frac{1}{2}$	+1	$\left(\frac{3}{2}, \frac{3}{2}\right)$	$\frac{1}{2}\left(\frac{3}{2}\right)^+$
3	Ω_{cc}^{+}	5165 ± 72	0	0	+1	$\left(\frac{3}{2}, \frac{3}{2}\right)$	$0\left(\frac{3}{2}\right)^+$
4	Ω_{ccc}^{++}	8710 ± 93	0	0	+1	$\left(\frac{3}{2}, \frac{3}{2}\right)$	$0\left(\frac{3}{2}\right)^+$

Difference between M_2 and M_1:

$M_2 - M_1 = 2644 - 1456 = 1188 \ MeV/c^2$

Similarly;

$M_3 - M_2 = 5100 - 2644 = 2456 \ MeV/c^2$

Also $1188 \times 2 = 2376 \ MeV/c^2$, which is very near to 2456 MeV/c^2 (with only difference of 80 MeV/c^2). It means;

$M_2 - M_1 = 1188 \ MeV/c^2$

$M_3 - M_2 = 2 (M_2 - M_1) + 80 = (2 \times 1188) + 80 \ MeV/c^2$

and

$M_4 - M_3 = 3(M_2 - M_1) + 46 = (3 \times 1188) + 46 \ MeV/c^2$

Now we can generalize these in one equation:

$$M_n = M_{n-1} + Charmness \times (1188) + Charge \times (\sqrt{188})$$
(3)

Where n=2, 3, 4
That is;

$M_2 = M_1 + 1 \times (1188) + 0 \times (\sqrt{1188})$

$= 1456 + 1188 = 2644 \ MeV/c^2$

$M_3 = M_2 + 2 \times (1188) + 1 \times (\sqrt{1188})$

$= 2644 + 2376 + 34 = 5054 \ MeV/c^2$

Here value of M_3 will be average of both the theoretical values, as there are no experimentally observed values for particles in this row. i.e.

$$M_3 = \frac{5100 + 5054}{2} = 5077 \; MeV/c^2$$

hence

$$M_4 = M_3 + 3 \times (1188) + 2 \times (\sqrt{1188})$$
$$= 5077 + 3564 + 69 = 8710 \; MeV/c^2$$

Thus the mass of Ω_{ccc}^{++} particle, estimated using the above method is equal to $8710 \pm 93 \; MeV/c^2$. Statistical Errors are the square root values of the particle masses. Experimentally observed Particle masses may be slightly differ from the above estimated values of masses of all the four particles, due to rough estimates. However in that case the values obtained experimentally should agree with theoretical mass values with in two standard errors. All the predicted masses of the four unknown particles and their other properties are listed in Table 3.

Now let us check what is the mass difference, $M_2 - M_1 = 1188 \; MeV/c^2$. It is actually mass of the Charm quark, which is the constituent of the particles. Charm number increases by +1 as we go up in the particles pyramid of Fig. 1, and Fig. 3. So this increase in the masses of the particles is due to the mass of the charm quark. Comparing this with the evaluated mass of the charm quark $M_c = 1270 \pm 30$ and $M_c = 1196 \pm 59 \pm 50 \; MeV/c^2$ listed in Ref. [5] gives satisfactory result. Hence it is also proved that splitting due to charm quarks in the $SU(4)$ particles multiplets is about an order of magnitude, equal to an average value of 80%, as was expected [6].

The calculations may also be expanded to the whole 20- multiplet, as shown in Fig. 1, so that a combined formula for all the baryons masses of this multiplet may be extracted.

In the Fig. 1, m_1 shows average mass of the particles forming de-couplet, with $C = 0$, and is equal to $1382 \; MeV/c^2$, $m_2 = 2602 \; MeV/c^2$ is average mass of the particles with $C = 1$, $m_3 = 5079 \; MeV/c^2$ is the average mass of particles

with $C = 2$ and $m_4 = 8710 \; MeV/c^2$ is the average mass of particle having $C = 3$.
General expression for these masses may be derived as under;

$$m'_n = m_{n-1} + Charmness \times (1188) + Charmness \times (\sqrt{1188})$$

Where n=2, 3, 4

Or more generally,

$$\boxed{m'_n = m_{n-1} + Charmness \times (1218)} \qquad (4)$$

with n=2, 3, 4

Let's try to find average mass of the particles multiplets using this relation;

$$m'_2 = m_1 + C \times (1218) = 1382 + 1 \times (1218)$$
$$= 2600 \; MeV/c^2 \approx m_2$$

$$m'_3 = m_2 + C \times (1218) = 2602 + 2(1218)$$
$$= 5038 \; MeV/c^2 \approx m_3$$

and

$$m'_4 = m_3 + C \times (1218) = 5079 + 3(1218)$$
$$= 8733 \; MeV/c^2 \approx m_4$$

Mass difference term $1218 \; MeV/c^2$ is also equal to the mass of the charm quark [5]. The mass symmetry braking ratio $\frac{m_2}{m_1} = \frac{m_4}{m_3}$ in the direction of the increasing mass in the Charm plane for $SU(4)$ multiplets, is of the order of an average value of 1.8 for baryons of $J^p = 3/2^+$.

III. CONCLUSIONS

$SU(4)$ multiplets of Standard Model have been analyzed in this article and some predictions have been made about the unknown masses and other properties of the Ξ_{cc}^{*++}, Ξ_{cc}^{*+} Ω_{cc}^{*+}, and Ω_{ccc}^{*++} hyperons. Their masses are estimated to be $\Xi_{cc}^{*++} (5036 \pm 71)$, $\Xi_{cc}^{*+} (5036 \pm 71)$, $\Omega_{cc}^{*+} (5165 \pm 72)$, and $\Omega_{ccc}^{*++} (8710 \pm 93)$ MeV/c^2. Statistical errors are the square root values of the estimated masses of particles. Experimentally observed Particles' masses may slightly differ from the estimated values of

masses of all the four particles, due to rough estimates. However in that case the values obtained experimentally should agree with theoretical mass values with in two standard errors. The mass symmetry braking ratio for $SU(4)$ multiplets, is estimated to be of the order of an average value of 1.8 for baryons of $J^P=3/2^+$. It is found that Ξ_{cc}^{*++} and Ξ_{cc}^{*+} have same isospin, equal to ½, so both have approximately equal masses. Ξ_{cc}^{+} has third component of isospin I_z equal to +1/2, while that of Ξ_{cc}^{*+} is equal to −1/2. A general formula for masses has been derived for the $SU(4)$ multiplets, which gives satisfactory results for observed and estimated masses of the particles of $SU(4)$. The mass difference in the multiplets of the $SU(4)$ is due to the mass of Charm quark, and its value is also equal to mass of the charm quark. The results in this research, if proved correct, will be helpful in understanding the particle physics, and will strengthen the Standard Model of particles.

REFERENCES

[1] Introduction to Elementary Particles, David J. Griffiths, John Wiley & sons, INC, New York, 2008.

[2] M. Gell-Mann, Proceedings of the International Conference on High-Energy Nuclear Physics, Geneva, Switzerland, 1962.

[3] S. Okubo, "Note on Unitary Symmetry in Strong Interactions", *Progr. Theoret. Phys.* (Kyoto) 27, 949 (1962)

[4] V. E. Barnes *et.al.*, "Observation of a hyperon with strangeness minus three", *Physical Review Letters*, 12 (8), 204, 1964.

[5] C. Patrignani *et al*. (Particle Data Group), *Chin. Phys. C*, 40, 100001 (2016)

[6] M. Gourdin, "Mass Formulae and Mixing in SU(4) Symmetry", (France) *Pages_from_C*75-03-02-1_229.pdf.

EFFECT OF MASONRY INFILL WALLS ON CAPACITYCURVE OF AN RC FRAME STRUCTURE BY NON-LINEAR STATIC PUSHOVER ANALYSIS

Faisal Pervez[1, a], Muhammad Shoaib Khan[1, b], Bashir Alam[2, c], Naveed Ahmad[3, d]

Abbas Khan [1, e], Jalal Habib Khan[1, f]

[1]Researcher, Department of Civil Engineering, UET Peshawar

[2]Professor, Department of Civil Engineering, UET Peshawar

[3]Assistant Professor, Department of Civil Engineering, UET Peshawar

Email address: [a]13pwciv3900@uetpeshawar.edu.pk [b]muhammadshoaib5308@gmail.com
[c]bashir@gwmail.gwu.edu [d]naveed.ahmad@uetpeshawar.edu.pk [e]abbas@cecos.edu.pk
[f]jalal.marwat@gmail.com

Abstract— *Reinforced concrete frame have masonry infill walls considered as non-structural element in analysis and design. Stiffness and strength capacity of masonry walls is ignored in analysis and its dead load are considered as load on frames. But in practice they resist lateral forces and for this masonry wall capacity is checked of high rise building with different configuration through non-linear static analysis (pushover analysis). Infill walls are simulated in SAP2000 with strut and its dimensions are calculated from equivalent strut method. Seismic performance of various configurations of infill in reinforced concrete frames is compared with bare frame model. It is concluded that infill wall in reinforced concrete frame reduces top story displacements, increases lateral stiffness, reduce time period of structure, and increase base shear.*

 Keywords: R.C Frame, Infill Wall, Pushover analysis, SAP2000, Lateral Stiffness, Base Shear

I.   INTRODUCTION

Most of the reinforced concrete structures consist of masonry infill walls which are not considered as structural elements because they do not contribute in resisting gravity and collapse of structure. Seismic performance of structures are greatly dependent on these walls as they have sufficient stiffness and strength. They are also used to protect from an environmental hazards. This paper presents the effect of masonry infill walls on the linear static analysis of RC frames using compressive strut approach. Investigation of infill walls behavior in high rise building are carried out under static nonlinear pushover analysis. Analysis and design of slab are carried out using moment coefficient and strip method. Design requirement for earthquake are different from wind force requirement as they are differ in their action. But the basic parameter in the design is the force that is compatible also for wind design in which the

loads on a structure. They are used to resist lateral action of earthquake, wind load which are of great concern because lateral forces causing sway in building resulting in damage exposed area of building subjected to forces

that is the force type loading. Larger shear forces results from the increase of in plane lateral strength of RC structures. Failure

Ductility of RC structure depends on the properties and reinforcement provided in
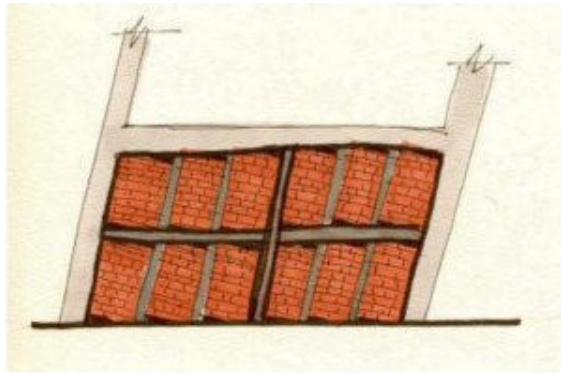
mode of structure is also correlated to the strength and properties of infill walls.

infill for for the control of cracking and failure.

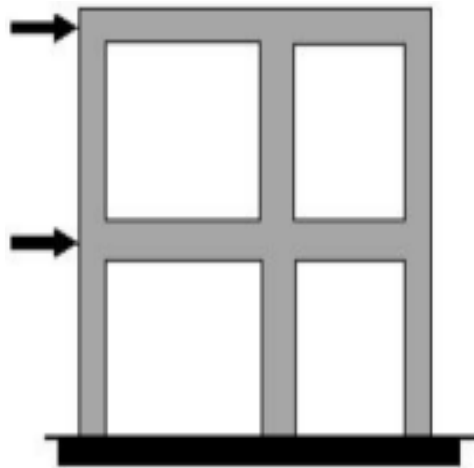*Figure 1. Effect of inertia in abuilding when shaken at its base*

Figure 3. Predominant truss action in infilled frame
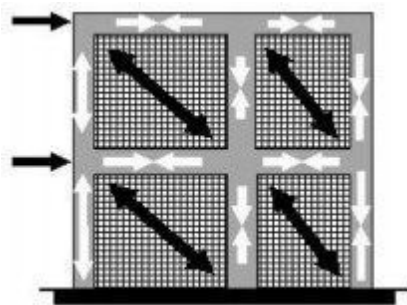
Figure 2. Frame action in bare frame

Building is subjected to inertial forces due to earthquake causing ground motion at the base that induce stresses that type of loading is called displacement type loading. Cyclic type of motion is induced in a ground during an earthquake. So the force type and displacement type loading is the demand for the structure.
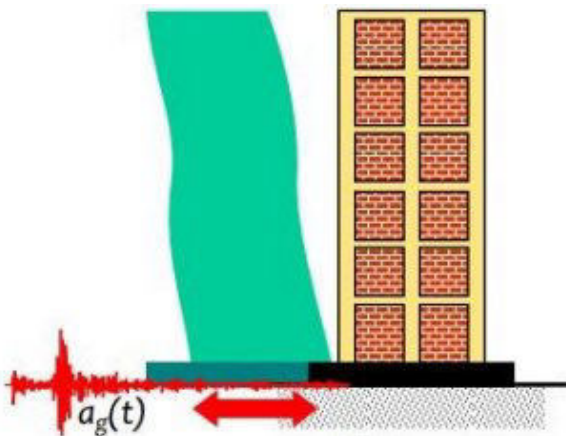
Figure 3. Earthquake Ground Motion At it Base
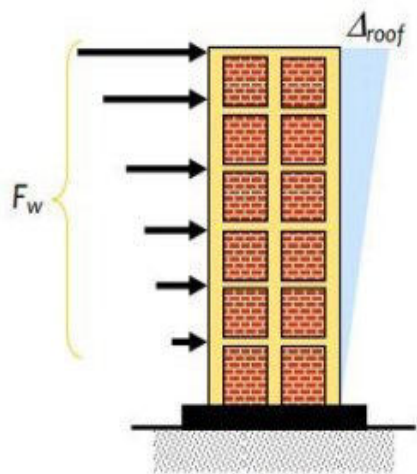
Figure 4. Wind Pressure on its Exposed Area

The structures mass is also important and should be taken into account in addition to stiffness of building because the inertial forces induced by earthquake is directly proportional to the mass of structure. It is very uneconomical to design a

building such that they have elastic behavior during the earthquake without damage. Therefore, several strength and serviceability limit states should be limited while designing a structure. Therefore the traditional methods and philosophy of designing a seismic resistant structures requires that normal structures should have sufficient resistance to minor shaking without having damage of structural and non-structural components and but undergo minor cracks to moderate earthquakes. Also during the severe shaking the structure must not undergo collapse phenomena so that to avoid fatalities and save lives. Therefore if the structure has to be designed such that it remain elastic during severe shaking and undergo a damage also then only (8-14%) of fraction of force has to be taken for design. But to reduce cracking due minor shaking, sufficient stiffness should be provided initially. Therefore careful balance to reduce cost and undergo acceptable damage is most viable during design.
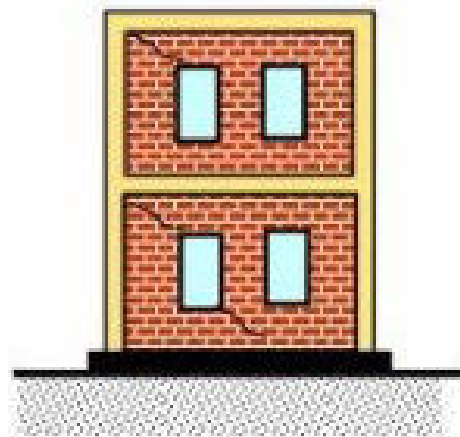

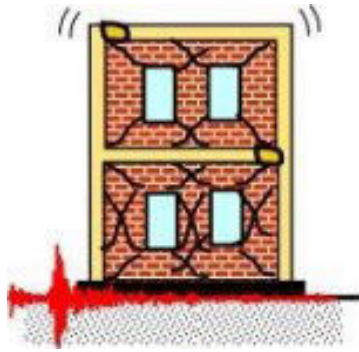Figure 5. Shows minor shaking and not considerable damage

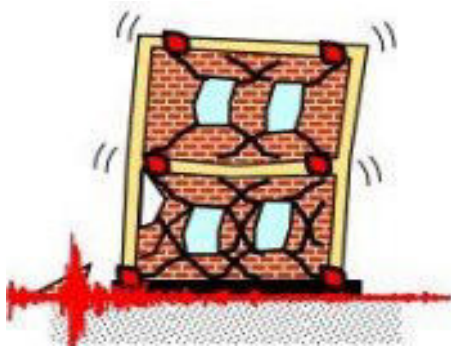Figure 6: shows minor damages due to moderate shaking

Figure 7. Shows damage due to severe shaking but no collapse

Figure 8. Summary of Push Over Analysis

II. METHODOLOGY

Masonry used in reinforced concrete structure are kiln bricks or hollow blocks. Its use are common due to its economy. In this study masonry walls are simulated as compression struts. Four methods usually used for seismic analysis includes, linear static analysis, non-linear static (Pushover analysis), linear dynamics, non-linear dynamics analysis. In this study non-linear static analysis of infill wall is done using SAP-2000 and its procedure can be shown in figure. Static nonlinear analysis in which structure is subjected to monotonic load pattern (displacement controlled) and vertical gravity loads increases continuously under which the structures behaves elastic and inelastic until reaches to ultimate limit states. When the structure is subjected to lateral loading then it causes base shear. The base shear is directly proportional to mass distribution of building. High rise building having high distribution of mass has least shear on the base. A curve showing strength versus deflection shows static pushover curve that is generated as an output. Strength of members correlated to the performance against deflection.

Usually stiffness is ignored of masonry walls but it can resist lateral forces and for this its simulated model is shown with equivalent compression strut of dimension "a" and is calculated from equation.
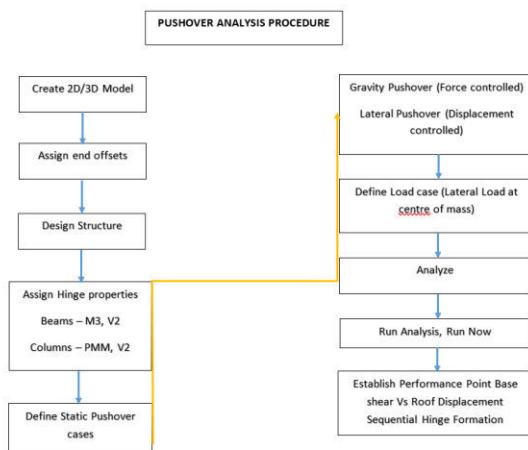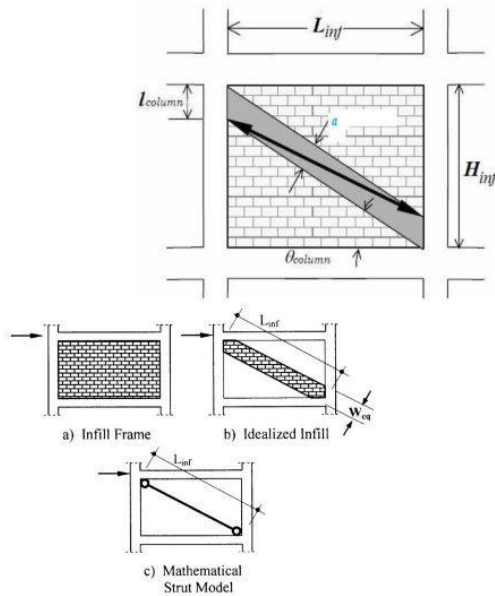
$$a=1.175(\lambda 1.hcol)^{-.4} Ldiag(in)$$

Figure 9. Diagnal Strut

Strength of structure are compared with load demands through use of Capacity Spectrum Method (CSM) in which capacity curve is obtained called pushover curve. Through pushover analysis, we can obtain the Capacity Curve of a structure shown in figure. The procedure consists of applying either a small lateral displacement or force to the structure, iteratively increasing this amount, re-analyzing the structure at each step, until the predefined damage state is obtained.
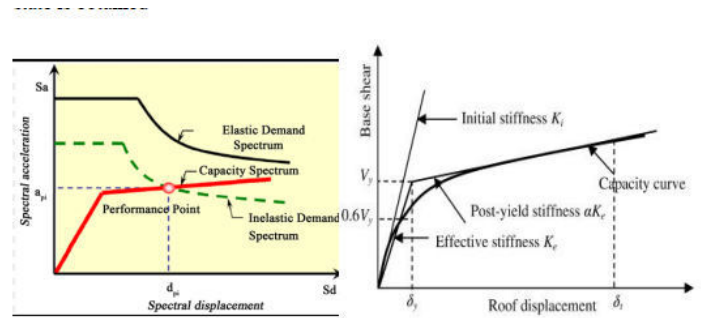

Figure 10. Capacity Spectrum

For the purpose of using different methods of Seismic Pushover analysis and then comparing their results, a building was selected which was situated in Seismic zone 2B (Peshawar). The analysis and design of the building were performed by first starting from Single story pushover analysis in one side struts, and then a 3D frame analysis in SAP2000.

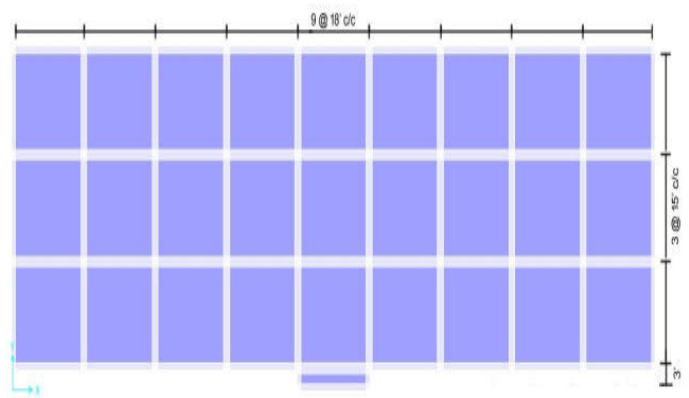The selected building was almost a regular building whose plan is shown in the figure given below.
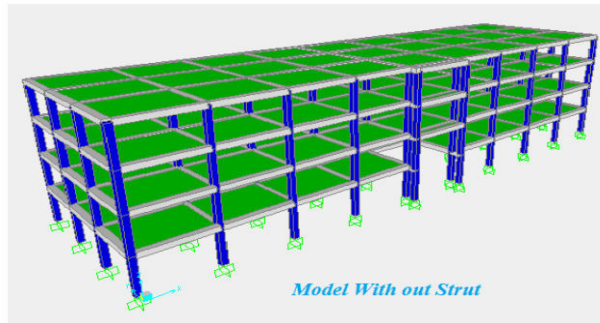

Figure 11.Plan of the selected RC Frame Structure
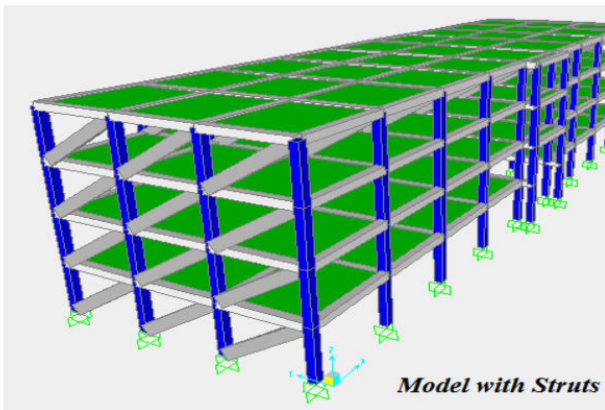
Figure 12. Bare Frame Model

Figure 13. Model with Struts

In Push over analysis (SAP2000) after analysis, the next step is to assign plastic hinges. Assign plastic Hinge to all frame members and run analysis & display the spectrums.

III.   RESULTS AND DISCUSSION

Through pushover analysis, we can obtain the Capacity Curve of a structure. The procedure consists of applying either a small lateral displacement or force to the structure, iteratively increasing his amount, re-analyzing the structure at each step, until the predefined damage state is obtained. Capacity curve and target displacement of reinforced concrete frame without and with infill walls are shown in figures 13, 14 below.
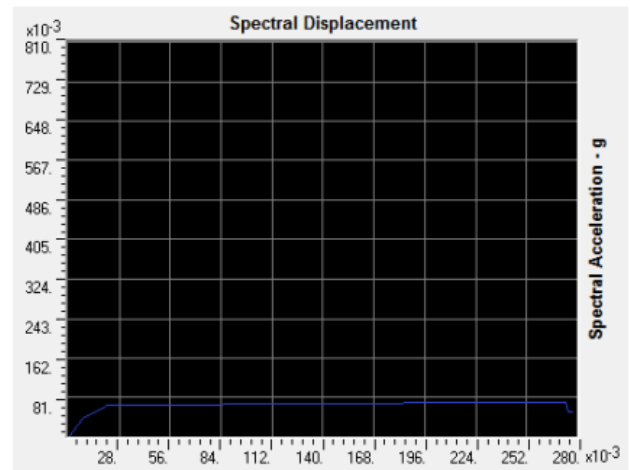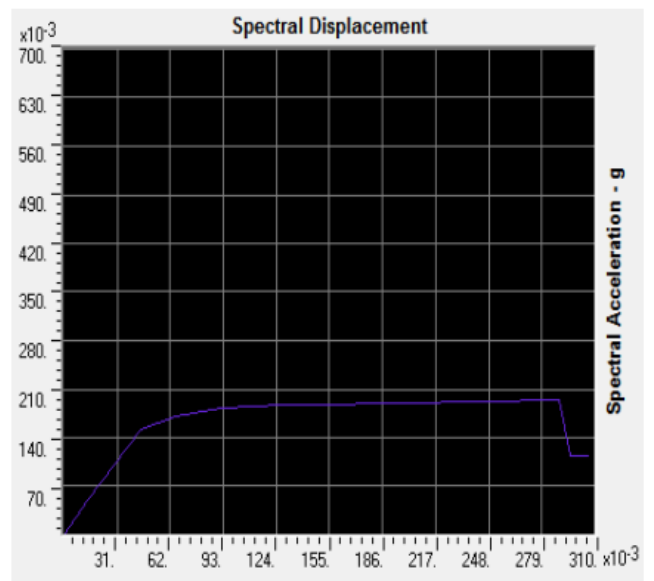

Figure 14. Capacity Curve without wall

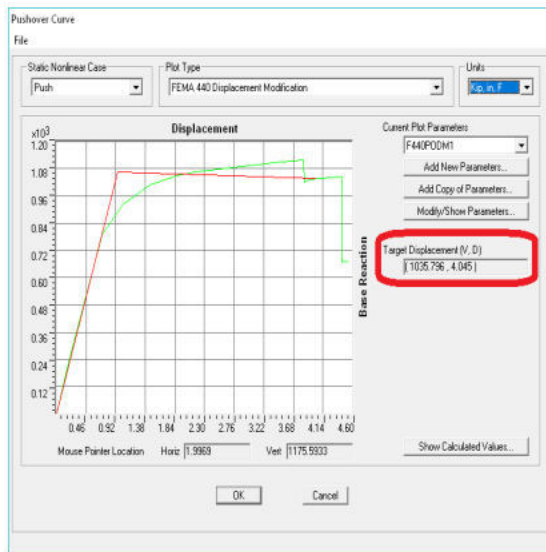*Figure 15. Capacity Curve with Infill walls*
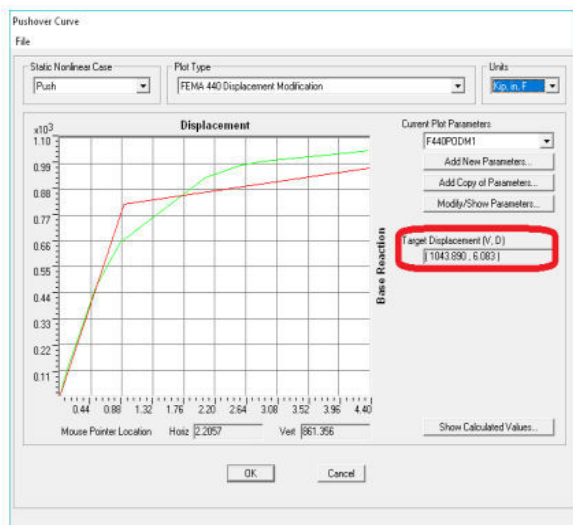
228

Figure 16. Target Displacement without wall

Figure 17. Target displacement with Infill Walls

Capacity curve of reinforced concrete frame with infill wall is increased and show that infill wall increases lateral stiffness of structure and hence improve capacity. Behavior of Various configuration of infill walls are examined under the seismic loads .plastic hinges formation take place at the joints in the bar frame that acts to resist bending moment under seismic loads. Infill

walls acts just like a truss mechanism of frame that resist loads with the help of bracing. Results has shown that Damage distribution in a structure is completely changed by infill masonry walls.

IV. CONCLUSION

i. Top storey displacement of high rise reinforced concrete frame is reduced with infill walls which increase global lateral stiffness.

ii. The time period of Building is reduced which increases base shear.

iii. Arrangement of these walls in soft storey changes displacement and base shear.

iv. Structural behavior of reinforced concrete having infill walls changes to large extent.

REFERENCES

[1]. "ACI standard building code requirements for reinforced concrete",
American Concrete Institute, Michigan, 2011.

[2]. Building Code of Pakistan, Seismic Provision, SP-2007, Ministry of Housing
and Works, Government of Islamic Republic of Pakistan, 2007.

[3]. D. Das and C.V.R. Murthy, "Brick Masonry infills in seismic of RC framed buildings: Part 1- Cost Implications", The Indian Concrete Journal, July 2004. Vol. 78, No.7, pp. 39-43.

[4]. H.B. Kaushik, D. C. Rai, and S. K. Jain, "Rational Approach to Analytical Modeling of Masonry Infill in Reinforced Concrete Framed Buildings", The 14th World Conference on Earthquake Engineering, October 12-17, 2008, Beijing, China.

[5]. Journal of Structures, Volume 2014 (2014), Article ID 493745, 15 pages Research Article "Effect of Soil Flexibility on Seismic Force Evaluation of RC Framed Buildings with Shear Wall: A Comparative Study of IS 1893 and EUROCODE8"

[6]. B. R. Jayalekshmi and H.K Chinmayi, Department of Civil Engineering, National Institute of Technology Karnataka, Surathkal 575025, India.

[7]. C.V.R.Murty, Rupen Goswami, A.R.Vijayan arayanan, Vipul V. Mehta Gujarat State Disaster Management Authority Government of Gujarat.

[8]. Design of Concrete Structures (14th edition) by Arthur H. Nilson, David Darvin, Charles W. Dolan

[9]. Pushover Analysis of High Rise Reinforced Concrete Building with and without Infill walls

[10]. "Uniform Building Code, 1997"

Comparative study of different forecasting models: A Case Study of 11 different cities of Pakistan

Hamza Hanif[1, a] and Imran Ahmed Siddiqui[1, b]

[1]University of Karachi

Email address: [a] hamzahanif2210@gmail.com and [b] imranahmadsiddiqui@yahoo.com

Abstract—Different forecasting models have been studied in this literature. The five forecasting model; three Statistical models (ARIMA, SARIMA, and SES) and 2 Machine Learning models (Prophet and Artificial Neural Network) has been employed for the forecasting of weather variable; Wind Speed on 11 different cities of Pakistan.

Keywords—forecasting, Environmental Physics, Data Science

I. INTRODUCTION

Forecasting is about predicting something in the future. In scientific term, it is about predicting about future as accurately, given all of the information available, including historical data and knowledge of any future events that might impact the forecast. The factors on which the probable for an event or quantity depends on (1) Availability of data, (2) Under stability of the factors, (3) whether the forecast influence the object which we are trying to forecast.[1]

Weather forecasting is a prime application in the domain of meteorology to prophesy the condition of the atmosphere. There are different usages of weather forecasting depending on the weather variable under consideration. Weather Forecasting has a major impact on people's lifestyle and also predicts the warning about the abrupt change in the near future that allows safeguarding of people's life, services, and trade.

The forecasting of wind speed shares greater importance in planning and developing of wind operating system. The forecasting of Wind speed has a direct effect on the power forecasting as the speed of wind is directly proportional to the cube root of wind power. Furthermore, the forecasts can play a vital role in keeping the costs competitive by reducing the need for wind curtailments and thereby, increasing revenue in electricity market operations. Therefore, ample efforts have been invested in the developments and improvements of wind speed and power forecasting. The better and accurate predicted wind power decreases chances of the worse outcome in wind power operating systems.

II. FORECASTING METHODS

There are many different models for forecasting purpose. The models which are generally used for forecasting and that been used in this literature are mentioned below. 1)ARIMA, 2)SARIMA, 3)Simple Exponential Smoothing Model(SES), 4)Prophet, 5)Artificial Neural Network (ANN)

The ARIMA, SARIMA, and SES are statistical models while Prophet and ANN belong to the class of Machine learning models.

A. ARIMA

ARIMA model stands for autoregressive integrated moving average. There are seasonal and Non-seasonal ARIMA models that can be used for forecasting. It comprises of the autoregressive model (AR) and moving average model (MA)

model. In an Auto-Regression(AR) model, we forecast the variable of interest using a linear combination of past values of the variable. The term auto regression indicates that it is a regression of the variable against itself. The MA model uses the dependency between an observation and a residual error from a moving average model applied to lag observations. The MA model is always stationary as compared to the AR model.

ARIMA model is a supplement of the ARMA model, which includes autoregressive terms, moving average terms, and differencing operations. [2] It is a Non Seasonal model. The "I" in ARIMA stands for Integrated (in this context, "integration" is the reverse of differencing), a model that uses differencing technique, a statistical transformation that performs on time-series data in order to make it stationary. This change causes the property of variables to be independent on time, eliminating the effects of trend and seasonality and steady the mean of time series. The Integrated model first applied to time series if differencing is required before any model can be applied. The ARIMA model, in general, using backshift notation can be written as,

$$(1 - \sum_{i=1}^{p} \phi_i B^i)(1-B)^d y_t = (1 - \sum_{i=1}^{q} \theta_i B^i) a_t \ ,$$

Where a_t is a white noise series and p is the order of the autoregressive part, d is the degree of first differencing involved and q is the order of moving average part.[2]

B. SARIMA

SARIMA stands for Seasonal Autoregressive Integrated Moving Average. The seasonality in a time series is defined as a regular pattern of changes that continual over 's' time periods, where 's' is the number of time periods until the pattern repeats again. [2] By utilizing the backshift operator, SARIMA(p,q,d) (P,Q,D)$_s$ can be written as.

$$(1 - \sum_{i=1}^{P} \phi_i B^{si})(1-B^s)^D(1 - \sum_{i=1}^{p} \phi_i B^i)(1-B)^d y_t = (1 - \sum_{i=1}^{q} \theta_i B^i)(1 - \sum_{i=1}^{Q} \theta_i B^{si}) a_t \ ,$$

Where a_t is a white noise series and p,q, d ,P , D and Q are non-negative integers.

C. Single Exponential Smoothing Model

The Single Exponential Smoothing (SES) also referred to as Simple Exponential Smoothing model is probably the most widely used method for short-term fore-casting. It was proposed in the late 1950s by Holt and Brown. The single Exponential model works fine with univariate time series which shows no trend or seasonal pattern. It depends upon a single parameter, named smoothing parameter or smoothing coefficient and it is a constant term, with values lies often in between 0 to 1. The value has a significant effect on the forecast, as it controls the rate at which weight decay exponentially. The computation of forecast based on the observation in time series $y_1, \dots, y_t$ can be done as follows,

$$y_{t+1|t} = \alpha y_t + (1 - \alpha) y_{t|t-1}$$

Where
$y_{t+1|t}$ = forecast value
α = smoothing constant

The large value of α, close to 1 indicates the model pay attention to most recent past observations which relates to a fast learning approach, where smaller value of that are close to 0 is a slow learning technique as it gives more weight to distant observations.

D. PROPHET

The Prophet is an open source computational tool for forecasting that is developed by the Facebook research team on February 23, 2017. The Prophet is built specifically to produce high-quality forecast in the business-related task. This method focuses on the difficulties related to business time series like seasonal effects due to human behavior as seen on a weekly, monthly and yearly cycles, ups, and downs on public holidays; variation in trend caused by the arrival of new products and market events[4]. It uses the curve fitting method instead of traditional times series model because it makes easier to fit the model,

handles missing data effectively and have adaptability in its computation.

Prophet built upon on Bayesian-based additive regression model and that compromises on the following main four components [4].

$$y(t) = g(t) + s(t) + h(t) + \in_t$$

Trend $g(t)$ represents non-periodic changes of the series. Seasonality $s(t)$ models periodic events. Holiday effect component $h(t)$ estimates information about holiday and events. Errors $\in_t$, that cannot be accounted for.

E. Artifical Neural Network

Neural network also called artificial neural network is a computational model that is built upon the human brain model or biological neural network [5]. However in recent years, the neural network has gained momentum in several domains, solving the complex task of different sectors like speech and image recognition, driverless car and robotics, data clustering and classification, time series forecasting.

A Neural Network can be characterized as a network of neurons, which is analogous to the interconnected neurons of our brain. The neurons also called nodes are stacked in layers and have an input layer, an output layer and also intermediate layer consists of hidden neurons. In the context of forecasting the input layer will be referred to as predictor layers and output layer will be called forecasts layers. A neuron can be defined as 'nonlinear, parameterized and bounded function' [5].

III. CASE STUDY

In this literature, forecasting of Wind Speed has been done by using different forecasting models that have been discussed in the previous section. The data are obtained from the World Bank[19], an essential source of providing financial and technical assistance to developing countries around the world. The data is recorded for a purpose, to help policymakers and service sectors in understanding the potential high-wind areas for

wind power generation in Pakistan. The data contains the daily report for wind speed, wind direction, air pressure, relative humidity, and temperature are collected with a time interval of 15 or 20 minutes from 11 wind masts located in different cities of Pakistan; Bahawalpur, Chakri, Gwadar, Haripur, Peshawar, Quaidabad, Sadiqabad, Sanghar, Sujawal, Tandho Ghulam Ali and Umerkot.

The Map of Pakistan featuring the locations of 11 wind masts.
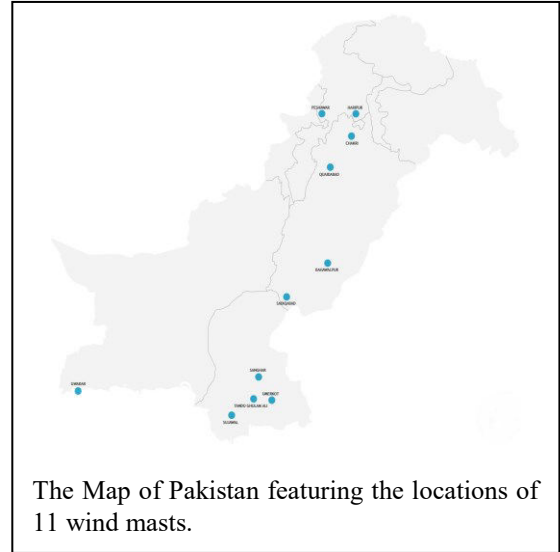
The data that been used in this literature have missing values, due to the instrumentation error or during the maintenance of equipment. The missing values replaced by neighboring values and then data was resampled to 1-hour interval. The training data set comprises of 4 weeks values and for test data set it include values of one day(24 values), to check the accuracy of different forecasting models.

A. Discussion

In order to find out, which model had the best performance, we calculate accuracy measurements; Root Mean Squared Error (RMSE) and Mean Absolute Percentage Error (MAPE) for each of the methods that been used to predict wind speed. Tables show the mean value of accuracy measurement of all 11 cities of test data set.

	ARIMA	SARIMA	SES
RMSE	1.373	0.966	0.966
MAPE	28.004	20.784	25.25

	PROPHET	ANN
RMSE	2.104	0.666
MAPE	39.42	14.362

.

Table demonstrates that ANN forecasting methods have the lowest error, while SARIMA and SES models being at the second place. The worst result was given by the ARIMA and Prophet. The given results can be explained by the following facts. ARIMA have a relatively simples algorithm and it is not able to deal with prediction of fast turnovers, and do not involve trend and seasonality component. The same reason accounts for the inaccuracy by the Prophet model as it does not support rapid changes in the data set, as it built for the econometric and financial time series analysis. SARIMA show promising results, might due to the seasonal components incorporated in it. ANN models with their ability to reproduce nonlinear dependencies presented the best forecasting results. The examination of MAPE values informs us that large error on average is expected in forecasting from the Prophet and ARIMA forecasting model, while SARIMA, SES, and AAN models have minimal error values in their forecasting.

The actual and predicted values of wind Speed of one of the city, Gwadar.
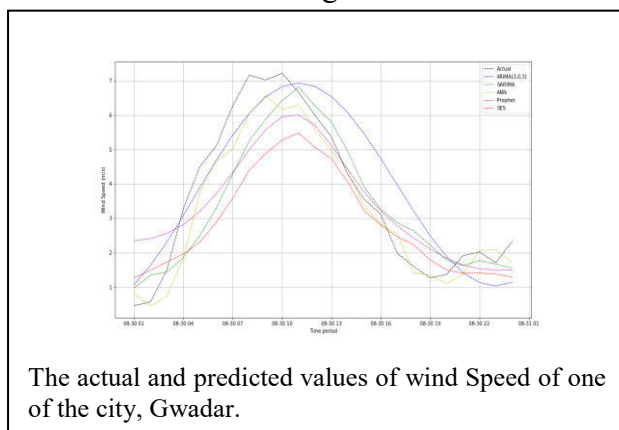
FURTHER WORK

There are other forecasting models that can also be reviewed. The Dynamic Regression (multivariate) models; ARIMAX and SARIMAX can be applied with the external factors taken into account. The variant models of ANN, like long short term memory (LSTM) or Recurrent Neural Network (RRN) can also be employed. The other models of Exponential Smoothing Model like Double Exponential and Triple Exponential Smoothing models may provide accurate compared to SES as their methods have trend and seasonal components.

REFERENCES

[1] Time Series Analysis: Forecasting and Control by Gregory C. Reinsel, Greta M. Ljung, George E. P. Box, Gwilym M. Jenkins.

[2] Forecasting: principles and practice By Rob J Hyndman, George Athanasopoulos.

[3] I. S. Jacobs and C. P. Bean, "Fine particles, thin films and exchange anisotropy," in Magnetism, vol. III, G. T. Rado and H. Suhl, Eds. New York: Academic, 1963, pp. 271–350.

[4] Sean J. Taylor and Benjamin Letham; "Forecasting at Scale'.

[5] Gerard Dreyfus; Neural Netwroks: Methodology and Applications.

[6] Data received from "World Bank via ENERGYDATA.info, under a project funded by the Energy Sector Management Assistance Program (ESMAP).
URL:
https://energydata.info/dataset/pakistan-wind-measurement-data